

JET PROPULSION

1958

A publication of the

AMERICAN ROCKET SOCIETY

Research and Development

VOLUME 28

DECEMBER 1958

NUMBER 12
SCIENCE & TECHNOLOGY

SURVEY ARTICLE

- Recent Advances in Determination of Radiative Properties of Gases at High Temperatures Joseph G. Logan Jr. 795

CONTRIBUTED ARTICLES

- The Ignition of Combustible Mixtures by Hot Gases H. G. Wolfhard 798
Digital Computer Analysis of Transients in Liquid Rocket Engines P. Kluger and E. C. Farrell 804
Precision Measurement of Supersonic Rocket Sled Velocity—Part II F. J. Beutler and L. L. Rauch 809
Meteorological Rocket Soundings in the Arctic W. G. Stroud 817

TECHNICAL NOTES

- Influence of Approach Boundary Layer Thickness on Premixed Propane-Air Flames Stabilized in a Sudden Expansion William T. Snyder 822
Visibility of Orbital Points W. J. Berger and J. R. Ricupito 825
Calculation of Re-Entry Velocity Profile Alfred A. Adler 827
Combustion Chamber Pressure Loss S. L. Bragg and S. P. Q. Byworth 829
An Empirical Method for Calculating Heat Transfer Rates in Resonating Gaseous Pipe Flow Gerald Marrell 829
The Gasification of Solid Ammonium Nitrate W. H. Andersen, K. W. Bills, A. O. Dekker, E. Mishuck, G. Moe and R. D. Schultz 831
Pressure Distributions on Blunt-Nosed Cones in Low Density Hypersonic Flow L. Talbot, S. A. Schaaf and F. C. Hurlbut 832
Note on Interplanetary Navigation Robert M. L. Baker Jr. 834
Ignition by Flow Over Hot Surfaces Welby G. Courtney 836
A New Instrument for Measuring Atmospheric Density and Temperature at Satellite Altitudes A. J. Dessler, W. B. Hanson, M. Hertzberg, D. D. McKibbin and R. C. Wrigley 837
Some Comments on Generalized Trajectories for Free Falling Bodies of High Drag William Squire 838
On the Classification of the Chemistry in Combustion Experiments Gerald Rosen 839
On the Importance of the Sensitive Time Lag in Longitudinal High-Frequency Rocket Combustion Instability Luigi Crocco, Jerry Gray and David T. Harrie 841

DEPARTMENTS

- Technical Comment 843 New Patents 846 Book Reviews 850 Technical Literature Digest 852
Annual Index—Volume 28, January-December 1958 866



NEW

*from the
Reaction
Motors
Division of
Thiokol*

**THE PRE-PACKAGED
LIQUID ROCKET ENGINE**

**ready for
instant firing**

**includes entire
engine system**

factory fueled

**no propellant handling
in the field**

**safe
flexible
storable**

A unique concept in liquid propellant rocket engines, the pre-packaged powerplant developed and now being produced by Thiokol's Reaction Motors Division stands as one of the most significant recent advances in the field of rocketry. It is high on reliability; can be held in "ready" state for extended periods of time; and in design will lend itself to many missile applications.

In your future development programs, you can consider pre-packaged liquid rocket engines as being available!

Thiokol®

CHEMICAL CORPORATION

REACTION MOTORS DIVISION, DENVER, N. J.

® Registered trademark of the Thiokol Chemical Corporation for its liquid polymers, rocket propellants, plasticizers and other chemical products.



Lino-Writ 4...fastest to use, fastest to process

Lino-Writ 4 is the *fastest, toughest, thinnest* paper you can use. Now with Du Pont's new low-odor Rapid Processing Chemicals Kit, it offers the additional advantages of fastest processing without sacrificing fine detail.

With this combination you can now use processing temperatures up to 120° F. and get better trace densities, cleaner records, higher photographic speeds and faster processing throughout.

No other photorecording paper-chemical team can offer these across-the-board "plus" features. Ask your Du Pont Technical Representative about Lino-Writ 4, the new low-odor Rapid Chemicals Kit and the entire Lino-Writ line.

E. I. du Pont de Nemours & Co. (Inc.), Photo Products Department, Wilmington 98, Delaware. In Canada: Du Pont Company of Canada (1956) Limited, Toronto.

This advertisement was produced exclusively by Phototypography



Better Things for Better Living . . . through Chemistry

JET PROPULSION

A publication of the
AMERICAN ROCKET SOCIETY

Research and Development

IRWIN HERSEY—DIRECTOR OF PUBLICATIONS

EDITOR

MARTIN SUMMERFIELD

ASSISTANT EDITOR

BARBARA NOWAK

ART EDITOR

JOHN CULIN

ASSOCIATE EDITORS

ALI BULENT CAMBEL, *Northwestern University*

IRVIN GLASSMAN, *Princeton University*

M. H. SMITH, *Princeton University*

CONTRIBUTORS

MARSHALL FISHER, *Princeton University*

GEORGE F. McLAUGHLIN

ADVERTISING PRODUCTION MANAGER

WALTER BRUNKE

ADVERTISING & PROMOTION MANAGER

WILLIAM CHENOWETH

ADVERTISING REPRESENTATIVES

D. C. Emery & Associates
155 East 42 St., New York, N. Y.
Telephone: Yukon 6-6855

James C. Galloway & Co.
6535 Wilshire Blvd., Los Angeles, Calif.
Telephone: Olive 3-3223

Jim Summers & Associates
35 E. Wacker Dr., Chicago, Ill.
Telephone: Andover 3-1154

R. F. Pickrell & Associates
318 Stephenson Bldg., Detroit, Mich.
Telephone: Trinity 1-0790

Louis J. Bresnick
304 Washington Ave., Chelsea 50, Mass.
Telephone: Chelsea 3-3335

John W. Foster
239 4th Ave., Pittsburgh, Pa.
Telephone: Atlantic 1-2977

AMERICAN ROCKET SOCIETY

Founded 1930

OFFICERS

President
Vice-President
Executive Secretary
Secretary
Treasurer
General Counsel

George P. Sutton
John P. Stapp
James J. Harford
A. C. Slade
Robert M. Lawrence
Andrew G. Haley

BOARD OF DIRECTORS

Terms expiring on dates indicated

Krafft Ehrlicke, 1959
S. K. Hoffman, 1958
Simon Ramo, 1960
H. W. Ritchey, 1959

H. S. Seifert, 1958
K. R. Stehling, 1958
Martin Summerfield, 1959
Wernher von Braun, 1960

Maurice J. Zucrow, 1960

TECHNICAL DIVISION CHAIRMEN

Lawrence S. Brown, Instrumentation and Guidance
Milton U. Clauser, Magnetohydrodynamics
Krafft A. Ehrlicke, Space Flight
Stanley V. Gunn, Nuclear Propulsion

Y. C. Lee, Liquid Rocket
Brooks T. Morris, Ramjet
David G. Simons, Human Factors
John Sloop, Propellants and Combustion
Ivan E. Tuhy, Solid Rocket

COMMITTEE CHAIRMEN

S. K. Hoffman, Finance
Simon Ramo, Publications
H. W. Ritchey, Membership

H. S. Seifert, Program
Kurt Stehling, Awards
Martin Summerfield, Policy

Scope of JET PROPULSION

This Journal is a publication of the American Rocket Society devoted to the advancement of the field of jet propulsion through the dissemination of original papers disclosing new knowledge or new developments. As used herein, the term "jet propulsion" embraces all engines that develop thrust by rearward discharge of a jet through a nozzle or duct; and thus it includes air-consuming engines and underwater systems as well as rockets. JET PROPULSION is open to contributions dealing not only with propulsion but with other aspects of jet-propelled flight, such as flight mechanics, guidance, telemetry, and research instrumentation. Increasing emphasis will be given to the scientific problems of extraterrestrial flight.

Information for Authors

Manuscripts must be as brief as the proper presentation of the ideas will allow. Exclusion of dispensable material and conciseness of expression will influence the Editor's acceptance of a manuscript. In terms of standard-size double-spaced typed pages, a typical maximum length is 22 pages of text (including equations), 1 page of references, 1 page of abstract, and 12 illustrations. Fewer illustrations permit more text, and vice versa. Greater length will be acceptable only in exceptional cases.

Short manuscripts, not more than one quarter of the maximum length stated for full articles, may qualify for publication as Technical Notes or Technical Comments. They may be devoted to new developments requiring prompt disclosure or to comments on previously published papers. Such manuscripts are usually published within two months of the date of receipt.

Sponsored manuscripts are published occasionally as an ARS service to the industry. A manuscript that does not qualify for publication according to the above-stated requirements as to subject, scope or length, but which nevertheless deserves widespread distribution among jet propulsion engineers, may be printed as an extra part of the Journal or as a special supplement, if the author or his sponsor will reimburse the Society for actual publication costs. Estimates are available on request. Acknowledgment of such financial sponsorship appears as a footnote on the first page of the article. Publication is prompt since such papers are not in the ordinary backlog.

Manuscripts must be double spaced on one side of paper only with wide margins to allow for instructions to printer. Include a 100 to 200 word abstract. State the author's positions and affiliations in a footnote on the first page. Equations and symbols may be handwritten or typewritten; clarity for the printer is essential. Greek letters and unusual symbols should be identified in the margin. If handwritten, distinguish between capital and lower case letters, and indicate subscripts and superscripts. References are to be grouped at the end of the manuscript and are to be given as follows: for journal articles: authors first, then title, journal, volume, year, page numbers; for books: authors first, then title, publisher, city, edition, and page or chapter numbers. Line drawings must be clear and sharp to make clear engravings. Use black ink on white paper or tracing cloth. Lettering should be large enough to be legible after reduction. Photographs should be glossy prints, not matte or semi-matte. Each illustration must have a legend; legends should be listed in order on a separate sheet.

Manuscripts must be accompanied by written assurance as to security clearance in the event the subject matter lies in a classified area or if the paper originates under government sponsorship. Full responsibility rests with the author.

Submit manuscripts in duplicate (original plus first carbon, with two sets of illustrations) to the Editor, Martin Summerfield, Professor of Aeronautical Engineering, Princeton University, Princeton, N. J. Preprints of papers presented at ARS national meetings are automatically considered for publication.

JET PROPULSION is published monthly by the American Rocket Society, Inc., and the American Interplanetary Society at 20th & Northampton Sts., Easton, Pa., U. S. A. Editorial office: 500 Fifth Ave., New York 36, N. Y. Price: \$12.50 per year, \$2.00 per single copy. Second-class mail privileges authorized at Easton, Pa. Notice of change of address should be sent to the Secretary, ARS, at least 30 days prior to publication. Opinions expressed herein are the authors and do not necessarily reflect the views of the Editors or of the Society. © Copyright 1958 by the American Rocket Society, Inc.

Recent Advances in Determination of Radiative Properties of Gases at High Temperatures

JOSEPH G. LOGAN Jr.

Space Technology Laboratories, Inc., Los Angeles, Calif.

After receiving a B.S. degree in Mathematics and Physics from the District of Columbia Teachers' College, the author was employed by the Aerodynamics Section of the National Bureau of Standards. In 1947, he joined the Aerodynamics Department of the Cornell Aeronautical Laboratory where he carried out research in propulsion and high temperature gasdynamics. He received his Ph.D. in Physics from the University of Buffalo in 1955, and is currently head of the Aerophysics Laboratory, Aerophysics Department, Space Technology Laboratories, Inc.

Introduction

AERODYNAMIC heating problems associated with hypersonic re-entry of ballistic missiles and satellites into the atmosphere have been greatly complicated by the necessity for considering new mechanisms for heat transfer caused by radiation and atomic surface recombination phenomena (16).¹ These processes, previously unencountered in aerodynamic phenomena, arise because a high speed re-entry vehicle is surrounded by a sheath of highly luminous, high temperature air composed of a complicated mixture of molecules, atoms, ions and electrons.

Early attempts (22,27) to assess the magnitude of the radiative contribution to heating indicated values equivalent to convective effects and stimulated extensive theoretical and experimental studies of the emissive characteristics of the high temperature air components. This article describes recent progress in the determination of the radiative properties of gases (primarily air) in the temperature range 3000 to 10,000 K. The review and bibliography are intended to serve only as a guide to current investigations and consequently are not complete. Electric arcs, for example, are known to produce temperatures in, and well above, this range. A comprehensive survey of recent advances in the determination of radiative gas properties must necessarily include mention of arc studies (10,11) as well as investigations of flames (48) and explosions (25,48).

Determination of Radiative Properties of Gases

A gas emits radiation as a result of rotational, vibrational and electronic transitions from excited energy levels to lower energy levels. The emitted radiant energy corresponding to these transitions is distributed over a wide wavelength region. The total radiant intensity emitted from a given quantity of gas is obtained by summing the radiant intensities corresponding to each of the individual energy transitions. The simplest approach to the determination of the radiative intensity of gases is based upon the determination of overall emissivities or absorptivities for gaseous mixtures as a function of pressure, temperature and path length (33). This approach involves only limited application of the fundamental relations determining the intensity

of absorbed or emitted radiant energy,² although it has been developed to the point where reasonable predictions can be made for practical applications.

Such calculations require knowledge of the following factors (17):

- 1 The number of molecules present in each of the various energy levels in thermal equilibrium.
- 2 The transition probabilities for each of the possible energy transitions.
- 3 The frequencies for the energy transitions.
- 4 The spectral line shape. The spectral line shape at high temperatures is primarily influenced by gas motion (Doppler broadening) and the presence of neighboring particles (pressure broadening).

In the temperature and density range of interest for missile and satellite re-entry, the most important air components according to concentration are N_2 , O_2 , NO_2 , NO , N , O , O^- , N_2^+ , O_2^+ , NO^+ , O^+ and electrons (14,24). Contributions to the observed radiant flux from these components can be conveniently classified as transitions yielding continuous spectra and transitions yielding discrete, line, spectra. Contributions to continuum radiation can further be classified as free-bound, wherein the electron-ion collision results in attachment, and free-free, wherein the electron-ion or electron-atom collision results in emission of energy without union between electron and particle.

Absorption Coefficients for Air Components

Calculations of the absorption coefficient of air in the temperature range 2000 to 18,000 K were first carried out by Magee and Hirschfelder (25) in connection with studies of radiation effects of atomic explosions. They considered photoelectric absorption by N , O and O^- , and absorption by NO_2 . The absorption spectra of the N_2 and NO band systems were not taken into account. When a state of thermodynamic equilibrium exists, the emission coefficient is related to the absorption coefficient through Kirchhoff's law, and either the emission coefficient or the absorption coefficient can be employed to describe the radiation.

The possible significance of NO as an important contributor to radiation in this region was pointed out by Teller (22) and Meyerott (27). In calculations of absorption coefficients, one of the important parameters, which is a measure of the intensity of a spectral line, is the oscillator strength, or f number, which relates the actual energy absorbed by a spectral line to the energy absorbed by a classical electron oscillator.

The major uncertainty in calculations of the NO contribution is related to the integrated oscillator strength or f number to be assigned to the NO molecule (27). Use of f values of 0.1 indicated that the NO molecule would be one of the most important constituents for absorption. However,

² In principle, rigorous solutions to the problem of emission of radiant energy from an assembly of gaseous emitters which are in thermal equilibrium can be evolved, based on quantum-mechanical considerations. In practice this is difficult because of uncertainty with regard to many of the fundamental atomic and molecular parameters; see for example (33).

Received Oct. 22, 1958.

¹ Numbers in parentheses indicate References at end of paper.

emissivity measurements by Keck made at Avco Research Laboratory, using a shock tube to produce the radiating gas, demonstrated that NO was not an important contributor (21,22,38). This result was substantiated by the absorption measurements made by Weber and Penner in cold NO (45). This work, combined with measurements by Marmo (26) and Hurowitz (28), indicated that the f values could be as small as 0.002.

Meyerott (27) carried out the first extensive calculations of the absorption coefficients for air components. In this work, which has now been modified to reflect the effect of recent experimental studies (28), 0.2 was taken for the electronic f number for all molecular electronic transitions. He considered the N_2 first and second positive systems and the N_2^+ first negative system. Contributors to the continuous absorption which appeared significant were photoelectric absorption by O^- , O , N and N_2 and free-free absorption by electrons in the fields of both positive ions and O .

Experimental Determination of Absorption Coefficients

Experimental determinations of absorption coefficients using room temperature gases are of limited value for studies of high temperature radiative properties, because many species make contributions to the absorption coefficient by absorption from excited states. Other techniques must be employed to evaluate contributions of excited species.

One of the most promising of these techniques centers around the use of the shock tube,³ and this technique has been used extensively by Keck, Kivel and Wentink (21,38,46) of the Avco Research Laboratory. A confined region of gas is shock-heated to the temperature, density and thermodynamic state of interest to hypersonic flight problems by reflecting a strong shock wave from the closed end of a shock tube. In this program, measurements of absolute intensities were carried out as well as measurements of time-resolved emission spectra.

Conclusions from these studies at 8000 K and sea level density were that in the visible and near-infrared regions, little structure can be observed. Above 5500 Å the radiation was attributed to the N_2 first positive system. Fig. 1 shows the measured wave length dependence of radiation from air at 8000 K. Significant contributors to radiation were determined to be NO (γ band), N_2 (second positive), N_2 (first positive), CN (violet), O^- (free-bound) and $O + e$ (free-free). Positive spectroscopic identification was obtained for the N_2 and CN band systems. One of the more significant results of these studies was the determination that in flight at a Mach number 20, at an altitude of approximately 100,000 ft, the radiative heat transfer from a 1-ft radius sphere would be only approximately 10 per cent of the aerodynamic stagnation point heat transfer.

Although the work of the Avco group has clarified many of the important questions about the absorption properties of air in the 8000 K temperature range (23), Meyerott (28) points out that additional work is needed in other temperature and density ranges and with different gas mixtures to isolate particular contributors. The relative importance of different species changes with temperature and density. For example, at 8000 K and 10^{-3} normal density, the relative importance of the N_2^+ first negative band increases, O^- becomes unimportant, and the photoelectric absorption from the excited states of N and O becomes a contributing factor. At 12,000 K and normal density, in addition to the N_2 first positive and second positive band systems, the N_2^+ first negative system, and O^- photoelectric absorption, the photoelectric absorption from the excited states of N and O , as well as free-free absorption by electrons in the field of positive ions, contribute to the total absorption. At 12,000 K and 10^{-3} normal density,

³ A detailed discussion of shock tube techniques is presented later in this paper.

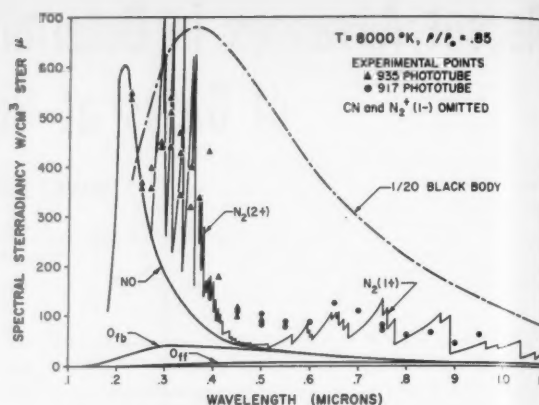


Figure 1 Monochromator-photocell measurements of the distribution and absolute intensity of the radiation from 1 cm of air at approximately 8000 K and $\rho/\rho_0 = 0.85$, compared to the estimated radiation

the molecules are dissociated, and the only remaining contributors are free-free absorption by electrons in the fields of positive ions and photoelectric absorption from the excited states of N and O . The contributions of many of these species are as yet poorly evaluated, and the possibility exists that a constituent other than those presently considered might make a significant contribution to radiation.

Shock tube studies of the radiative properties of high temperature air have also been carried out by Wurster, Glick and Treanor at Cornell Aeronautical Laboratory (49,50) in the temperature range 4000 to 7000 K. From absorption studies, the gross absorption coefficient for air was obtained. Typical features of the spectrum observed were: NO α bands at 6000 K and normal density; strong continuum absorption below 2600 Å at 4000 K and four times normal density; CN bands at 3900 Å and sequences of the second positive system of N_2 in emission at 7000 K, and high vibrational transitions of the O_2 Schumann-Runge system.

Such studies of the radiative properties of high temperature air will be of increasing significance for hypersonic photo-reconnaissance and satellite re-entry applications (13,28). They may also provide improved recognition techniques for countermeasure applications.

Recent Theoretical Studies of Radiation From High Temperature Gases

One of the outgrowths of the recent interest in determination of the emissivity of high temperature air has been the renewed interest in the development of theoretical approaches which will permit more accurate prediction of the radiation from gaseous mixtures at high temperatures. Jarman, Fraser, Nicholls and Turner (19), at the University of Western Ontario, have made extensive studies of molecular band intensities. In particular, they have carried out a detailed investigation of the N_2 first positive system and have computed overlap integrals for the NO β and γ bands. Kivel, Mayer and Bethe (22) have extended the latter results.

Breene⁴ (2,3,4,5) at the Aerophysics Laboratories of the General Electric Company is undertaking an extensive program to calculate diatomic vibrational wave functions, molecular electronic wave functions, atomic wave functions and wave functions for free electrons in the fields of various atoms. The primary objective is the development of a theoretical approach which will permit the accurate prediction of radiation from high temperature gas mixtures.

⁴ R. G. Breene Jr. (private communication).

Radiation Phenomena in Rocket Thrust Chambers

Radiation phenomena similar to those encountered in ballistic missile applications are also of importance for the design of cooling systems for rocket exhaust systems. As emphasis is placed on achieving greater specific impulse and thrust values in chemical rocket engines, combustion chamber temperatures tend to increase to values approaching 3000 K. As combustion chamber temperatures increase, greater percentages of heat will be transferred to the nozzle wall by radiative processes. The problem, therefore, exists of determining how large a fraction of the total heat transfer is produced by radiant energy. At the present time, only the transitions corresponding to the infrared vibration-rotation bands make important contributions to the total radiant heat transfer at the temperatures of interest in connection with combustion chamber studies (1,33).

As a typical example of this problem, studies were carried out at the Jet Propulsion Laboratory for the RFNA-hydrazine propellant system (29). Although water vapor was the only component of the combustion products capable of emitting energy, experimental measurement of the emissivity indicated that, in terms of heat transfer to the combustion chamber, radiation could contribute 10 to 30 per cent of the total heat transfer.

In many cases, the problem of radiant heat transfer in rocket exhaust systems is more serious than the corresponding ballistic missile problem in that the combustion chamber pressures tend to be extremely high, between 300 and 600 psi. Since the density is correspondingly large, the radiant energy in the rocket combustion chamber can contribute a much greater fraction of the total overall heat transfer.

The problem of the accurate determination of radiant energy contributions in rocket combustion systems will, in the future, be an extremely complex one, since new fuels, both liquid and solid, are being considered which will operate at increasingly higher combustion chamber temperatures. In many cases very little information is available concerning the chemical composition of these fuels at high temperatures, and, consequently, the problem of determining the radiative contributions will become increasingly difficult.

Use of Shock Tube for Study of High Temperature Radiation Phenomena

The shock tube is now recognized as one of the more promising of the experimental tools for studies of high temperature radiation phenomena. Kantrowitz was one of the first to recognize its importance for the creation of high temperatures in a controlled manner. At Cornell University, studies of radiation produced by high temperature argon were initiated, and high speed spectrographic techniques were developed (36).

The combination of the development of the shock tube and the refinement of high speed recording techniques (18,34,37,43) has enabled investigations of radiation phenomena in regions which were previously inaccessible. Recent developments in shock tube driver heating techniques involving the use of plasma generators for inert driver gas heating promise achievement of enthalpy and temperature conditions even higher than those currently obtainable by hydrogen and combustion driver methods (40,41,42).⁵ The development of this technique will permit the controlled investigation of radiation phenomena not accessible at the present time by any but microsecond duration electric heating techniques (20,52).

Many current investigations of chemical and physical phenomena are based on studies of the emission or absorption characteristics of high temperature gases (8,15,30,44). In shock tube studies of kinetic phenomena in air, Camac,

Camm, Keck and Petty (6,7) have determined the concentration of O_2 in the ground vibrational state by measuring the gas opacity to Schumann-Runge radiation. Such studies yield information on both vibration and chemical relaxation rates in air. Roth and Gloersen (39) have studied the visible continuum emission from xenon in the temperature range 6000 to 11,000 K and have determined the activation energy for this emission corresponding to the energy of the metastable state of the xenon atom (39). Windsor, Davidson and Taylor (47) have studied the energy exchange between translation and vibration and rotation in CO through study of the infrared emission.

The fundamental knowledge concerning internal structure of gas molecules, collision phenomena, reaction rates and relaxation processes formerly supplied primarily by studies of the radiation from electrical discharges and combustion processes,⁶ is now being greatly extended through the use of shock tube facilities for the generation of high gas temperatures under controlled density and temperature conditions. Information derived from these studies is making a significant contribution to the solution of the problem of radiation from high temperature gases in thermal equilibrium. For an excellent review of the use of the shock tube for the investigation of physical and chemical phenomena the reader is referred to the paper by Penner, Harshbarger and Vali (34).

References

- 1 Benitez, L. E. and Penner, S. S., "The Emission of Radiation from Nitric Oxide: Approximate Calculations," *J. Applied Physics*, vol. 21, Sept. 1950, pp. 907-908.
- 2 Breene, R. G., Jr., "Analytic Wave Functions I. Atoms with 1s, 2s, and 2p Electrons," *The Physical Review*, Aug. 15, 1958.
- 3 Breene, R. G., Jr., "Infrared Emissivity Theory," General Electric Co., Aerophysics Laboratory Operation Technical Memorandum no. 44.
- 4 Breene, R. G., Jr., *J. Chemical Physics*, vol. 29, no. 3, Sept. 1958, p. 512.
- 5 Breene, R. G., Jr. and Todd, M. N., Jr., "Vibrational Matrix Elements of NO ," *J. Chemical Physics*, vol. 28, no. 1, Jan. 1958, pp. 11-15.
- 6 Camac, M., Keck, J. and Petty, C., "Relaxation Phenomena in Air Between 3000 and 8000°K," Avco Research Laboratory, Research Report 22, Everett, Mass., March 13, 1958.
- 7 Camm, J. and Keck, J., "Radiative Relaxation Behind a Shock Wave," Presented before American Physical Society, Washington, D.C., April 1957.
- 8 Eastmond, J. and Hales, R. W., "Observation of Stark Effect Broadening to Determine Ionic Conditions in Shock Tubes," *Bull. American Physics Soc.*, vol. 2, Sept. 5, 1957, p. 302.
- 9 Feast, M. W., "Investigation of the Spectrum of the High Voltage Arc in Carbon Dioxide: the CO Flame Spectrum," *Proc. Physics Society of America*, vol. 63, 1950, pp. 772-774.
- 10 Finkelburg, W. and Maeker, H., *Encyclopedia of Physics*, vol. XXII, Springer-Verlag, Berlin, Göttingen, Heidelberg, 1956, pp. 254-439.
- 11 Fischer, H. and Mansur, L. C. (ed.), "Conference on Extremely High Temperatures," John Wiley and Sons, Inc., New York, 1958.
- 12 Fowler, R. G., *Encyclopedia of Physics*, vol. XXII, Springer-Verlag, Berlin, Göttingen, Heidelberg, 1956, pp. 209-253.
- 13 Gazley, C., Jr. and Masson, D. J., "Recovery of Circum-Lunar Instrument Carrier," Presented under the auspices of the American Rocket Society, Eighth Int. Astronautical Congress, Barcelona, Spain, Report 488-57, Oct. 1957, pp. 1-22, 6-12.
- 14 Gilmore, F. R., "Equilibrium Composition and Thermodynamic Properties of Air to 24,000°K," U.S. Air Force Project, Rand Research Memorandum RM-153, Aug. 1955.
- 15 Greene, E. F., Taylor, R. L. and Patterson, W. L., Jr., "Pyrolysis of Simple Hydrocarbons in Shock Waves," *J. Physical Chemistry*, vol. 62, 1958, p. 238.
- 16 Griffith, W. C., "Recent Advances in Real Gas Effects in

⁵ L. Lees (private communication).

⁶ For typical examples of these studies see (9, 12, 32, 34, 35, 48, 51).

Hypersonic Flow," *JET PROPULSION*, March 1958, pp. 157-159.
 17 Hindmarsh, W. R., "Radiation from Gases," A.E.R.E. GP/2028, Atomic Energy Research Establishment, 1956.

18 Hooker, W., Lapp, M., Weber, D. and Penner, S. S., "Multiple-Path Technique for the Determination of Physico-Chemical Data Behind Shock Fronts," *J. Chemical Physics*, vol. 25, 1956, p. 1087.

19 Jarman, W. R., Fraser, P. A. and Nicholls, R. W., *Astrophysical J.*, vol. 118, 1953, p. 228; Jarman, W. R. and Nicholls, R. W., *Canadian J. Physics*, vol. 32, 1954, p. 201; Turner, R. G. and Nicholls, R. W., *Canadian J. Physics*, vol. 32, 1954, p. 468; Fraser, P. A., *Canadian J. Physics*, vol. 32, 1954, p. 515; Nicholls, R. W., *Canadian J. Physics*, vol. 32, 1954, p. 722.

20 Josephson, V., "Production of High-Velocity Shocks," *J. Applied Physics*, vol. 29, Jan. 1958, pp. 30-32.

21 Keck, J., Kivel, B. and Wentink, T., "Emissivity of High Temperature Air," Avco Research Laboratory, Research Report 8, Everett, Mass., April 1957.

22 Kivel, B., Mayer, H. and Bethe, H., "Radiation from Hot Air. Part I. Theory of Nitric Oxide Absorption," *Annals of Physics*, vol. 2, July 1957, pp. 57-80.

23 Kivel, B. and Bailey, K., "Tables of Radiation from High Temperature Air," Avco Research Laboratory, Research Report 21, Everett, Mass., Dec. 1957.

24 Logan, J. G., Jr. and Treanor, C. E., "Tables of Thermodynamic Properties of Air from 3000°K to 10,000°K at Intervals of 100°K," Cornell Aeronautical Laboratory Report no. BE-1007-A-3, Jan. 1957.

25 Magee, J. L. and Hirschfelder, J. O., "Thermal Radiation Phenomena," Los Alamos Scientific Laboratory, LA-1020, chap. IV, pp. 8, 13, 47.

26 Marmo, F. F., "Absorption Coefficients of NO in the Vacuum Ultraviolet," *J. Optical Society of America*, vol. 47, 1953, pp. 1186-1190.

27 Meyerott, R. E., "Absorption Coefficient of Air from 2000°K to 18,000°K," Rand Corp., Santa Monica, Calif.

28 Meyerott, R. E., "Radiation Heat Transfer to Hypersonic Vehicles," Lockheed Missile Systems Division Report 2264, 1957.

29 Omori, T. T. and Powell, W. B., "Radiation of Rocket Motor Combustion Gases," *JET PROPULSION* Laboratory, Progress Report no. 20-166, Pasadena, Jan. 15, 1953.

30 Palmer, H. B., "Emission and Two-Body Recombination in Bromine," *J. Chemical Physics*, vol. 26, 1957, p. 648.

31 Pearce, W. J., "Argon Line Shifts in an Argon Stabilized Arc," Aerodynamics Laboratory Investigations, Missile and Ordnance Systems Department, General Electric, Dec. 31, 1957.

32 Pearce, W. J., "Measurement of Temperature of Arc Plasmas," Aerodynamics Laboratory Investigations, Missile and Ordnance Systems Department, General Electric, Technical Memorandum no. 28, June 30, 1958.

33 Penner, S. S., "The Emission of Radiation from Diatomic Gases. I. Approximate Calculations," *J. Applied Physics*, vol. 21, July 1950, pp. 685-695.

34 Penner, S. S., Harshbarger, F. and Vali, V., "An Introduction to the Use of the Shock Tube for the Determination of Physico-Chemical Parameters," Combustion Researches and Reviews, Butterworths Scientific Publications, London, 1957.

35 Penner, S. S. and Björnerud, "Experimental Determination of Rotational Temperatures and Concentrations of OH in

Flames from Emission Spectra," *J. Chemical Physics*, vol. 23, no. 1, Jan. 1955, p. 143.

36 Petschek, H., Rose, P. H., Glick, H. S., Kane, A., and Kantrowitz, A., "Spectroscopic Studies of Highly Ionized Argon Produced by Shock Waves," *J. Applied Physics*, vol. 26, Jan. 1955, pp. 83-95.

37 Rosa, R. J., "Shock Wave Spectroscopy," *Physical Review*, vol. 99, July 15, 1955, p. 633.

38 Rose, P. H., "Physical Gas Dynamics Research at the Avco Research Laboratory," Presented at the Eleventh Meeting of the Wind Tunnel and Model Testing Panel, Scheveningen, Holland, July 1957.

39 Roth, W. and Gloersen, P., "A Shock Tube Study of Luminosity in Xenon," Aerodynamics Laboratory Investigations, Missile and Ordnance Systems Department, General Electric, Memo Report P-155. (To be published in *J. Chemical Physics*.)

40 Russell, G. and Lamb, L., Space Technology Laboratories, to be published.

41 Russo, A. and Hertzberg, A., "A Method for Improving the Performance of Shock Tubes," *JET PROPULSION*, vol. 27, no. 11, Nov. 1957, pp. 1191-1195.

42 Schexnayder, C. J., Jr., "On the Performance of a Double-Diaphragm Shock Tube Using the Reflected-Shock Method and a Light-Gas Buffer," *J. Aero/Space Sciences*, vol. 25, no. 8, Aug. 1958, pp. 527-528.

43 Turner, E. B., "Radiation from a Strong Shock Front in Krypton," *Physical Review*, vol. 99, July 15, 1955, p. 633.

44 Turner, E. B., "The Production of Very High Temperatures in the Shock Tube with an Application to the Study of Spectral Line Broadening," AFOSR-TN-56-150, ASTIA Document no. AD-86309, May 1956.

45 Weber, D., "Approximate Intensity Estimates for Several Ultraviolet β -Bands of NO," California Institute of Technology, Report no. 23, March 1957; Weber, D. and Penner, S. S., Report no. 18, Pasadena, Calif., April 1956.

46 Wentink, T., Jr., Planet, W., Hammerling, P. and Kivel, B., "Infrared Continuum Radiation from High Temperature Air," *J. Applied Physics*, vol. 29, April 1958, pp. 742-743.

47 Windsor, M., Davidson, N. and Taylor, R., "A Study of Vibrational Relaxation in Carbon Monoxide by Shock-Waves and Infra-Red Emission," Presented at the Seventh Combustion Symposium, England, 1958.

48 Wolfe, H. C. (ed.), "Temperature—Its Measurement and Control in Science and Industry, vol. II," Reinhold Publishing Corp., New York, 1955.

49 Wurster, W. H., and Glick, H. S., "Ultraviolet Spectrum of Air at 5750°K," *J. Chemical Physics*, vol. 27, Nov. 1957, p. 1218.

50 Wurster, W. H., Glick, H. S. and Treanor, C. E., "Radiative Properties of High Temperature Air," Cornell Aeronautical Laboratory, Report no. CM-997-A-1, AF29(601)-176, Sept. 1957.

51 Yos, Jerrold, "Interpretation of Rotational Temperature Measurements," Avco Research Laboratory, Rad Technical Memo 2-TM-58-58, Everett, Mass., May 19, 1958.

52 Ziemer, R. W. and Bush, W. B., "Magnetic Field Effects on Bow Shock Stand-Off Distance," *Physical Review Letters*, vol. 1, no. 2, July 15, 1958, pp. 58-59.

The Ignition of Combustible Mixtures by Hot Gases¹

H. G. WOLFARD²

Bureau of Mines, U. S. Department of the Interior, Pittsburgh, Pa.

Fuel-air mixtures are ignited by a jet of hot gas which is heated in a ceramic furnace. The igniting gas is continuously injected into the cold explosive mixture. Lu-

minous reactions can be seen to occur in the center of the hot jet if its initial temperature approaches a critical temperature. On further raising the temperature of the

Received March 5, 1958.

¹ Sponsored in part by Project Squid, which is supported by the Office of Naval Research under Contract Nonr 1858(25), NR-

098-038. Reproduction in full or in part is permitted for any use of the U. S. Government.

² Research Scientist, Div. of Explosives Technology. Member A.R.S.

jet, the luminosity increases and a laminar luminous pencil extends up to 30 cm above the furnace exit. A flame can then be seen to originate from the top of this column and propagate into the cold mixture outside. Two types of experiments are performed: The ignition of cold fuel-air mixtures by hot neutral gases, such as nitrogen or carbon dioxide; and the ignition of cold fuel by hot air. In the second case only a diffusion flame can be ignited which, under favorable conditions, floats on top of the hot air jet. These "hot gas ignition temperatures" bear little relation to the "spontaneous ignition temperatures."

Introduction

THE ignition of combustible mixtures by hot burned gases from flames is of importance in many appliances, such as ramjet burners or rocket combustion chambers. In the ignition of methane-nitric oxide mixtures by pilot flames, it was found (1)² that the size and temperature of the pilot flame determined ignition. For small pilot flames (volume flow of the order of a few cc/sec), the parameter responsible for ignition was the energy flow of the flame (cal/sec), whereas for large flames, ignition became independent of flame size and was determined by a minimum temperature of the flame (the requirement being expressed in cal/cc). Intermediate pilot sizes had to be characterized by both energy and temperature statements for ignition of the surrounding mixture.

It was first proposed to extend this investigation by burning pilot flames in hydrocarbon-air mixtures. However, both extremely small and larger but highly dilute, i.e., cooler, pilot flames invariably led to ignition, and minimum conditions for ignition could not be investigated in an apparatus allowing only relatively small flow rates. It was necessary therefore to heat gases in a furnace, and then lead them into explosive mixtures. It is difficult to heat small gas flows in a furnace because of inevitable heat losses at the furnace exit. The present investigation deals, therefore, with the minimum condition of fuel-air ignition by relatively large flows of hot gas. The influence of velocity of the hot gas on ignition could not be investigated for reasons explained later. This investigation was limited to ignition by a steady stream of hot gas. Ignition by sudden bursts of hot gas is outside the scope of this paper.

Experimental Arrangement

The source of ignition was a steady flow of hot nitrogen, carbon dioxide, air, etc. The gas entered the furnace from below. After being heated, it flowed into the explosive mixture or pure fuel, which in turn flowed slowly through the outer vessel (Fig. 1) to avoid dilution by the jet of hot gas. This jet of hot gas was surprisingly coherent; for instance, a sheet of paper held 10 cm above the jet was punctured initially with a very small hole followed by ignition of the paper. The furnace consisted of an inner ceramic tube through which the gas flowed. This tube was surrounded by a spiral of platinum wire embedded in ceramic paste. A larger tube enclosed the inner tube and was sintered to the inner tube with the ceramic paste. Additional ceramic tubes around both these tubes served as insulation (Fig. 2). Gases could be heated to a maximum of 1400 C before the furnace was damaged due to melting of the ceramic and platinum wire in localized spots within the furnace.

The temperature of the gas jet was measured directly above the furnace outlet with a platinum-platinum rhodium thermocouple before and after each ignition experiment. The thermocouple wire was 0.005 in. thick; a small bead formed the junction (Fig. 2). Furnaces 1 and 3, which had an inner tube of 4 mm internal diameter, were suitable for heating flows of around 30 to 50 cc/sec. Flows above 100 cc/sec showed temperature profiles with layers close to the wall

² Numbers in parentheses indicate References at end of paper.

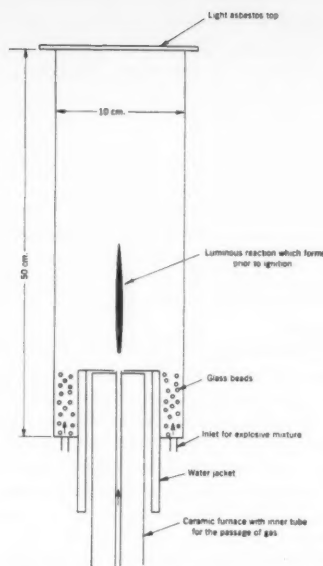


Fig. 1 Experimental arrangement

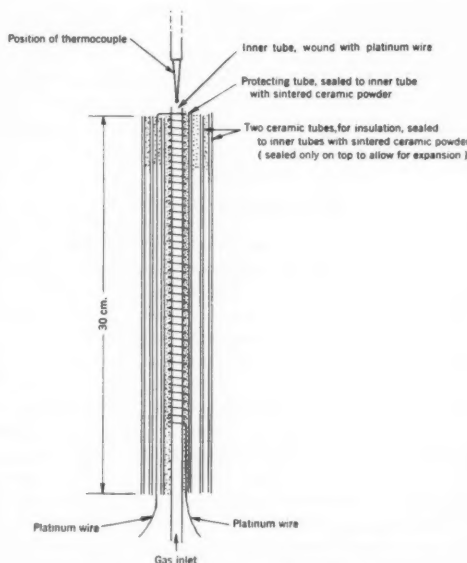


Fig. 2 The construction of the furnace

hotter than those at the center. Flows below 20 cc/sec were unsuitable; the layers close to the wall were much cooler than those at the center, due to the cooling of the last 5 mm of the inner tube which had no heating coil, since it protruded through the water jacket. Furnace 2 was suitable for slightly larger flows, since the inner tube was larger (7 mm diam).

To keep results comparable, flows of 35 cc/sec were always used (unless stated otherwise) for furnaces 1 and 3, and a flow of 60 cc/sec for furnace 2. Helium and hydrogen jets were difficult to work with, because heat dissipated very fast at the outlet of the furnace, and this could be overcome only by larger flows. In the initial stage of an experiment, the igniting gas flowed through the furnace, and steady furnace conditions had to be attained. At this stage, an inert gas, such as nitrogen or carbon dioxide, was used for the outer gas stream instead of the explosive mixture to be ignited.

The temperature at the center of the hot jet was measured directly above the inner tube. The thermocouple was then removed, and the explosive mixture was substituted for the inert atmosphere in the outer vessel. Ignition or nonignition was observed. The inert atmosphere was introduced again, and the temperature checked with the thermocouple. The outer explosive mixture to be ignited by the hot jet flowed at a steady rate, usually 100 to 300 cc/sec. No difference in minimum ignition temperatures could be observed between these flow limits. The outer explosive mixture was kept as close as possible to room temperature. However, as the cooling water in the furnace jacket usually was at a slightly higher temperature, the gas may have been closer to 40 C than to room temperature.

Ignition temperatures with a hot nichrome wire were measured for comparison with the hot gas ignition temperatures. A 40/1000-in. wire 9 cm long was suspended horizontally in a tube 9 cm in diameter and 50 cm in length. The explosive mixture flowed past the wire at a rate of about 200 cc/sec, corresponding to a flow velocity around 3 cm/sec. Our purpose was not to make a detailed study of ignition by hot wires, but to obtain ignition temperatures for a variety of fuels under comparable conditions. The temperature of the wire was measured with a pyrometer and reported directly as measured, i.e., the black body temperature of the wire at 6500 AE. No correction for emissivity was applied, because the wire acquired an oxide coating following some preliminary experiments, making the emissivity of the surface doubtful. The wire was heated by slowly increasing the electrical current, following the temperature rise of the wire with the pyrometer. The ignition temperature was defined as the temperature immediately prior to ignition, detected by the sound. All gases used were taken from cylinders (Matheson Co.). Carbon monoxide was of commercial grade.

Accuracy of Results

The gas ignition temperatures were reproducible within ± 10 C, for example when checking the value for ethane following measurements with propane or a similar hydrocarbon. The ignition temperatures, however, were not the same for different furnaces and depended on the history of each furnace. Because of the heat losses of the hot gas jet in the exit of the furnace, the temperature across the jet was not a constant, and the resulting profile depended on the conductivity of the sintered material on the furnace top. After prolonged use, the furnace usually developed cracks in this sintered material, leading to smaller heat losses and an improved temperature profile, which in turn led to a lowering in ignition temperatures. After aging, all furnaces built during this investigation gave ignition temperatures agreeing to within ± 20 C. A new furnace, however, initially gave values up to 150 C too high. Intentional aging would have been beneficial, but it was difficult to predict at which temperatures aging or total destruction of the furnace would have occurred.

Accordingly results are reported with the following limitations: Furnaces 1 and 2 were aged before the measurements recorded in Tables 2, 3, and 4 were made, and ignition temperatures were reproducible throughout. Furnace 3 was new when used for the recorded data, but aging occurred during the experiments (see remarks in Tables 2 and 4).

The temperatures recorded were measured directly with the thermocouple and potentiometer. It is believed that heat losses of the thermocouple due to conductivity are very small as a great length of wire was immersed in the hot gas jet. No radiation corrections were applied, since they are uncertain and may falsify the results. As a guide, the corrections in Table 1 are believed to be approximately valid for an air or nitrogen jet of 35 cc/sec, from a 4 mm diameter tube.

Ignition temperatures with the hot wire were reproducible to within ± 10 C or better. Difficulties were encountered only with very rich ethylene mixtures, rich acetylene mixtures

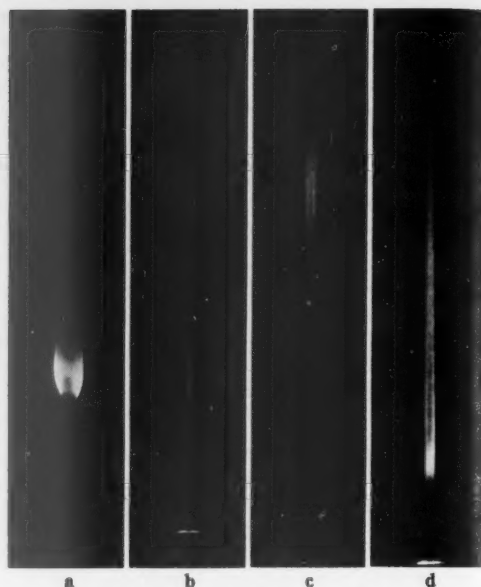


Fig. 3 (a) Flame developing with a 35 cc/sec hot air jet in ethane. (b) Luminosity within hot argon jet in stoichiometric ethane-air mixture. (c) Luminosity within hot argon jet in a very rich ethane-air mixture. (d) Luminosity within hot argon jet in a very lean ethane-air mixture

Table 1 Corrections for thermocouple, deg C

Temperature as measured	Correction
500	5
700	15
900	30
1100	60
1300	100

and all hydrogen mixtures except those near the lean limit. In these cases, catalytic surface reactions contributed to the wire heating. No results are reported for these mixtures.

Results

The process of hot gas ignition will be described first. Two types of ignition flames must be distinguished: 1 Flames which develop when a jet of hot air flows into cold fuel, and 2 flames which develop when hot air or hot inert gas flows into a cold explosive mixture.

1 A jet of hot air at slightly below ignition temperature introduced into a cold fuel, such as ethane, leaves little visible trace of reaction. When the air temperature is raised, a small flame suddenly appears floating about 5 cm above the furnace tube. This flame has a bluish base topped by a bright green section (Fig. 3a). When the temperature of the jet is reduced, this flame disappears. When the temperature of the air jet is increased above the minimum ignition temperature, this flame may become self-propagating and may flash back onto the furnace tube forming a diffusion flame with abundant carbon formation. Reduction of the air temperature no longer extinguishes this flame. For the 7 mm jet, this flame has a greater tendency to flash back and sit on the furnace tube, whereas smaller jets (4 and 2 mm diam) give rise to floating flames which give the impression of stationary self-ignition flames.

2 An inert gas, such as nitrogen, flowing into a cold explosive mixture gives rise to a luminous column where slow reactions take place at temperatures below the minimum ignition temperature (Fig. 3b). Increasing the temperature of the jet makes the column longer and brighter. Finally, the column branches out at some point up to 30 cm above the furnace tube, and a flame propagates throughout the vessel. A report and the blowing off of the lid are further evidence of ignition. Ignition can also be approached by making the outside mixture too rich and slowly reducing the fuel content. The luminous column is quite bright, with a purple color for the first 10 cm of the jet, followed by a bright green region. As before, ignition occurs from the top of the column. Figs. 3c and 3d show luminous columns with a jet temperature high enough to ignite stoichiometric mixtures, the actual mixture being either just too lean or too rich for ignition.

Table 2 shows ignition temperatures for hot air jets flowing into pure cold fuel. In all instances, small flames are formed which float between 2 and 5 cm above the furnace exit. In some instances, this flame may subsequently flash back to form a full diffusion flame.

Table 2 Ignition temperatures in deg C for a hot air jet into cold fuel

Fuel	Furnace 1 (aged) Jet diam 4 mm 35 cc/sec air	Furnace 2 (aged) Jet diam 7 mm 60 cc/sec air	Furnace 3 (new) Jet diam 4 mm 35 cc/sec air
methane	1180	1135	1180 ^a
ethane	920	905	990 ^b
propane	980	960	1070
n-butane	960	...	1075
ethylene	840	840	890 ^c
propylene	1040	1020	1085
iso-butylene	1030	...	1110
carbon monoxide	745	760	765
hydrogen	655	670	665 ^a
acetylene	700	...	700 ^a

^a Furnace aged

^b 920 C after aging

^c 845 C after aging

Furnaces 1 and 2 were used at high temperatures for preliminary experiments, and therefore were aged, giving lower values than furnace 3, which was used directly for final measurements. The hydrogen and acetylene experiments in furnace 3 were run following an experiment (referred to in Table 4) in which the jet temperature was raised to 1300 C, with subsequent aging. The methane experiments were last in each set.

In one experiment, 35 cc/sec oxygen was substituted for air in furnace 1. This reduced the ignition temperature of propane from 980 to 960 C. With hydrogen and carbon monoxide, it is possible to reverse the ignition experiment and cause ignition in air with a jet of hot fuel. Table 3 shows the results.

Table 3 Ignition temperatures in deg C for air into fuel and fuel into air with furnace 1

Hot jet	Cold medium	Ignition temp.
air	H ₂	655
H ₂	air	820
air	CO	745
CO	air	860

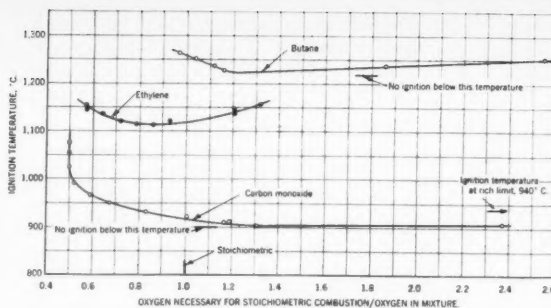


Fig. 4 Change of hot gas ignition temperature with mixture strength

Table 4 gives ignition temperatures of fuel-air mixtures ignited by a jet of hot nitrogen. The temperatures recorded correspond to the mixture compositions which gave the lowest ignition temperatures.

Table 4 Ignition temperatures in deg C for a jet of hot nitrogen into fuel-air mixtures

Fuel in fuel-air mixture	Furnace 2 (aged) N ₂ jet, 60 cc/sec	Furnace 3 (new) N ₂ jet, 35 cc/sec
methane	>>1200	Close to 1425 (aged)
ethane	1015	1110 (1050 after aging)
propane	1110	1200
n-butane	1095	1220
ethylene	985	1110
propylene	1150	1305
iso-butylene	1155	1295
carbon monoxide	795	905
hydrogen	<755	not tested
acetylene	not tested	not tested

Methane-air mixtures could not be ignited. At 1425 C (furnace 3) a strong luminous column formed in the hot jet, indicating that the ignition temperature was near, but further raising of the temperature made the furnace break. Furnace 2 broke above 1200 C when trying to ignite methane-air. Hydrogen-air mixtures gave a violent explosion when ignited with a jet of nitrogen at 755 C, so the accurate ignition temperature could not be measured. Acetylene was not tested for the same reason.

An attempt was made to measure not only the lowest temperature at which a 35 cc/sec hot nitrogen jet ignites the most favorable fuel-air mixture, but also the ignition temperatures over the whole range of mixture compositions. Fig. 4 gives ignition temperature (furnace 3) vs. mixture composition curves for butane, ethylene and carbon monoxide. The curves are quite flat, i.e., ignition temperature does not change much with mixture composition, making it difficult to locate the minimum accurately. Hydrocarbons seems to ignite slightly better when the fuel is rich, with the exception of ethylene for which the minimum is on the lean side. With propylene the minimum corresponds to a stoichiometric mixture, whereas with butylene the minimum is again on the fuel-rich side. Carbon monoxide ignites much more readily when the fuel is rich.

The ignition of fuel-air mixtures by hot air, instead of nitrogen, also has been investigated. (See Fig. 5.) For pure fuel the values are identical to those in Table 2 (furnace 3). The addition of air even in rather large amounts affects the ignition temperature very little. The resulting flame obtained is

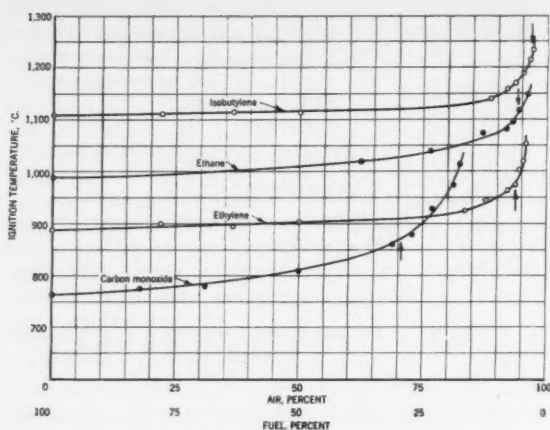


Fig. 5 Ignition of fuel-air mixtures by hot air (35 cc/sec). Arrow marks stoichiometric point

simply a suspended diffusion flame. As the mixture composition approaches the rich limit, the ignition temperature begins to rise and continues steadily upward toward the lean limit. Within the explosive range, a flame moves through the whole vessel after ignition, instead of remaining suspended. Table 5 summarizes the ignition of stoichiometric fuel-air mixtures by a 35 cc/sec jet of hot air.

Table 5 Ignition of a stoichiometric fuel-air mixture by hot air (35 cc/sec) furnace 3 (new)

Fuel	Ignition temp., deg C
methane	not tested
ethane	1120
propane	1160
n-butane	1170
ethylene	980
propylene	1200
iso-butylene	1215
carbon monoxide	870

The influence of the nature of the hot gas on ignition has been further investigated by substituting carbon dioxide, argon or helium for nitrogen or air as the igniting gas. Table 6 gives details for ethylene-, ethane- and carbon monoxide-air mixtures ignited by hot nitrogen, argon, helium or carbon dioxide jets.

Table 6 Ignition temperature of most favorable mixture by inert hot jets, deg C (35 cc/sec) furnace 3

Fuel	Nitrogen	Argon	Helium	Carbon dioxide
ethane	1100	1175	1290	1100
ethylene	1110	1165	1265	1075
carbon monoxide	900	925	1000	870

The foregoing values are the result of separate experiments, and the values for nitrogen are not identical, although close, to those reported in Table 4. The flow of helium was adjusted to 100 cc/sec for the ethane and ethylene experiments, and to 60 cc/sec for the carbon monoxide test, because the end effects of the furnace influenced the helium temperature too much with a flow of 35 cc/sec. The furnace tended to over-heat for low helium flows. Carbon dioxide seemed to be as effective as nitrogen for ignition. Argon required slightly higher temperatures, but helium did not ignite well at all.

The oxygen index of the explosive mixtures has little influence on the ignition temperature. An increase of the oxygen index from 0.21 to 0.25 in an ethylene-air mixture ignited by hot nitrogen reduced the ignition temperature by less than 20 C. Higher oxygen indexes could not be considered, because the explosion became too violent.

The results of the wire ignition experiments are summarized in Fig. 6. The ignition temperatures are not very sensitive to mixture composition. With the exception of carbon monoxide, all ignition temperatures are lower for lean flames. However, the slope is more pronounced for methane, propylene, butane and butylene than for the other gases. Hydrogen and acetylene could only be measured satisfactorily on the very lean side for reasons already explained. The oxygen index was altered for an ethane-"air" mixture. The ignition temperature is affected very little by this change (see Fig. 7).

Discussion

Little information is available in the literature on the ignition of explosive mixtures by hot gases. Wright and Becker (2) appear to have been the only investigators to attempt this problem. They heated air or nitrogen on quite a large scale with a heat exchanger and circulated fuel-air mixtures around the hot jet. They were able to heat the inner jet to just above 1000 C. This was only sufficient to ignite an outer acetylene-air mixture, which required an inner jet temperature of 752 C. Propane could be ignited only when the outside mixture also was heated. Thus hardly any data are available for comparing Wright and Becker's work and the work reported here. Their value for acetylene is slightly higher than our value for hot air into pure acetylene, but they do

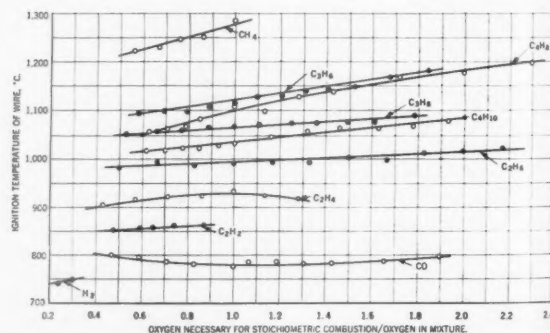


Fig. 6 Ignition of fuel-air mixtures by a 0.04-in. nichrome wire

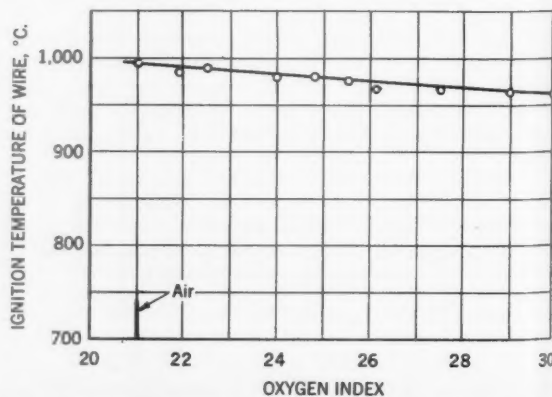


Fig. 7 Ignition of C_2H_6 -"air" mixture by hot nichrome wire. Effect of oxygen index

Table 7

Fuel	Gas ignition temp. ^b deg C	Spontaneous ignition temp. with air deg C	Minimum ignition energy ^a	
			Stoichiometric mixture with air	Optimum mixture with air
methane	1180	537	0.34	0.28×10^{-2} joules
ethane	920	472	0.31	0.25
propane	980	493	0.40	0.25
n-butane	960	408	0.70	0.25
ethylene	840	490	0.11 ^c	...
propylene	1040	458	0.41 ^c	...
iso-butylene	1030	443
carbon monoxide	745	609
hydrogen	655	572	0.02	0.02
acetylene	700	305	0.03 ^c	...

^a Interpolated from Figs. 185, 187 in (4)^b From Table 2^c From Calcote in (5) (Flange electrode)

not say whether this value is for hot nitrogen or hot air. Moreover, their mass flows were very large compared to ours. However, Wright and Becker were the first to note that a luminous reaction precedes the spreading of the flame. They call this reaction an "initial flame." We doubt whether, at least in our case, this is a flame, as it does not have such flame characteristics as self-propagation. Accordingly, we prefer to call it a luminous column.

It is tempting to compare ignition temperatures as measured here with other flame characteristics, such as spontaneous ignition temperatures (as measured in furnaces), minimum spark ignition energies, etc. The values found in the literature on spontaneous ignition temperatures vary widely; the values recommended by Scott et al (3) are recorded in the second column of Table 7. They are compared to the lowest values obtained for ignition by hot gas, i.e., when hot air is injected into pure fuel. It is clear that little or no correlation exists. For hydrocarbons the hot gas ignition temperature is very roughly double the spontaneous ignition temperatures, when expressed in deg C, whereas that for hydrogen or carbon monoxide is only slightly higher. Even within a series of hydrocarbons, there is no correlation. Table 4 shows that this also holds for ignition with hot nitrogen.

Table 7 also gives minimum ignition energies as reported in (4). If there is a correlation between hot gas ignition and minimum spark ignition energy, one would expect the relation to be with the energy for the most favorable mixture. However, paraffin hydrocarbons show very little change. A certain correlation does appear to exist for the values taken at stoichiometric ratio, especially as hydrogen and acetylene have very low minimum ignition energies. If carbon monoxide also had low ignition energies this would be an important proof. However, this is very unlikely, and no measurements could be found in the literature. Any anticipated correlation breaks down, if we consider that an increase in oxygen index has very little influence on the hot gas ignition temperature, whereas it affects the minimum ignition energy greatly (see (4)).

It is because of this lack of correlation that the hot wire experiments were performed. A comparison between Fig. 6 and either Table 2 or Table 4 shows that the correlation is nearly perfect. This holds also for the values obtained with a different oxygen index, as in both instances little change is indicated. This close correlation suggests that an important characteristic of flame ignition has been found.

Correlation with lean limit temperatures leads to some agreement as hydrogen, carbon monoxide and acetylene have a low lean limit temperature compared with paraffin hydrocarbons. (For values see Egerton (6).) However, methane

does not fit into the order, since its limit temperature is much the same as that of other hydrocarbons. It is also known that the oxygen index has little effect on the lean limit.

The ignition process itself will now be considered in more detail. It is important to note that when hot nitrogen is injected into a fuel-air mixture, a luminous reaction occurs in the core of the hot jet. The hot jet gradually loses heat to the surrounding gas, but at the same time mass transfer takes place, i.e., nitrogen flows radially from the jet and is replaced by an explosive mixture. This explosive mixture will react if the residual temperature of the jet is high enough. If the heat produced along the jet is less than that lost by conduction, the reaction dies out, and there is no ignition. If the initial jet temperature is increased, the luminous column becomes longer, and a propagating flame originates at the center of the jet. Theoretical calculations for a two-dimensional model (hot gas in contact with cool explosive mixture) have predicted this behavior (Marble (7), Cheng (8), Spalding (9)). Wright and Becker were able to observe it in their high-speed ignition arrangement. It has now been shown to be applicable in a wide variety of experiments.

Therefore, ignition is dependent on the reaction rate at a given temperature level in the core of the jet. The ignition temperatures in Table 4 measure the relative reaction rates of the fuel-air mixtures. However, the reaction rate is not the only factor influencing ignition. If it were, a jet of hot air into cold hydrogen would have the same ignition temperature as hot hydrogen into cold air. In fact, the temperatures differ by 165 C. Mass transfer must be considered. More air must diffuse into hydrogen to form a reaction mixture than hydrogen into air, for reasons of stoichiometry. More information as to the importance of diffusivity and the specific heat of the jet is available from the experiments with hot argon, helium and carbon dioxide. Carbon dioxide is not essentially better than nitrogen, and the heat content or energy of the jet does not seem to be of great importance. The ignition temperature of argon is only slightly higher than that of nitrogen. However, the high diffusivity of helium is clearly responsible for the large increase in ignition temperature as compared to argon. The higher jet velocity which had to be used with the helium jet is not responsible for the increase in ignition temperature, since the influence of jet velocity on ignition temperature is small for laminar jets. This subject will be considered in a separate paper.

That the oxygen index is of little importance is also understandable, since temperature controls the reaction rate to a greater degree than does concentration, and dilution with nitrogen decreases the ignition temperature only slightly.

It has been known for some time that gas ignition by hot

wires occurs in the wake of the wire, at least as long as the wire does not give rise to catalytic effects. This ignition also will be determined by whether the reaction rate is greater than the heat loss by conductivity. The close similarity between hot wire ignition and hot gas ignition becomes understandable. More difficult is the question of why hot wire ignition is so insensitive to mixture concentration, whereas hot gas ignition shows a minimum. A definitive answer cannot be given at the moment. It can only be pointed out that, whereas hot gas ignition depends on a reaction rate in a given volume, hot wire ignition can expand the useful volume of reacting gases along the wire axis.

Although diffusivity as well as reaction rate determines ignition for hot gas and hot wire ignition, it is rather surprising that so little similarity exists between those modes of ignition and spontaneous gas ignition. Hot gas and hot wire ignition require higher temperatures than does spontaneous ignition. As different fuels have very different activation energies, a rise in temperatures entirely reverses the reaction rates, i.e., carbon monoxide seems to have a higher reaction rate than propylene at 800 C, whereas at lower temperatures the reverse is true.

More information is needed to establish the influence of jet diameter and jet velocity. In this investigation, the diameter was varied from 2 to 7 mm, and ignition temperature showed little change. The results with the 2 mm diameter were not reported here, as they were less accurate due to the difficulty of measuring temperatures in such a limited space. Much larger diameters must be used in the future to investigate this effect. The velocity of the hot jet could not be altered significantly in our experiments because of the change of the

temperature profile of the hot jet. Investigation of the diameter and velocity effect in the future is hoped for.

I wish to thank Mr. A. E. Bruszak for conducting part of the ignition experiments.

References

- 1 Wolfhard, H. G. and Burgess, D. S., "The Ignition of Combustible Gases by Flames," *Combustion and Flame*, vol. 2, 1958, pp. 3-12.
- 2 Wright, F. H. and Becker, T. L., "Combustion in the Mixing Zone Between Two Parallel Streams," *JET PROPULSION*, vol. 26, 1956, pp. 973-978.
- 3 Scott, G. S., Jones, G. W., and Scott, F. E., "Determination of Ignition Temperatures of Combustible Liquids and Gases," *Analytical Chemistry*, vol. 20, 1948, pp. 238-241.
- 4 Lewis, B. and von Elbe, G., "Combustion, Flames and Explosions of Gases," Academic Press, New York, 1951.
- 5 Calcote, H. F., Gregory, C. A., Jr., Barnett, C. M. and Gilmer, R. B., "Spark Ignition," *Indust. Engrg. Chem.*, vol. 44, 1952, pp. 2656-2662.
- 6 Egerton, A. C., "Limits of Inflammability," Fourth Symposium (International) on Combustion, Williams & Wilkins Co., Baltimore, 1953, pp. 4-13.
- 7 Marble, F. E. and Adamson, T. C., Jr., "Ignition and Combustion in a Laminar Mixing Zone," "Selected Combustion Problems," AGARD, Butterworths Scientific Publications, London, 1954, pp. 111-131.
- 8 Cheng, S. I. and Kovitz, A. A., "Ignition in the Laminar Wake of a Flat Plate," Sixth Symposium (International) on Combustion, Reinhold Publishing Corp., New York, 1957, pp. 418-427.
- 9 Spalding, D. B., "Some Fundamentals of Combustion," Butterworths Scientific Publications, London, 1955.

Digital Computer Analysis of Transients in Liquid Rocket Engines

P. KLUGER¹ and E. C. FARREL²

Aerojet-General Corp., Sacramento, Calif.

A digital computer program for engine transient study has been developed to obtain an evaluation of pressure surges in the propellant system during startup and shutdown. This technique is intended to supplement and eventually replace analog computer start and shutdown transient analysis which does not provide realistic simulation of propellant lines and combustion dead times. The mathematical model used for propellant line representation was based on the water-hammer theory as originally developed by Allievi, i.e., hydraulic oscillations appear as pressure surges caused by the conversion of kinetic to potential energy, where the kinetic energy changes are a result of system impedance changes taking place during engine start or shutdown. Line equations and component transfer functions have been programmed in a general manner, allowing routine parameter changes to be executed without the need of major reprogramming. The analysis determined the values of instantaneous propellant flow and transient pressures at points of interest in the system for successive time intervals.

Received Oct. 17, 1957.

¹ Design Engineer, Systems and Controls Department, Liquid Rocket Plant. Member ARS.

² Design Engineer, Systems and Controls Department, Liquid Rocket Plant.

Nomenclature

A	= area, ft ²
b	= pipe wall thickness, ft
c	= velocity of sound, ft/sec
c^*	= characteristic velocity, ft/sec
c_v	= specific heat at constant volume, Btu/lb/F
c_p	= specific heat at constant pressure, Btu/lb/F
C_1	= constant
D	= pipe diameter, ft
E	= pipe modulus of elasticity, lb/ft ²
e	= water-hammer slope, lb-sec/ft ³
e'	= modified water-hammer slope, sec/ft ²
F	= function denoting a pressure wave
f	= function denoting a pressure wave
g	= acceleration of gravity, ft/sec ²
h	= film coefficient of heat transfer, Btu/sec F ft ²
h_f	= heat of vaporization, Btu/lb
I	= moment of inertia, ft-lb-sec ²
K, K'	= constants or bulk modulus, (min/rev) ² , lb/ft ²
k	= thermal conductivity, Btu/sec F ft
L	= length, ft
M	= molecular weight, lb/mol
\bar{n}	= interaction index
Nu	= Nusselt number
p	= pressure, lb/ft ²
Pr	= Prandtl number
Q	= volume flow, ft ³ /sec

diam-
art of
Com-
1958,
a the
ston,
ation
ses,"
Ex-
and
44,
Sym-
Co.,
Com-
Prob-
don,
inar
on
pp.
on,"
ON

- q = heat flow, Btu/sec
- R = gas constant, ft/R
- R' = resistance coefficient, $\text{sec}^2/\text{ft}^2\text{-lb}$
- Re = Reynolds number
- r = gear ratio
- T = temperature, R
- T_L = turbine power transmission losses
- t = time, sec
- V = volume, ft^3
- v = fluid velocity, ft/sec
- W = weight, lb
- \dot{W} = flow rate, lb/sec
- X = LOX quality
- γ = density, lb/ ft^3
- Δ = difference
- η = efficiency
- θ = pump or turbine speed, rpm
- μ = torque, ft/lb
- ν = kinematic viscosity, ft^2/sec
- λ = valve or injector admittance, $\text{lb-ft}^2/\text{sec}^2$
- τ = combustion time lag, sec
- ψ = pump constant, $\text{sec}^2\text{-ft/lb}$
- ω = angular velocity, radians/sec

Subscripts

- b = burned propellants
- c = thrust chamber
- d = pump discharge
- F = flow
- f = fuel or filled condition
- g = gas
- H = heating
- i = inlet
- j = injector
- l = line
- L = liquid
- m = metal
- n = efficiency
- o = oxidizer
- p = pump
- s = pump suction
- T = turbine
- t = time or thrust chamber throat
- tp = turbopump
- V = valve

Introduction

A METHOD was developed to analyze transients in liquid rocket engines by means of a high-speed digital computer. The basic mathematical model was developed and its physical counterpart is shown schematically. An example illustrates the use of the method on a pressure fed system, and the results are compared with test data.

Object of Transient Analysis

The reproducibility of desired starting and shutdown transients is one of the most important factors in designing a rocket engine with a specified performance. Almost all malfunctions and performance shortcomings result from an unexpected development during the starting transient. Conversely though, not all unusual transients will result in component failures. Therefore, an understanding of the mechanism of transient phenomena is required to predict system tolerances and their effect on the prescribed performance. The analysis relates pressure and flow oscillations in the propellant lines to transient phenomena during starting and shutdown.

Mathematical Model

The physical system analyzed is shown in Fig. 1. The following is the breakdown required for mathematical representation of the main components:

The mathematical model for the propellant lines was based on water-hammer theory as originally developed by Allievi,

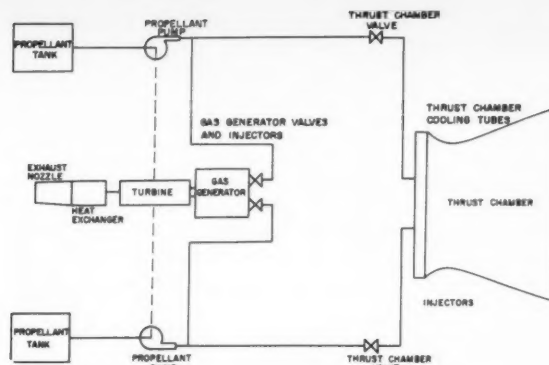


Fig. 1 Basic rocket engine schematic used for digital computer representation

i.e., hydraulic oscillations appear as static pressure surges caused by the conversion of kinetic to potential energy.

From (1)³ the conjugate water-hammer equations are given by

$$\begin{aligned} p_{x,t} - p_{x,t+\Delta t} &= e(v_{x,t} - v_{x,t+\Delta t}) \\ p_{x,t} - p_{x,t-\Delta t} &= -e(v_{x,t} - v_{x,t-\Delta t}) \end{aligned} \quad [1]$$

where $e = c\gamma/g$.

Equation [1] assumes frictionless flow. To account for frictional pressure drop, two assumptions were made:

1 Frictional drop is proportional to the square of the line flow.

2 Friction may be lumped at the end of each pipe section. The form of Equation [1] as used for digital programming will be shown later.

The characteristics of the mixed flow centrifugal propellant pumps are given by

$$p_d - p_s = K_\theta \theta_p^2 - \psi_1 v_p |v_p| \quad [2]$$

The values of K_θ and ψ_1 are determined by solving the equation at two values of $p_d - p_s$ and v_p for the same θ , where $p_d - p_s$ and v_p are taken from the head capacity curves of the pump. Other type pumps can be represented by modifying the right hand side of Equation [2]. The pump efficiency is represented by the equation

$$\eta_p = \frac{Q_p}{\theta_p} \left(K_n - K_n' \frac{Q_p}{\theta_p} \right) \quad [3]$$

The values of K_n and K_n' are determined in the same manner as K_θ and ψ_1 where Q_p and η_p are taken from the pump efficiency curves. The pump torque for a single pump is given by

$$\mu_p = \frac{Q_p}{\eta_p h \theta_p} (p_d - p_s) \quad [4]$$

where $h = 2\pi/60$, conversion factor from rpm to radians/sec.

In the above equations, Q_p and v_p are related by $Q_p = A_p v_p$ where A_p is the pump inlet area.

Substituting [2 and 3] into [4]

$$\mu_p = \frac{K_\theta \theta_p^2 - \psi_1 v_p |v_p|}{h \left(K_n - K_n' \frac{Q_p}{\theta_p} \right)} \quad [5]$$

Equations [2, 3, 4 and 5] apply for either the fuel or the

³ Numbers in parentheses indicate References at end of paper.

oxidizer pump. Total torque required by the two pumps is given by μ_T where

$$\mu_T = [r_f \mu_{pf} + r_o \mu_{po}] T_L \dots [6]$$

where T_L = transmission losses, $\theta/\theta_f = r_f$ and $\theta/\theta_o = r_o$ represent the gear ratios of the fuel and oxidizer pumps, respectively.

The accelerating torque

$$\mu_T = -I \tau_p \frac{d\omega}{dt} \dots [7]$$

For a short time interval, the torque can be written approximately as

$$\frac{1}{2} [\mu_T(t-\Delta t) + \mu_T t] = -\frac{I \tau_p}{\Delta t} [\omega_t - \omega(t-\Delta t)] = \frac{\pi I \tau_p}{30 \Delta t} [\theta(t-\Delta t) - \theta_t] \dots [8]$$

Substituting [6] into Equation [7]

$$\frac{1}{2} T_L [(\mu_{pf} r_f + \mu_{po} r_o)(t-\Delta t) + (\mu_{pf} r_f + \mu_{po} r_o)_t] = \frac{\pi I \tau_p}{30 \Delta t} [\theta(t-\Delta t) - \theta_t] \dots [9]$$

$$\frac{1}{2h} \left\{ \left[\frac{K_{\theta f} \frac{\theta^2}{r_f} - \psi_{1f} v_{pf} |v_{pf}|}{K_{nf} - K'_{nf} \frac{Q_{pf}}{\theta} r_f} + \frac{K_{\theta o} \frac{\theta^2}{r_o} - \psi_{1o} v_{po} |v_{po}|}{K_{no} - K'_{no} \frac{Q_{po}}{\theta} r_o} \right]_{(t-\Delta t)} + \left[\frac{K_{\theta f} \frac{\theta^2}{r_f} - \psi_{1f} v_{pf} |v_{pf}|}{K_{nf} - K'_{nf} \frac{Q_{pf}}{\theta} r_f} + \frac{K_{\theta o} \frac{\theta^2}{r_o} - \psi_{1o} v_{po} |v_{po}|}{K_{no} - K'_{no} \frac{Q_{po}}{\theta} r_o} \right]_t \right\} = \frac{\pi I \tau_p}{30 \Delta t} [\theta(t-\Delta t) - \theta_t] \dots [10]$$

Equation [10] holds while the pump is operating as a pump. When the flow reverses, ψ_1 is replaced by ψ_2 which is estimated to be $3\psi_1$. The range of transient behavior considered includes positive shaft speed, positive head and positive and negative fluid flow.

The pump heads taken from the head capacity curves include the difference between the velocity heads at the discharge and suction points. Since the desired pressures are static pressures, an allowance must be made for the velocity head by subtracting the differences between the rated system pump head and the calculated rated pump head.

The valve equation used for either propellant line is given by

$$\dot{w}_{vi}^2 = \lambda_{vi}^2 (p_{1i} - p_{2i}) \dots [11]$$

λ_{vi} is the valve admittance factor and is usually available as a function of valve opening.

The condition of the oxidizer (liquid oxygen) in the tank and feed lines is at, or slightly above, the saturation temperature at atmospheric pressure (normal boiling point). When the LOX valve is opened, liquid flows through the valve into the injector manifold. Since the injector is at ambient temperature, the LOX will absorb heat from the injector and vaporize. The quality of the oxygen and the weight flow rate of the liquid into the combustion chamber had to be determined as a function of time from initial valve opening.

Since the liquid is at its saturation temperature, all the heat will be used to vaporize a portion of the liquid. The heat transferred will be primarily by convection.

$$q/A_H = h(T_m - T_o) \dots [12]$$

The forced convection heat transfer equation is

$$Nu = 0.023 (Re)^{0.8} (Pr)^{0.3} \dots [13]$$

or

$$\frac{hD}{k} = 0.023 \left(\frac{VD}{\nu} \right)^{0.8} (Pr)^{0.3} \dots [14]$$

From continuity equation $\gamma v = (w_o/A_F)$

$$h = 0.023 \frac{k}{D} \dot{w}_o^{0.8} \left(\frac{D}{\rho \nu A_F} \right)^{0.3} (Pr)^{0.3} \dots [15]$$

or

$$h = C_1 \dot{w}_o^{0.8}$$

where

$$C_1 = 0.023 \frac{k}{D} \left(\frac{D}{\rho \nu A_F} \right)^{0.8} (Pr)^{0.3} \dots [16]$$

Substituting in [12] and rearranging

$$q = A_H C_1 \dot{w}_o^{0.8} (T_m - T_o) \dots [17]$$

The heat transferred into the liquid must come from heat capacity of the metal, hence

$$C_1 A_H \dot{w}_o^{0.8} (T_m - T_o) = C_{pm} W_m \frac{dT_m}{dt} \dots [18]$$

Solution of this differential equation yields

$$T_{m,t} = T_o + (T_{m,t=0} - T_o) e^{-B \int_0^t \dot{w}_o^{0.8} dt} \dots [19]$$

where

$$B = \frac{C_1 A_H}{C_{pm} W_m}$$

Continuity requires that

$$\dot{w}_o = \dot{w}_{lo} + \dot{w}_{go} \dots [20]$$

where l and g denote liquid and gaseous conditions.

The quality of LOX, X , is defined as the fraction by mass of liquid in the mixture

$$\dot{w}_{lo} = X \dot{w}_o \dots [21]$$

In Equation [17] q is also equal to $h_f \dot{w}_{go}$, where h_f is the heat of vaporization of oxygen

$$h_f \dot{w}_{go} = A_H C_1 \dot{w}_o^{0.8} (T_m - T_o)$$

and

$$h_f (\dot{w}_o - \dot{w}_{ol}) = h_f (\dot{w}_o - X \dot{w}_o) = A_H C_1 \dot{w}_o^{0.8} (T_m - T_o)$$

$$X = 1 - \frac{A_H}{h_f} C_1 \dot{w}_o^{-0.2} (T_m - T_o) \dots [22]$$

and substituting from Equation [19]

$$X = 1 - \frac{A_H}{h_f} (T_{m,t=0} - T_o) (\dot{w}_o)^{-0.2} e^{-B \int_0^t \dot{w}_o^{0.8} dt} \dots [23]$$

From the mass balance, the weight of oxygen flowing into the injector must equal the weight flowing out plus the rate of change of gaseous and liquid oxygen contained in the injector, i.e.

$$\dot{w}_o = \dot{w}_o' + \frac{dW_{go}}{dt} + \frac{dW_{lo}}{dt} \dots [24]$$

where \dot{w}_o' = LOX flow rate through injector.

If the perfect gas law is assumed, $P_{oj}V = (W_{go}/M)RT$, the

total change is expressed as

$$\left(1 + \frac{RW_{go}}{MC_v}\right) \frac{dV_g}{dt} = V_g \left(\frac{1}{W_{go}} \frac{dW_g}{dt} - \frac{1}{P_{oj}} \frac{dP_{oj}}{dt} \right) \dots [25]$$

also from [20 and 21]

$$\dot{w}_o = \frac{\dot{w}_{go}}{1 - X} \dots [26]$$

and

$$V_g = \text{volume of injector manifold } (V_{oj}) - \text{volume of LOX in injector manifold} = V_{oj} - \frac{W_{Lo}}{\gamma_o} \dots [27]$$

Equations [23 through 27], after being expressed in finite difference form are sufficient to express the injector pressure P_{oj} in terms of the valve flow \dot{w}_{vj} .

From the assumed incompressibility of the fuel (in the manifold), after the injector is full, the flow out must equal the flow in, if no leakage flow is assumed during filling.

$$\dot{w}_{fj} = \begin{cases} 0 & t < t_f \\ \dot{w}_f & t > t_f \end{cases} \dots [28]$$

where t_f is the time at which the injector is filled, also

$$\int_a^{t_f} \dot{w}_f dt = \text{capacity of fuel manifold by weight} \dots [29]$$

Equations [28 and 29] allow the solution for t_f . Air and fuel vapor compression during the filling interval were neglected, since experimental evidence indicates this factor to be of secondary importance.

After the manifolds are filled, the injector equation is

$$\dot{w}_{it}^2 = \lambda_j^2 (p_{it} - p_{ct}) \dots [30]$$

The injector admittance λ_j is constant for all flows.

Propellants injected into the combustion chamber after time $(t - \tau)$ will not have burned at time t due to a combustion time lag τ . The total amount of propellants burned from $t' = 0$ to $t' = t$ is given by

$$\int_0^t \dot{w}_{b(t')} dt' = \int_0^{t-\tau} \dot{w}_{i(t')} dt' \dots [31]$$

differentiating

$$\dot{w}_{b(t)} = \left(1 - \frac{d\tau}{dt}\right) \dot{w}_{i(t-\tau)} \dots [32]$$

From Crocco and Cheng (2)

$$1 - \frac{d\tau}{dt} = 1 + \frac{\dot{n}}{p_c} [p_{c(t)} - p_{c(t-\tau)}] \dots [33]$$

Using Equation [32]

$$\begin{aligned} \dot{w}_{b(t)} &= \left[1 + \frac{\dot{n}}{p_c} (p_{c(t)} - p_{c(t-\tau)})\right] \dot{w}_{i(t-\tau)} \\ &= \frac{A_t}{C^*} p_{ct} + \frac{V_c}{RT_c} \frac{dp_c}{dt} \dots [34] \end{aligned}$$

but

$$\dot{w}_{i(t-\tau)} = (\dot{w}_{fj} + \dot{w}_{oj})(t-\tau)$$

$$\begin{aligned} \therefore (\dot{w}_{fj} + \dot{w}_{oj})(t-\tau) \left[1 + \frac{\dot{n}}{p_c} (p_{c(t)} - p_{c(t-\tau)})\right] &= \\ \frac{A_t}{C^*} p_{ct} + \frac{V_c}{RT_c} \frac{dp_c}{dt} \dots [35] \end{aligned}$$

where $\dot{w}_{i(t)}$ or $\dot{w}_{i(t-\tau)}$ indicates time at which variable is evaluated.

The aforementioned components of the mathematical model are typical and identical in form to the models used for

the gas generator loop. For this loop, however, a number of additional equations were necessary, describing the quasi-steady condition of the hot gases at the turbine outlet.

Programming Details and Computing Logic

The programming of the mathematical model was done in a general form. Not only can system parameters be changed at will, but components of the system may be replaced with other components of different characteristics. To some extent, rocket engine models may be synthesized with available component models.

Techniques

All system components, such as valves, injectors and pumps, were numbered and given a type annotation. The equations describing the components and the equations connecting the component to the upstream and downstream component were then programmed.

Since the connecting equations are all line equations, any line component can be linked to another line component when the type and the next upstream component to which it is to be connected are specified. This scheme allows line configurations to be changed at will.

An important digital feature of the compressible fluid flow equation is the fact that the equations use past time values for the extreme ends of the upstream and downstream lines. This allows each component to be computed without the necessity of knowing present time values at the other components.

The thrust chamber and the gas generator combustion chambers are particularly amenable to this type of solution due to the combustion time delay. Present time pressures are thus computed from past time flows and mixture ratio.

Solution of the turbopump loop required the most involved handling. Here the energy input to the system is transferred from the gas generator to the propellant lines, and involves simultaneous solution of the turbopump system and the propellant suction and discharge lines. In addition, the available energy absorbed by the turbine is dependent on the exhaust conditions. In this section of the program, there are two separate iterations within an iteration.

Modification of Line Equations

The line Equation [1] is modified by the addition of two friction terms

$$p_{xt} - p_{x_{t_1}} = e' (\dot{w}_{xt} - \dot{w}_{x_{t_1}}) + R_x' \dot{w}_{xt} |\dot{w}_{xt}| + R_{x_1}' \dot{w}_{x_{t_1}} |\dot{w}_{x_{t_1}}| \dots [36]$$

where

$$e' = \frac{c\gamma}{g} \cdot \frac{1}{A_1\gamma} = \frac{c}{gA_1}$$

is a constant converting velocity into mass flows, where R_x' is the resistance coefficient at section x , and R_{x_1}' is the resistance coefficient at section x_1 .

The use of the absolute mass flow term is to keep the friction acting in the proper direction whenever the flow direction reverses.

Computing Time Interval

The computing time interval and the line transmission time are determined as follows:

Pressure disturbances travel through a medium with sonic velocity, and the transmission time of a line equals the length of the line divided by the speed of sound in the medium.

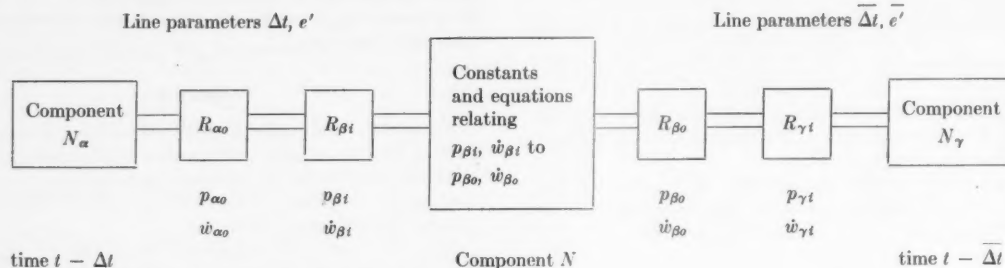
In Equation [36] the transmission time determines time t_1 , since $t - t_1$ equals transmission time.

When the transmission times of all the lines are determined, the shortest time is the computing interval. For the

rest of the lines, the transmission time is divided by the computing interval, and the closest multiple integer is used as the number of computing intervals between end points of the line.

Computer Logic

The diagrammatic representation of a system link is shown below.



The equations representing the computation logic for this schematic are

$$p_{\beta 1}(t) = -e' [\dot{w}_{\beta 1}(t) - \dot{w}_{\alpha 0}(t - \Delta t)] + p_{\alpha 0}(t - \Delta t) - R_{\beta 1} \dot{w}_{\beta 1}(t) | \dot{w}_{\beta 1}(t) | - R_{\alpha 0} \dot{w}_{\alpha 0}(t - \Delta t) | \dot{w}_{\alpha 0}(t - \Delta t) | \dots \dots \dots [37]$$

$$\begin{bmatrix} p_{\beta 1}(t) \\ \dot{w}_{\beta 1}(t) \end{bmatrix} = \begin{bmatrix} 2 \times 2 \\ \text{Matrix of} \\ N \\ \text{transfer function} \end{bmatrix} \times \begin{bmatrix} p_{\beta 0}(t) \\ \dot{w}_{\beta 0}(t) \end{bmatrix} \dots \dots \dots [38]$$

$$p_{\beta 0}(t) = \bar{e}' [\dot{w}_{\beta 0}(t) - \dot{w}_{\gamma 1}(t - \bar{\Delta t})] + p_{\gamma 1}(t - \bar{\Delta t}) + R_{\beta 0} \dot{w}_{\beta 0}(t) | \dot{w}_{\beta 0}(t) | + R_{\gamma 1} \dot{w}_{\gamma 1}(t - \bar{\Delta t}) | \dot{w}_{\gamma 1}(t - \bar{\Delta t}) | \dots \dots \dots [39]$$

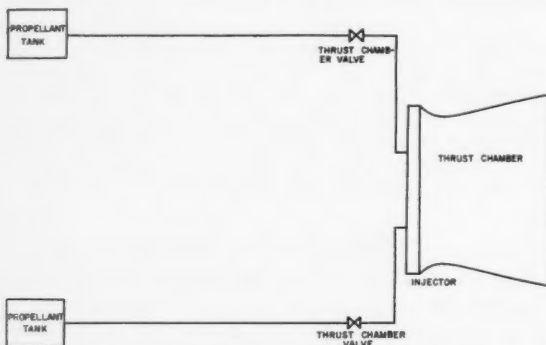


Fig. 2 Schematic of pressure fed thrust chamber used for transient comparison

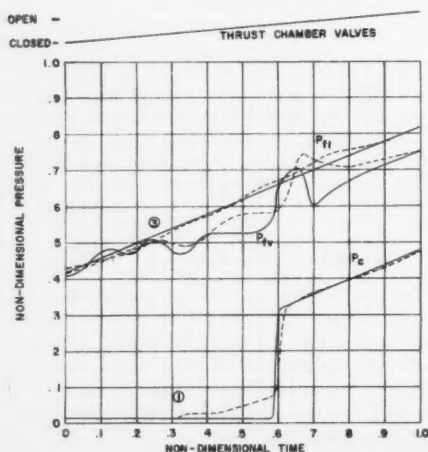


Fig. 3 Comparison of start transient pressures

Computer Simulation of a Pressure Fed System

A rocket engine system, comprised of the elements shown in Fig. 2, was mathematically represented and programmed into the digital computer. The following equations represented the system:

- 1 Line equations, similar in type to Equation [36].
- 2 Valve equation, similar in type to Equation [11].
- 3 Manifold equations similar in type to [12 to 29].

- 4 Injector equations similar in type to Equation [30].
 - 5 Combustion chamber equations similar in type to Equation [35].
- Valve opening times and other pertinent initial data were found from an actual firing.

Start Transient

The functions plotted for comparison are chamber pressure (P_c), fuel thrust chamber valve inlet pressure (P_{fv}), fuel tank pressure (P_{ft}), oxidizer thrust chamber valve inlet pressure (P_{ov}) and oxidizer tank pressure (P_{ot}). The following points of interest are highlighted in Figs. 3 and 4:

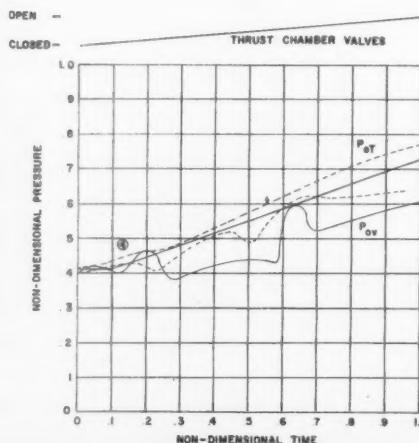


Fig. 4 Comparison of start transient pressures

1 In the actual engine, combustion begins at this point as oxidizer and fuel begin leaking through the injector. The manifolds are not fully pressurized yet.

2 The manifolds are filled at this point and are fully pressurized, allowing appreciable flow to enter the chamber, resulting in a sharp rise in chamber pressure. The computer results do not show the slow rise in chamber pressure between 1 and 2 because no injector fuel flow exists between these points.

3 Initial fuel flow through the fuel thrust chamber valve, indicated by a drop in valve inlet pressure.

4 Initial oxidizer flow through the oxidizer thrust chamber valve.

The computer results follow the test data in general appearance and within about 10 per cent in magnitude. The main differences are attributed to approximations of valve characteristics and line configuration. The effect of bends on pressure waves is not included in the mathematical model, and small changes in pipe cross-sectional area and wall thickness are not taken into account.

Shutdown Transient

The points of interest for the shutdown comparison are shown in Fig. 5:

1 Test data drop in the oxidizer valve inlet pressure is apparently due to the oxidizer valve lagging the fuel valve in starting to close. The result is an increase in oxidizer flow caused by the drop in chamber pressure and the increased flow reducing the valve inlet pressure.

2 The valve inlet pressures increase during the valve closure due to the conversion of velocity head to static pressure and the resulting pressure-wave action.

3 Indication of combustion instability due to feed-line dynamics. The computer indicated a loss of chamber fuel flow at this point.

Summary

Approximations in the mathematical model are those due to lumped resistances and the assumption of straight piping. The former does not materially affect the accuracy of the analysis. The latter, however, could be important in a system having numerous bends. Bends act as reflective elements, passing some of the pressure waves and reflecting the others. Thus, a length of tubing with a bend at some intermediate point will show pressure oscillations of a line having a length up to the bend, modulated by a lower frequency oscillation

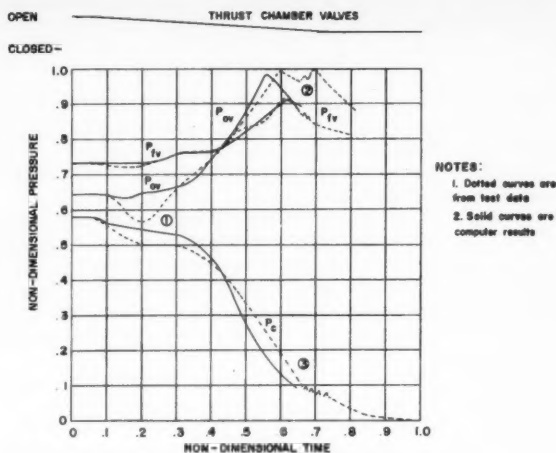


Fig. 5 Comparison of shutdown transient pressures

due to the entire pipe length. This has been observed in a number of tests.

In order to obtain conservative results with respect to pressure surge amplitudes, pumps were considered to pass pressure waves without attenuation. A contemplated improvement of the present digital program will incorporate a variable attenuation factor to be determined from test records.

The present digital program requires approximately 30 min of IBM 704 time for each engine starting transient solution; a basic computing interval of a little over 1 millisecc was used. A simplified program is under development which will neglect the transients in the pump discharge line; however, the transients in the longer suction lines will still be retained. This program is expected to require less than 10 min for solution and will allow rapid evaluation of transients for numerous conditions.

References

- 1 Parmakian, J., "Waterhammer Analysis," New York, Prentice-Hall, 1955.
- 2 Crocco, L., and Cheng, Sin-I, "Theory of Combustion Instability in Liquid Propellant Rocket Motors," London, Butterworths Scientific Publications, 1956, pp. 22-24.

Precision Measurement of Supersonic Rocket Sled Velocity—Part II¹

F. J. BEUTLER² and L. L. RAUCH³

University of Michigan, Ann Arbor, Mich.

This continuation of a previous paper (Reference 1) analyzes the possibility of measuring the velocity of a rocket sled to an accuracy of 0.1 ft/sec (root mean square)

Received Jan. 4, 1958.

¹ This paper represents work performed by the authors in their respective capacities as Member of the Technical Staff and Consultant of the Ramo-Wooldridge Corp., Los Angeles, Calif.

² Assistant Professor of Aeronautical Engineering.

³ Professor of Instrumentation.

over a 100 cps bandwidth. It is shown that a track coil system alone cannot achieve this goal using reasonable techniques. However, the addition of a sled-borne accelerometer of moderate accuracy suffices to insure attainment of the quoted velocity accuracy, if accelerometer and track coil data are combined in an optimum manner. Finally, an error analysis is performed on a practical computational procedure for combining accelerometer and track coil data. It is concluded that the desired accuracies

can be achieved with present day components using the SNORT track.

Introduction

PART I of this paper (1)⁴ was devoted to an expository discussion on the measurement of sled velocity to an accuracy of 0.1 ft/sec rms over a 100 cps bandwidth. This part of the paper contains the analytical justification for the results stated in Part I.

In section 2, we analyze the possibility of attaining the desired measurement of velocity with the existent track coil system. It is shown that any practicable system utilizing only discrete position data cannot achieve satisfactory results, even when markers are spaced 2 ft apart with an accuracy of 0.024 in. rms, and time measurement is accurate to 0.1 microsec.

The third section is devoted to a study of velocity measurement through use of an optimum combination of position and acceleration data in a distortionless filter scheme. It is shown that velocity accuracy and bandwidth specifications can be met without imposing too stringent requirements on the measurement of position or acceleration. In fact, it is demonstrated that this approach is feasible within the present state of the art.

A practical computational procedure for combining accelerometer and track coil data is presented in section 4. The equations which must be mechanized are given. A complete error analysis is performed, indicating that an accuracy of 0.1 ft/sec rms over a 100 cps bandwidth can be achieved by practical components and computation techniques.

2 Differentiation of Track Position Data

If track markers are used, the data obtained will consist of the time intervals required for the sled to pass from one marker to the next. Solely for simplicity in analysis, however, we shall treat position as a function of time. We shall assume that the sled position is sampled at equal intervals of time. The velocity is then calculated by numerical differentiation of discrete data. (For a discussion of discrete differentiation, see (2).)

The problem at hand may be stated as follows: Using a system of physical markers, is it possible to achieve a velocity measurement accuracy of 0.1 ft/sec with a bandwidth of 100 cps? It should certainly be possible if the spacing between markers is sufficiently accurate and if the distance between them is extremely small. However, we shall show that the accuracy and bandwidth requirements cannot both be met by any system of markers now available or conceivable from the standpoint of time, manpower and the present state of engineering achievement.

The block diagram of Fig. 1 shows how the velocity-measurement error arises. It is seen that there are two sources of this error. First, the discrete differentiation process can only approximate true (continuous) differentiation. Thus, except for restricted inputs (e.g., constant acceleration for certain numerical differentiation processes), there will be an error because the operation performed on the position data is not a true differentiation. Second, the noise input indicated in Fig. 1 also yields an error.

We may now proceed directly from Fig. 1 to the power spectrum of the velocity error. Let $A(\omega)$ be the power spectrum of the sled acceleration. Since an integrator has a transfer function $1/\omega$, the sled position spectrum is $A(\omega)/\omega$ (4). $G(\omega)$ denotes the transfer function of the discrete differentiation process, and $N(\omega)$ the spectrum of the position noise input. Since the transfer function of a true differentiator is $i\omega$, the power spectrum of the velocity-measurement error is

$$\Phi(\omega) = \left| G(\omega) \right|^2 N(\omega) + \left| i\omega - G(\omega) \right|^2 \frac{A(\omega)}{\omega^4} \dots [1]$$

⁴ Numbers in parentheses indicate References at end of paper.

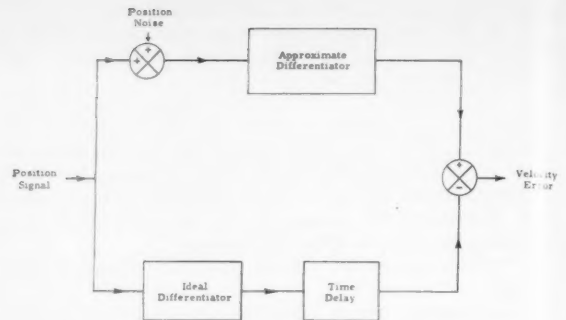


Fig. 1 Block diagram of error computational process

from Fig. 1.

Since $A(\omega)$ and $N(\omega)$ are fixed by the characteristics of the sled, track and marker system, the value of $\Phi(\omega)$ depends on the choice of $G(\omega)$. Evidently, $G(\omega)$ should be selected to minimize $\Phi(\omega)$, subject to the limitation that only discrete samples of sled position are available with time interval h .

The general subject of optimum discrete filters is sufficiently complex to merit further mention, but without a complete—and therefore prohibitively involved—analysis. The reader is referred to (3), which treats in detail discrete filters that permit zero lag for certain classes of signals (polynomials) while minimizing the error due to noise. Because our data need not be available instantaneously, the zero lag requirement is relaxed to optimum lag, which improves the filtering possibilities considerably. In other words, the present velocity of an object can be estimated more closely by a device which looks into past and future for time T than by a system which uses only data in the past over a time interval $2T$.

For the purpose of this analysis, we shall construct a discrete differentiator (filter) which is optimum in a more restricted sense. We shall then show that, even with the most optimistic assumptions about the marker system, no possible discrete differentiator can meet the specified accuracy and bandwidth requirements.

A discrete filter, using $2M + 1$ samples at time intervals h , may be described by

$$v^*(t) = \sum_{j=-M}^{+M} W_j x(t + jh) \dots [2]$$

where $x(\tau)$ is the sled position at time τ , and $v^*(t)$ is the velocity-measurement output of the filter.

If it can be assumed that $N(\omega)$ is white noise, we find that for $M = 5$ (eleven sample points) the first term of Equation [1] is minimized by

$$W_j = \frac{j}{110h} \dots [3]$$

if we require that there be no measurement error [$\Phi(\omega) = 0$] when $N(\omega) = 0$, and when the sled position is representable by an arbitrary quadratic equation in t over any time interval $(t - 5h, t + 5h)$; that is, the acceleration is constant.

Proceeding as explained in Part I (1), we find that the transform of the discrete differentiation (or filtering process) described by Equations [2 and 3] is

$$G(\omega) = \frac{i}{55h} \sum_{j=1}^5 j \sin jh\omega \dots [4]$$

for $\omega < \pi/h$.

We evaluate $N(\omega)$ on the assumption that the errors in marker position are independent of one another. Let the

⁵ Without this constraint, it is obvious that the noise error is minimized by $W_j = 0$ (all j), and therefore $G(\omega) = 0$.

standard deviation of such errors be σ_x . There is also an error in measuring the time between successive markers. The actual timing operation consists of counting cycles of a frequency standard into a register, the counting being initiated and terminated by a pulse emitted the instant a marker is passed. We assume a counting frequency f , and note that the error in timing any interval may be incorrect by as much as 1, i.e., $\delta t = 1/f$. However, it is equally probable that the time error is any lesser figure in the interval $(-1/f, +1/f)$. The distribution of timing errors is then rectangular, with the mean square deviation $1/3f^2$. Converting this into an equivalent marker location error gives $\frac{1}{3}(v/f)^2$, since v/f is the distance traveled by the sled per cycle of the frequency standard. The total mean square equivalent error in marker location is therefore

$$\sigma^2 = \sigma_x^2 + \frac{1}{3} \left(\frac{v}{f} \right)^2 \quad [5]$$

Because the position sampling interval is h , and the errors on successive samples (marker positions) are independent of one another, the form of $N(\omega)$ can be taken to be that of white noise—perfectly flat—except that it is cut off at $|\omega| = \pi/h$ and is zero for all larger $|\omega|$. But since its mean square value is σ^2 , it follows that

$$\sigma^2 = \int_0^{\pi/h} N(\omega) d\omega \quad [6]$$

and therefore

$$N(\omega) = \begin{cases} \frac{\sigma^2 h}{\pi}, & |\omega| < \frac{\pi}{h} \\ 0, & |\omega| \geq \frac{\pi}{h} \end{cases} \quad [7]$$

Lastly, we must assume a value for $A(\omega)$. In a typical case, the acceleration spectrum might be covered by a white noise spectrum of sufficient magnitude. A value of $A(\omega)$ which is somewhat pessimistic but of the proper order of magnitude for a number of applications is

$$A(\omega) = A_0^2 = 1000 \quad (\text{ft/sec}^2)^2/\text{rad/sec} \quad [8]$$

To reduce the measurement error, we should consider only those frequencies below some cutoff frequency ω_c , such as the 100 cps requirement. This is exactly equivalent to passing the measurement error through an ideally flat filter with a sharp cutoff at ω_c . Since $\Phi(\omega) > 0$ for every ω , this can only reduce the error. Further, the error increases very rapidly if $\omega_c/2\pi$ has a value comparable to $1/2h$ due to the frequency foldover effect of the sampling. We must have $\omega_c \ll \pi/h$ then, so that expressions containing $\sin h\omega$ can be approximated by the leading terms of their power series expressions. By this series of steps we obtain successively from [1]

$$\Phi(\omega) = \frac{\sigma^2 h}{\pi} \left| \frac{i}{55h} \sum_{j=1}^5 j \sin jh\omega \right|^2 + \left| i\omega - \frac{i}{55h} \sum_{j=1}^5 j \sin jh\omega \right|^2 \frac{A_0^2}{\omega^4} \quad [9]$$

and by approximating the sines as described above

$$\Phi(\omega) = \frac{\sigma^2 h \omega^2}{\pi} + \left(\frac{89}{30} \right)^2 h^4 A_0^2 \omega^2 \quad [10]$$

With a cutoff ω_c the mean square velocity measurement error becomes

$$\bar{\epsilon}_v^2 = \int_0^{\omega_c} \Phi(\omega) d\omega \quad [11]$$

which in view of Equations [8 and 10] reduces to

$$\bar{\epsilon}_v^2 = \omega_c^3 h (0.106 \sigma^2 + 2930 h^3) \quad [12]$$

To express this in terms of sled velocity and distance between markers we note that this distance Δx is given by

$$\Delta x = hv \quad [13]$$

so that the final expression for the mean square error is

$$\bar{\epsilon}_v^2 = \frac{\omega_c^3 \Delta x}{v} \left[0.106 \sigma^2 + 2930 \left(\frac{\Delta x}{v} \right)^3 \right] \quad [14]$$

We now estimate the rms error under the assumption that a maximum effort is made on a crash basis to instrument a 22,000 ft track. If $\Delta x = 2$ ft, and $\sigma_x = 0.002$ ft, 11,000 markers have to be surveyed and placed along the track with a mean deviation of only 0.024 in. Also, take $f = 10$ mc. The cutoff frequency is taken as $\omega_c = 200\pi$ (100 cps). Then, for $v = 1000$ ft/sec,

$$\sqrt{\bar{\epsilon}_v^2} = 3.42 \text{ ft/sec} \quad [15]$$

Equation [1], as well as those subsequent to it, have two separate terms, corresponding to the two sources of error described earlier. The first of these is associated only with the noise input (physically, marker location and timing errors), and may be called noise error. The second is due solely to the difference between approximate (discrete) differentiation and true differentiation; we shall denote this by the term "frequency response error." Let these types of errors be designated by $(\bar{\epsilon}_v^2)_n$ and $(\bar{\epsilon}_v^2)_{fr}$, respectively. We have, then, from Equation [14]

$$\sqrt{(\bar{\epsilon}_v^2)_n} = 0.459 \text{ ft/sec} \quad [16]$$

and

$$\sqrt{(\bar{\epsilon}_v^2)_{fr}} = 3.40 \text{ ft/sec} \quad [17]$$

It is evident that changing the weighting coefficients W_i in

$$v^*(t) = \sum_{j=-M}^M W_j x(t + jh) \quad [18]$$

will alter the value of rms error. Consequently, the question arises whether, by increasing M and/or varying the W_j 's, a smaller error than Equation [15] may be obtained.

Consider first an increase in M (the above implies $M = 5$) so as to employ a greater number of samples. Since we have used a perfectly flat filter to a cutoff ω_c , we already have an infinite memory filter, i.e., every sample obtained along the track is used. Thus, if such a filter is represented by

$$v^*(t) = \sum_{i=-\infty}^{\infty} Y_i v(t + ih) \quad [19]$$

there follows

$$v^*(t) = \sum_{i=-\infty}^{\infty} Y_i \sum_{j=-M}^M W_j x(t + (i+j)h) \quad [20]$$

from which

$$v^*(t) = \sum_{k=-\infty}^{\infty} V_k x(t + kh) \quad [21]$$

with

$$V_k = \sum_{j=-M}^M Y_{k-j} W_j \quad [22]$$

Now a change in V_k implies a change in Y , W , or both. If Y is varied (without, however, affecting ω_c which is specified) the filter must depart from flatness in the region $0 \leq \omega \leq \omega_c$. Suppose the variation is such as to compensate for the

* A filter of this type and the meaning of infinite memory with respect to such a filter may be found in Valley and Wallman (4), p. 722, and, more generally, on pp. 721-727.

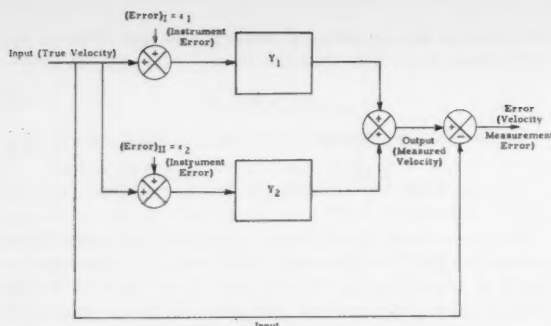


Fig. 2 Block diagram of velocity measurement error when velocity is measured by two separate, independent devices

drop in the frequency response due to W , and the limited value of M . This would be a lead or differentiation filter which, while improving the frequency response error, would increase the noise error which is already excessive. Any other change in Y might decrease the noise error at the expense of the frequency response error, or possibly even increase both errors.

Consider also the changes in W . But W has already been optimized with respect to the noise error, and therefore any change whatever in W must increase the noise error.

Thus we have proved that any change in the discrete filtering coefficients must either enlarge the frequency response error, the noise error, or both. Since either error is in itself excessive (see Eqs. [16 and 17]), it follows that there is no system of weighting coefficients which can reduce the total error to 0.1 ft/sec on an rms basis with the parameters used.

It should be noted again that the parameters—that is, the marker spacing of 2 ft, mean deviation in marker placement of 0.024 in., and counting frequency of 10 mc—are all marginal with respect to the techniques available and the time required. Therefore, any marker system using feasible parameters will have still greater measurement errors than those quoted and considered excessive.

The problem may also be approached from an alternative viewpoint, namely, what bandwidth can be achieved with the above parameters, given that the rms error is to be 0.1 ft/sec or less. Using Equation [14], it is seen that this cutoff frequency is $\omega_c = 59.5$ rad/sec.

It must be concluded, therefore, that a system of markers along the track, unaided by other means of velocity measurement, presents little promise of fulfilling the requirements set forth in Part I.

3 Optimum Combination of Position and Acceleration Data

We wish to find a lower bound for rms velocity measurement error when linear, non-time-varying filtering methods are employed to treat independently position and acceleration data to obtain velocity. The lower bound so calculated serves the dual purpose of:

1 Determining whether it is at all possible to attain the desired accuracy with existent track coil and accelerometers.

2 Evaluating specific filter scheme accuracy relative to the best accuracy which can be achieved by any method.

Starting from more general considerations, we assume that the same time-varying quantity is to be measured by two separate, independent devices. The outputs of these devices are passed through filters of responses $Y_1(\omega)$ and $Y_2(\omega)$. Defining the error as being the difference between the measured and actual quantity, we see that the block diagram of Fig. 2 is applicable.

Suppose that the signal and both errors are stationary and mutually uncorrelated. In particular, let the input (signal)

spectrum be $\phi_s(\omega)$, and the spectra of e_1 and e_2 be $\phi_1(\omega)$ and $\phi_2(\omega)$, respectively. Then, according to Fig. 2, the output (error) spectrum $\Phi(\omega)$ is

$$\Phi(\omega) = |Y_1(\omega)|^2 \phi_1(\omega) + |Y_2(\omega)|^2 \phi_2(\omega) + |1 - Y_1(\omega) - Y_2(\omega)|^2 \phi_s(\omega) \dots [23]$$

and the mean square error $\bar{\epsilon}^2$ is given by

$$\bar{\epsilon}^2 = \int_0^\infty \Phi(\omega) d\omega \dots [24]$$

In general, ϕ_1 , ϕ_2 and ϕ_s are determined by the measuring devices. The problem of minimizing $\bar{\epsilon}^2$ must then be attacked by choosing Y_1 and Y_2 in an optimum fashion. This is exactly the Wiener filter problem. However, an arbitrarily long lag can be permitted in the process of data reduction, so that filter realizability is not a problem.

Turning to Equation [23], we see that $\Phi(\omega)$ (and therefore $\bar{\epsilon}^2$) is minimized by Y_1 and Y_2 , which are real and non-negative. Thus, we need only differentiate $\Phi(\omega)$ with respect to the magnitudes of Y_1 and Y_2 , set the derivatives to zero, and solve for the magnitudes. Whenever reasonably accurate instrumentation is employed, $\phi_s(\omega) \gg \phi_1(\omega)$ and $\phi_s(\omega) \gg \phi_2(\omega)$ so that the procedure described yields approximately

$$Y_1(\omega) = \frac{\phi_2(\omega)}{\phi_1(\omega) + \phi_2(\omega)}$$

and

$$Y_2(\omega) = \frac{\phi_1(\omega)}{\phi_1(\omega) + \phi_2(\omega)} \dots [25]$$

The corresponding mean square error is

$$\bar{\epsilon}^2 = \int_0^\infty \frac{\phi_1(\omega)\phi_2(\omega)}{\phi_1(\omega) + \phi_2(\omega)} d\omega \dots [26]$$

The analysis will now be applied to velocity measurement of a rocket sled by means of markers spaced equally along the track in time, aided by an accelerometer mounted on the sled itself.

Let $\phi_1(\omega)$ be taken as the error spectral density resulting from measurements by the markers alone. Ordinarily, $\phi_1(\omega)$ would be expected to contain terms resulting from aliasing effects, imperfect differentiation,⁷ and marker spacing and timing errors.

Aliasing effects in the marker data will be due to sled motion frequency components at frequencies higher than half the sampling frequency. If the time interval between successive markers is Δt , this is equivalent to position samples being taken with sampling angular frequency $2\pi/\Delta t$. Aliasing of this data can be eliminated if the position samples contain only frequencies below $\pi/\Delta t$, that is, if it is possible to eliminate higher frequency components in some manner. These frequency components may actually be eliminated as follows: Pass the accelerometer output through a unity gain high-pass filter with low frequency cutoff $\pi/\Delta t$, integrate twice to obtain position, sample the integrator output at the same instant the position is sampled by the marker systems and subtract this result from the marker system samples. In this way all the aliasing error can be eliminated, except for a small residual entirely due to accelerometer errors at the higher frequencies. The latter effect is small (especially since the high-frequency accelerometer errors are integrated twice) and may be disregarded in this analysis.

We treat next the error due to imperfect differentiation, again assuming an interval Δt between successive track markers. The position samples may be passed through an

⁷ Ordinary differentiation cannot be applied to a signal consisting of sampled data.

interpolation filter flat to an angular frequency of $\pi/\Delta t$, and cutting off sharply at that frequency. The resulting continuous signal can be differentiated in ordinary fashion; aside from aliasing and spacing errors, the differentiation will be perfect up to angular frequency $\pi/\Delta t$. In the calculations which follow, it will be assumed that outputs of all frequencies are available to the filter $Y_1(\omega)$. This is not strictly correct in light of the above. However, it will be seen that the response of $Y_1(\omega)$ cuts off well below $\omega = \pi/\Delta t$, and that only a truly insignificant portion of the total output is due to the track coil data at frequencies above $\pi/\Delta t$.

Marker spacing and timing errors may both be regarded as errors in position samples. In practice, the greater part of this error is attributable to sled bending and flexing, so that errors may be assumed independent from marker to marker. The effect is then the same as a band limited white noise position error, whose spectra density is $\Delta t \sigma_x^2 / \pi$ up to a frequency $\pi/\Delta t$ where σ_x^2 is the mean deviation of marker position. When the position data are differentiated as indicated in the preceding paragraph, the resulting error spectral density of the velocity calculated from the marker position samples is

$$\phi_1(\omega) = \begin{cases} \frac{\omega^2 \Delta t \sigma_x^2}{\pi}, & 0 \leq \omega < \frac{\pi}{\Delta t} \\ 0, & \text{otherwise} \end{cases} \quad [27]$$

For the power spectrum $\phi_2(\omega)$ of the integrated output of the sled-borne instrumentation accelerometer, we consider a zero offset, a scale factor error p and a noise spectrum $R(\omega)$ generated on the acceleration output within the accelerometer.

The zero offset contributes to the power spectrum as a delta function at the origin. By Equation [25], $Y_2(0) = 0$, and there is no net error due to the offset.

The scale factor error may be virtually eliminated by the first correction method proposed in section 4 of this paper. Consequently, the validity of these calculations is not compromised by omitting consideration of the extremely small inaccuracy which remains after scale factor compensation.

Lastly, the accelerometer noise error is taken to have a spectral density of $R(\omega)$, so that the velocity which is derived by integrating the accelerometer data has an error spectral density of

$$\phi_2(\omega) = \frac{R(\omega)}{\omega^2} \quad [28]$$

If the optimum filters $Y_1(\omega)$ and $Y_2(\omega)$ are used, the total spectral density is computed to be

$$\Phi(\omega) = \frac{\omega^2 R(\omega)}{\omega^4 + \frac{\pi R(\omega)}{\Delta t \sigma_x^2}} \quad [29]$$

In the absence of further information, it is reasonable to suppose that the acceleration spectrum is white. We assume then, that

$$R(\omega) = N^2 (\text{ft/sec}^2)^2 / \text{rad/sec} \quad [30]$$

With this substitution, the mean square error is determined by straightforward integration. We have

$$\bar{\epsilon}_v^2 = \frac{\pi^{1/4}}{2\sqrt{2}} (N^2)^{1/4} (\Delta t \sigma_x^2)^{1/4} \quad [31]$$

where $\bar{\epsilon}_v^2$ is the mean square velocity error.

In order to evaluate the mean square velocity error, one chooses values of N^2 and σ_x^2 which are well within the range of achievement, and require no development time and effort.

Markers are available at 100-ft intervals to an accuracy of

0.01 ft rms. Then, if v represents sled velocity in ft/sec

$$\begin{aligned} \Delta t &= \frac{100}{v} \text{ sec} \\ \sigma_x^2 &= 10^{-4} (\text{ft})^2 \\ N^2 &= 0.0318 (\text{ft/sec}^2)^2 / \text{rad/sec} \text{ (see footnote 8)} \end{aligned} \quad [32]$$

and the rms velocity measurement is

$$\sqrt{\bar{\epsilon}_v^2} = \frac{0.1403}{v^{1/4}} \text{ ft/sec} \quad [33]$$

where v is in ft/sec. It is seen that the rms velocity error is below 0.1 ft/sec for any velocity in excess of 15 ft/sec. At a speed of 200 ft/sec, this error is only 0.073 ft/sec. By the time 2000 ft/sec velocity is reached, the rms error has dropped to 0.054 ft/sec. Furthermore, these figures apply to an arbitrarily large bandwidth, since the upper limit of the integral of the error spectral density was taken to be infinity.

It is possible to speak of the frequency response of $Y_1(\omega)$ and $Y_2(\omega)$ in the usual sense. For example, by substituting the expressions for $\phi_1(\omega)$ and $\phi_2(\omega)$ into Equation [25] for $Y_1(\omega)$, we see that

$$Y_1(\omega) = \frac{1}{1 + \left[\frac{(\Delta t \sigma_x^2)}{\pi N^2} \right] \omega^4} \quad [34]$$

which is a low pass filter with a cutoff frequency⁹ of 1.8 $v^{1/4}$ rad/sec and an attenuation of 24 db/octave.

Since $Y_2(\omega) = 1 - Y_1(\omega)$, it follows that $Y_2(\omega)$ is a high pass filter, with the same cutoff and attenuation characteristics.

It was stated earlier that, while the filter $Y_1(\omega)$ on the track coil data exhibited response beyond half the sampling frequency, the response was so small that the sharp cutoff assumption on $\phi_1(\omega)$ (see Eq. [27]) was of little consequence in shaping $Y_1(\omega)$. Since half the sampling angular frequency is given by $\pi v/100$, a substitution of that figure into Equation [34] shows that the response at that frequency is down by a factor of more than $10^5/v^3$, or about 10^{-4} at a velocity of 1000 ft/sec. Response inaccuracy at higher frequencies is still smaller, related inversely as the fourth power of frequency.

The filters $Y_1(\omega)$ and $Y_2(\omega)$ have to be closely matched, otherwise the third term of Equation [23] becomes prohibitively large. This consideration (together with the discrete nature of the marker data) suggests that a discrete (digital) filter of the form

$$v(t) = \sum_{n=-N}^{+N} U_i u(t - j\delta t) + W_i w(t - j\delta t) \dots [35]$$

is appropriate, with u and w representing the outputs of the marker system and sled-borne accelerometer, respectively, and with U_i , W_i , N and δt chosen to give a discrete representation of $Y_1(\omega)$ and $Y_2(\omega)$.

4 A Practical Method of Obtaining Velocity From Position and Acceleration Data

We shall now present a constructive method of velocity measurement. The computational procedure necessary to accomplish the measurement of velocity will be given explicitly, so that the method should prove directly useful.

An error analysis of the scheme described here constitutes

⁸ This figure has been chosen to be consistent with the noise values used in section 4. The actual choice of this number is explained in greater detail there.
⁹ The cutoff frequency is defined as that frequency for which the attenuation is 3 db.

a part of this section. In this fashion, the adequacy of the technique is established for a measurement accuracy of 0.1 ft/sec rms over any bandwidth.

The method of this section is not claimed to be the optimum method. It does have the virtues of computational simplicity and accuracy close to that of an optimum method. Indeed, without an exact knowledge of the sled acceleration spectrum and the sled-borne accelerometer error spectrum it is impossible to design a truly optimum filter. Furthermore, the work of section 3 indicates that, even under simple assumptions on the two spectra, the computational mechanization of the filter scheme is rather complex.

A brief description of the velocity measurement method under discussion will precede its analytical representation. If the sled-borne instrumentation accelerometer has bias and scale factor errors, these may be estimated by comparing the doubly integrated accelerometer output with track coil data from three coils along the track. Corrections based on the bias and scale factor error estimates may then be made to the accelerometer output. The correction just outlined will be called the "gross correction." Its calculation is so quick and simple that it may serve to provide "quick look data" available almost immediately after the end of a run.

The gross correction may result in data adequate for many purposes; however, to achieve an accuracy of 0.1 ft/sec or better, further effort is required. A final correction is made by comparing the average velocity obtained by differencing successive track coils with the average velocity obtained from accelerometer data on which the gross correction process has already been performed. This entire process is illustrated in Fig. 3.

The actual output of the accelerometer $a^*(t)$ may be expressed as

$$a^*(t) = K_0 + (1 + K_1)a(t) + a'(t) \dots \dots \dots [36]$$

where K_0 is the bias error, K_1 the scale factor error, $a'(t)$ all other accelerometer errors (including particularly random noise), and $a(t)$ the true sled acceleration.

In order to perform the gross correction, it is necessary to estimate K_0 and K_1 . If the sled starts at time zero and passes by the j th and k th track coils at times t_j and t_k , respectively, the doubly integrated (position) accelerometer output is

$$x^*(t_j) = K_0 \frac{t_j^3}{2} + (1 + K_1)x(t_j) + x'(t_j) \dots \dots \dots [37]$$

and

$$x^*(t_k) = K_0 \frac{t_k^3}{2} + (1 + K_1)x(t_k) + x'(t_k) \dots \dots \dots [38]$$

at times t_j and t_k , where $x(t)$ is the true sled position.

The track coil passed at t_j is thought to be at position x_j rather than $x(t_j)$ because of surveying errors, sled flexing and vibration. Hence, there is a track position error ϵ_j which is equal to

$$\epsilon_j = x(t_j) - x_j \dots \dots \dots [39]$$

The track error ϵ_j should also include an error which results because the time of passing a given track coil is not measured exactly, but only to a given increment. The SNORT track instrumentation is capable of measuring this time to the nearest microsecond, so that the resulting error is small compared to an estimated one sigma track error of 0.01 ft.

Equations [37 and 38] yield

$$K_0 = \frac{2}{A(j, k)} \{x_k[x^*(t_j) - \epsilon_j(1 + K_1) - x'(t_j)] - x_j[x^*(t_k) - \epsilon_k(1 + K_1) - x'(t_k)]\} \dots \dots \dots [40]$$

$$K_1 = \frac{2}{A(j, k)} \{t_j^2[x^*(t_k) - \epsilon_k(1 + K_1) - x'(t_k)] - t_k^2[x^*(t_j) - \epsilon_j(1 + K_1) - x'(t_j)]\} - 1 \dots \dots \dots [41]$$

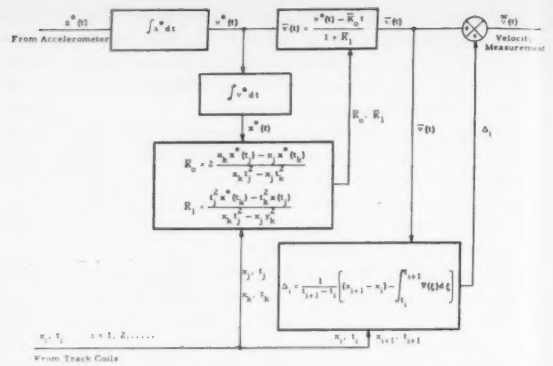


Fig. 3 Block diagram of practical method for obtaining velocity from acceleration and position data

where

$$A(j, k) = x_k t_j^2 - x_j t_k^2 \dots \dots \dots [42]$$

In Equations [40 and 41] we know the values of $x^*(t)$, x_j , x_k , t_j and t_k . This enables us to construct estimates \bar{K}_0 and \bar{K}_1 for K_0 and K_1 , respectively. We shall use

$$\bar{K}_0 = \frac{2}{A(j, k)} [x_k x^*(t_j) - x_j x^*(t_k)] \dots \dots \dots [43]$$

and

$$\bar{K}_1 = \frac{1}{A(j, k)} [t_j^2 x^*(t_k) - t_k^2 x^*(t_j)] - 1 \dots \dots \dots [44]$$

If the error in estimating K_0 is defined as $d\bar{K}_0 = K_0 - \bar{K}_0$, and similarly for K_1 , one may write

$$d\bar{K}_0 = \frac{2}{A(j, k)} [(x_j \epsilon_k - x_k \epsilon_j)(1 + K_1) + x_j x'(t_k) - x_k x'(t_j)] \dots \dots \dots [45]$$

$$d\bar{K}_1 = \frac{1}{A(j, k)} [(t_k^2 \epsilon_j - t_j^2 \epsilon_k)(1 + K_1) + t_k^2 x'(t_j) - t_j^2 x'(t_k)] \dots \dots \dots [46]$$

We shall assume that $a'(t)$ has zero mean (any constant non-zero mean is absorbed in K_0), as do track coil errors ϵ_j and ϵ_k . Then the estimates \bar{K}_0 and \bar{K}_1 are unbiased.

At any time t the true velocity of the sled is

$$v(t) = \frac{v^*(t) - K_0 t - v'(t)}{1 + K_1} \dots \dots \dots [47]$$

from [36]. Our estimate $\bar{v}(t)$ of the velocity shall be

$$\bar{v}(t) = \frac{v^*(t) - \bar{K}_0 t}{1 + \bar{K}_1} \dots \dots \dots [48]$$

which is easily computed after \bar{K}_0 and \bar{K}_1 are calculated from [43 and 44]. The error in this estimate of $v(t)$ is

$$d\bar{v}(t) = - \frac{(d\bar{K}_1)v(t) + (d\bar{K}_0)t + v'(t)}{1 + \bar{K}_1} \dots \dots \dots [49]$$

In our application, a so-called 1 per cent accelerometer or better is required. Then $|K_1| < 0.01$, and likewise \bar{K}_1 will be

small. On the basis of this argument it is legitimate to approximate $d\bar{v}(t)$ by

$$d\bar{v}(t) = -(d\bar{K}_1)v(t) - (d\bar{K}_0)t - v'(t) \dots [50]$$

As stated previously, the gross correction described above may suffice for some purposes, and in any case proves useful for quick look data. Therefore, we shall calculate the rms error in the measured velocity after the gross correction has been applied.

Since \bar{K}_0 and \bar{K}_1 are unbiased estimates, and $a'(t)$ has zero mean, the mean square value of $d\bar{v}(t)$ will be identical with the variance.¹⁰ To perform the required calculation, $d\bar{v}(t)$ is squared, and its expectation taken. We shall denote "expectation of" by prefixing the letter E to the appropriate quantity. Now

$$E\{[d\bar{v}(t)]^2\} = v^2(t)E[(d\bar{K}_1)^2] + t^2E[(d\bar{K}_0)^2] + E\{[v'(t)]^2\} + 2tv(t)E[(d\bar{K}_0)(d\bar{K}_1)] + 2v(t)E[(d\bar{K}_1)v'(t)] + 2tE[(d\bar{K}_0)v'(t)] \dots [51]$$

The remainder of the work will be greatly eased if a few assumptions are made at this point. Since these assumptions will correspond closely with fact, no apology is necessary. The great preponderance of the track coil error is due to flexing and bending of the sled itself, so that ϵ_j and ϵ_k are orthogonal for any $j \neq k$. The track coil error is also assumed to be uncorrelated with the accelerometer error. With regard to the latter, K_0 , K_1 and $a'(t)$ are all mutually (pairwise) uncorrelated.

An additional supposition applicable only to the gross correction analysis is that $E(\epsilon_i^2) \ll E\{[x'(t_i)]^2\}$. The justification lies in the fact that the rms value of ϵ_i is about 0.01 ft, while $x'(t_i)$ has an rms magnitude of 8.2 ft in the representative example which is to follow, and $x'(t_k)$ has an even larger rms value. Consequently, the calculation of the expectations in [50] will omit all considerations of track error. Since $E\{[x'(t)]^2\}$ tends to grow as t^2 , the same approximation is not appropriate to the final correction in which we deal with time intervals of the order of 0.1 sec.

Reference to Equations [45, 46 and 51] will show that terms such as $E[x'(t_1)x'(t_2)]$ occur in the evaluation of $d\bar{v}(t)$. To show how such terms are evaluated we define first the covariance $E[a'(t_1)a'(t_2)]$ by

$$R_{aa}(t_1, t_2) = E[a'(t_1)a'(t_2)] \dots [52]$$

and similarly

$$R_{vx}(t_1, t_2) = E[v'(t_1)x'(t_2)] \dots [53]$$

$$R_{xx}(t_1, t_2) = E[x'(t_1)x'(t_2)] \dots [54]$$

Given $R_{aa}(t_1, t_2)$, these covariances may be computed as follows

$$R_{vv}(t_1, t_2) = \int_0^{t_1} \int_0^{t_2} R_{aa}(\tau_1, \tau_2) d\tau_1 d\tau_2 \dots [55]$$

$$R_{vx}(t_1, t_2) = \int_0^{t_1} R_{vx}(\tau_1, t_2) d\tau_1 \dots [56]$$

$$R_{xx}(t_1, t_2) = \int_0^{t_1} \int_0^{t_2} R_{vv}(\tau_1, \tau_2) d\tau_1 d\tau_2 \dots [57]$$

As an example, we shall calculate $d\bar{v}(t)$ for a rocket sled traveling along a 20,000-ft track. We shall assume that the sled accelerates at 200 ft/sec² for 10 sec, and then decelerates at the same rate for the same length of time. Then, with $x_i = 10,000$ ft, and $x_k = 20,000$ ft we shall have $t_i = 10$ sec, and $t_k = 20$ sec. The accelerometer has an assumed noise error $a'(t)$ of 3.2 ft/sec² rms, flat from 0 to 50 cps; this implies a spectral density $N^2 = 0.0318$ (ft/sec²)²/rad/sec. We may thus write $R_{aa}(t_1, t_2) = 0.0318 \delta(t_1 - t_2)$ as an approximation to white noise over the entire frequency spectrum. The difference between the exact R_{aa} and the one just given implies

¹⁰ This statement is true if the approximation of [50] is valid.

an error of less than 1.05×10^{-4} (ft/sec)² in R_{vv} , and an error of less than 10^{-9} (ft)² in R_{xx} .

If the indicated calculations are carried out

$$E[d\bar{v}^2(t)] = 0.1t + 0.096t^2 - 0.0025t^3 \quad (\text{ft/sec})^2 \dots [58]$$

whenever $t \leq t_j$. For $t_j \leq t \leq t_k$, we have instead

$$E[d\bar{v}^2(t)] = 0.1t + 0.0356t^2 + 0.0035t^3 \quad (\text{ft/sec})^2 \dots [59]$$

In particular, if $t = t_j = 10$ sec, the rms value of $d\bar{v}(t)$ is

$$\sqrt{E[d\bar{v}^2(t)]} = 3.0 \text{ ft/sec} \dots [60]$$

and

$$\sqrt{E[d\bar{v}^2(t)]} = 6.7 \text{ ft/sec} \dots [61]$$

when $t = t_k = 20$ sec. The rms values of $d\bar{K}_0$ and $d\bar{K}_1$ are 0.115 ft/sec² and 0.00167, respectively. Without the proposed correction, a 1 per cent instrument might have $K_0 = 3$ ft/sec² and $K_1 = 0.01$, so that errors would be in excess of 60 ft/sec!

Since only three track coils have been used to correct the accelerometer, it is evident that better results may be achieved through further corrections made by use of track position data obtained from other track coils. The procedure which is proposed here consists of correcting the singly integrated accelerometer output by the difference between average velocities between two track coils as determined from track coils and accelerometer over that interval. That is, in the time interval $t_i \leq t < t_{i+1}$ our new estimate of sled velocity is $\bar{v}(t)$, where

$$\bar{v}(t) = \bar{v}(t_i) + \Delta_i + \int_{t_i}^t \bar{a}(\xi) d\xi \dots [62]$$

in which the difference between average velocities Δ_i is given by

$$\Delta_i = \frac{1}{\Delta t_i} \left[(x_{i+1} - x_i) - \int_{t_i}^{t_{i+1}} \bar{v}(\xi) d\xi \right] \dots [63]$$

and Δt_i is defined by

$$\Delta t_i = t_{i+1} - t_i \dots [64]$$

The error in our estimate is then

$$d\bar{v}(t) = \frac{\epsilon_{i+1} - \epsilon_i}{\Delta t_i} + d\bar{v}(t) - \frac{d\bar{x}(t_{i+1}) - d\bar{x}(t_i)}{\Delta t_i} \dots [65]$$

It will be noted that aliasing does not appear in any of the error terms of [65] regardless of the frequency components of the rocket sled motion. This is to be expected, because the track coil data are used only to determine the average velocity between two track coils as shown by [62 and 63].

For the purposes of our error analysis we shall assume that the i th and $(i+1)$ track coils are not identical to either the j th or the k th (on which \bar{K}_0 and \bar{K}_1 have been estimated). Since there are 200 coils along the track, this assumption will generally hold. If the assumption is not true, $E\{[d\bar{v}(t)]^2\}$ will contain terms in addition to those that we shall calculate. However, these terms are small for practical ϵ_i , so that our error estimates will apply along the entire track.

The mean square error of velocity measurement is most conveniently expressed as

$$E\{d\bar{v}(t)^2\} = \frac{2E[\epsilon^2]}{(\Delta t_i)^2} - \frac{2}{\Delta t_i} \int_{t_i}^{t_{i+1}} E[d\bar{v}(t)d\bar{v}(\xi)] d\xi + E\{[d\bar{v}(t)]^2\} + \frac{E\{[d\bar{x}(t_{i+1}) - d\bar{x}(t_i)]^2\}}{(\Delta t_i)^2} \dots [66]$$

Here $d\bar{v}(t)$ is given by [50] in terms of $d\bar{K}_0$, $d\bar{K}_1$, and $v'(t)$. In turn, $d\bar{K}_0$ and $d\bar{K}_1$ are expressed as functions of $x'(t_i)$ and $x'(t_{i+1})$ in [45 and 46]. Making the first indicated set of substitutions yields

$$E\{[d\bar{v}(t)]^2\} = \frac{2E[\epsilon^2]}{(\Delta t_i)^2} + [v(t) - v_i]^2 E[(d\bar{K}_1)^2] + 2[v(t) - v_i] \left(t - \frac{t_{i+1} + t_i}{2} \right) E[(d\bar{K}_0)(d\bar{K}_1)] + \left(t - \frac{t_{i+1} + t_i}{2} \right)^2 E[(d\bar{K}_0)^2] \\ + 2 \left\{ [v(t) - v_i] \left(E[v'(t)(d\bar{K}_1)] - \frac{1}{\Delta t_i} \int_{t_i}^{t_{i+1}} E[v'(\xi)(d\bar{K}_1)] d\xi \right) + \left(t - \frac{t_{i+1} + t_i}{2} \right) \left(E[v'(t)(d\bar{K}_0)] - \frac{1}{\Delta t_i} \int_{t_i}^{t_{i+1}} E[v'(\xi)(d\bar{K}_0)] d\xi \right) \right\} \\ + \frac{1}{\Delta t_i} \left\{ \int_{t_i}^{t_{i+1}} d\eta \left[\frac{1}{\Delta t_i} \int_{t_i}^{t_{i+1}} R_{vv}(\xi, \eta) d\xi - 2R_{vv}(t, \eta) \right] \right\} + R_{vv}(t, t) \dots [67]$$

where for brevity of notation, we write the average velocity over the interval (t_i, t_{i+1}) as

$$v_i = \frac{x(t_{i+1}) - x(t_i)}{\Delta t_i} \dots [68]$$

In some cases it may be sufficient to obtain an upper bound for $E[d\bar{v}(t)]^2$. The following inequalities are useful for this purpose

$$\left| t - \frac{t_{i+1} + t_i}{2} \right| \leq \frac{\Delta t_i}{2} \dots [69]$$

$$\left| v(t) - v_i \right| \leq \frac{\Delta t_i}{2} a_{\max} \dots [70]$$

where a_{\max} is the maximum expected acceleration. Then

$$E\{[d\bar{v}(t)]^2\} \leq \frac{2E[\epsilon^2]}{(\Delta t_i)^2} + \frac{(\Delta t_i)^2}{4} \left\{ a_{\max} \sqrt{E[(d\bar{K}_1)^2]} + \sqrt{E[(d\bar{K}_0)^2]} \right\}^2 + \Delta t_i \sqrt{R_{vv}(t_{i+1}, t_{i+1}) - R_{vv}(t_i, t_i)} \times \\ \left\{ a_{\max} \sqrt{E[(d\bar{K}_1)^2]} + \sqrt{E[(d\bar{K}_0)^2]} \right\} + \frac{1}{\Delta t_i} \left\{ \int_{t_i}^{t_{i+1}} \eta \left[\frac{1}{\Delta t_i} \int_{t_i}^{t_{i+1}} R_{vv}(\xi, \eta) d\xi - 2R_{vv}(t_{i+1}, \eta) \right] \right\} + R_{vv}(t_{i+1}, t_{i+1}) \dots [71]$$

Equation [70] may be obtained from [66] by repeated use of the Schwarz and Minkowski inequalities (5).

A numerical example will indicate the order of accuracy attainable by the velocity measurement scheme under discussion. We shall again assume that the sled travels down a 20,000-ft track, first accelerating at a rate of 200 ft/sec² for a period of 10 sec, and then decelerating at the same rate for the same period of time. The rms position errors on the track coils will be taken as 0.01 ft, and the acceleration noise error in the accelerometer as 3.2 ft/sec² rms uniformly over a 50 cps bandwidth. We shall again base our calculation on white noise of the same spectral density. The accelerometer may also have bias and scale factor error; these do not enter into our equation as per the discussion on the first correction. The maximum acceleration, a_{\max} , is 300 ft/sec² for the purpose of this computation.

Fig. 4 gives an upper bound for rms velocity measurement error by the method of this section. Equation [71] has been used to find the numerical values for the graph.

The error analysis demonstrates that the measurement

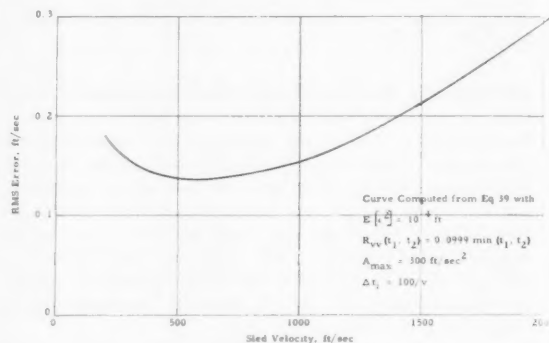


Fig. 4 Upper bound on rms velocity measurement error vs. sled velocity

method presented here promises sufficient accuracy to approach the specifications. Indeed, the figures presented here refer to upper bounds based on pessimistic accuracy estimates, so that greater precision should be realized in practice.

References

- 1 Beutler, F. J. and Rauch, L. L., "Precision Measurement of Supersonic Rocket Sled Velocity, Part I," *JET PROPULSION*, vol. 27, 1957, pp. 1021-1024.
- 2 Milne, W. E., "Numerical Calculus," Princeton University Press, 1949, chapter IV.
- 3 Johnson, K. R., "Optimum, Linear, Discrete Filtering of Signals Containing a Nonrandom Component," *IRE Transactions on Information Theory*, vol. IT-2, no. 2, June 1956, pp. 49-55.
- 4 Valley, G. E., Jr. and Wallman, H., "Vacuum Tube Amplifiers," McGraw-Hill (Radiation Laboratory Series), New York, 1948, pp. 721-727.
- 5 Graves, L. M., "Theory of Functions of a Real Variable," McGraw-Hill, New York, 2nd ed., 1956, pp. 233-234.

Meteorological Rocket Soundings in the Arctic¹

W. G. STROUD²

U. S. Army Signal Research and Development Laboratory, Fort Monmouth, N. J.

Some thirty upper atmosphere rocket soundings have been made in the Arctic so far in the International Geophysical Year to measure temperature, pressure, density and winds. Aerobees in the various models and Nike-Cajuns have been the vehicles. The experiments have included the freely-falling sphere for measuring densities, the rocket-grenade experiment for measuring pressures and densities in the supersonic flow, yielding the ambient conditions by theoretical conversion. Data from a number of these firings have been reduced and compared to those taken at other latitudes. The preliminary analysis indicates different temperature, pressure and density distributions than elsewhere. Also, these parameters seem to be more sensitive to the time of measurement than at lower latitudes.

Introduction

THE meteorological parameters of temperature, pressure, density and winds have been and are being measured in the Arctic during the International Geophysical Year by a variety of techniques developed over the previous ten years by various groups in this country that have been carrying out the upper atmosphere rocket research program. The scope of the program has been described elsewhere (11).³ Tables 1 and 2 are summaries of the meteorological firings.

Table 1 Meteorological rocket soundings (Arctic)

Experiment	No. firing	Location	Time
sphere	8	North Atlantic and Churchill	W,D
grenade	10	Churchill	W,S D,N
aerodynamic	6	Churchill	W,S D,N
gage	3	Churchill	W,S D,N
USSR	6	Franz Joseph Land	W,D

W = winter, S = summer, D = day, N = night

The IGY is only a year old at present; most of the rocket research groups are still in the middle of their firing schedules; the results, in terms of reduced data that are available at this time, are quite limited. The scientists themselves have not had the opportunity to publish their information. Therefore, this paper is intended to review the techniques that are being used in the Arctic to measure the meteorological parameters and to present a few of the preliminary results that the working scientists have so kindly made available. Other published data have been included when pertinent.

In the planning of the IGY rocket program for Fort Churchill, a guiding principle was that proven rocket-borne techniques would be used. Each of the methods used,

whether sphere, aerodynamic, grenade or gage, has been tested at White Sands Proving Ground and has yielded significant data (1a,b). Thus, there is added the significance of having measurements made with the same method in different geographic locations.

Descriptions of Methods

There follow quite simplified descriptions of the various experiments for measuring the meteorological parameters of temperature, pressure, density and winds at rocket altitudes. References (1) give more thorough discussions.

The Freely-Falling Sphere Experiment (2)

This method of measuring the density of the atmosphere has been developed by the University of Michigan group under L. M. Jones, first under Signal Corps sponsorship using

Table 2 Meteorological rocket soundings (Arctic)

IGY no. ¹	Date ²	Location	Experiment	Alt. km
AM 6.08	20 Oct.—	North	sphere (D)	90
AM 7.12	20 Nov. 56 D	Churchill	aero (T)	113
AM 6.31	20 Oct. 56 D	"	aero (T)	145
AM 2.21	23 Oct. 56 N	"	grenade (T, W)	68
SM 1.01	12 Nov. 56 N	"	gage (P, D)	210
NN 3.12	17 Nov. 56 D	"	grenade (T, W)	92
SM 1.02	21 July 57 N	"	grenade (T, W)	87
SM 1.03	23 July 57 N	"	gage (P, D)	210
NN 3.13	29 July 57 D	"	grenade (T, W)	74
F		"	grenade (T, W)	93
SM 1.04	12 Aug. 57 D	"	grenade (T, W)	130
SM 1.05	19 Aug. 57 N	"	aero (T)	160
SM 2.06	25 Aug. 57 D	"	grenade (T, W)	85
AM 4.01	1 Sept. 57 D	"	grenade (T, W)	97
SM 1.07	11 Dec. 57 N	"	aero (T)	160
SM 1.08	14 Dec. 57 D	"	grenade (T, W)	98
AM 6.02	25 Jan. 58 D	"	grenade (T, W)	152
SM 1.09	27 Jan. 58 N	"	sphere (D)	130
SM 2.10	27 Jan. 58 D	"	aero (T)	160
AM 6.36	27 Jan. 58 D	"	sphere (D)	160
AM 6.03	29 Jan. 58 N	"	aero (T)	144
AM 6.37	24 Feb. 58 N	"	gage (P, D)	206
NN 3.14	24 Feb. 58 N	"	sphere (D)	170
F		"	aero (T)	137
AM 6.05	4 March 58	"	sphere (D)	170
AM 6.38	24 March 58	"	aero (T)	137

¹ IGY no.: A code number indicating the sponsoring agency, the instrumenting agency and the type and number of the vehicle used.

² The D or N after the year indicates day or night respectively. "Aero" is the aerodynamic technique of N. Spencer, Univ. of Mich. "Sphere" is the freely-falling sphere technique of L. M. Jones of the Univ. of Mich. "Grenade" is the rocket-grenade experiment of W. G. Stroud of the Army Signal Corps. "Gage" is the multiple-gage technique of H. LaGow of the Naval Research Laboratory. P, T, D and W are pressure, temperature, density and winds, respectively.

¹ Presented at the ARS Semi-Annual Meeting, Los Angeles, Calif., June 9-12, 1958.

² Chief, Space Research Instrumentation, Applied Physics Division. Member ARS.

³ Numbers in parentheses indicate References at end of paper.

Aerobees and later under Air Force sponsorship using Nike-Cajuns. The present procedure consists of carrying aloft a 7-in. diam, 9-lb sphere, ejecting it from the Nike-boosted Cajun, and measuring its drag by means of an internal accelerometer as it falls through the atmosphere.

The basic equations are

$$F = M(g - a) \dots \dots \dots [1]$$

and

$$\text{drag} = \frac{1}{2} D v^2 C_D A \dots \dots \dots [2]$$

where

- D = density of air
- v = velocity of sphere
- C_D = drag coefficient
- A = cross-sectional area

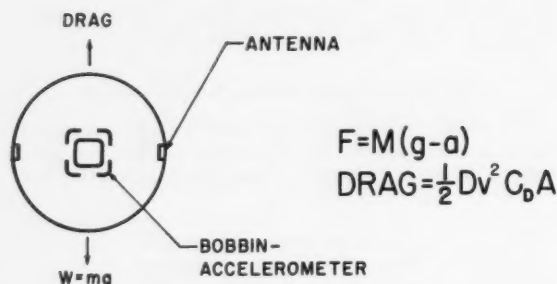


Fig. 1 The sphere experiment

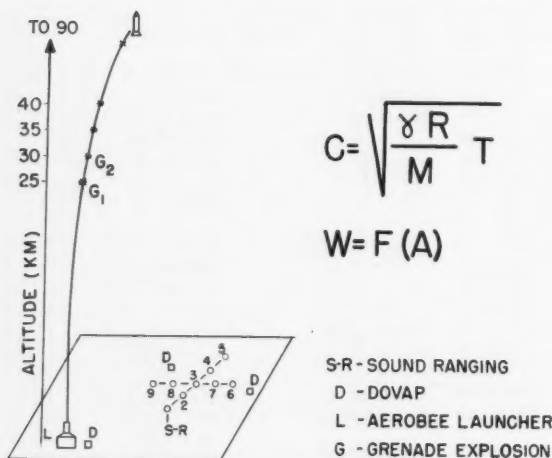


Fig. 2 The grenade experiment

$$\frac{P_x}{P_y} = \frac{f(x, T, v, \alpha, \theta, m, \gamma)}{f(y, T, v, \alpha, \theta, m, \gamma)}$$

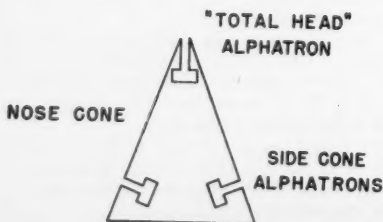


Fig. 3 The aerodynamic method

The deceleration is measured; the drag coefficients are known from scaled wind tunnel tests at low pressures; the velocity is obtained from the free-fall from peak, and the other known quantities permit the calculation of D .

The altitude range over which the experiment is effective depends on the height from which the sphere is dropped, the ratio of area to mass of the sphere, and the sensitivity of the accelerometer. The present configuration yields data between 10 and 90 km. The accuracy is about 10 per cent over this altitude range, the primary limitation being the uncertainty in the coefficient of drag over the range of Mach and Reynolds numbers. Pressures and temperatures may be derived from the computed densities by means of the hydrostatic equation.

The Rocket-Grenade Experiment (3,4)

The temperatures and winds of the upper atmosphere have been measured by sound-ranging on successive explosions created by carrying aloft and ejecting charges from Aerobees. The present experiment is conducted jointly by the Army Signal Corps group under W. G. Stroud and the University of Michigan group under L. M. Jones. The fundamental parameters measured are the positions and times of the explosions in space, and the times and angles of arrival of the successive sound waves at the ground. The experimentally determined altitude limit for the method is about 90 km above which sufficient sound energy cannot be coupled into the atmosphere.

The average temperatures in the layers between grenades are calculated from the relationship

$$C = \sqrt{\frac{\gamma RT}{M}} = K(T)^{1/2} \dots \dots \dots [3]$$

where

- C = the velocity of sound in the layer
- γ = ratio of specific heats of air
- R = gas constant
- T = temperature
- M = average molecular weight of air
- K = constant over the altitude range

The average wind speeds and directions in the layers between grenades are determined by measuring the differences between the true positions of the explosions and their apparent positions as given by the angles of arrival of the sound waves at the ground. The accuracy of the measurements is limited by that with which the times of arrivals of the low frequency sound waves at the individual microphones can be measured. The average temperatures have an accuracy of $\pm 5^\circ \text{C}$, the winds, ± 10 m/sec and ± 18 deg in azimuth as determined in previous firings.

The Aerodynamic Experiment (1,5)

By means of the Taylor-Maccoll (6) theory concerning supersonic flow around right-circular cones and the Kopal tables (7) for such cones in yaw, it is possible to determine ambient temperatures from a supersonic rocket by measuring the ram pressures and cone sidewall pressures by appropriate gages. Spencer of the University of Michigan has applied alphas for such pressure measurements using both Aerobees and Nike-Cajuns. Pressures at the nose tip and roughly 0.8 of the distance back along the right-circular cone are measured.

Thus, the pressure P_x at a distance x back along the cone is given by

$$P_x/p = f(x, T, v, \alpha, \theta, m, \gamma) \dots \dots \dots [4]$$

where T is the ambient temperature, v the speed of the missile, α and θ its angles of attack and roll, and m and γ the molecular weight and ratio of specific heats, respectively. For gages at

different distances, x and y

$$\frac{P_s}{P_a} = \frac{f(x, T, v, \alpha, \theta, m, \gamma)}{f(y, T, v, \alpha, \theta, m, \gamma)} \quad [5]$$

For any rocket flight, all these quantities are known or determined point by point except T , which may be computed point by point along the trajectory. The pressures may be derived from these temperatures using the hydrostatic equation. The temperatures obtained over the region 40 to 90 km are accurate to $\pm 10^\circ\text{C}$.

The Gage Methods (8,9)

LaGow and his colleagues of the Naval Research Laboratory have applied the earlier work (8) of NRL to Aerobee-Hi borne measurements in the Arctic. These measurements of pressure and density (from which the temperature may be derived) are carried out as follows: A family of pressure gages is scattered over the surface of the rocket measuring stagnation, ambient and cone pressures. Bellows, Pirani and Philips gages and the Havens-cycle gage measure the pressures in different pressure ranges. See Table 3. Roll

Table 3 Ranges of sensitivity of various pressure-density gages

Gage	Range mm Hg
Bellows	760 to 20
Pirani (conductivity)	$2 \text{ to } 3 \times 10^{-3}$
Havens-cycle	$10^3 \text{ to } 10^{-5}$
Philips (ionization)	$10^3 \text{ to } 10^{-6}$
Alphatron	$10^3 \text{ to } 10^{-2}$

modulation appearing on the side cone gages also permits the determination of the pressure at higher altitudes (10^{-7} mm). The distribution of the gages along the walls of the vehicle is critical, since ambient pressures are measured directly by various gages located about 7 calibers behind the stagnation probe. These Aerobees are sealed throughout to prevent outgassing and permit the extension of the measurements to the limits of gage sensitivity.

The density is determined from the Rayleigh supersonic pitot tube formula which takes the form

$$D = \frac{0.144 P_s - 0.066 P_a}{V^2} \left(\frac{\text{gm}}{\text{m}^3} \right) \quad [6]$$

where

P_s = stagnation pressure
 P_a = ambient pressure
 V = total velocity

This multiple-gage approach has made possible measurements to much higher altitudes than the other techniques. Its accuracies, as given by NRL, are

	Altitude, km	Error, per cent
Pressure data	25-80	5-15
	110-150	20-50
Density data	30-80	2-10
	110-300	20-200

Other Methods

Two other methods of measuring the density at rocket altitudes should be mentioned. Aerobee flight NN 3.17 by NRL, which was instrumented with time-of-flight mass spectrometers for gas and ion composition (10), obtained density data because the rocket's altitude stayed within 54

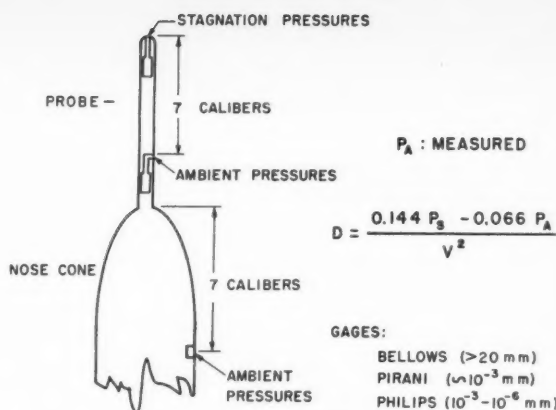


Fig. 4 The gage method

deg of the trajectory during ascent, and the spectrometer at the tip yielded density data between 110 and 170 km. These are winter night data. Also, it has been observed in the grenade experiment that at the time of each explosion a period disturbance appears on the Dovap cycle record. This disturbance is apparently a measure of the velocity of propagation of the shock wave from the explosion which is a function of the ambient density—thus the density at each grenade altitude may be determined. Bartman of the University of Michigan is at present working out this technique.

A specific problem in the comparison of the rocket data is the time variations. Simultaneous measurements with the different experiments is highly desirable but difficult, because of the limited space on the vehicles and the limited facilities for launching and tracking on range. However, on Jan. 27, 1958 at noon, an Aerobee carrying the rocket-grenade experiment and a small sphere was fired. Twenty-nine minutes later a Nike-Cajun carrying the aerodynamic experiment was successfully fired. A comparison of these results from three techniques will be particularly interesting and valid.

The USSR Method

The USSR is also conducting Arctic and, in addition, Antarctic meteorological rocket sounding programs (14) using their meteorological sounding rocket (15,16) to measure temperatures and pressures up to about 110 km. Between November 1957 and March 1958, six rockets were launched in Franz Joseph Land and four near Mirnyy in the Antarctic.

As described in the literature, the instrumentation consists of thermal (Pirani?) and membrane manometers for measuring pressure, and an electric resistance thermometer for temperatures. A unique feature of their technique is the use of a parachute throughout the entire downward leg of the trajectory to orient and slow the separated instrumentation section in its fall. A telemeter is used to recover the data which apparently are now being processed.

Previously published USSR results for the upper-middle latitudes (16) show general agreement with the U. S. literature in this field.

Results

Of the twenty-seven firings, including the pre-IGY group, that have been conducted so far, data from only about ten have been reduced or even partially reduced. The responsible scientists have had only limited opportunities to publish their results. The data presented in the following paragraphs must be considered preliminary. Except for the grenade experiment which is the author's responsibility, the inclusion of data in this paper is due to the cooperation of the responsible scientist.

The Sphere Experiment

In a series of five Nike-Cajun firings in the North Atlantic in November 1956, as part of the pre-IGY test program, three successful measurements of the density distributions at three

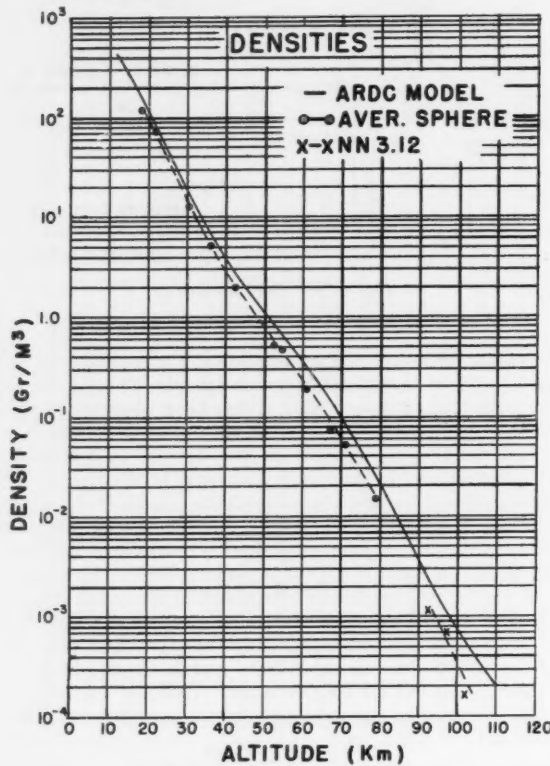


Fig. 5 Densities—sphere

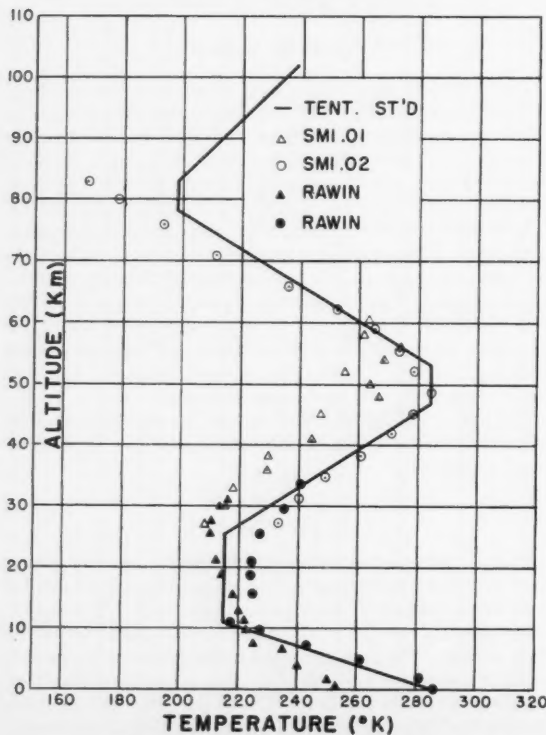


Fig. 6 Grenade data—temperatures

latitudes up to 80 km altitude have been obtained by the University of Michigan. The averaged preliminary data are shown in Fig. 5. An initial conclusion is that in this region of the atmosphere the densities are lower than the White Sands measurements which are the basis for the ARDC model atmosphere. Also plotted on the graph in the region 90 to 100 km are several points from Aerobee NN 3.12, fired at the same latitude at about the same time (Nov. 1956). The data are consistent.

These sphere samplings taken at latitudes of 49, 58 and 66 deg N when compared with the sphere data from Wallops Island (38 deg N) and White Sands (32 deg N) suggest a strong latitude variation in the densities at 50 km of about 2 per cent per deg of latitude. This is greater than we might have suspected.

The Grenade Experiment

The ten planned Aerobee-grenade firings of the joint Signal Corps-University of Michigan (Jones) program at Churchill have been successfully completed. Five winter firings and five summer firings were made. Some were daytime, some nighttime; on Jan. 27, 1958 firings were made at midnight and at noon, to measure the diurnal variation of temperatures and winds up to 90 km.

The reduction of the grenade data involves the determination of the positions of each of the grenade explosions from the Dovap records and the calculation of the angles of arrival of the sound waves. The calculation of the temperatures and winds (12) from these elements has been programmed on an IBM 650 computer so that the final steps of the reduction go quickly. But the Dovap reduction for positions is a matter of hand counting of the Doppler cycles, some 100,000 of them per firing, which takes several months. Data from firings SM 1.01 (Nov. 1956) and SM 1.02 (July 1957) have been reduced, and the preliminary results are shown in Figs. 6 (temperatures) and 7 (winds). We are not ready to assign probable errors to these measurements.

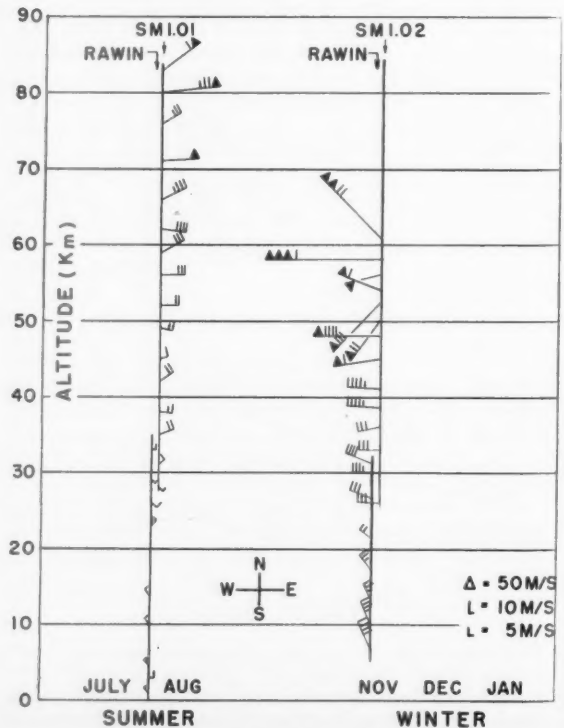


Fig. 7 Grenade data—winds

The temperature data show a difference between the summer and winter distributions throughout the entire altitude region. At 50 km, a maximum in the temperature distribution, the spread is about 20 C, a significant amount. The winter measurement is characterized by low temperatures below 50 km and large scatter from layer to layer. The summer sounding is, by contrast, quite smooth and shows an extremely low temperature at 80 km of 165 K. This is the lowest temperature we have measured in the atmosphere.

The temperature data obtained from radiosondes flown at the times of the rocket soundings are also plotted in the figure. The soundings overlap in the 30 km altitude region, and the data match quite well.

The grenade winds, shown in Fig. 7, have the characteristic summer-winter difference we have observed in the lower latitude measurements (4). The winds are weak and from the east in the summer, very strong and from the west in the winter. We have every reason to believe the data at this time, even the 150 m/sec velocity at 58 km. However, the analyses are preliminary.

An additional finding of the Churchill firings is the fact that above about 90 km the experiment does not work. Even with the 4-lb explosives, sufficient energy cannot be coupled into the atmosphere to permit sound arrivals at the ground. This is consistent with Schrodinger's early work on the absorption of sound in the atmosphere, since the mean-free-path at these altitudes is about equal to the wave lengths of the sound waves.

The Aerodynamic Experiment

As do all other experiments except the sphere experiment, the aerodynamic method needs detailed trajectory data before the alphasat measurements of the soundings can be converted to atmospheric parameters. At present no data from the six aerodynamic experiments on both Aerobees and Nike-Cajuns have been made available.

The Gage Experiments

Again, since the accurate trajectory data required for the complete analysis of measured parameters have taken considerable time and effort, the data reduction of the gage experiments is incomplete and preliminary; however, three successful firings have been carried out at Churchill. An initial reduction of data from NN 3.12 fired in November 1956 is plotted on Fig. 8, densities vs. altitude. Again throughout the entire region of the measurement, the densities are lower than those previously measured at White Sands (13). This is true up to about 200 km. The group of points in the lower right-hand corner are single measurements taken at the peaks of the other rocket trajectories when the velocities were minimal. Summer day (SD) densities are a factor of 20 higher than those of winter night (WN), and winter day (WD) a factor of 10 higher than winter night. The confirmation of these results will provide an extremely interesting insight into the dynamics of the high atmosphere. The winter night data are from NN 3.17.

Another measurement of interest was the ion-composition spectrometer firing of November 1956 (NN 3.17) which, because of favorable altitude throughout the upper leg of the trajectory, yielded density data between 100 and 200 km. These data are plotted on Fig. 9 with a comparison with the Panel data (13) and the average ascent-descent data of NN 3.12 (Fig. 8). If real, the day-night difference in densities at altitudes above 160 km is consistent with our present picture of the radiation processes in the ionosphere.

The USSR Results

We have seen no detailed results from the Russian meteorological soundings and suspect that the problem is the same as that of the American groups. The data processing takes

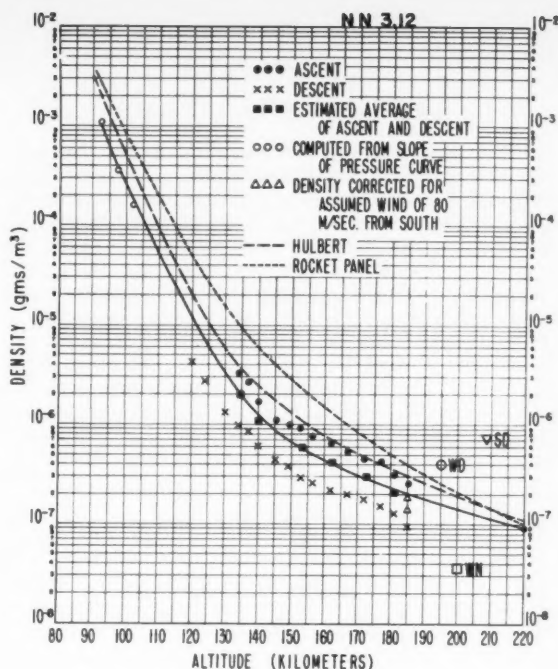


Fig. 8 NN 3.12 densities

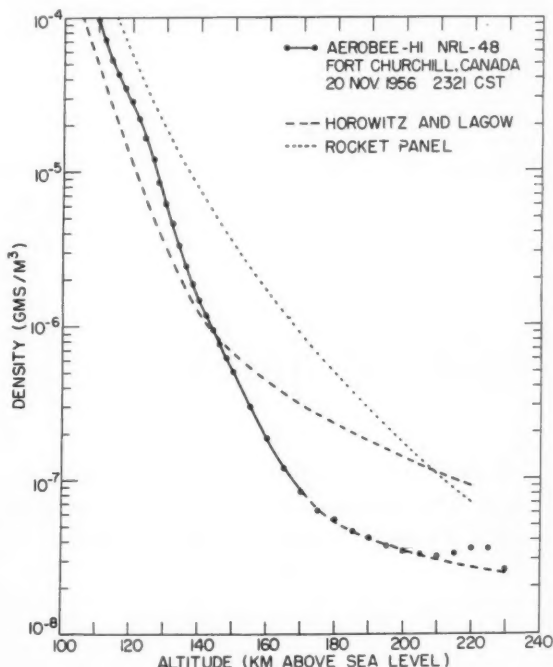


Fig. 9 NRL-48 (NN 3.17) densities

at least as long as the preparations. However, a Russian geophysical rocket, carrying ionization and magnetic gages in flight to 473 km, made measurements at 260 km on both ascent and descent. Results: Pressure at 260 km was 10^{-7} mm Hg. This could be compared to the ARDC model atmosphere in which at 260 km the pressure is 3×10^{-8} mm Hg. This suggests, as do the satellite data, that the densities at these altitudes above 200 km is higher than the

previous extrapolations of rocket soundings had led us to expect.

Some Comparisons of Results

Despite the tentative character of the results that have been presented here, the various figures have been drawn comparing these recent high latitude measurements with the ARDC or Panel model atmospheres which were based largely on the rocket data taken in middle latitudes. That there would be differences between the Arctic and the middle latitude data could be suspected; the winds in the atmosphere certainly suggest it. Thus, at high latitudes the density is apparently lower than the ARDC model up to about 200 km, above which altitude the densities are higher, as suggested by some of the satellite densities. A difficulty with the satellite measurements is that they are averages over changing geographic regions of the atmosphere; our recent data suggest considerable time and space variations in these parameters.

Conclusions

It would be premature to attempt to draw any far-reaching conclusions from the limited data now available. However, the number of successful firings that have been conducted when combined with those still to be fired within the IGY should yield an amount of data of sufficient quality to give a good understanding of the world-wide circulation patterns and the dynamic processes of the upper atmosphere. By the end of the IGY meteorological rocket soundings will have been made 60 deg N (Fort Churchill), 50 deg N (Russia), 32 deg N (White Sands), 12 deg N (Guam), and from shipboard at 50 to 65 deg N (North Atlantic) and 60 to 70 deg S (Antarctic). The analysis and interpretation of the data present an exciting prospect.

Acknowledgments

In addition to his colleagues at the Signal Research and Development Laboratory, particularly Dr. W. Nordberg and Capt. W. R. Bandeen, the author wishes to acknowledge the great contributions of the University of Michigan group

under L. M. Jones and F. L. Bartman in the conduct of the grenade experiment and in supplying the advance copy of the sphere data. H. E. LaGow, J. W. Townsend and C. Y. Johnson of the Naval Research Laboratory have contributed their data and time for discussion, as has Mr. N. W. Spencer of the University of Michigan.

References

- 1 General references: (a) Newall, H. E. "High Altitude Rocket Research," Academic Press, New York, 1953. (b) Boyd, R. L. F. and Seaton, M. J. (ed.), "Rocket Exploration of the Upper Atmosphere," Pergamon Press, London, 1954.
- 2 Jones, L. M. and Bartman, F. L., "Scientific Uses of Earth Satellites," ed by J. A. Van Allen, Univ. of Mich. Press, Ann Arbor, 1956, chap. 10.
- 3 Stroud, W. G. et al., *RSI*, vol. 26, 1955, p. 427.
- 4 Stroud, W. G., Nordberg, W. and Walsh, J. R., *Journal of Geophysical Research*, vol. 61, 1956, p. 45.
- 5 Sicsinsky, H. S., Spencer, N. W. and Down, W. G., *Journal of Applied Physics*, vol. 25, 1954, p. 161.
- 6 Taylor, G. I. and Maccoll, J. W., *Proc. Royal Society*, vol. 139A, London, 1939, p. 278.
- 7 Kopal, Z., Cambridge Technical Reports 1, 1947; 3, 1947, and 5, 1949.
- 8 Havens, R. J., Koll, R. T. and LaGow, H. E., *Journal of Geophysical Research*, vol. 57, 1952, p. 67.
- 9 LaGow, H. E. and Ainsworth, J., *Journal of Geophysical Research*, vol. 61, 1956, p. 77.
- 10 Townsend, J. W., *RSI*, vol. 23, 1952, p. 538.
- 11 Spencer, N. W., "Forty-seven Rocket Firings at Fort Churchill," ARS preprint no. 635-58, June 1958.
- 12 (a) Stroud, W. G., U. S. Army Signal Res. and Dev. Lab., Technical Memo 1570, April 1, 1954. (b) Nordberg, W., U. S. Army Signal Res. and Dev. Lab., Technical Memo 1856, Feb. 1, 1957.
- 13 "The Rocket Panel," *Physics Review*, vol. 88, 1952, p. 1027.
- 14 Soviet Bloc IGY Information, U. S. Dept. of Commerce, Office of Technical Services, Washington, D. C., April 4, 1958.
- 15 Blagonravov, A. A., *Vestnik Akad. Nauk, USSR*, vol. 6, 1957, p. 25; trans. E. R. Hope, Directorate of Sci. Inform. Service, DRB, Canada.
- 16 Mizhnevich, V. V., "Measurement of Pressure in the Upper Atmosphere," Rocket and Satellite Conference, Sept. 30-Oct. 5, 1957, National Academy of Sciences, Washington, D. C.

Technical Notes

Influence of Approach Boundary Layer Thickness on Premixed Propane-Air Flames Stabilized in a Sudden Expansion

WILLIAM T. SNYDER¹

Gas Dynamics Laboratory, Northwestern University,
Evanston, Ill.

Nomenclature

δ = boundary layer thickness

Received June 14, 1958.

¹ Now Assistant Professor of Mechanical Engineering, North Carolina State College, Raleigh, N. C.

L = distance from leading edge of flat plate to point of flame stabilization
 Re = Reynolds number
 V_0 = free stream velocity
 ρ = free stream density
 V_B = blowout velocity
 a, b = parameters in the equation $V_B = a + bRe$
 m = mass flux per unit width in boundary layer
 u = local velocity in boundary layer
 y = distance from flat plate
 ϕ = equivalence ratio

Introduction

THE stabilization of premixed flames in high velocity streams has received much attention in recent years. Nevertheless, there are a number of aspects of flame stabilization which deserve further study and consideration. One of these is the influence of the upstream boundary layer thickness

EDITOR'S NOTE: The Technical Notes and Technical Comments sections of JET PROPULSION are open to short manuscripts describing new developments or offering comments on papers previously published. Such manuscripts are published without editorial review, usually within two months of the date of receipt. Requirements as to style are the same as for regular contributions (see masthead page).

on the performance of a flameholder. In previous work, Putnam (3)² studied the importance of laminar boundary layers on the stability limits of premixed propane-air flames stabilized on axial rod flameholders. Putnam controlled the boundary layer thickness by providing suction grooves along the rod and varied the boundary layer thickness by a factor of two. He found that as long as the boundary layer and the main flow are nonturbulent, the thickness of the former has little bearing on the limits of stabilization. Gross (2) studied stabilization on the trailing edge of a very thin plate aligned parallel to a laminar flow. He determined that with a laminar boundary layer, a flame may be stabilized on a flat plate without separation and in the absence of turbulent eddies. In his analysis Gross showed that the velocity gradient may be used conveniently in the correlation of the data. The work of both Gross and Putnam was concerned with laminar boundary layers, and their applicability to the turbulent regime requires further study.

Zierner and Cambel (5) experimentally investigated the stabilization of propane-air flames in the boundary layer of a heated flat plate maintained at constant temperature. Their investigation was concerned with true boundary layer burning in which a mechanism of recirculation of hot gases was not necessary for stabilization. They demonstrated that the point of stabilization of a flame in a laminar boundary layer corresponds to a position at which the local velocity in the boundary layer equals the flame propagation velocity.

With a laminar boundary layer, there will be some point in the boundary layer at which the velocity is equal to the burning velocity of the combustible mixture, and thus a flame may be stabilized. However, the existence of such a condition is not a sufficient condition for flame stabilization, but the quenching distance must be considered also. Flame stabilization may be expected if the burning velocity equals the local velocity at a distance from the solid boundary at least equal to the quenching distance. However, it is well known that for flame stabilization in highly turbulent streams a zone of recirculation is necessary.

In this investigation the effect of the approach boundary layer on flame stabilization was studied. In particular, a Reynolds number range of 1.5×10^5 to 8.65×10^5 was considered. It was noticed that decreasing the boundary layer thickness at the flameholder decreased the maximum blowoff velocity and the range of the stability curves while shifting them in the direction of richer mixtures.

For a turbulent boundary layer, the thickness is given by Schlichting (4) by the following equation

$$\delta(L) = \frac{0.37L}{(Re)^{1/5}} \quad [1]$$

where the Reynolds number is defined as

$$Re = \frac{V_0 L \rho}{\mu} \quad [2]$$

It follows from Equations [1 and 2] that the boundary layer thickness increases as $L^{4/5}$.

Description of Apparatus and Experiments

The tests were conducted in a combustion tunnel of conventional design having a rectangular cross-section test chamber. The flame was stabilized at the edge of a sudden expansion in the chamber walls (1). In accordance with Equation [1], the boundary layer thickness at the point of stabilization was varied by changing the characteristic length L preceding the sudden expansion. The flameholder geometry is illustrated in Fig. 1. In making the boundary layer calculations, no corrections were made for the laminar boundary layer present in the initial stage of boundary layer development.

The blowout data for the three approach lengths used are shown in Fig. 1. The curves indicate that the flameholder

² Numbers in parentheses indicate References at end of paper.

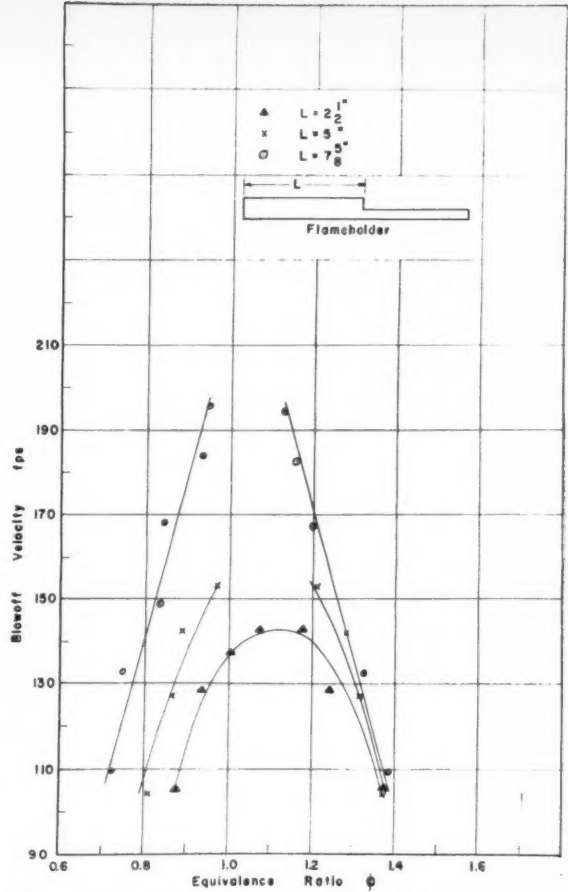


Fig. 1 Blowout velocity vs. equivalence ratio for different approach lengths

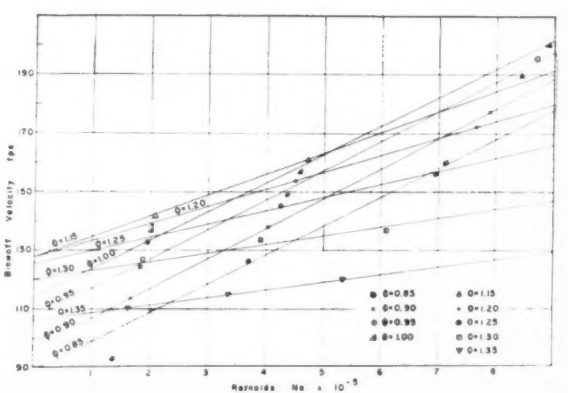


Fig. 2 Blowout velocity vs. Reynolds number for constant equivalence ratio

performance is improved as the thickness of the boundary layer at the point of stabilization is increased. The blowout data were correlated in the following manner. From Fig. 1, a cross plot of blowout velocity vs. Reynolds number at constant equivalence ratio was made. This family of curves is shown in Fig. 2. The curves of Fig. 2 can be described analytically as

$$V_B = a + bRe \quad [3]$$

Since the family of curves in Fig. 2 has the equivalence

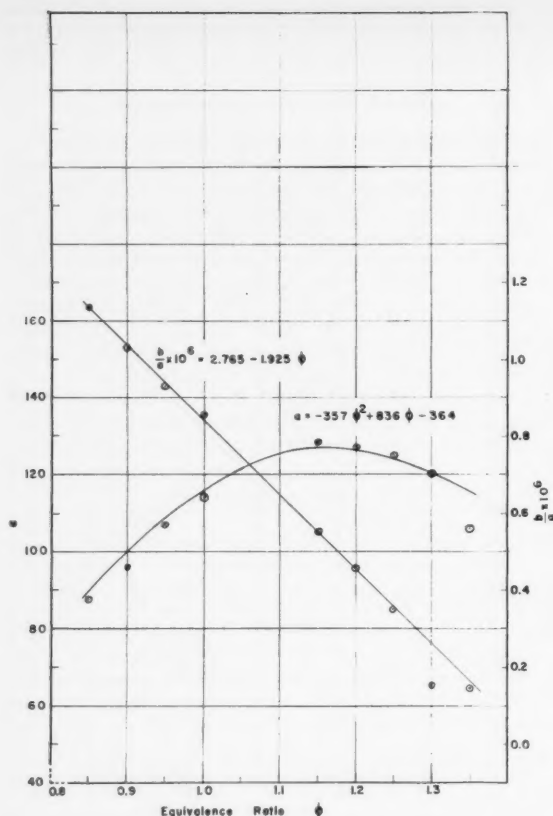


Fig. 3 Curves of parameters a and b/a vs. equivalence ratio

ratio as parameter, it follows that the following functional expressions may be written

$$V_B = f(\phi, Re) \dots \dots \dots [4]$$

$$a = F(\phi) \dots \dots \dots [5]$$

$$b = G(\phi) \dots \dots \dots [6]$$

Values of a and b were determined from Fig. 2, and analytical expressions for a and b in terms of equivalence ratio were obtained. Fig. 3 illustrates the degree of scatter of the experimental values of a and b from the analytical curves obtained. The ratio b/a is plotted in Fig. 3 for later use.

Since the curves of Fig. 1 indicated that thickening the boundary layer at the point of stabilization widened the stability limits, it seemed reasonable to expect some degree of correlation between blowout velocity and mass flow rate in the boundary layer. Such a correlation was obtained as follows:

The mass flow rate per unit width in the boundary layer is given by the expression

$$m = \int_0^\delta \rho u dy \dots \dots \dots [7]$$

Since the boundary layer at the sudden expansion is turbulent, a velocity distribution obeying the $\frac{1}{7}$ law is assumed. Thus

$$\frac{u}{V_0} = \left(\frac{y}{\delta}\right)^{1/7} \dots \dots \dots [8]$$

Substituting [8] in [7] and integrating yields

$$m = \frac{7}{8} V_0 \delta \rho \dots \dots \dots [9]$$

In integrating Equation [7], the fluid may be assumed in-

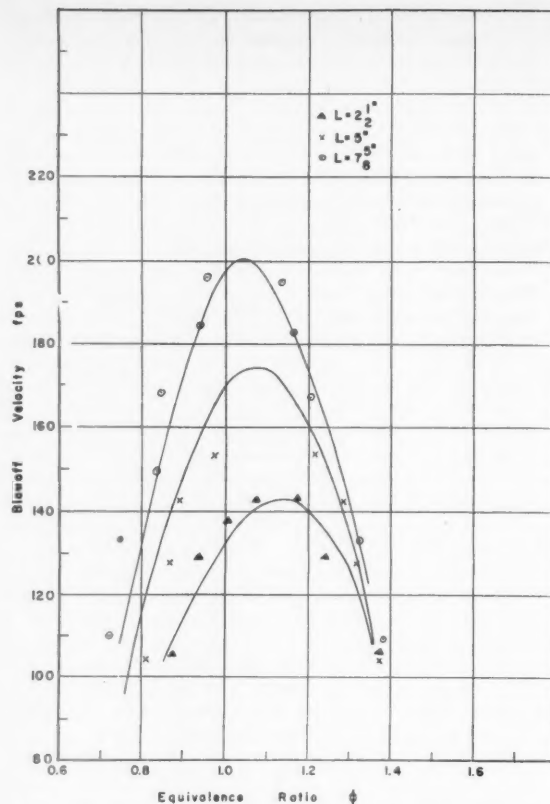


Fig. 4 Analytical blowout curves with experimental data

compressible, because of the relatively low free stream velocities preceding the flameholder. Combining Equations [1, 2 and 9] yields

$$m = 10.42 \mu Re^{4/5} \dots \dots \dots [10]$$

Substituting the value of μ for a stoichiometric air-propane mixture at 70 F gives

$$m = (10.42)(3.31 \times 10^{-7}) Re^{4/5} \dots \dots \dots [11]$$

or

$$Re = 671 m^{5/4}$$

Combining Equations [3 and 11] yields

$$V_B = c(1 + dm^{5/4}) \dots \dots \dots [12]$$

where

$$c = c(\phi) = -357\phi^2 + 836\phi - 364 \dots \dots \dots [13]$$

$$d = d(\phi) = 10^{-8}(1.855 - 1.29\phi) \dots \dots \dots [14]$$

Using Equations [12, 13 and 14], blowout curves were calculated for the three characteristic lengths used in the experiments. These curves are shown in Fig. 4 along with the experimental points for comparison. Fig. 4 serves to define the maximum blowout points which were not obtainable experimentally due to an inadequate air supply. This correlation of data indicates that for the recessed wall flameholder in the operating range covered by these experiments, the parameters determining the blowout velocity are the equivalence ratio and the mass flow rate in the boundary layer at the sudden expansion.

The length of the recirculation zone was observed by NaCl

injection and was found to be essentially constant above a certain minimum Reynolds number, about 2.5×10^6 . At a fixed value of ϕ , the transport of active chemical species and thermal energy from the recirculation zone to the mixing zone must increase, up to a certain point, as the velocity of the main stream increases. Since the data correlation indicated that for a fixed value of ϕ , the boundary layer mass flow rate increased with an increasing blowout velocity, it appears that a thickened boundary layer improves flameholder performance by increasing the time rate of recirculation of hot gases. This reasoning can be made more plausible by a physical argument which follows.

A necessary condition for recirculation to occur is the existence of an adverse pressure gradient. Recirculation then occurs because the boundary layer fluid near the wall does not possess sufficient momentum to penetrate the increasing pressure field. Hence, fluid particles with relatively low momentum are decelerated, reach a zero velocity in the downstream direction, and are ultimately accelerated in the upstream direction. Thus as the boundary layer at the sudden expansion is thickened, more fluid becomes available with insufficient momentum to penetrate the adverse pressure gradient. This results in an increase in time rate of recirculation of hot gases. An increased rate of recirculation means an increased rate of energy and species flux to the mixing zone resulting in improvement of flameholder performance.

Acknowledgments

This paper is based on the M.S. thesis of the author. The author is indebted to the General Electric Company for a fellowship grant and to Northwestern University for financial aid through Faculty Research Project FR P103-54. Special thanks are due to Professor Ali Bulent Cambel, teacher and friend, for suggesting the topic and giving needed advice and encouragement.

References

1. Huellmantel, L. W., Ziemer, R. W. and Cambel, A. B., "Stabilization of Premixed Propane-Air Flames in Recessed Ducts," *JET PROPULSION*, vol. 27, Jan. 1957, p. 31.
2. Gross, R. A., "Boundary Layer Flame Stabilization," *JET PROPULSION*, June 1955, p. 288.
3. Putnam, A. A., "The Effect of Boundary Layer Thickness on Flame Stability," *Fuel*, July 1954, p. 355.
4. Schlichting, H., "Boundary Layer Theory-Turbulent Flows," U. S. NACA T.M. 1218, April 1949.
5. Ziemer, R. W. and Cambel, A. B., "Flame Stabilization in the Boundary Layer of Heated Plates," *JET PROPULSION*, vol. 28, no. 9, Sept. 1958, pp. 592-599.

Visibility of Orbital Points

W. J. BERGER¹ and J. R. RICUPITO²

Convair-Astronautics Division of General Dynamics Corp., San Diego, Calif.

Equations are developed for computing the values of time at which a vehicle, moving in a known ballistic orbit, appears visible to line-of-sight instrumentation at any specified geodetic station. Transformations are found for describing the vehicular position in orbital-plane coordinates, in geocentric fixed star coordinates, and in local spherical coordinates originating at the observing station.

Introduction

MODERN activity in astronautics has created a need for a simplified mathematical discussion concerning visi-

Received June 24, 1958.

¹ Sr. Research Engineer.

² Sr. Research Engineer. Now Research Specialist, Lockheed Missile Systems Division, Sunnyvale, Calif.

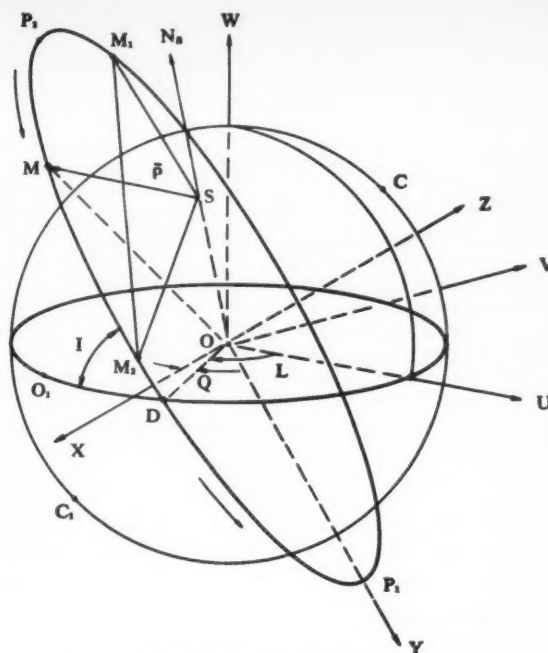


Fig. 1 Geometric configuration for satellite orbits

bility of orbital points. By "visibility of an orbital point" we mean that there exists a mathematical line joining a fixed station on Earth to an instantaneous position of an orbiting vehicle such that the line does not cut through the Earth. Neglecting refraction, this characterization of visibility applies especially to all "line-of-sight" instrumentation systems, e.g., optical cameras, radar, Dovap, Azusa, Minitrack, etc. Questions of visibility occur not only in test flights of missiles but also in tracking of satellite vehicles and in detection of enemy ICBM's.

General Theory

The general basis of the problem may be outlined as follows: In Fig. 1 let CC_1 represent the curved surface of the Earth; let S be an instrumentation station on the Earth, and let the curve M_1, M, M_2 denote the path of a vehicle (missile or artificial moon) moving in a gravitational orbit about the Earth. The plane tangent to the Earth at S cuts the orbit at points M_1 and M_2 , and we suppose that the vehicle passes M_1 before M_2 .

Assume a geocentric equatorial Cartesian system with (U, V, W) axes having constant directions relative to the "fixed stars."³ The W axis may be taken coincident with the axis of rotation of the Earth.⁴ In the (U, V, W) system let the orbit of M be represented by the functions

$$U = \alpha(t) \quad V = \beta(t) \quad W = \gamma(t) \dots \dots \dots [1]$$

As an approximate picture, sufficient for our purpose, we can consider the orbit of M to be a fixed track relative to the equatorial (U, V, W) system, with the Earth spinning about the W axis at constant angular velocity Ω . Because of gravitational perturbations and other disturbing effects, such as collisions of the vehicle with ions and micrometeorites, the elements of an orbit may vary slowly with time. If such

³ The "fixed stars," an old astronomical term, denotes the stellar system which defines sidereal time.

⁴ Because of precession and nutation, the axis of the Earth is not strictly constant in direction, but these effects are negligible in our problem.

variations are known functions of time, they can be readily included in our theory, since they enter only algebraically, and we do not have occasion to evaluate their time derivatives. Any station S on the Earth has known coordinates as functions of time.

$$\begin{bmatrix} U \\ V \\ W \end{bmatrix} = \begin{bmatrix} \rho \cos \Omega t \\ \rho \sin \Omega t \\ S_w \end{bmatrix} \dots \dots \dots [2]$$

where ρ and S_w are constants determined by the figure of the Earth.

When a particular mathematical model is assumed to represent the figure of the Earth, we can specify, as a known function of time, the unit vector \bar{N}_S normal to the Earth at S . We can construct, as a function of time, the vector $\bar{P} = \overline{SM}$ joining S to any orbital point M regardless of whether or not this vector cuts through the Earth.

Any value of time for which M is visible from S must satisfy the inequality

$$\bar{P} \cdot \bar{N}_S \geq 0 \dots \dots \dots [3]$$

If $\bar{P} \cdot \bar{N}_S < 0$, then the point M is not visible from S . Values of time t_{M_1} and t_{M_2} such that $\bar{P} \cdot \bar{N}_S = 0$ determine the first and the last visible points M_1 and M_2 .

For $t_{M_1} \leq t \leq t_{M_2}$ it will be of interest to transform (α, β, γ) into local coordinates originating at S .

Specialized Kinematic Theory

To obtain a simple mathematical method, we assume that

$$r = a - ae \left[1 - (1 + 2e + 3e^2 + 4e^3)\theta^2 - \frac{e}{3}(1 + 5e + 15e^2)\theta^4 + \dots \right] \dots \dots \dots [7]$$

the orbiting vehicle describes a Keplerian ellipse with the centroid of the Earth as one focus. Since the gravitational potential function of the Earth is not spherically symmetrical, the elliptical orbit will be subject to dynamic perturbations which we shall not consider. However, we retain the spheroidal shape of the Earth insofar as it influences the geometry of the problem.

POSITION IN THE ORBITAL PLANE In Fig. 1, curve M_1, M, M_2 now represents an ellipse with one focus at the centroid O of the Earth. Let X, Y and Z be orthogonal Cartesian axes originating at O with the Z axis normal to the plane of the orbit and the Y axis pointing toward the perigee P_1 . We suppose the orientation to be such that, if \bar{X}, \bar{Y} and \bar{Z} are unit vectors along these axes, then the rotation of the X axis into the Y axis gives the sense of motion of the orbiting vehicle provided that the vector product $\bar{X} \otimes \bar{Y} = \bar{Z}$.

In classical mechanics, six "elements" are necessary to define an elliptical orbit. These are

- a = semimajor axis of the ellipse
- e = eccentricity
- t_0 = time of perigee passage

and three angles (I, L, Q) which fix the orientation of the orbit. Usually these angles are defined as being

- I = inclination of the orbit. We take I positive when measured from the equatorial plane toward the orbital plane on the descending side of the orbit.
- L = longitude of a node (ascending or descending). In Fig. 1 we show L as positive measured westward in the equatorial plane from the U axis to the line OD which points to the descending node D .
- Q = angle between the major axis of the orbit and a nodal line. We take Q positive when measured from the X axis to the line OD of the descending node D .

The position of the vehicle in the orbit is described by Kepler's equations

$$\begin{aligned} r &= a(1 - e \cos E) \\ \frac{2\pi(t - t_0)}{T} &= \theta = E - e \sin E \dots \dots \dots [4] \\ \tan \frac{A}{2} &= \left(\frac{1+e}{1-e} \right)^{1/2} \tan \frac{E}{2} \end{aligned}$$

where

- t_0 = time of perigee passage
- t = any later time
- T = periodic time
- E = eccentric anomaly
- $r = |\overline{OM}|$ = radial distance of the vehicle at time t
- θ = "mean anomaly"
- A = "true anomaly" = angle described by OM in the orbital plane during the time between the most recent perigee passage and the present position at time t .

As in the text by Smart (4),⁶ series expressions for E, A and hence r can be developed in terms of θ , namely

$$E = \theta + \left(e - \frac{e^3}{8} \right) \sin \theta + \frac{e^2}{2} \sin 2\theta + \frac{3e^3}{8} \sin 3\theta + \dots \dots \dots [5]$$

$$A = \theta + \left(2e - \frac{e^3}{4} \right) \sin \theta + \frac{5e^2}{4} \sin 2\theta + \frac{13e^3}{12} \sin 3\theta + \dots \dots \dots [6]$$

These expansions (2) were originally obtained by Lagrange.

Laplace proved that Equation [5] converges if $e < 0.662743$; a condition which happens to hold for orbits of most ballistic missiles and satellites.

Adding $\pi/2$ to A , we obtain ψ , the usual polar angle of OM measured in the orbital plane counterclockwise from the X axis.

Hence

$$\begin{aligned} x &= r \cos \psi = -r \sin A \\ y &= r \sin \psi = r \cos A \\ z &= 0 \end{aligned} \dots \dots \dots [8]$$

gives the position of the vehicle in the (X, Y, Z) system at any time t .

POSITION IN THE (U, V, W) SYSTEM By vectorial geometry (3), with $(\bar{X}, \bar{Y}, \bar{Z})$ and $(\bar{U}, \bar{V}, \bar{W})$ as unit orthogonal vectors along the respective axes, we find

$$\begin{bmatrix} \bar{X} \\ \bar{Y} \\ \bar{Z} \end{bmatrix} = \begin{bmatrix} x_u x_v x_w \\ y_u y_v y_w \\ z_u z_v z_w \end{bmatrix} \begin{bmatrix} \bar{U} \\ \bar{V} \\ \bar{W} \end{bmatrix} \dots \dots \dots [9]$$

where

$$\begin{aligned} x_u &= \cos L \cos Q - \cos I \sin L \sin Q \\ x_v &= -\sin L \cos Q - \cos I \cos L \sin Q \\ x_w &= \sin I \sin Q \\ y_u &= \cos L \sin Q + \cos I \sin L \cos Q \\ y_v &= -\sin L \sin Q + \cos I \cos L \cos Q \\ y_w &= -\sin I \cos Q \\ z_u &= \sin I \sin L \\ z_v &= \sin I \cos L \\ z_w &= \cos I \end{aligned}$$

⁵ Traditionally the mean anomaly is denoted by the symbol M which then conflicts with the symbol for mass.

⁶ Numbers in parentheses indicate References at end of paper.

Since Equation [8] gives the components (x, y, z) of the position vector $\bar{R}(t)$ of the vehicle in the (X, Y, Z) system, we have by Equation [9]

$$\bar{R} = (x, y, z) \begin{bmatrix} \bar{X} \\ \bar{Y} \\ \bar{Z} \end{bmatrix} = (x, y, z) \begin{bmatrix} x_u & x_v & x_w \\ y_u & y_v & y_w \\ z_u & z_v & z_w \end{bmatrix} \begin{bmatrix} \bar{U} \\ \bar{V} \\ \bar{W} \end{bmatrix} \dots [10]$$

CRITERION OF VISIBILITY

If

- \bar{S} = position vector of station S relative to O
- Ω = angular velocity of Earth rotation
- ρ = distance from the W axis to S
- ϕ = geodetic latitude (1) of station S
- t_0 = time of perigee passage
- λ_0 = longitude of the station S at t_0

measured in the (U, V) plane from the U axis in same sense (clockwise) as L , then the angle η between U and the projection of S in the (U, V) plane, measured counterclockwise from U is given by

$$\eta = \Omega(t - t_0) - \lambda_0 \dots [11]$$

Hence

$$\bar{S} = S_u \bar{U} + S_v \bar{V} + S_w \bar{W} \dots [12]$$

$$\begin{bmatrix} S_u \\ S_v \\ S_w \end{bmatrix} = \begin{bmatrix} \rho \cos \eta \\ \rho \sin \eta \\ S_w \end{bmatrix} \dots [13]$$

and \bar{N}_s , the unit normal vector at S , is given by

$$\bar{N}_s = N_u \bar{U} + N_v \bar{V} + N_w \bar{W} \dots [14]$$

$$\begin{bmatrix} N_u \\ N_v \\ N_w \end{bmatrix} = \begin{bmatrix} \cos \phi \cos \eta \\ \cos \phi \sin \eta \\ \sin \phi \end{bmatrix} \dots [15]$$

By Equations [3, 12, 14], the criterion of visibility is

$$(\bar{R} - \bar{S}) \cdot \bar{N}_s \geq 0 \dots [16]$$

POSITION RELATIVE TO THE STATION At the station S , let (S_1, S_2, S_3) be an orthogonal coordinate system with the S_3 axis pointing upward (along \bar{N}_s), and the S_1 and S_2 axes pointing east and north, respectively.

Let ($\bar{S}_1, \bar{S}_2, \bar{S}_3$) be unit vectors along the (S_1, S_2, S_3) axes.

We have already defined $\bar{S}_3 = \bar{N}_s$ by Equations [14 and 15]. Similarly

$$\bar{S}_1 = (-\sin \eta) \bar{U} + (\cos \eta) \bar{V} \dots [17]$$

$$\bar{S}_2 = -(\sin \phi \cos \eta) \bar{U} - (\sin \phi \sin \eta) \bar{V} + (\cos \phi) \bar{W} \dots [18]$$

Since $\bar{M} = \bar{R} - \bar{S}$ is the position of the vehicle M relative to S , then the coordinates of M in the (S_1, S_2, S_3) system are

$$(\bar{M} \cdot \bar{S}_1, \bar{M} \cdot \bar{S}_2, \bar{M} \cdot \bar{S}_3) \dots [19]$$

Other useful coordinates relative to S are the azimuth α_s , elevation ϵ_s , and range R_s of M given by

$$\alpha_s = \arctan \frac{\bar{M} \cdot \bar{S}_1}{\bar{M} \cdot \bar{S}_2} \dots [20]$$

$$\epsilon_s = \arctan \frac{\bar{M} \cdot \bar{S}_3}{|\bar{M}|} \dots [21]$$

$$R_s = |\bar{M}| \dots [22]$$

References

- 1 Bomford, B. G., "Geodesy," Oxford University Press, London, England, 1952.
- 2 MacMillan, W. D., "Statics and the Dynamics of a Particle," McGraw-Hill, New York, 1927.
- 3 Milne, E. A., "Vectorial Mechanics," Interscience Publishers, Inc., New York, 1948.
- 4 Smart, W. M., "Spherical Astronomy," Cambridge University Press, England, 1956.

Calculation of Re-Entry Velocity Profile

ALFRED A. ADLER¹

Bell Aircraft Corp., Buffalo, N. Y.

A simple approximate equation, widely used to compute the velocity vs. altitude profile of a ballistic missile re-entering the Earth's atmosphere, gives quite a good approximation of the results sought. Modifications to the derivation of this equation are presented which include the effect of gravity and provide for a more accurate representation of the air density variation. These refinements, to a large extent, eliminate the deleterious effects of the assumptions made in the more simple equation without unduly increasing the complexity of the final relation. Two equations result, one covering the altitude range from initial re-entry down to 75,000 ft, the other providing for the remaining distance to sea level.

Nomenclature

- V = velocity, ft/sec
- h = altitude, ft
- ρ = air density, lb sec²/ft⁴
- $\beta = \frac{1}{h} \ln \frac{\rho_0}{\rho}$
- C_D = vehicle drag coefficient
- S = vehicle reference area, ft²
- W = vehicle weight, lb
- g = gravitational acceleration, ft/sec²
- γ = flight path angle with respect to local horizontal
- r = geocentric radius, ft
- $\lambda = g_s r_s^2, 14058.65 \times 10^{12}$ ft³/sec²
- $E' = \text{total energy per unit mass, } \frac{V^2}{2} - \frac{\lambda}{r}, \text{ ft}^2/\text{sec}^2$

Subscripts

- 0 = initial condition
- s = sea level
- k = assumed constant value

IN COMPUTING the velocity vs. altitude profile of a ballistic vehicle re-entering the Earth's atmosphere, the following equation is widely used

$$V = V_0 e^{-\alpha e^{-\beta h}} \dots [1]$$

where

$$\alpha = \frac{\rho_0 C_D S}{2 \beta_k W \sin |\gamma|} = \text{const}$$

and

$$\beta = \beta_k = 41.5 \times 10^{-6} \text{ ft}^{-1}$$

This equation results from solving the general equation of motion in the velocity direction, assuming that the effect of gravity is negligibly small compared to the drag effect, and assuming that β and α are constant. These assumptions are necessary to obtain a very simple solution.

Although Equation [1] yields a good approximation to the results sought for certain uses, a comparison of these predictions with a machine-computed numerical solution to the equation of motion assuming only that α remains constant, indicates that the assumptions of zero gravity and constant β made in the derivation of Equation [1] are to be avoided if possible. Due to the lack of a gravity term, the velocity predicted by Equation [1] decreases slowly with decreasing altitude for large values of altitude, whereas actually the velocity increases with decreasing altitude at high altitudes. Thus,

Received June 10, 1958.

¹ Aeromechanics Section, Space Flight Division. Member ARS.

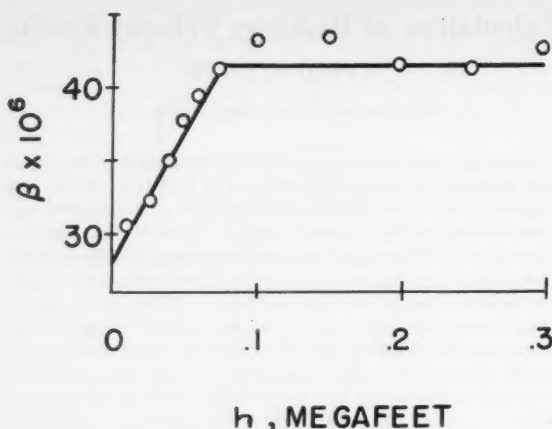


Fig. 1 β From ARDC 1956 data

$$\frac{C_D S}{W \sin \gamma} = .0013$$

$$V_0 = 20,000 \text{ FPS} ; h_0 = .3 \times 10^6 \text{ FT.}$$

----- $V_{\text{EQ. 1}} - V_{\text{NUM. SOL.}}$

———— $V_{\text{EQS. 2 \& 3}} - V_{\text{NUM. SOL.}}$

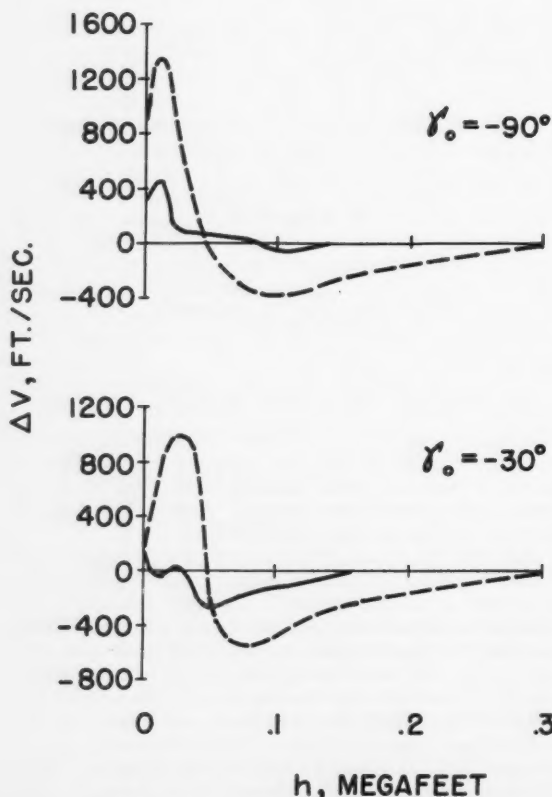


Fig. 2 Comparison of velocity profile results

the velocity vs. altitude profile given by Equation [1] for a particular problem will depend on the assumed initial re-entry altitude. The assumption that β remains constant, though a simplifying assumption, is at variance with published data (1).² It will be shown that it is possible to make modifications to the derivation of Equation [1] which, to a large extent, eliminate the deleterious effects of these two assumptions without increasing the complexity of the final relation unduly.

It is reasonable to state that the velocity of a re-entering ballistic vehicle at any point in its descent is the sum of the initial re-entry velocity, the velocity gained since initial re-entry due to gravity, and the velocity lost since initial re-entry due to drag. The velocity gained due to gravity can be determined by considering the interchange between potential and kinetic energy in an inverse square central force field. The velocity lost due to drag is essentially given by Equation [1]. Thus

$$V = \sqrt{2} \sqrt{E_0' + \frac{\lambda}{r_s + h}} + V_0(e^{-\alpha e^{-\beta h}} - 1) \dots [2]$$

This relation amounts to an analytical solution of the equation of motion assuming β and α are constant and that the gravity and drag effects are linearly independent. The addition of the gravity dependence increases the accuracy of the solution considerably, and makes the final result no longer dependent on the choice of initial re-entry altitude.

A plot of β vs. altitude from ARDC 1956 data (see Fig. 1) indicates that while $\beta = \text{const}$ is a good approximation above 75,000 ft, below this altitude β is more nearly a linear function of altitude. If Equation [1] is rederived, holding α constant and letting $\beta = \beta_k - m(75,000 - h)$ rather than a constant, and the results substituted in Equation [2] in place of the drag term, the relation to be used below 75,000 ft becomes

$$V = \sqrt{2} \sqrt{E_0' + \frac{\lambda}{r_s + h}} + V_0 \left\{ e^{-\alpha e^{-\beta_k h}} \times \exp \left(\frac{\alpha \beta_k e^b}{\sqrt{m}} \frac{\sqrt{\pi}}{2} [\text{erf}(\sqrt{m} h + \sqrt{b}) - \text{erf}(75,000 \times \sqrt{m} + \sqrt{b})] \right) - 1 \right\}$$

From Fig. 1, $\sqrt{m} = 13.416 \times 10^{-6} \text{ ft}^{-1}$, $\sqrt{b} = \beta_0/2\sqrt{m} = 1.0435$. Substituting these values

$$V = \sqrt{2} \sqrt{E_0' + \frac{\lambda}{r_s + h}} + V_0 \left\{ e^{-0.044490\alpha} \times \exp(8.1446\alpha[\text{erf}(13.416 \times 10^{-6} h + 1.0435) - 0.99626]) - 1 \right\} \dots [3]$$

Thus, the velocity vs. altitude profile calculation should be made using Equation [2] over the altitude range from initial re-entry down to 75,000 ft, and using Equation [3] from 75,000 ft to sea level. It is apparent that these equations may readily be adapted to the use of a piecewise constant α to allow for variable $C_D S/W \sin |\gamma|$.

A comparison of the differences between the velocity vs. altitude profiles computed by use of Equation [1] and by use of Equations [2 and 3] and the results of a machine-computed numerical solution of the equation of motion, holding α constant, is presented in Fig. 2 for two initial re-entry conditions. The results indicate that where greater accuracy is required without undue effort, Equations [2 and 3] may be used.

² Minzer, R. A. and Ripley, W. S., "The ARDC Model Atmosphere, 1956," Air Force Surveys in Geophysics no. 86, AFCRC TN-56-024, Dec. 1956.

Combustion Chamber Pressure Loss

S. L. BRAGG¹ and S. P. Q. BYWORTH²

Rolls-Royce Ltd., Derby, England

THE characteristic velocity and thrust coefficient values calculated for an ideal thrust chamber are based on the total pressure at the throat, P_t . The normal test bed measurement is that of static pressure at the injector plate, p_c . The following analysis demonstrates a simple method of calculating the ratio between the two pressures.

The equation of motion of flow in the combustion chamber, which is assumed to be parallel, and of area A_c , is

$$A_c p_c + Z = \frac{\dot{M} V}{g} + A_c p \dots [1]$$

where

Z = axial momentum of the liquid propellants at entry

\dot{M} = total propellant flow

p = static pressure at combustion chamber exit

V = velocity at combustion chamber exit

The actual characteristic velocity is defined by the relation

$$c^* = \frac{A_t P_t g}{\dot{M}} \dots [2]$$

where A_t is the throat area.

Substituting for \dot{M} in Equation [1] and rearranging

$$\frac{P_t}{p_c} = \left(1 + \frac{Z}{A_c p_c}\right) / \left(\frac{A_t V}{A_c c^*} + \frac{p}{P_t}\right) \dots [3]$$

Now the dimensionless groups V/c^* and p/P_t are functions of the area ratio A_t/A_c and the physical characteristics of the exhausting gases. The figure shows the variation of the denominator function

$$\left(\frac{A_t V}{A_c c^*} + \frac{p}{P_t}\right)^{-1}$$

with area ratio, for extreme values of the specific heat ratio $\gamma = 1.0$ and $\gamma = 1.4$. Also shown are two curves for the expansion of a typical mixture (2.35:1, oxygen:kerosene), assuming shifting (equilibrium) composition, and constant (frozen)

Received May 15, 1958.

¹ Supervisor, Performance Department, Rocket Division. Member ARS.

² Performance Engineer, Rocket Division.

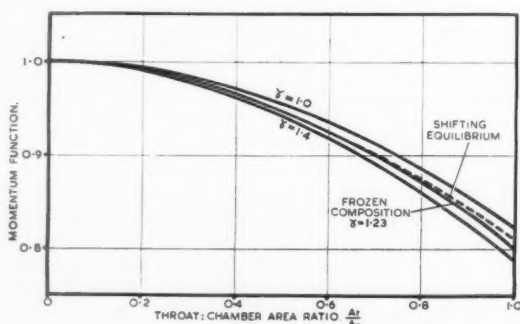


Fig. 1 Curves of momentum function $\left(\frac{A_t V}{A_c c^*} + \frac{p}{P_t}\right)^{-1}$ against throat: chamber area ratio A_t/A_c .

composition, respectively. The latter corresponds to $\gamma = 1.23$ approximately.

It is apparent that the value of γ , or the assumptions made as to composition changes during expansion, have comparatively little effect on the relation between the denominator function and the area ratio. Thus the relation is probably also unaffected by combustion inefficiency, or any other departure from ideal performance in the combustion chamber, and the mean curve can safely be used for practical analysis.

The term $Z/A_c p_c$ is usually small but *not* negligible compared to unity. If each propellant is injected under an injection pressure differential ΔP , through ports of effective area A_p , inclined at θ to the chamber axis

$$Z = \sum 2A_p \Delta P \cos \theta \dots [4]$$

This equation, used in conjunction with Equation [3] and the graph, enables the throat total pressure at any operating condition to be calculated from the measured injector end static pressure, in a very simple way.

An Empirical Method for Calculating Heat Transfer Rates in Resonating Gaseous Pipe Flow

GERALD MORRELL¹

National Aeronautics and Space Administration, Cleveland, Ohio

KUBIANSKII (1)² has shown experimentally that a sound field at resonance can produce an increase in heat transfer rate from a heated surface to surrounding air provided the velocity perturbations are at least as large as the steady velocity. Male, Kerslake and Tischler (2) have reported large increases in wall erosion rates (hence, heat transfer rates) accompanying large amplitude resonance burning in cylindrical rocket combustors. Since exact solutions of the energy and flow equations even for simplified cases of linear perturbations are tedious and difficult (3), it appeared that an approximate method suitable for many engineering applications would be worthwhile.

In this presentation the following major assumptions have been made:

1 The perturbations are sufficiently similar to shocks that the one-dimensional pressure-velocity relations for normal shock waves can be used.

2 The usual Stanton number-Reynolds number-Prandtl number relation applies to both resonance and steady flow provided suitable average conditions behind the shock are selected.

3 The effect of aerodynamic heating due to the oscillations can be treated as a correction factor to the quasi-steady state solution.

The ratio of resonance heat transfer to steady-state heat transfer may be defined as

$$R \equiv \frac{q_{res}}{q_0} = \frac{h_s(T_s - T_w)}{h_0(T_s - T_w)}$$

where T is absolute temperature, and subscripts s , 0 and w refer to average conditions behind the shock, steady conditions, and wall conditions, respectively. The latter condition is assumed the same for both cases. The film coefficient h is given by

$$h \propto c_p \rho V \left(\frac{DV_p}{\mu}\right)^{-0.2} \left(\frac{c_p \mu}{k}\right)^{-0.6}$$

Received June 20, 1958.

¹ Chief, Rocket Chemistry Branch, Lewis Research Center. Member ARS.

² Numbers in parentheses indicate References at end of paper.

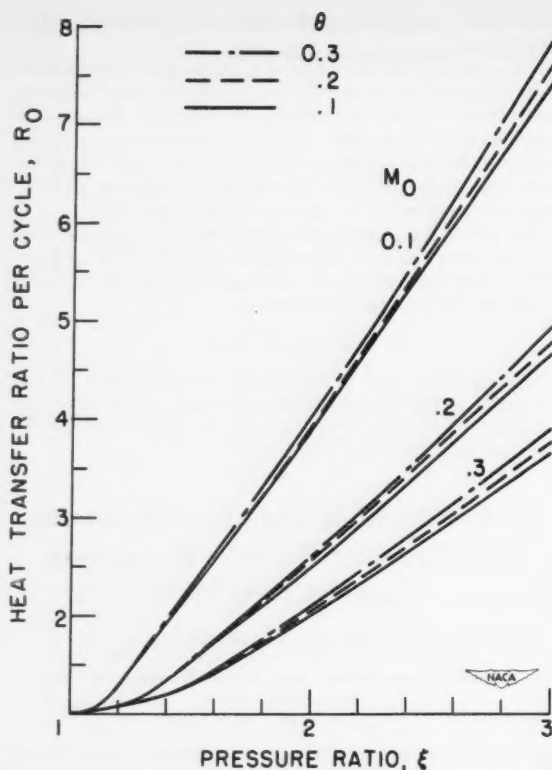


Fig. 1 Typical curves of heat transfer ratio as a function of pressure ratio for several values of Mach number M_0 and temperature ratio θ

where the symbols have their usual meaning. Assuming that the ideal gas law applies, that (μ/k) , molecular weight and heat capacity are invariant, and that $\mu \propto T$, the heat transfer ratio becomes

$$R = \left(\frac{V_s}{V_0}\right)^{0.8} \left(\frac{p_s}{p_0}\right)^{0.8} \left(\frac{T_s}{T_0}\right)^{-0.8} \left(\frac{T_s - T_w}{T_0 - T_w}\right)$$

where p is pressure.

The ratio of maximum pressure behind the shock to steady-state pressure is assumed to be nearly equal to the shock pressure ratio

$$\xi \equiv \frac{p_2}{p_1} \approx \frac{p_{s,\max}}{p_0}$$

and the shock temperature ratio T_2/T_1 as given in (4) is assumed to be nearly equal to the ratio of maximum temperature behind the shock and steady-state temperature

$$\frac{T_2}{T_1} = \frac{\xi(\xi + \alpha)}{\alpha\xi + 1} \approx \frac{T_{s,\max}}{T_0}$$

where $\alpha = (\gamma + 1)/(\gamma - 1)$ and γ is the specific heat ratio. For one-dimensional flow, the particle velocity behind the shock (5) is given by

$$V_{s,\max} = V_0 \pm \frac{(\alpha - 1)(\xi - 1)a_0}{\sqrt{(\alpha + 1)(1 + \alpha\xi)}}$$

where a_0 is the speed of sound at temperature T_0 , the plus sign is for a wave moving in the same direction as the undisturbed velocity V_0 , and the minus sign is for a wave moving in the opposite direction. For a reflected wave, the heat transfer ratio per cycle will be given by the average of these two conditions.

For these calculations average conditions behind the shock were chosen

$$x_s = 0.5x_0 \left(\frac{x_{s,\max}}{x_0} + 1 \right)$$

where x is velocity, pressure or temperature. The expressions for heat transfer ratio become

$$R_+ = \frac{0.5[A_+ + 1]^{0.8}(\xi + 1)^{0.8}[0.5(B + 1) - \theta]}{(B + 1)^{0.6}(1 - \theta)}$$

and

$$R_- = \frac{0.5[A_- + 1]^{0.8}(\xi + 1)^{0.8}[0.5(B + 1) - \theta]}{(B + 1)^{0.6}(1 - \theta)}$$

where the plus subscript is for the forward facing wave and the minus subscript for the reflected wave, and

$$\theta = \frac{T_w}{T_0}$$

$$A_+ = 1 + \frac{(\alpha - 1)(\xi - 1)}{M_0\sqrt{(\alpha + 1)(1 + \alpha\xi)}}$$

$$A_- = 1 - \frac{(\alpha - 1)(\xi - 1)}{M_0\sqrt{(\alpha + 1)(1 + \alpha\xi)}}$$

$$B = \frac{\xi(\xi + \alpha)}{\alpha\xi + 1}$$

and M_0 is the Mach number of the undisturbed flow.

The correction for aerodynamic heating due to gas oscillations is assumed to be given by Ostrach's derivation (6) for an oscillating flat plate. The expression, in terms of a heat transfer ratio, may be written

$$R' = 1 + \frac{V_s^2\sqrt{Pr}(\pi - \sqrt{Pr})}{4c_pT_0(1 - \theta)}$$

and

$$R'_+ = 1 + \frac{\sqrt{Pr}(\pi - \sqrt{Pr})\left(\frac{\alpha + 1}{\alpha - 1}\right)R_uM_0^2}{16\pi m(1 - \theta)} (A_+^2 + 2|A_+| + 1)$$

$$R'_- = 1 + \frac{\sqrt{Pr}(\pi - \sqrt{Pr})\left(\frac{\alpha + 1}{\alpha - 1}\right)R_uM_0^2}{16\pi m(1 - \theta)} (A_-^2 + 2|A_-| + 1)$$

where Pr is Prandtl number, R_u is the universal gas constant and m is gas molecular weight.

The overall heat transfer ratios are

$$R_{0+} = R_+ R'$$

and

$$R_{0-} = R_- R'$$

and for a reflecting wave, the heat transfer ratio per cycle is given by

$$R_0, \text{ per cycle} = \frac{R_{0+} + R_{0-}}{2}$$

For small values of M_0 and large values of ξ , $|A|$ for the two cases will be nearly the same, and it becomes unnecessary to perform the averaging process in view of the other approximations involved. Fig. 1 is a plot of R_0 per cycle as a function of ξ for several values of θ and M_0 , and for $c_p = 0.3$ Btu/lb deg R, $\gamma = 1.25$ ($\alpha = 9$), $m = 22$, and $Pr = 0.75$. The latter values are typical of some rocket combustion gases.

If the erosion rates of (2) are assumed to be proportional to heat transfer rates, these data may be used to check the calculation method. From the engine performance data the

values of M_0 and T_0 are calculated to be 0.125 and 3650 R, respectively. The values of c_p , α , m and Pr may be assumed to be the same as those above. The softening point of the plastic used for a wall material is given in (7) as 713 deg R, so that θ is approximately 0.2. For longitudinal waves the only measured value of ξ was about 2, and the experimental value of R_0 was about 3; the calculated value of R_0 is 3.37. For the traveling wave form of the transverse oscillations ξ is about 3.7, and the maximum experimental value of R_0 is about 11. Assuming the same values for M_0 and θ (this neglects the difference in direction for V_0 and V_s) and considering only the forward traveling wave, the calculated value of R_0 is 9.86. This agreement indicates that the calculation method presented can give useful engineering estimates of the heat transfer rates produced in a resonating flow.

References

- 1 Kubianskii, P. N., "Effect of Acoustical Vibrations of Finite Amplitude on the Boundary Layer," *Journal Tech. Phys. (USSR)*, vol. 22, 1952, p. 593.
- 2 Male, T., Kerslake, W. R. and Tischler, A. O., "Photographic Study of Rotary Screaming and Other Oscillations in a Rocket Engine," NACA RM E54A29, 1954.
- 3 Illingworth, C. R., "The Effects of a Sound Wave on the Compressible Boundary Layer on a Flat Plate," *Journal of Fluid Mechanics*, vol. 3, pt. 5, 1958, p. 471.
- 4 Ames Research Staff, "Equations, Tables, and Charts for Compressible Flow," NACA Rep. 1135, 1953, p. 8. (Supersedes NACA TN 1428.)
- 5 Courant, R. and Friedrichs, K. O., "Supersonic Flow and Shock Waves," Interscience Pub. Inc., 1948, chap. III, C.
- 6 Ostrach, S., "Note on the Aerodynamic Heating of an Oscillating Surface," NACA TN 3146, 1954.
- 7 Hodgman, C. D. (ed.), "Handbook of Chemistry and Physics," Thirty-eighth ed., Chem. Rubber Pub. Co., 1955-1956.

The Gasification of Solid Ammonium Nitrate¹

W. H. ANDERSEN,² K. W. BILLS,³ A. O. DEKKER,⁴
E. MISHUCK,⁵ G. MOE⁶ and R. D. SCHULTZ⁷

Aerjet-General Corp., Azusa, Calif.

When the surface of solid ammonium nitrate is superheated by a high flux heating technique the ammonium nitrate decomposes in a different manner than the bulk phase liquid.

Introduction

IN ORDER to understand the burning of ammonium nitrate (AN) composite propellants, information is required about the rates and the nature of the chemical reactions occurring in the surface layer of initially solid oxidizer which is exposed to the flame zone. A number of investigations have been directed toward an elucidation of the mechanism of the thermal decomposition of AN (1).⁸ However, in all instances, the studies were carried out with the molten salt. There is general agreement that N_2O and H_2O are the chief products of the decomposition of the liquid, from 169.6 C

(melting point) to about 260 C, and at atmospheric pressure. At higher temperatures and pressures, side reactions occur in the gas phase between the small amounts of the dissociation products, HNO_3 and NH_3 . The extent to which these side reactions occur increases with the temperature of the liquid and with the ratio of the exposed surface to the volume of the melt. Kinetically, the liquid phase (bulk) decomposition is a first order reaction, having an activation energy of about 38 kcal/mole (2). The reaction is exothermic to the extent of about 9 kcal/mole.

This note describes some experiments in which the surface of solid AN is heated at such a high rate of heat input that the surface gasifies at a rate which is much greater than the bulk decomposition rate. Under these conditions the surface gasification reaction proceeds by a mechanism which involves a small activation energy (about 7 kcal/mole), is highly endothermic, and produces essentially only HNO_3 vapor and NH_3 as the primary products. This surface reaction is the direct result of the fast rate of heating of the surface, and appears to involve the same phenomena of solid superheating reported by Schultz and Dekker for ammonium chloride (2).

Experiment

The linear gasification rate of solid AN was measured as a function of surface temperature (T_s) with an improved version of the "hot plate" device described by Schultz and Dekker (2). This method has the important advantage of close simulation of conditions that exist during propellant burning. Briefly, the measurements were made by pressing strands of AN against a heated surface, and measuring the linear rates of regression of the surface of the samples as a function of T_s . T_s was measured by means of a thin, flattened thermocouple which was interposed between the sample surface and a thin sheet of mica covering the hot element. The apparatus used was a prototype of the hot plate pyrolysis apparatus which is described in detail elsewhere (3). The samples were pressed vertically against the surface of the heating element with a constant loading pressure of about 750 gm/cm². The measurements were made in an atmosphere of nitrogen at pressures of 3, 14.7 and 600 psia. In the experiments, the samples gasified cleanly; little evidence for the accumulation of liquid or solid residues was observed.

The AN strands were prepared for pyrolysis by pressing dry, cp AN powder (particle size about 10 μ) in a steel die to a pressure of 17,000 psi. Density measurements (oil immersion method) indicated that average strand densities of about 1.69 gm/cm³ were obtained. The strands thus were close to crystal density, 1.72 gm/cm³.

Results and Discussion

The experimental linear pyrolysis rates B for strands of AN are shown in Fig. 1. The dependence of the pyrolysis rate on surface temperature in the range 180 to 300 C can be represented to good approximation by the equation

$$B = 120 \exp(-7100/RT_s) \text{ cm/sec.} \dots \dots \dots [1]$$

where T_s is the surface temperature, K, and R is the gas constant. With the available apparatus, the activation energy is believed to be reliable to only about ± 3 kcal. However, this fact does not affect the main point of this note, namely, that the surface gasification of AN is entirely different from the bulk decomposition reaction.

The linear pyrolysis of AN is a highly endothermic process, as is evidenced by the fact that a very large amount of heat is removed from the hot plate during the pyrolysis of the sample. This, together with analyses of the pyrolysis products,⁹ indicated that the overall process occurring in a very

⁹ Semiquantitative infrared and mass spectrometric analyses show that the major pyrolysis product is sublimed ammonium nitrate; very small amounts of NO_2 , NO , N_2 , H_2O , NH_3 and perhaps O_2 are also present. Below 200 C, N_2O was also found.

Received June 17, 1958.

¹ This work was supported by the U. S. Air Force under Contract AF 33(616)-2551, WADC, and Contract AF 18(603)-74 with the Air Force Office of Scientific Research.

² Research Chemist, Chemical Division.

³ Assistant Senior Chemist, Chemical Division.

⁴ Associate Director, Propellant Development Division. Member ARS.

⁵ Principal Chemist, Chemical Division.

⁶ Senior Chemist, Chemical Division.

⁷ Technical Specialist, Chemical Division.

⁸ Numbers in parentheses indicate References at end of paper.

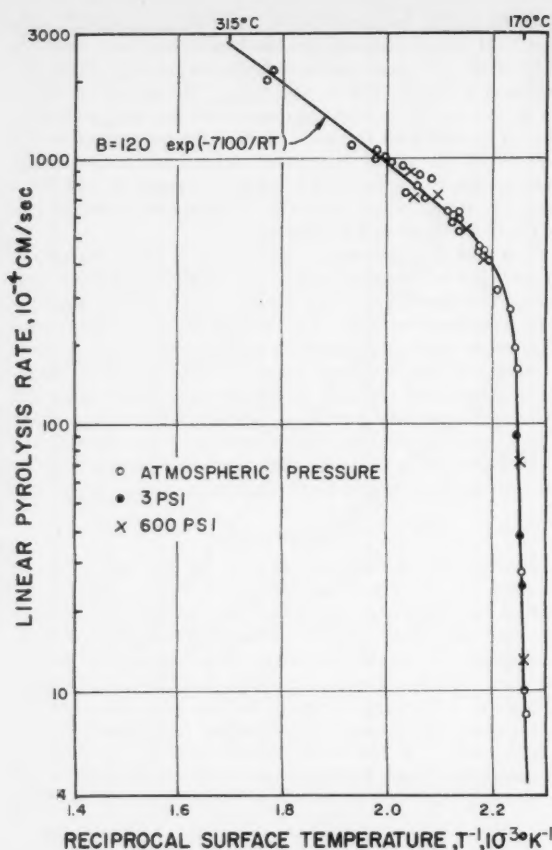
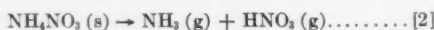


Fig. 1 Linear pyrolysis rate of ammonium nitrate as a function of surface temperature

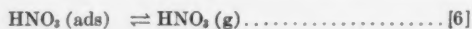
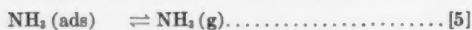
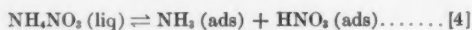
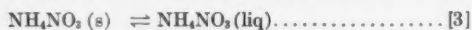
thin layer of AN exposed to a heat source, such as a hot plate or a flame, is chiefly the dissociation reaction



which has an endothermicity of about 40 kcal/mole. Surprisingly, the activation energy for the linear pyrolysis of AN is only about 7 kcal/mole, indicating that a stepwise surface process is probably involved. The situation thus appears to be similar to that in NH_4Cl , where the dissociation reaction is likewise highly endothermic, whereas the rate of reaction is controlled by a low activation energy (2).

Fig. 1 shows that below about 180°C, the pyrolysis rates drop sharply, and become essentially independent of temperature. Moreover, the rates appear independent of pressure in the range studied. These results imply that the sharp decrease in pyrolysis rate below about 180°C is related to a melting process rather than a sublimation process, as in the case of NH_4Cl (2).

The mechanism of the surface dissociation of AN is not known, but possibly involves the following sequence of steps



where $\text{NH}_3 (\text{ads})$, $\text{HNO}_3 (\text{ads})$ represent molecules physically adsorbed on a microscopically thin (solid or liquid) AN surface layer. The heat of vaporization of pure liquid HNO_3 is of the same magnitude as the activation energy for pyrolysis,

and hence it is reasonable to assume that during the linear pyrolysis of AN the desorption of HNO_3 , reaction [6], may be the rate-controlling step. The heat of fusion of AN is 1460 cal/mole, and it is thus unlikely that reaction [3] is rate controlling.

The thermal decomposition of any material at a given temperature proceeds by the fastest mechanism compatible with the conditions. The preceding results and discussion indicate that the rate of the solid surface decomposition of AN is greater than that for the bulk decomposition. This has important consequences for the interpretation of combustion phenomena involving the surface thermal decomposition of AN. In particular, it has led to new models for interpretation of the burning (4, 5) and detonation (6) characteristics of AN.

In conclusion it is suggested that, according to the observations described above, the rate-controlling process in the linear pyrolysis of solid AN occurs in the surface layer only, and not below the surface. The surface reaction is highly endothermic. The possibility of partial decomposition in the subsurface layers is not ruled out, but this partial decomposition is not considered to be rate-controlling.

References

- 1 See, for example: Robertson, A. J. B., "Thermal Decomposition of Pentaerythritol Tetranitrate, Nitroglycerin, Ethylenediamine Dinitrate and Ammonium Nitrate," *J. Society of Chemical Industry*, London, vol. 67, 1948, p. 221; Cook, M. A. and Abegg, M. T., "Isothermal Decomposition of Explosives," *Industrial Engineering Chemistry*, vol. 48, 1956, p. 1090; Cawthon, T. M. and Taylor, H. S., "Kinetics of the Thermal Decomposition of Ammonium Nitrate," Tech. Note no. 17, Report Control no. OSR-TN-54-334, Princeton University, Nov. 1954; Wood, B. J. and Wise, H., "Acid Catalysis in the Thermal Decomposition of Ammonium Nitrate," *Journal of Chemical Physics*, vol. 23, 1955, p. 693.
- 2 Schultz, R. D. and Dekker, A. O., "The Absolute Thermal Decomposition Rates of Solids," Fifth Symposium (Int.) on Combustion, Reinhold Publishing Co., New York, 1955, p. 260.
- 3 Barsh, M. K., Andersen, W. H., Bills, K. W., Moe, G. and Schultz, R. D., "Improved Instrument for the Measurement of Linear Pyrolysis Rates of Solids," *Review Scientific Instruments*, vol. 29, 1958, p. 392.
- 4 Andersen, W. H., Bills, K. W., Mishuck, E., Moe, G. and Schultz, R. D., "A Model Describing Combustion of Solid-Composite Propellants Containing Ammonium Nitrate," submitted to *Combustion and Flame*.
- 5 Chaiken, R. F., "A Thermal Layer Mechanism of Combustion of Solid Composite Propellants: Application to Ammonium Nitrate Propellants," *Combustion and Flame*.
- 6 Andersen, W. H. and Chaiken, R. F., "Application of Surface Decomposition Kinetics to Detonation of Ammonium Nitrate," to be published in *JET PROPULSION*.

Pressure Distributions on Blunt-Nosed Cones in Low Density Hypersonic Flow¹

L. TALBOT,² S. A. SCHAAF³ and F. C. HURLBUT⁴

University of California, Berkeley, Calif.

THIS note describes an experimental investigation of surface pressures on a class of blunt bodies in low density hypersonic flow. The general object of this study was to investigate the effect of viscous interaction on the surface pressure.

The configuration which was studied was a family of cones

Received July 29, 1958.

¹ This work was supported by the Bell Aircraft Corporation, under Government contract AF18(600)1607.

² Associate Professor, Aeronautical Sciences.

³ Professor, Aeronautical Sciences.

⁴ Lecturer, Aeronautical Sciences.

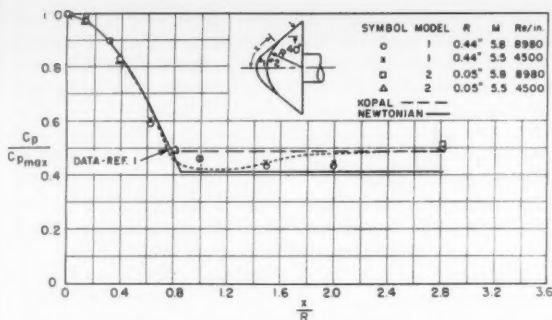


Fig. 1 Surface pressure distribution, 40 deg cone angle

with spherically-blunted noses. These cones were similar to those investigated by Machell and O'Bryant (1).⁵ The latter experiments were performed at flow conditions $M_\infty \approx 5.8$ and $6 \times 10^4 < Re_{R_\infty} < 1.6 \times 10^5$, where M_∞ is the free stream Mach number, and Re_{R_∞} is the Reynolds number based on free stream conditions and the nose radius. The present tests covered the range $3.6 < M_\infty < 5.8$, but were at considerably lower Reynolds numbers, in the range $2 \times 10^2 < Re_{R_\infty} < 5 \times 10^3$. At these lower Reynolds numbers, some viscous interaction effects can be expected to be present, and comparisons between the present tests and the results of (1) thus serve to indicate the magnitude of such effects.

The model dimensions are shown in Figs. 1 to 5. All models were of base diameter 1.75 in. The data points indicate the location of the pressure orifices, in terms of x/R , with x measured from the stagnation point along the surface of the model. Most of the tests were conducted in the nominal Mach 6 nozzle, under two flow conditions: $M_\infty \approx 5.8$, $Re_{R_\infty}/in. \approx 8980$, and $M_\infty \approx 5.5$, $Re_{R_\infty}/in. \approx 4500$. A few additional results were obtained in the nominal Mach 4 nozzle. Typical flow conditions are listed in Table 1. Accuracy of the present experiments is estimated to be within ± 2 per cent in pressure, ± 5 per cent in free stream Reynolds number and ± 1 per cent in Mach number. The values of x/R are accurate to ± 2 per cent on all but the models with 0.05 in. nose radius. For these models, the orifices on the spherical portions could be located to about ± 10 per cent accuracy in x/R .

It is convenient to discuss the results in terms of two regions on the model surface, the stagnation region, and the "transition" region, which is the region of the surface in the vicinity of the change in curvature between the spherical nose and the conical afterbody.

Stagnation Region

Figs. 1 to 5 show that in the stagnation region the surface pressures follow quite closely the "modified-Newtonian" approximation

$$C_p = C_{p_{\max}} \cos^2 \theta \quad [1]$$

where $C_p = 2(p - p_\infty)/\rho_\infty U_\infty^2$ is the local pressure coefficient, $C_{p_{\max}}$ the value of the pressure coefficient at the stagnation point, and θ the angle between the local normal to the surface and the direction of the undisturbed free stream velocity U_∞ . This agreement with the modified-Newtonian values was also found by Machell and O'Bryant. The fact that modified-Newtonian theory predicts the surface pressures in the stagnation region even at the Reynolds numbers of the present tests is really not too surprising. It has been pointed out by several authors (see (2) for a review of the subject and a comprehensive bibliography) that the success of the modified-Newtonian result can be "explained" by the fact

⁵ Numbers in parentheses indicate References at end of paper.

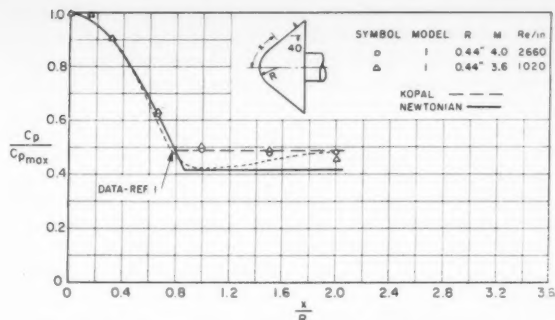


Fig. 2 Surface pressure distribution, 40 deg cone angle

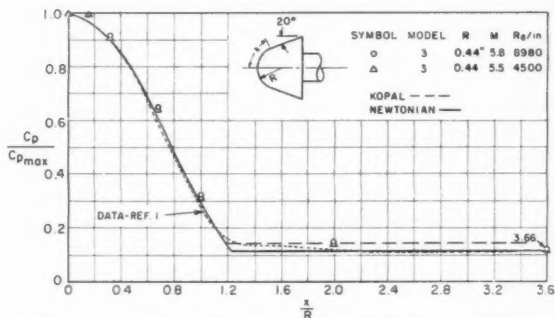


Fig. 3 Surface pressure distribution, 20 deg cone angle

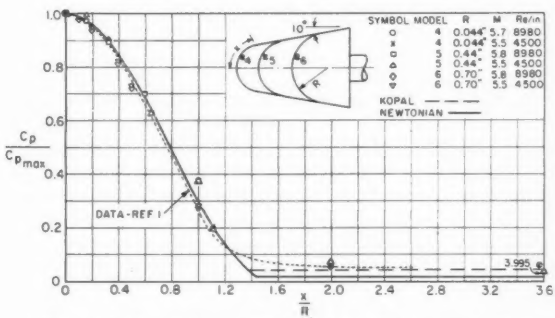


Fig. 4 Surface pressure distribution, 10 deg cone angle

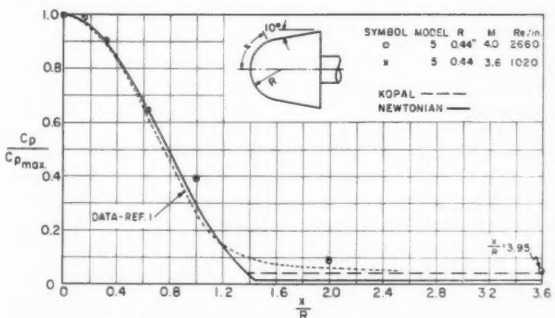


Fig. 5 Surface pressure distribution, 10 deg cone angle

that the decrease in surface pressure, caused by centrifugal effects (which yields the Newtonian-plus-centrifugal formula $C_p = 2 \cos^2 \theta - (2/3) \sin^2 \theta$), is almost exactly balanced by the increase in surface pressure due to the fact that the shock wave curvature is less than the body curvature. Now, the pressure drop through the shock layer $\Delta p \approx (1/3)(\rho_\infty U_\infty^2 \sin^2 \theta)$ is independent of the shock layer thickness δ , to first order in $k = \rho_\infty/p_2$, where subscript 2 refers to conditions

behind the normal shock. The same appears to be true for the counterbalancing pressure increment due to lack of concentricity of shock and body, because the modified-Newtonian theory is accurate over a wide range of δ/R .

The effect of the boundary layer in the stagnation region is to change the effective thickness of the shock layer by the δ^* , the boundary layer displacement thickness. Detailed calculations show that in the stagnation region, because of the strong favorable pressure gradient, δ^* grows very slowly with x and is in fact practically constant. Hence, one might expect the modified-Newtonian result to hold accurately in hypersonic flow even when δ^* is not negligible, perhaps even up to the point where δ^* approaches the inviscid shock layer thickness δ , and the two layers merge. Now, under wind tunnel conditions at $M \approx 6$, $\delta^*/R \sim 1/\sqrt{Re_{R_\infty}}$ (8); and to first approximation the shock layer thickness is given by $\delta/R \sim k$ (2). Thus the two layers can be expected to be distinct provided $\delta^*/\delta \sim 1/k\sqrt{Re_{R_\infty}}$ is somewhat less than unity. In the present tests, $\delta^*/\delta < 0.4$.

The actual values of C_{pmax} found in the tests agreed, within experimental error, with their theoretical inviscid flow values given by the Rayleigh pitot tube formulas. Viscous effects on impact pressures (3) begin to be important (for rounded bodies) for $Re_{R_\infty} \sim 100$ and less, which is a little lower than the range of the present data. Noncontinuum effects (i.e., slip flow phenomena) were likewise totally indiscernible in the data. It is now well established that such effects, if present, are overshadowed by viscous interaction phenomena at a "moderately low" Reynolds number (perhaps even for Reynolds numbers as low as $Re_{R_\infty} \sim 10$). In view of the fact that in the experiments the viscous interaction effects themselves were unimportant, at least in the stagnation region, the absence of noncontinuum phenomena is only to be expected.

Transition Region

In this region of the body surface, the pressure distribution departs from modified-Newtonian to approach its final downstream value on the conical afterbody. The ideal inviscid flow value on the cone is the Taylor-Maccoll value, as given in the Kopal Tables (4). The Kopal value is greater than the modified-Newtonian value for the cone surface, although for small cone angles the two are close together.

The inviscid pressure distributions for blunt cones with large cone angle, as found by Machell and O'Bryant, are indicated in the figures. In the vicinity of the change in curvature, the flow overexpands, and the pressure drops to nearly the modified-Newtonian value for the cone. A recompression region follows, and the final pressure is the Kopal value. The amount of overexpansion becomes progressively less as the cone angle is decreased. (Of course, the Kopal and modified-Newtonian values are nearly equal for small cone angles.) For blunt-nosed slender bodies (5) the overexpansion vanishes altogether.

The present data, in comparison with those of (1), exhibit less overexpansion in the transition region. Also, the lengths of the transition regions on the models, measured in units of x/R , are somewhat greater in the present tests. It seems probable that these differences are caused by viscous interaction. One may note that, at the lower Reynolds numbers of the $M_\infty \approx 4$ data, there is no overexpansion at all evident on Model 1.

Far back on the cone, downstream of the transition zone, one expects that due to weak interaction viscous effects the surface pressure will be slightly higher than the inviscid flow value, as is observed on slender pointed cones (6, 7) and slender blunt-nosed bodies (2, 5). The present tests were not designed to provide the high accuracy of pressure measurement in the weak interaction region necessary for a careful study of this region, and, in any case, the shortness of the models would have rendered any such measurements highly suspect. But within the accuracy of measurement, the pres-

sures downstream of the transition zone were found to be slightly higher than the ideal Kopal values, the differences being of magnitudes commensurate with the predictions of the weak interaction theories (7). Of course, for large angle cones, the viscous interaction pressure increase in the weak interaction region is a very small fraction of the Kopal pressure, and is not even noticeable on the scale to which the data have been plotted.

Table 1 Flow conditions of tests

M_∞	p_∞ (μ Hg)	Measured C_{pmax}	Re_∞ /in.
3.69	57.2	1.80	1020
4.05	111	1.81	2660
5.46	66.7	1.83	4500
5.80	107	1.85	8980

References

- 1 Machell, R. M. and O'Bryant, W. T., "An Experimental Investigation of the Flow over Blunt-Nosed Cones at a Mach Number of 5.8," Galtit Hypersonic Research Project, Memorandum 32, June 15, 1956; also, Readers' Forum, *Journal of the Aeronautical Sciences*, vol. 23, Nov. 1956, pp. 1054-1055.
- 2 Lees, Lester, "Recent Developments in Hypersonic Flow," *JET PROPULSION*, Nov. 1957.
- 3 Sherman, F. S., "New Experiments on Impact Pressure Interpretation in Subsonic and Supersonic Rarefied Air Streams," NACA TN-2995, Sept. 1955.
- 4 Staff of the Computing Section, Center of Analysis, M.I.T., under the direction of Zdenek Kopal, "Tables of Supersonic Flow Around Cones," Technical Report no. 1, 1947.
- 5 Kubota, T., "Inviscid Hypersonic Flow over Blunt-Nosed Slender Bodies," Paper presented at 1957 Heat Transfer and Fluid Mechanics Institute, June 19-21, 1957, California Institute of Technology, Pasadena, Calif.; also, Galtit Hypersonic Research Project, Memorandum 40, June 25, 1957.
- 6 Talbot, L., "Viscosity Corrections to Cone Probes in Rarefied Supersonic Flow at Nominal Mach Number of 4," NACA TN-3219, 1954.
- 7 Talbot, L., Koga, T. and Sherman, P. M., "Hypersonic Viscous Flow over Slender Cones," U. C. Eng. Project Report HE-150-147, June 1957; also NACA TN 4327, 1958.
- 8 Cohen, C. B. and Reshotko, E., "The Compressible Laminar Boundary Layer with Heat Transfer and Arbitrary Pressure Gradient," NACA Report 1294, 1956.

Note on Interplanetary Navigation

ROBERT M. L. BAKER Jr.¹

Aeronutronic Systems, Inc., Newport Beach, Calif.

BECAUSE mass onboard the interplanetary vehicle would be so expensive and reliability so important, techniques should be found for minimizing the amount of in-flight observation and computation required by making the maximum use of terrestrial precomputation of trajectories. Thus, observations would, for example, take the form of comparing the predicted and observed positions of all observable solar system bodies against the fixed star background, while the onboard computations would deal only with the differences between the precomputed and the actual trajectories. Preliminary studies have shown that these procedures would result in a substantial savings in equipment weight and complexity, and that such a self-contained navigational unit would probably be superior to the employment of Earth-bound computers and a data link.

Basically, it would seem that the navigational requirements for an interplanetary voyage would be twofold: First,

Received Aug. 3, 1958.

¹ Staff Member. Member ARS.

to determine the true orbit that the space vehicle is proceeding along, and, second, to compute the corrective thrusts needed to place the vehicle on an orbit that will accomplish the desired mission (implicit in the latter is a knowledge of the vehicle's orientation); see (1, 2 and 3).² These requirements need not, however, be carried out explicitly. In fact, it will probably never be necessary to determine exactly *where* the vehicle is, since the real question is *how* to get it to its objective. By eliminating the middleman (i.e., by eliminating the determination of the vehicle's actual orbit), a great savings can be achieved in computer complexity and computational time. Under the assumption that the vehicle must determine its own corrective maneuver, the navigator or navigational device will have certain raw data available, such as star and planetary positions (obtained by celestial observations or by star-trackers) and some electronic information (perhaps radar near the Earth or the target planet and a LORAN type signal in midcourse), all information of comparable accuracy being useful. Such rough data must be reduced to terms from which a corrective thrust program can be calculated. Precomputation would permit these calculations to be carried out mainly before the flight.

In general, observational inputs (probably obtained at different times throughout a month or so of flight), which are denoted by $O_1, O_2, O_3, \dots, O_i$, must be processed by the on-board computer. If the orbit is a ballistic one, then the corrective thrust is specified by α, β, γ, T and t_0 , where α, β , and γ are angles that define the thrust direction with respect to some reference system, T is the magnitude of the corrective thrust, and t_0 is the time when the corrective thrust should be applied. These five variables are, of course, implicitly related to the O_i 's. If the orbit is a low thrust one, then the thrust program modification, i.e., $\alpha(t), \beta(t), \gamma(t)$ and $T(t)$, must be specified as a function of the time t , and these variables will likewise be implicitly related to the O_i 's.

Precomputation, based upon accurate astronomical constants and accurate stellar and planetary position data would provide a set of the values of the observational quantities O_i that would be observed from the space vehicle if it were on the ideal computed orbit (i.e., a "prediction ephemeris"). Of course, the space vehicle will not actually move along the ideal trajectory because of various unpredictable errors in the thrust program, uncertainties in certain astronomical conversion factors (which, for example, reflect themselves in incorrect takeoff initial conditions), unaccounted for perturbations, malfunctions, etc., so that the observed quantities will differ from the computed values by small differences, denoted by $\Delta_{oc} = O_i$ (actually observed) - O_i (computed) (4). The accurate precomputation could, however, provide coefficients $\alpha_{11}, \alpha_{12}, \dots, \beta_{11}, \beta_{12}, \dots, \gamma_{11}, \gamma_{12}, \dots$, and T_{11}, T_{12}, \dots , and t_{11}, t_{12}, \dots that will determine the corrective thrusts *directly* from these differences, e.g.

$$\alpha = \alpha_{11}\Delta_{oc}(O_1) + \alpha_{12}\Delta_{oc}(O_2) + \dots \\ + \alpha_{21}\Delta_{oc}^2(O_1) + \alpha_{22}\Delta_{oc}^2(O_2) + \dots$$

$\alpha \rightarrow \beta, \gamma, T$ and t_0 . Consequently, the actual orbit need never be explicitly determined.

This Taylor-series or other slightly more complex representation can be expanded to any number of terms, as required by the expected vehicle inaccuracy and by the nature of the mission. The evaluation of these series would then be carried out by a simplified onboard computer. This can be designed to employ a large recirculating magnetic tape as its main memory with, perhaps, a second recirculating tape of smaller size which would contain the arithmetic registers and the logical structure of the computer. Such a computer would be exactly tailored to the requirements for processing observational data on the basis of precomputed information. This device can be made with a minimum of flip-flops, thus increasing its reliability. (It should be noted in passing that the importance of reliability cannot be overrated.)

Preliminary investigations indicate that our lack of precise knowledge concerning the conversion of certain astronomical constants might make a completely predetermined trajectory inadequate for all except the most rudimentary of interplanetary missions (5). Such a circumstance, however, makes the employment of a differential correction procedure even more attractive, since differential corrections could be simply interpreted as a form of "homing," in which the differentials Δ_{oc} indicate the aiming error that must be eliminated by corrective thrusts; e.g., after converting from a geocentric to a heliocentric reference system in midcourse, much of the constant error can be automatically eliminated since the observations will be made in the heliocentric system. Even if such a homing type of navigational scheme is found to be useful for certain missions, the requirements for precision orbits cannot be relaxed. In the case of such terminal guidance, one would have to consider the trade-off between better observational information obtained nearer to the objective planet as opposed to less corrective thrust required further away. Essentially, precision orbital techniques, involving precomputed data, would provide for the most efficient reduction of the earlier, less refined observational information and hence would provide for a more economical employment of corrective thrusts.

Of course, a midcourse correction will always be required, no matter how accurately the orbit was established, in order to account for the inclination between the Earth's and the planet's orbit plane. (This inclination effect would result in maximum errors of 3,960,000 miles for Venus and 4,560,000 miles for Mars.)

It has been found (6) that (unless Venus at the time of landing were passing through the line of nodes) the optimum manner in which to transfer from the Earth's heliocentric orbit plane to that of Venus or Mars would be to carry out the transfer in midcourse (in fact, almost precisely in midcourse). It is evident that if such a maneuver were carried out at take-off, it would be impossible to design a doubly tangent Earth-planet orbit without passing over the celestial pole—a maneuver that would be extremely costly in view of the fact that no advantage could be taken of the Earth's speed; in fact this speed would have to be cancelled out. Other than double tangent heliocentric orbits are found to be rather inefficient, and even if this inefficiency were discounted, the penalty paid to transfer into any Earth-sun-planet orbit initially can become exorbitant. Spherical trigonometry can be employed to demonstrate that the minimum inclination angle between the Earth-sun-rocket plane and the planet-sun-rocket plane³ would occur when the radius vector from the sun to the rocket and from the sun to the predicted position of the planet at landing is 90 deg. Thus, excluding other effects, the inclination maneuver is made most efficiently at this point (and *not* at the line of nodes of the Earth-planet plane; see (1)).

The author acknowledges the contributions made to this note through discussions held with Drs. Samuel Herrick, Eric Durand and L. G. Walters of Aeronutronic Systems, Inc.

References

- Porter, J. G., "Navigation Without Gravity," *Journal of the British Interplanetary Society*, vol. 13, no. 2, 1954, pp. 68-74.
- Stuhler, Ernst, "The Flight Path of an Electrically Propelled Space Ship," *JET PROPULSION*, vol. 27, no. 4, 1957, pp. 410-414.
- Lawden, D. F., "Correction of Interplanetary Orbits," *Journal of the British Interplanetary Society*, vol. 13, no. 4, 1954, pp. 215-223.
- Herrick, S., "Astrodynamics," Van Nostrand, N. Y. (to be published).
- Herrick, S., Baker, R. M. L., Jr. and Hilton, C. G., "Units and Constants for Geocentric Orbits," ARS preprint 497-57, 1957, iii + 62 pp.
- Baker, R. M. L., Jr., "Thoughts on Interplanetary Rocket Travel," paper presented to S. Herrick and J. Kaplan, 1954.

² Numbers in parentheses indicate References at end of paper.

³ I.e., planet where it would be at predicted time of arrival.

Ignition by Flow Over Hot Surfaces

WELBY G. COURTNEY¹

Experiment Incorporated, Richmond, Va.

ALTHOUGH it has long been known that a combustible material could be ignited by a hot surface, an interpretation of ignition phenomena in terms of heat transfer and chemical reactions has been severely limited by turbulence (1).² Ignition during laminar flow over a heated flat surface (or in the laminar boundary layer when the free stream is turbulent) was treated theoretically by Chambré (2) and Toong (3). However, the present experimental work indicates that small-scale turbulence at the hot surface may be difficult to avoid in ignition during flow over hot surfaces.

Received Aug. 21, 1958.

¹ Senior Scientist.

² Numbers in parentheses indicate References at end of paper.

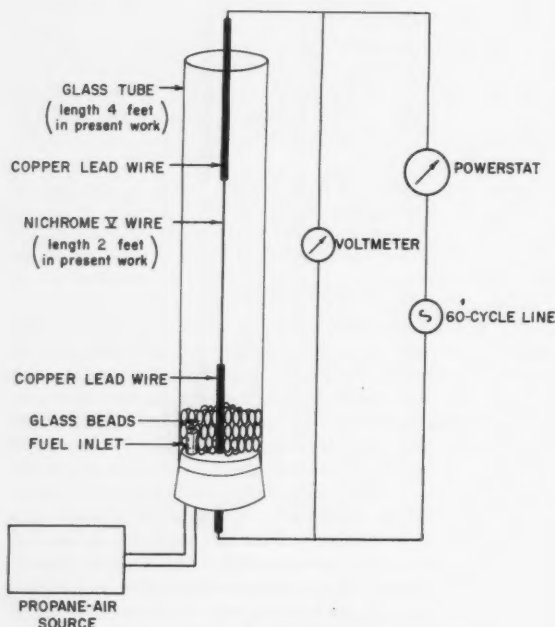


Fig. 1 Flow-ignition apparatus

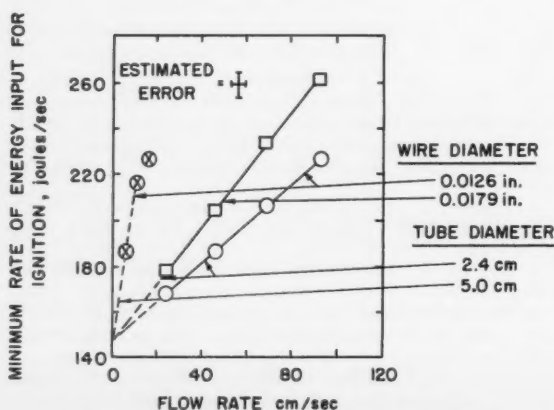


Fig. 2 Effect of flow rate, equivalence ratio 0.62

Experimental Procedure

Premixed propane-air gas at ambient temperature and pressure was passed at a constant initial linear flow velocity (volume feed rate/tube area) up an electrically heated nichrome wire positioned vertically in a glass tube (Fig. 1). When a minimum voltage was applied to the wire, flame formed at the top of the wire and then rapidly moved down the tube until it stabilized on the wire at a point which depended upon the initial flow velocity, burning velocity of the combustible mixture, flame-holding behavior of the wire and the voltage³ on the wire.

The minimum total rate of energy input required for ignition was calculated from the minimum voltage for ignition and the wire resistance and length. The minimum rate depended critically upon the placement of the wire and tube, with the lowest minimum rate being measured when the tube and wire were vertical and the wire was located in the center part of the tube. The ignition data reported below corresponded to the minimum conditions obtained in the present work.

Results and Discussion

Shadowgraph examination of the gas as it exited from the tube indicated that the gas near the wire was in laminar flow when the wire was cold, became turbulent when the wire was warmed, and was highly turbulent when the wire was heated to a temperature sufficient to give ignition. Although the free stream was always laminar, turbulence always formed near the wire when the heat flux was sufficient to give ignition.

The turbulence extended with a 2 mm radius into the gas stream. Although low shadowgraph sensitivity did not permit observation of the flow pattern immediately adjacent to the wire surface, Eckert and Soehngen (4) reported turbulence "right up to the surface" during free convection with a vertical heated plate. Since the present heat fluxes were considerably larger than those used by Eckert and Soehngen, the gas immediately at the heated wire in the experiment discussed in this paper was probably also in turbulent motion. Therefore, a theoretical treatment of ignition assuming laminar flow at the surface would not apply to the present work and may in general be of limited usefulness in interpreting ignition during flow over a hot surface.

Empirically, the minimum total rate of energy input for ignition dE/dt increased with increasing initial flow velocity and increasing wire or tube diameter (Fig. 2) but was essentially independent of equivalence ratio⁴ (Fig. 3). The present limited results corresponded to

$$dE/dt = aV + b$$

where V is the initial linear flow velocity, a is a constant which depends upon the wire and tube diameters but is independent of equivalence ratio, and b is a constant which is independent of wire and tube diameters and equivalence ratio. The independence of dE/dt on gas composition is probably due to the heat capacity of the combustible gas being essentially independent of composition. Interpretation of the effects of wire and tube diameter is uncertain at present. The increase in dE/dt with increasing flow velocity is undoubtedly related to decreasing contact time, but this relationship is obscured by the presence of turbulence. Ignition presumably involves heating a volume element of the combustible gas to the temperature range where autoignition readily occurs, but the temperature history of the volume element as it passes in turbulent flow along the wire is difficult to describe. Further work is planned.

The author is pleased to acknowledge the advice of Dr. L. E. Line Jr. and I. R. King and the assistance of J. T. Scheurich, who performed the experimental work.

³ The stabilized flame could be moved up or down the wire by decreasing or increasing the voltage on the wire (i.e., by changing the wire temperature).

⁴ Stoichiometric air/fuel ratio divided by actual air/fuel ratio.

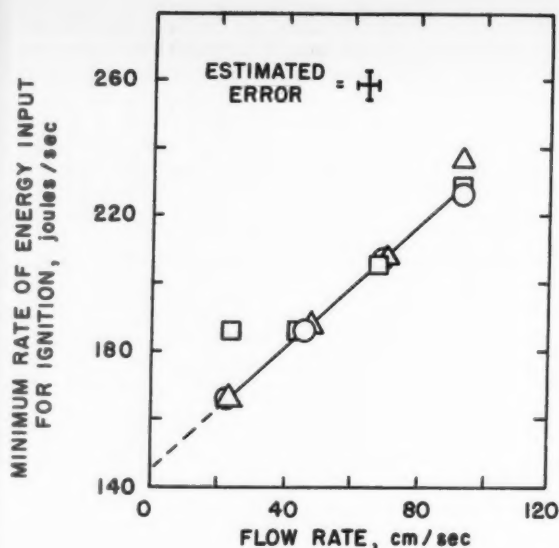


Fig. 3 Effect of equivalence ratio; wire diameter 0.0126 in., tube diameter 2.4 cm

References

- 1 Mullen, J. W., II, Fenn, J. B. and Irby, M. R., "The Ignition of High Velocity Streams of Combustible Gases by Heated Cylindrical Rods," in "Third Symposium on Combustion and Flame and Explosion Phenomena," Williams and Wilkins, Baltimore, 1949, p. 317. The extensive literature regarding ignition with heated surfaces is reviewed.
- 2 Chambré, P. L., "On the Ignition of a Moving Combustible Gas Stream," *Journal of Chemical Physics*, vol. 25, 1956, p. 417.
- 3 Toong, T.-Y., "Ignition and Combustion in a Laminar Boundary Layer over a Hot Surface," in "Sixth Symposium (Int.) on Combustion," Reinhold, New York, 1957, p. 532.
- 4 Eckert, E. R. G. and Soehngen, E., "Interferometric Studies on the Stability and Transition to Turbulence of a Free-Convection Boundary Layer," *Proc. of the General Discussion on Heat Transfer*, Institution of Mechanical Engineers, London, 1951, p. 321.

A New Instrument for Measuring Atmospheric Density and Temperature at Satellite Altitudes

A. J. DESSLER,¹ W. B. HANSON,² M. HERTZBERG,³
D. D. McKIBBIN⁴ and R. C. WRIGLEY⁵

Missile Systems Division, Lockheed Aircraft Corp.,
Palo Alto, Calif.

A simple rugged instrument is described which can measure, at satellite altitudes: Atmospheric density, at-

mospheric temperature and satellite or ballistic missile angle of pitch and yaw. When placed in a satellite, the present instrument is sensitive enough to operate up to altitudes of at least 300 miles. It is not affected by vehicle outgassing and will measure only the properties of the ambient atmosphere.

Introduction

A NEW instrument which is capable of the direct measurement of atmospheric density and temperature at very high altitudes has been developed and tested in our Space Physics Laboratory. This instrument can measure the atmospheric mass density continuously and hence can provide not only the time- and space-averaged density, but also its variation with altitude, latitude and local time. Thus, one successful satellite flight should yield a detailed description of the atmospheric density profile and its variations.

Satellite tracking data must be averaged over many orbits in order to be useful in the derivation of atmospheric density data. Therefore, analyses of satellite trajectories have thus far yielded values of atmospheric density which are a long term space and time average of the true density. The severity of this averaging process is indicated by rocket data now available.⁶ Rocket measurements at 125 miles altitude show variations in density of a factor of more than 10, depending on the time and place of measurement.

The Instrument

When a high velocity vehicle moves through the upper atmosphere, the ambient gas molecules produce an impact pressure on its forward side equal to $k\rho v^2$, where k is a constant determined by the accommodation coefficient ≈ 1 , ρ is the atmospheric density, and v is the velocity of the vehicle. This impact pressure is measured by a very sensitive microphone which is the sensing element for the instrument. The impact pressure is a direct measure of the density drag, or, since the satellite velocity is independently known, the pressure is also a direct measure of the density.

By mechanically chopping the beam of gas molecules striking the microphone, an a.c. signal is produced whose amplitude is proportional to ρv^2 . To achieve a narrow bandwidth and hence low noise, the microphone signal is detected at a phase sensitive detector with a signal from the chopper used as a reference. All of the electronic circuitry necessary for this instrument has been completely transistorized.

If a small hole is cut in the front part of a satellite moving through the upper atmosphere, the beam of ambient gas particles which passes through the hole will spread, due to the transverse thermal velocity components of the individual molecules. The amount of thermal spreading will be proportional to the square root of the absolute temperature. Thus, when the microphone is placed a short distance behind the sensing hole and moved transversely to map the intensity distribution across the beam, a measure of the amount of thermal spreading may be obtained. This distribution of the impact pressure behind the hole is an absolute measure of the kinetic temperature of the ambient atmosphere if the molecular weight of the gas is known. Direct methods for measuring the ambient gas temperature at altitudes greater than about 100 km are limited by radiation effects which are larger than the heat transfer to a detector by the ambient gas.

The direction of a molecular beam which passes through an aperture in the vehicle's skin is obviously determined by the vehicle's direction of motion. A suitable combination of apertures and detectors can be used to measure this beam direction with respect to the body axes and hence provide pitch and yaw information.

⁶ For a discussion of these data see "Atmospheric Density from Present Rocket and Satellite Measurements," by R. A. Minzner, presented at the Symposium on Satellite Geophysical Studies, at the Washington meeting of the American Geophysical Union on May 6, 1958.

Received June 22, 1958.

¹ Group Leader, Space Physics Dept. Member ARS.

² Group Leader, Space Physics Dept.

³ Senior Scientist, Space Physics Dept.

⁴ Scientist, Space Physics Dept.

⁵ Associate Scientist, Space Physics Dept.

Calibration

The sensitivity of the density gage has been measured in the laboratory with the aid of a simple molecular beam apparatus. The entire gage was placed in a large vacuum chamber which was maintained at a pressure of less than 10^{-4} mm Hg. An aperture of area 0.1 cm^2 , which was located 19 cm from the microphone, separated the large vacuum chamber from the beam source chamber. The gas pressure in the source chamber was controlled by a needle valve and measured with a Phillips ionization gage. Argon gas or air at room temperature was used for the beam. The product ρv^2 was adjusted to simulate the impact pressure which would be encountered in a satellite. Thus, although ρ and v independently do not duplicate satellite conditions, the product ρv^2 will be correct. Even a change in the accommodation coefficient from 0 to 1 cannot change the product $k\rho v^2$ by more than 30 per cent.

In a typical calibration run, a source pressure of 5×10^{-4} mm Hg was used. Allowing for spreading of the beam after passing through the 0.1 cm^2 hole, this source pressure corresponds to a ρv^2 at the microphone of about 6×10^{-4} dynes/cm². The voltage signal to noise ratio at the detector was about 4 under these conditions, using a 3 cps bandpass. This is the value of ρv^2 which would be experienced in a satellite moving through a gas of density 10^{-15} gm/cm^3 . Taking the lowest atmospheric density values of Jastrow,⁷ 10^{-15} gm/cm^3 corresponds to an altitude of 375 miles. The voltage signal to noise ratio at 300 miles should be better than 12. Hence, quite reliable density values should be obtained at this altitude.

Conclusion

The instrument described above provides a simple rugged detector which, with suitable modifications, can be used to measure as a continuous function of position: Atmospheric density, atmospheric kinetic temperature and vehicle angle of pitch and yaw. Since the operation of the detector is dependent on the impact of high velocity gas molecules on a sensitive microphone element, it will not be greatly affected by vehicle outgassing. Laboratory tests indicate that this detector, when moving through the upper atmosphere at satellite velocities, should operate at altitudes up to at least 300 miles in its present form. Calculations show that improvements are possible which can extend this altitude capability considerably.

Acknowledgment

We wish to thank Dr. F. S. Johnson for his efforts in getting this project started. We also wish to thank J. Drake, C. Searing and W. Page for their aid in the construction of the instrument.

⁷ Jastrow, R., *Bull. Am. Phys. Soc.*, vol. 3, no. 189, 1958.

Some Comments on Generalized Trajectories for Free Falling Bodies of High Drag

WILLIAM SQUIRE¹

Bell Aircraft Corp., Buffalo, N. Y.

IN A recent note (1)² Turnacli and Hartnett have discussed the velocity-altitude relation for a body with a constant drag coefficient falling through an atmosphere with an exponential density variation. This problem was apparently

Received Aug. 20, 1958.

¹ Aerodynamicist, Aerophysics Department.

² Numbers in parentheses indicate References at end of paper.

first treated by Munk (2) in 1944. In 1951 a number of notes (3 to 5) appeared on the general problem of a body with a drag proportional to the velocity and velocity squared in an exponential atmosphere.

The treatment given below is essentially based on Munk's analysis. The novel feature is a graphical construction which with the use of a variable scale³ gives particular solutions very rapidly.

Analysis

If distance is measured from sea level the basic differential equation is

$$\frac{d\bar{v}^2}{d\bar{x}} = \bar{K}_0 \frac{\rho}{\rho_0} \bar{v}^2 - 2 \dots \dots \dots [1a]$$

and

$$\frac{\rho}{\rho_0} = e^{-\bar{x}} \dots \dots \dots [1b]$$

where as in (1)

$$\bar{x} = x/\alpha$$

$$\bar{v}^2 = v^2/g_0\alpha$$

and

$$\bar{K}_0 = C_D \frac{\rho_0 A \alpha}{m}$$

A new variable $\bar{z} = \bar{K}_0 e^{-\bar{x}}$ is introduced, transforming [1a] into

$$\frac{d\bar{v}^2}{d\bar{z}} + \bar{v}^2 = \frac{2}{\bar{z}} \dots \dots \dots [2]$$

The solution is

$$\bar{v}^2 = e^{-\bar{z}} [C + 2\bar{E}i(\bar{z})] \dots \dots \dots [3]$$

where C is an integration constant and

$$\bar{E}i(\bar{z}) = \int_{\bar{z}}^{\infty} \frac{e^{-t}}{t} dt \dots \dots \dots [4]$$

is the exponential integral, several tables of which are available (6, 7). Besides the expansion

$$\bar{E}i(\bar{z}) = \ln \gamma \bar{z} + \sum_{n=1}^{n=\infty} \frac{\bar{z}^n}{n - n!} \dots \dots \dots [5]$$

$$\ln \gamma = 0.5772$$

cited in (1), there is an asymptotic expansion

$$\bar{E}i(\bar{z}) \sim \frac{e^{-\bar{z}}}{\bar{z}} \times \sum_{n=0}^{n=\infty} \frac{n!}{\bar{z}^n} \dots \dots \dots [6]$$

which is useful for large values of \bar{z} .

Graphical Solutions

Since \bar{v}^2 is a linear function of C , if \bar{v}^2 is plotted for two values of C , the value for any other value of C can be found by linear interpolation or extrapolation which is conveniently performed with a variable scale. Furthermore since

$$\bar{x} = \ln \bar{K}_0 - \ln \bar{z} \dots \dots \dots [7]$$

a plot against $\ln \bar{z}$ is easily adapted to any value of \bar{K}_0 .

The values for $C = 100$ and $C = 20$ are given in Table 1 and plotted in Fig. 1.

The values 20 and 100 taken for C are of course arbitrary, and it is a simple matter to make up curves for any ranges of interest to the user with the values of C selected for easy interpolation.

The first example given in (1) corresponds to $\bar{v}^2 = 31$ at

³Gerber Scientific Instrument Co., Hartford, Conn.

Table 1* Numerical values for trajectory analysis

$\ln \bar{z}$	\bar{p}^2 ($C = 100$)	\bar{p}^2 ($C = 20$)	$\bar{E}_i(\bar{z})$
-10.00	81.15	1.15	-9.4228
-9.00	83.15	3.15	-9.4227
-8.00	85.12	5.15	-7.4225
-7.00	87.08	7.15	-6.4217
-6.00	88.85	9.13	-5.4203
-5.00	90.55	17.09	-4.4165
-4.605	91.05	11.84	-4.0179
-3.507	91.42	13.78	-2.8991
-2.996	90.62	14.52	-1.6228
2.303	87.55	15.16	-0.8218
-1.609	80.53	15.03	+0.1047
-0.916	67.16	13.54	+0.7699
-0.511	55.73	11.82	+1.3474
-0.223	46.14	10.20	+1.8951
0.000	38.18	8.75	4.9542
0.262	28.74	6.93	2.7214
0.531	19.70	5.08	2.7214
0.693	14.87	4.05	4.9542
1.099	5.97	1.99	3.9210
1.386	2.55	1.09	19.631
1.792	0.67	0.48	85.990
2.079	0.33	0.30	44.038

* The first six values were obtained by using $\bar{E}_i(\bar{z}) = \ln \gamma \bar{z} + \bar{z}$. For the others the values were taken from Jahnke-Emde (7).

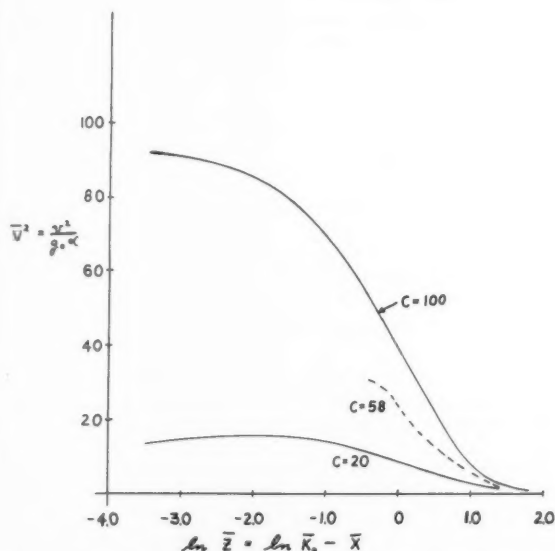


Fig. 1 Curve for rapid calculation of descent through an exponential atmosphere

$\bar{x} = 8$. The value of \bar{K}_0 is 1900 deg, so $\ln \bar{K}_0$ is 7.55; therefore, the value of $\ln \bar{z}$ is -0.45, and the value of C is found to be 58. The rest of the curve is shown dotted in Fig. 1.

Discussion

Because of the very large range of densities and velocities under consideration at present, it is extremely doubtful that the assumption of a constant drag coefficient holds. With the present rapid method of computation, it is possible to assume a drag coefficient which is constant in a limited range of Mach and Reynolds numbers, and piece together a number of such solutions.

In connection with the application made by (1) to oblique flight, it should be noted that the path will only be a straight

line, as they assume, when the drag is much greater than the force of gravity, i.e., when the exponential integral term can be neglected.

References

- 1 Turnacli, R. D. and Hartnett, J. P., "Generalized Trajectories for Free Falling Bodies of High Drag," *JET PROPULSION*, vol. 28, April 1958, pp. 263-266.
- 2 Munk, M. M., "Mathematical Analysis of the Vertical Dive," *Aero Digest*, Feb. 15, 1944, pp. 114, 213.
- 3 Sexl, T., "On the Motion of a Point Mass in a Resisting Medium of Variable Density," *Acta Physica Austriaca*, vol. 5, 1951, pp. 148-151.
- 4 Louchak, G., "The Fall of a Particle through the Atmosphere," *American Journal of Physics*, vol. 19, Oct. 1951, p. 426.
- 5 Squire, W., "Motion of a Particle through a Resisting Medium of Variable Density," *American Journal of Physics*, vol. 19, Oct. 1951, pp. 426-427.
- 6 "Tables of Sine, Cosine and Exponential Integrals," Mathematical Tables Project, vols. 5 and 6, GPO Washington, 1940.
- 7 Jahnke, E. and Emde, F., "Tables of Functions," Dover, New York, 1945.

On the Classification of the Chemistry in Combustion Experiments

GERALD ROSEN¹

Hughes Aircraft Co., Culver City, Calif.

Nomenclature

- A = constant "frequency factor" of the Spalding approximation, gr-cal/cm⁴-sec²-K
 C_p = constant specific heat of the mixture, cal/gr-K
 $f(T)$ = volumetric production of the product species, gr/cm³-sec
 H = $C_p(T_b - T_u)$, heat of reaction, cal/gr
 $k(T)$ = thermal conductivity of mixture, cal/cm-sec-K
 M_u = molecular weight of unburned gas, gr/mole
 P = pressure, kcal/cm³
 R = universal gas constant, 1.986 kcal/mole-K
 T = temperature, K
 T_u = temperature of unburned gas, K
 T_b = temperature of burned gas, K
 τ = $(T - T_u)/(T_b - T_u)$, dimensionless temperature rise

Introduction

D. B. Spalding (1)² has recently considered reaction rate expressions for the laminar flame which take the form

$$k(T)f(T) \cong A(1 - \tau)^m \tau^n \dots \dots \dots [1]$$

This approximate representation of the overall chemical kinetics provides a decisive simplification in the theoretical treatment of many combustion problems. The exponent m , the well-known effective order of the overall chemical reaction, can be determined empirically from the pressure sensitivity of the laminar burning velocity (2); it should be remarked that m , then, is not necessarily an integer. The exponent n , which we shall call the effective index of the overall chemical reaction, seems to be an equally appropriate parameter for a generic classification of combustion experiments.

The principal reason for assigning $\{m, n\}$ labels to a flame experiment is that these parameters completely determine the approximate dimensionless structure of the flame, as a consequence of [1] and the flame equations. A knowledge of the changes in the $\{m, n\}$ labels, in response to changes in the

Received July 22, 1958.

¹ National Science Foundation Predoctoral Fellow. Present address: Palmer Physical Laboratory, Princeton University. Member ARS.

² Numbers in parentheses indicate References at end of paper.

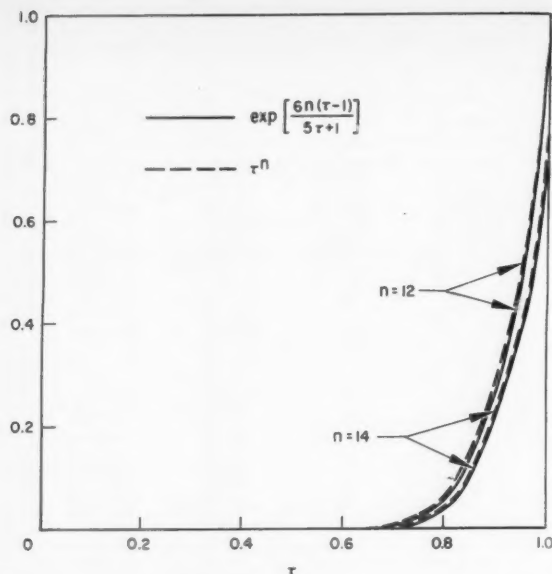
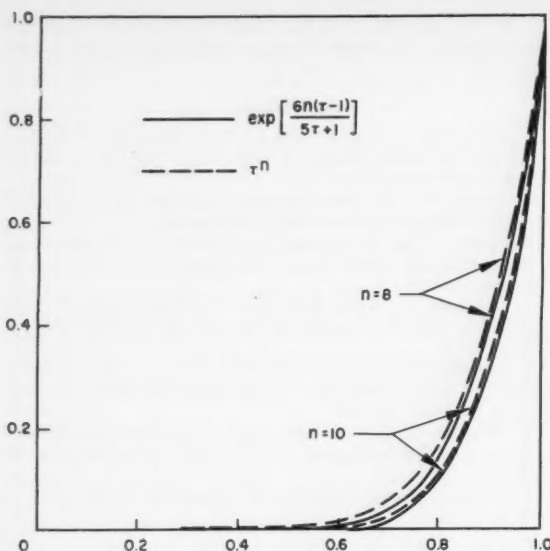


Fig. 1 The Spalding approximation for typical values of the index n

preparation of the flame, will provide theorists with a clue for understanding the associated changes in flame structure.

The purpose of this note is twofold. First, to show how the *index* can be related to the more venerable parameters of combustion chemistry. Second, to give up-to-date theoretical expressions for the empirical determination of $\{m, n\}$ labels from laminar flame experiments.

Theory

According to flame theory (1, 3, 4), the *laminar burning velocity*

$$S_u = \frac{RT_u}{PM_u} \left[\frac{1}{\lambda H} \int_{T_u}^{T_b} k(T) f(T) dT \right]^{1/2} \quad [2]$$

with the dimensionless eigenvalue parameter λ somewhat less than $\frac{1}{2}$ for practical reaction rate expressions. The traditional semitheoretical approach estimates the temperature dependent functions with the forms

$$k(T) = k_b \left(\frac{T}{T_b} \right)^g \quad [3]$$

$$f(T) = B(1 - \tau)^m \left(\frac{P}{RT} \right)^m \left(\frac{T}{T_b} \right)^h \exp \left(-\frac{E}{RT} \right) \quad [4]$$

Comparing these expressions with the Spalding approximation [1], we see that

$$A = Bk_b \left(\frac{P}{RT_b} \right)^m \exp \left(-\frac{E}{RT_b} \right) \quad [5]$$

and

$$\tau^n \cong \left(\frac{T}{T_b} \right)^{g+h-m} \exp \left(\frac{E}{R} \left[\frac{1}{T_b} - \frac{1}{T} \right] \right) \quad [6]$$

It will be noticed that [6] has been adjusted so that both sides become exactly equal at $T = T_b$ ($\tau = 1$). We determine the *index* n by requiring that the derivatives of both sides become equal at $T = T_b$. This gives

$$n = \frac{H}{C_p T_b} \left(\frac{E}{RT_b} + g + h - m \right) \cong \left(\frac{H}{C_p T_b} \right) \left(\frac{E}{RT_b} \right) \quad [7]$$

In the figures we have plotted both sides of [6] for the

typical case of $g + h = m$, $H/C_p T_b = 5/6$, and for several values of the index, $n = 5/6$ (E/RT_b). Through the entire range of physical interest, the semitheoretical and Spalding approximations correspond uniformly to within about 2 per cent. (See figures.)

Now we substitute [1] into [2]. Using [5 and 7], we obtain

$$S_u \cong \left[\frac{\beta(m, n)}{\lambda(m, n)} \frac{Bk_b}{C_p M_u^2} \exp(g + h - m) \right]^{1/2} \times \left[\frac{P}{RT_b} \right]^{(m/2)-1} \left\{ \left(1 - \frac{H}{C_p T_b} \right) \exp \left(-\frac{C_p T_b n}{H} \right) \right\} \dots [8]$$

with the Euler product of Gamma functions

$$\beta(m, n) \equiv \frac{\Gamma(m+1)\Gamma(n+1)}{\Gamma(m+n+2)} \quad [9]$$

Thus, if the burning velocity of a combustible mixture is measured at different pressures with the same flame temperature, we have the influence coefficient

$$\left(\frac{\partial(\ln S_u)}{\partial(\ln P)} \right)_{T_b} \cong \frac{m}{2} - 1 \quad [10]$$

On the other hand, suppose the burning velocity of a combustible mixture is measured at *neighboring* flame temperatures with the same pressure, by varying the initial temperature and density. Since the influence coefficient receives predominant contributions from the terms within the braces in [8], we have

$$\left(\frac{\partial(\ln S_u)}{\partial(\ln T_b)} \right)_P \cong \frac{1}{\frac{C_p T_b}{H} - 1} + \frac{C_p T_b n}{H} \quad [11]$$

Rewriting [10 and 11], the experimental definitions of the $\{m, n\}$ labels appear as

$$m \equiv 2 \left[1 + \left(\frac{\partial(\ln S_u)}{\partial(\ln P)} \right)_{T_b} \right] \quad [12]$$

$$n \equiv \frac{2H}{C_p T_b} \left[\left(\frac{\partial(\ln S_u)}{\partial(\ln T_b)} \right)_P - \frac{1}{\frac{C_p T_b}{H} - 1} \right] \quad [13]$$

References

- 1 Spalding, D. B., "Theory of Laminar Flame Propagation," *Combustion and Flame*, vol. 1, 1957, p. 287.
- 2 Gray, P., Lee, J. C. et al., "Propagation and Stability of the Decomposition Flame of Hydrazine," Sixth Symposium (Int.) on Combustion, Combustion Institute, 1957, p. 255.
- 3 Rosen, G., "An Action Principle for the Laminar Flame," Seventh Symposium (Int.) on Combustion, Combustion Institute, 1958 (in publication).
- 4 Rosen, G., "Generalization of the Laminar Flame Action Principle for Arrhenius-type Rate Expressions," *Combustion and Flame*, vol. 3, Jan. 1959 (in publication).

On the Importance of the Sensitive Time Lag in Longitudinal High-Frequency Rocket Combustion Instability

LUIGI CROCCO,¹ JERRY GREY² and DAVID T. HARRJE³

Princeton University, Princeton, N. J.

It was determined experimentally that there is an upper limit to the chamber length at which each mode of longitudinal high-frequency pressure oscillations will occur, and that this limit was accurately predicted for the fundamental mode by Crocco's sensitive time lag theory over a wide range of mixture ratios. The technique of using longitudinal stability boundaries for simple and direct experimental determination of the sensitive time lag and associated parameters was established as valid and may be used to replace the complicated and difficult chamber transfer function measurements described in previous publications.

Introduction

AN EXTENSIVE experimental study was performed on a small uncooled rocket motor using liquid propellants (95 per cent ethyl alcohol and liquid oxygen) in order to establish accurately the nature of the stability boundaries for longitudinal high-frequency combustion pressure oscillations. This study comprised a small part of an overall program⁴ aimed at the attainment of sufficient systematic knowledge to provide ultimate elimination of rocket combustion instability phenomena.

Experimental Data

The experiments discussed in this note consisted basically of determining the effects on high-frequency stability of varying mixture ratio and combustion chamber length. The length changes were achieved by adding and removing cylindrical sections of the experimental chamber (1),⁵ and the mixture ratio was changed by adjustment of injector pressure levels. Steady-state chamber pressure (nominally 300 psia) and mixture ratio were maintained constant on each run by a servo control system (2). Thrust level was approximately 250 lb. The experimental data included measurements of amplitude and frequency of combustion pressure oscillations, approximate axial distribution of steady-state chamber gas velocity, and the usual steady-state performance parameters. Details of the experimental apparatus and methods have been described in a number of previous publications (e.g., (1,2) and their bibliographies) and need not be repeated here.

A brief summary of the experimental results is presented in

Received Nov. 3, 1958.

¹ Robert H. Goddard, Professor of Jet Propulsion. Fellow Member ARS.

² Assistant Professor of Aeronautical Engineering. Member ARS.

³ Staff Research Engineer. Member ARS.

⁴ Sponsored by the Powerplant Division, Bureau of Aeronautics, U. S. Navy, Contract NOas 53-817-c.

⁵ Numbers in parentheses indicate References at end of paper.

Fig. 1, which plots the observed stability boundaries as functions of mixture ratio and chamber length. The experimental definition of these boundaries is demonstrated in the three-dimensional plot of Fig. 2 (which includes, for clarity, only the fundamental mode), showing the measured amplitude of pressure oscillations as a function of length and mixture ratio. Fig. 2 and photos of the observed wave shape demonstrated clearly that shock-type pressure waves occurred quite close to the stability boundaries.

Discussion

The experimental results of Figs. 1 and 2 corroborate directly the Crocco theory's well documented qualitative prediction (e.g. (1, 2) and Ref. 1, 2 of (4) etc.) that there exists an upper limit of chamber length beyond which any given longitudinal mode of oscillations cannot develop, as well as the lower limit which has been observed by a number of other experimenters (e.g., Berman, Tischler, Zucrow and their respective collaborators). Note that this existence of an upper limit clearly invalidates the oscillation-producing mechanism advanced by Zucrow and Osborn (3) as discussed by Crocco (4) since this mechanism cannot account for the observed cessation of oscillations with increasing chamber length (see Figs. 1 and 2).

Besides being the only mechanism which predicts qualitatively the upper longitudinal stability boundary, however,

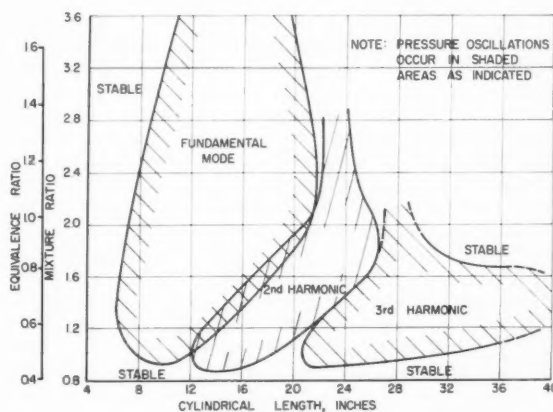


Fig. 1 Experimental longitudinal stability boundaries. Clarity of definition of the boundaries is shown in Fig. 2

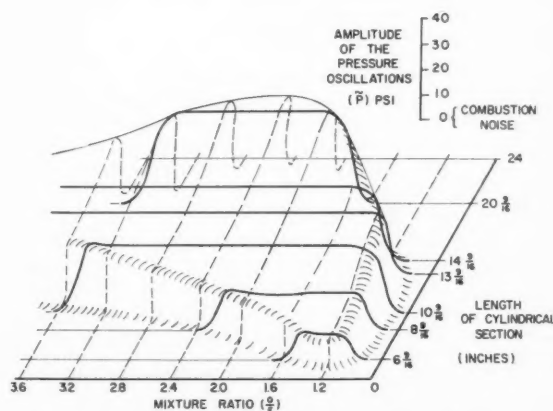


Fig. 2 Three-dimensional plot of the experimental fundamental mode longitudinal stability boundary, showing the definition obtained. Nominal chamber pressure is 300 psia. (Second and third harmonic boundaries are omitted for clarity)

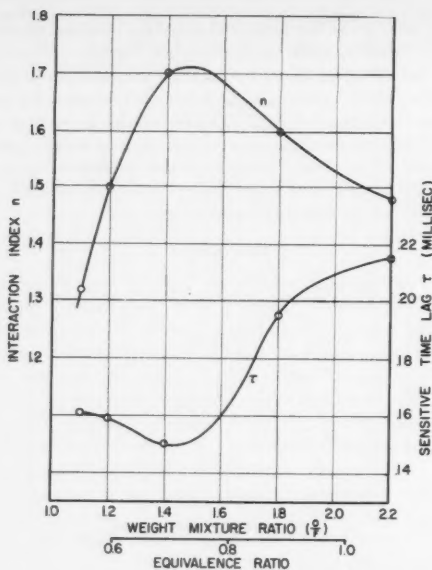


Fig. 3 Values of sensitive time lag τ and interaction index n obtained by using experimental data from the lower first mode stability boundary

the theory based on the sensitive time lag concept as first outlined by Crocco is unique in its capability for quantitative prediction of stability behavior. Previous publications giving results of the Princeton program have demonstrated that the theory has predicted quite well the effects on longitudinal stability boundaries of nozzle configuration and chamber pressure (e.g. (1) and Ref. 5 of (4), etc.) using measurements of the time lag and its associated parameters obtained for a few cases from chamber transfer function determinations (2). A more general, simpler and more direct experimental proof of the quantitative accuracy of the sensitive time lag theory as developed in detail in Ref. 2 of (4) will now be given, using the experimental data which appear here in Fig. 1.

It is demonstrated in the cited reference that for the general case of longitudinal pressure oscillations in a rocket motor,⁶ the theoretical conditions for neutral oscillations (i.e., the stability boundaries) may be expressed by

$$n = n(\omega, \alpha, \gamma, u(x), L, \epsilon, k)$$

$$\tau = \tau(\omega, \alpha, \gamma, u(x), L, \epsilon, k, m)$$

[1]

where

- τ = sensitive time lag
- n = interaction index relating time lag to the chamber parameters (primarily pressure and temperature). It represents in a synthetic way the degree of sensitivity of τ to variations in the chamber conditions
- ω = observed frequency at which neutral oscillations occur (i.e., at the stability boundary)
- α = complex nozzle admittance parameter, calculated by the theory of (5) and conclusively verified by experiments described in (6) and later papers

⁶ Fortunately, it no longer appears absolutely necessary to justify the application of a linearized analysis to so nonlinear a process as the shock-type pressure oscillations observed. The use of linearized equations to predict stability boundaries, at which no finite oscillations exist, is a well-known technique applied in the instability analyses of practically every field of dynamics. Further, it has been demonstrated experimentally for this rocket motor configuration that longitudinal shock waves, artificially produced by cartridges, had a negligible effect on the stability boundaries measured in the undisturbed rocket chamber (2).

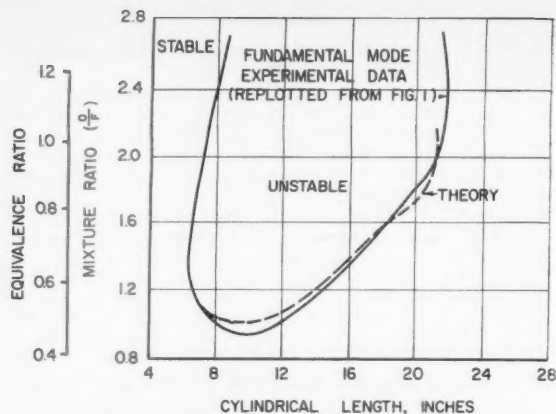


Fig. 4 Comparison of theoretical prediction with experimental observation of the upper fundamental mode stability boundary. The theoretical prediction is based on values of τ and n from Fig. 3, obtained from measurements at the lower boundary

- γ = mean value of specific heat ratio of combustion gases
- $u(x)$ = axial chamber gas velocity distribution
- x = axial space coordinate
- L = chamber cylindrical length
- ϵ = mean speed of sound in chamber
- m = mode of longitudinal oscillation (e.g., $m = 1$ corresponds to fundamental mode, $m = 2$ to second harmonic, etc.)
- k = estimated liquid droplet drag coefficient

Details of Equations [1] and the definitions of some of the above parameters are not essential to the present discussion, and in the interest of brevity, since they are thoroughly documented in the references cited, no further comment will be made here. It suffices to note that all quantities on the right-hand sides of Equations [1] were readily measured or inferred experimentally at the stability boundaries shown in Fig. 1.

First, Equations [1] were used to calculate the critical values of τ and n , using experimental data measured at the chamber lengths corresponding to the lower stability boundary (fundamental mode) of Fig. 1 at a number of the observed mixture ratio points. (Calculations to cover the full mixture-ratio range of Fig. 1 are now in process.) These values⁷ of n and the sensitive time lag τ are shown in Fig. 3.

Note that the values which appear in Fig. 3 do not in themselves constitute any check on the theory, since they are merely calculated from the measured lower stability boundaries of Fig. 1 and the theoretical Equations [1]. However, if the theory used to obtain the values of τ and n shown in Fig. 3 is correct, and if τ and n are, as the theory postulates, a valid mechanism for description of the rocket combustion processes, then at each experimental mixture ratio, Equations [1] solved for L and ω using the τ and n values of Fig. 3 should be capable of predicting quantitatively the chamber length and frequency at which the upper stability limit should appear.

Fig. 4 compares the theory's predictions of the upper first mode stability boundary with the experimental findings, replotted from Fig. 1. Quantitative calculations for the higher modes, whose existence is predicted by the theory, are now in process and will be presented in the complete report. The degree of correlation shown in Fig. 4 provides satisfactory verification of the sensitive time lag theory.

⁷ It should be pointed out that good agreement had been found between these calculations and previous measurements of τ and n at one mixture ratio by the more complicated method involving chamber transfer function measurement, as indicated in earlier publications, e.g., (1, 2). This, in effect, had constituted a limited but nevertheless quantitative verification of the theory.

Conclusions

1 It was observed conclusively by experiments on oxygen-alcohol hardware that there exists an upper limit to the chamber length above which a mode of longitudinal high-frequency pressure oscillation cannot occur in a rocket motor, as predicted by Crocco's sensitive time lag theory. This upper limit cannot be explained by any other mechanism advanced to date.

2 The sensitive time lag theory as developed in Ref. 2 of (4) has been used to predict *quantitatively* the upper stability boundary (i.e., chamber length) of the fundamental mode of longitudinal high-frequency oscillation over a wide range of mixture ratios. These results constitute a considerable extension of the previously established experimental verification for the lower fundamental mode stability boundary at one mixture ratio.

3 The longitudinal stability-boundary method of determining the combustion parameters τ and n , used to establish the above results, provides a remarkably simple and accurate determination of these important high-frequency stability criteria. This technique is expected to replace the former difficult and complicated transfer-function method described in previous publications.

Extension of Results

The above results were obtained for a single chamber pressure, propellant combination and injector type. Similar experiments for different chamber pressures, widely different injector characteristics, and several combinations

of fuels and oxidizers have been in process for some time. This rather complete survey of longitudinal rocket instability, of which the results given in this paper form a small part, will be included in a more comprehensive report at an early time.

Acknowledgments

The authors gratefully acknowledge the invaluable assistance of Frederick H. Reardon, Dr. Eva A. Kronenberg and members of the technical staff of the Jet Propulsion Research Group. Financial support by the U. S. Navy's Powerplant Division, Bureau of Aeronautics, made this study possible.

References

- 1 Crocco, L. and Grey, J., "Measurement of High-Frequency Limits of Stability in a Liquid Bipropellant Rocket Motor," *L'Aerotecnica*, vol. 38, June 1958, p. 135.
- 2 Crocco, L. and Grey, J., "Combustion Instability in Liquid Propellant Rocket Motors," Princeton University Aeronautical Engineering Report no. 216, Quarterly Installments Sept. 1, 1952, through Sept. 1, 1958.
- 3 Zucrow, M. J. and Osborn, J. R., "An Experimental Study of High-Frequency Combustion Pressure Oscillations," *JET PROPULSION*, vol. 28, Oct. 1958, p. 654.
- 4 Crocco, L., "Comments on the Zucrow-Osborn Paper on Combustion Pressure Oscillations," *JET PROPULSION*, vol. 28, Dec. 1958, p. 843.
- 5 Crocco, L., "Supercritical Gaseous Discharge with High-Frequency Oscillations," *L'Aerotecnica*, vol. 33, 1953, p. 46.
- 6 Lambiris, S., "Experimental Verification of Nozzle Admittance Theory in a Simulated Rocket Chamber," Project Squid Technical Report PR75-R, Sept. 15, 1957.

Technical Comment

Comments on the Zucrow-Osborn Paper on Combustion Oscillations

LUIGI CROCCO¹

Princeton University, Princeton, N. J.

THE idea that the phenomenon of high-frequency combustion instability in liquid propellant rockets should be related to the effect of pressure waves on the local rates of combustion was first introduced in a paper which I published in this JOURNAL in 1952 (1).² By means of the analytical treatment of a simple combustion model I was able to show, indeed, that the appearance of instability is determined by (a) a space condition, that is, the regions of maximum energy release must be sufficiently far away from pressure nodes, and (b) a time condition, that is, the ratio between a characteristic combustion time, called the *sensitive time lag*, and the period of the oscillations must lie in certain ranges. Observe that the sensitive time lag is not the same as the *total time lag* (on which the theory of *low frequency* rocket combustion instability is centered), and actually it must be much shorter in order to justify the high frequencies encountered. These ideas, applied later to more complicated models, are summarized in a monograph (2) which also includes the experimental confirmations available at the time. Many additional publications by various authors, both in the United States and abroad, have shown that in general the mechanism on which these theories are based has been accepted as correct.

A different mechanism, which does not involve the idea of a time lag, has been advanced in a recent publication (3) by Zucrow and Osborn, based on the interpretation of experimen-

tal results obtained through a technique similar to that already used in recent years at Princeton (4). The main difference in the experiments at Purdue consists of the use of premixed gaseous propellants, and promises to furnish interesting comparative results by eliminating the processes of atomization, evaporation and mixing always present when the propellants are liquid and unmixed. The conclusions reached by Zucrow and Osborn can be summarized as follows:

1 The unstable burning observed is due to the effect of pressure waves in increasing the local burning rates.

2 The tendency toward instability is greater when the amount of propellant injected during one period of oscillation is larger, and therefore increases with decreasing frequency.

3 As a result of argument 2, and in agreement with experimental observations, a *critical combustion chamber length* exists below which the frequencies are too high for an appreciable pressure oscillation to be produced, and above which the always decreasing frequency provides the conditions for unstable operation with a pressure amplitude that steadily increases with increasing chamber length.

4 The same argument can be applied to transversal types of instability to explain the aptitude of large rocket motors of small aspect ratio to exhibit this type of instability.

5 The shock-fronted pressure waves traveling in the combustion chambers are a type of detonation wave.

Analyzing these statements in order, we see that:

1 This suggestion is exactly the same as the one advanced in my 1952 paper (1), and since then reformulated by various authors.

2 This argument does not stand a more critical examination, since in the appearance and maintenance of the unstable process what counts is not the absolute value of the excess energy released during one cycle as a consequence of the modified combustion rates, but the balance between this ex-

Received Nov. 3, 1958.

¹ Robert H. Goddard Professor of Jet Propulsion. Fellow Member ARS.

² Numbers in Parentheses indicate References at end of paper.

cess energy and the excess energy absorbed during the whole cycle by dissipative processes and by the nozzle. With decreasing frequency both the released and the absorbed excess energies increase, and hence the balance is not particularly sensitive to the frequency level. In other words, it is not the excess energy during one cycle which determines the possibility of unstable combustion, but rather the excess energy per unit time, or the excess power.

3 This statement is contradicted by the results of some careful experiments carried out at Princeton. The first indications from these experiments have already been released, e.g., (4, 5 and 6). More complete results will soon be published in a full report now in preparation, but a preliminary release was believed necessary at this stage and is the object of a separate Technical Note in this same issue (7). It is clearly shown by these results that it is not true that only a lower critical length exists, above which oscillations become more and more severe, but that for each mode of longitudinal oscillation there exists a range of lengths outside which the operation is stable, while inside it is unstable. Thus, by sufficiently increasing the chamber length, the operation becomes stable again for a given mode (though it may still be unstable for higher modes). This result invalidates the mechanism suggested by Zucrow and Osborn (if a proof is still needed of its fundamental incorrectness). It also is a clear confirmation of the existence of a characteristic combustion time and of its fundamental importance in determining whether a rocket will operate under stable or unstable conditions. The analysis of the data actually allows the determination of this characteristic combustion time (which we have called the sensitive time lag, or simply the time lag), and of other important characteristic quantities related to combustion, and gives a proof of the fundamental correctness of the combustion model which is the basis for the existing theoretical treatments of rocket combustion instability (2). This is shown in the Technical Note in this issue (7).

4 Systematic quantitative experimental information about transversal instability is not yet available. The Princeton group and others in this country are actively engaged in an effort to provide data of this kind. But even before these results become available, I believe I may predict that no matter what is the actual mechanism responsible for instability, the time lag will again play a fundamental role, and that its ratio to the period of the oscillations will have to lie in well determined ranges if instability is to occur. The fact that in large rocket motors unstable operation is more likely to appear is probably related to the fact that in a chamber of no matter what shape there exists an infinite series of frequencies of natural oscillation corresponding to various modes and starting from a well determined minimum value. For small chambers, this minimum frequency may be such that the corresponding period of oscillation is too short compared to the sensitive time lag, and for no oscillation mode will the chamber be in a condition conducive to unstable operation. If, however, one of the dimensions of the chamber is increased, lower minimum frequencies and longer oscillation periods may be produced, thus upsetting the balance with the time lag (if, as is likely to happen, this has not changed in the same proportion) and favoring the appearance of instability. If the length of the chamber is increased, the instability, when produced, is of the longitudinal type. If the diameter is increased, transversal instability is the result. By further increasing the dimensions, other modes may always produce frequencies in the range proper for the appearance of instability, so that it is quite possible that stability cannot be found again by just increasing the dimensions, but that, in order to

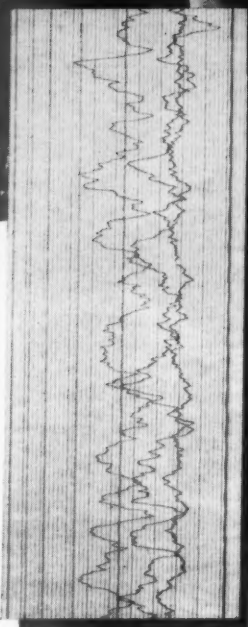
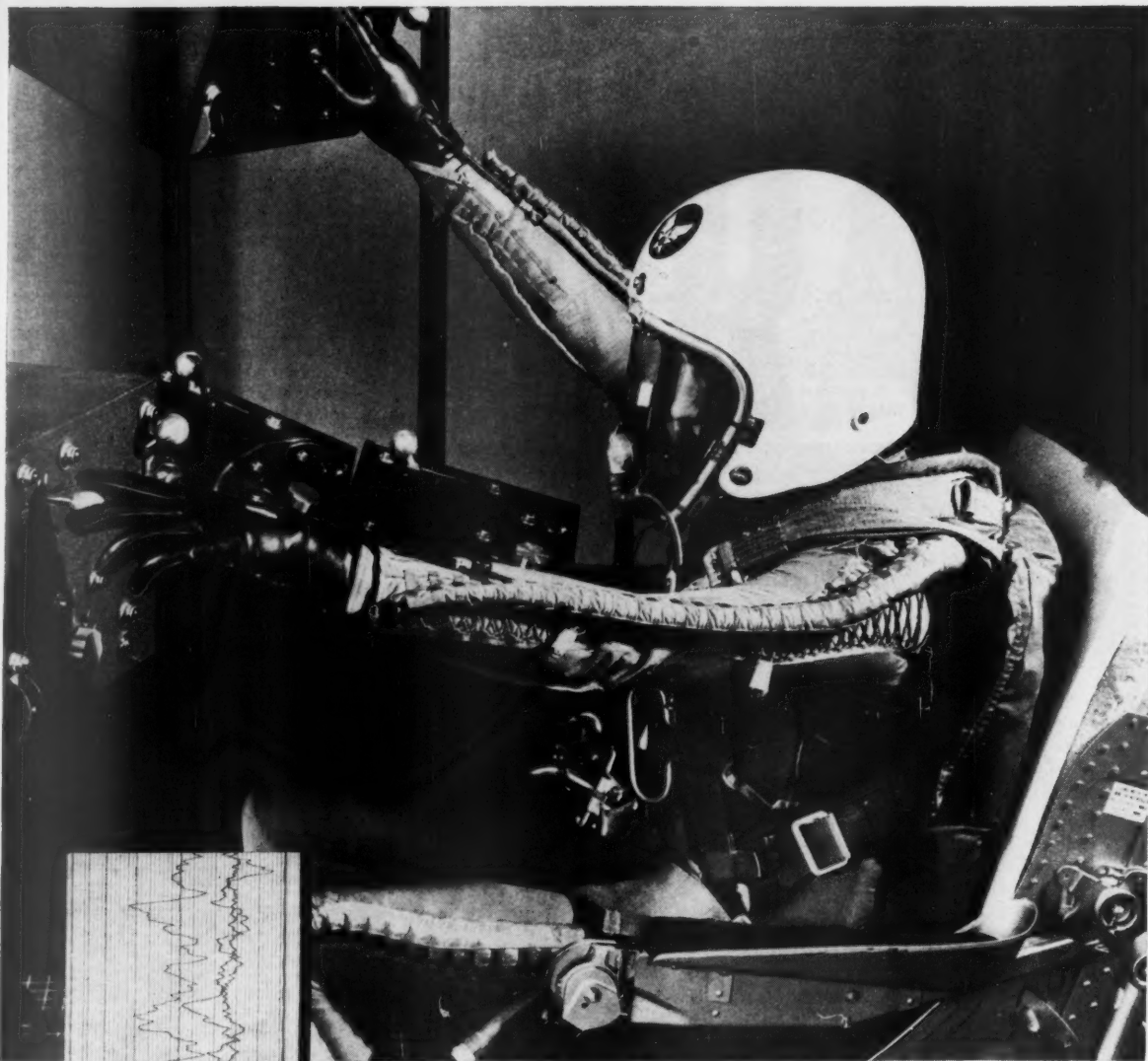
obtain stable combustion with large chambers, the overall energy balance must be modified through a change in the space distribution of combustion or an increase of damping. This may be particularly necessary in the case of transversal instability, since an unpublished theoretical study shows that the damping effect of the nozzle is absent for transversal oscillations. In principle, there would also be the possibility of obtaining stability through a suitable increase of the time lag. But in practice, this may be either impossible (if the sensitive time lag is essentially determined by the chemical properties of the propellants, as it certainly is for premixed gaseous propellants) or undesirable (because it may result in the necessity of a larger chamber to maintain the performance level).

5 The concept that the waves propagating in the chamber are a kind of detonation wave is somewhat misleading. In fact, in a rocket chamber the shock wave (when it exists) merely accelerates the rates of a combustion process which would take place even in the absence of the shock wave, while in a detonation wave the chemical change is initiated by the passage of the shock wave, on which it essentially depends. Moreover, the velocities and amplitudes of the shock waves are much below the values they would achieve for an ordinary detonation wave (which, by the way, are very well defined for the case of premixed gaseous propellant as used in the Purdue experiments). Finally, to introduce the concept of this type of detonation wave as essential to the phenomenon of instability would make a different mechanism necessary for the case when the waves are of a sinusoidal nature, as they are in many instances of fully developed instability, and always at the onset of a self-started instability (see, for instance, Fig. 5 of (3)).

It is surprising that a highly competent group such as that headed by Professor Zucrow at Purdue University should advance a new mechanism to explain the combustion instability in rockets, without any reference to previous formulations extensively used in the published literature. Perusal, even limited, of this literature would probably have indicated to the authors the incorrectness of their conclusions.

References

- 1 Crocco, L., "Aspects of Combustion Instability in Liquid Propellant Rocket Systems, Part I," *JOURNAL OF THE AMERICAN ROCKET SOCIETY*, vol. 21, Nov.-Dec. 1951, p. 163; Part II, *ibid.*, vol. 22, Jan.-Feb. 1952, p. 7.
- 2 Crocco, L. and Cheng, S. I., "Theory of Combustion Instability in Liquid Propellant Rocket Motors," AGARD Monograph no. 8, Butterworths Scientific Publications, London, 1956.
- 3 Zucrow, M. J. and Osborn, J. R., "An Experimental Study of High-Frequency Combustion Pressure Oscillations," *JET PROPULSION*, vol. 28, Oct. 1958, p. 654.
- 4 Crocco, L. and Grey, J., "Measurement of High-Frequency Limits of Stability in a Liquid Bipropellant Rocket Motor," *L'Aerotecnica*, vol. 38, June 1958, p. 135.
- 5 Grey, J., "Experimental Determination of the Longitudinal Limits of Stability in a Liquid Bipropellant Rocket Motor," Third Conference on Rocket Combustion Instability, Princeton University, October 20-22, 1955. (Also Appendix D to Fourteenth Quarterly Installment of Princeton University Aeronautical Engineering Report no. 216-n, Dec. 1, 1955.)
- 6 Crocco, L. and Harrie, D. T., "Combustion Instability in Liquid Propellant Rocket Motors," 24th Quarterly Progress Report, Princeton University Aeronautical Engineering Report no. 216-x, June 1, 1958.
- 7 Crocco, L., Grey, J. and Harrie, D. T., "On the Importance of the Sensitive Time Lag in Longitudinal High-Frequency Combustion Instability," *JET PROPULSION*, vol. 28, no. 12, p. 841.



Why wait for the answers?

... Observe and evaluate phenomena *as they occur*—with new Kodak Linagraph Direct Print Paper!

This new photorecording paper gives *immediate readout* in moving-mirror galvanometer oscillographs—with *no photochemical developing*. Gives sharp, legible traces over a wide range of recording frequencies—from 0 cps to 3000 cps.

Linagraph Direct Print records can be used in recording system readers, accept pen and pencil notations readily. They have adequate permanence and may be stabilized for extended archival storage.

Now available in 5" x 200', 6" x 100', 7" x 200', and 12" x 200' rolls. Other sizes on request. For complete details, write:

EASTMAN KODAK COMPANY
Graphic Reproduction Division
Rochester 4, N. Y.

Kodak
TRADE MARK

New Patents

George F. McLaughlin, Contributor

Object locating apparatus (2,842,760). J. L. McLucas, State College, Pa., assignor to Haller, Raymond and Brown, Inc.

Means for selectively energizing a cathode-ray tube control grid with the output of a radar receiver or the output of a facsimile pickup head.

Moving target indicator radar system (2,842,761). J. M. Downs, Glen Cove, N. Y., assignor to Sperry Rand Corp.

Detector connected to a receiver with means to delay reflected signals at least one cycle of pulse repetition frequency. Subtracting and adding means integrate delayed and undelayed versions of the signals.

Collision warning radar (2,842,764). N. L. Harvey, Eggertsville, N. Y., assignor

EDITOR'S NOTE: Patents listed above were selected from the Official Gazette of the U.S. Patent Office. Printed copies of patents may be obtained from the Commissioner of Patents, Washington 25, D. C., at a cost of 25 cents each; design patents, 10 cents.

to Sylvania Electric Products, Inc.

Ranging apparatus with bandpass filter tuned to reject all frequencies outside the band corresponding to the Doppler shift in the echo-signals frequencies received.

Infrared transmitting mirror (2,852,980). H. Schroder, Munich, Germany.

Mirror for reflecting visible rays from a light source and transmitting the heat rays. Reflector consists of layers of a transparent material nonabsorbent of infrared rays, and alternate layers of material having a high index of refraction.

Swingaway support for missiles (2,852,981). C. A. Caya, Los Angeles, Calif.

U-shaped suspension member on a bomb rack engaging a hood on the top of the missile and permitting the hook to swing from an upwardly extending position to a folded position within the missile upon release.

Aerial carry and release mechanism (2,852,982). C. W. Musser, Philadelphia, Pa., assignor to the U. S. Army.

Hooks in holding grooves in a pair of

supports released by firing a cartridge-actuated initiator which moves a piston in a cylinder. Mechanical linkage from the piston disengages the hooks attached to the store to be released.

Control apparatus (2,853,255). A. P. Rasmussen and F. J. Huddleston, Millersville, Md., assignors to Westinghouse Electric Corp.

System for controlling a control surface of an aircraft. A decoupling link is placed between a manual controller and a servo controller. Means responsive to the power supply operates the decoupling link from one position to the other.

Aircraft ejection seat (2,853,258). O. F. Polleys, Windsor, Conn., assignor to Chance Vought Aircraft, Inc.

Capsule, with a body and cover, spaced behind the pilot's seat. The seat may be moved into the capsule body, completely covered and ejected from the aircraft.

Motion measuring system (2,853,287). C. S. Draper and C. L. Emmerich, Cambridge, Mass., assignors to Research Corp.

Viscous damped mass element mounted



Small parts requiring very close tolerances and numerous machine operations have been our specialty during the past half-century! We invite your quotation requests and suggest that you write for our illustrated brochure to see how our facilities can be put to work for you!

LaVezzi MACHINE WORKS
4635 WEST LAKE ST., CHICAGO, ILLINOIS



Aircraft Controls
for all types of flight vehicles

TEMPERATURE & POSITIONING CONTROLS

AIR VALVES

ACTUATORS

GROUND TEST EQUIPMENT

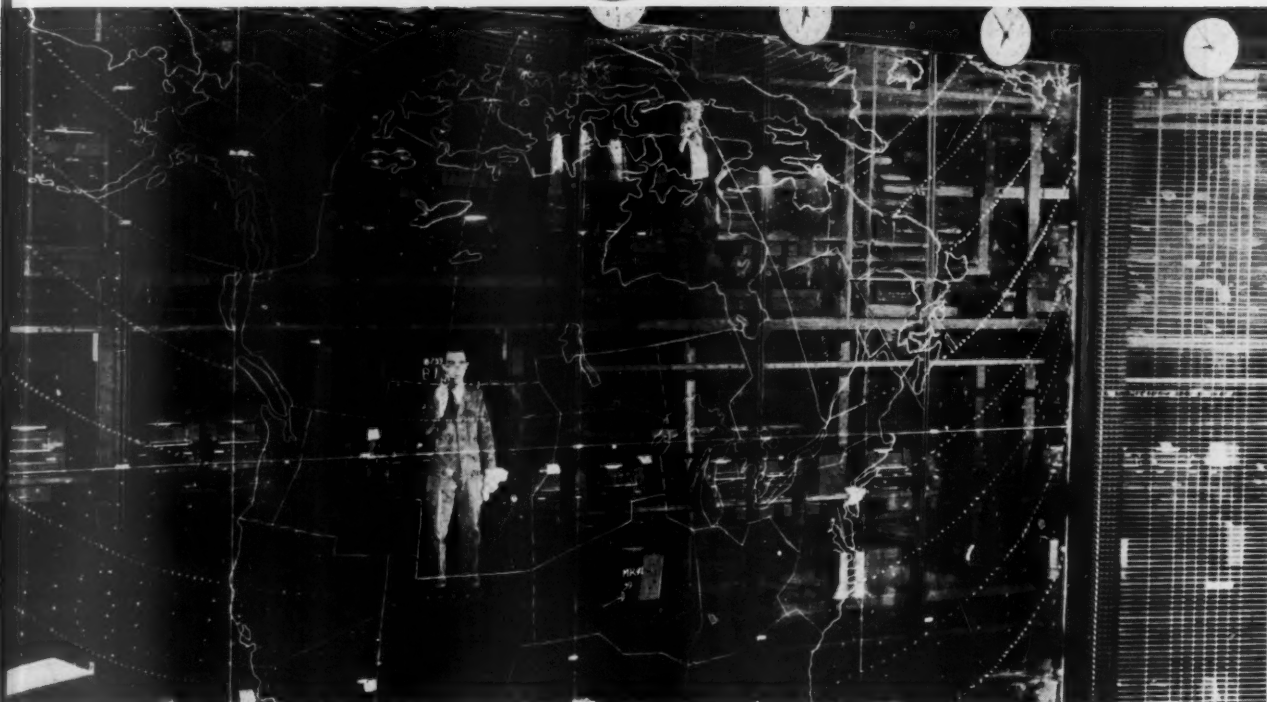
Write for complete data or consult the Barber-Colman engineering sales office nearest you: Los Angeles, Seattle, Fort Worth, New York, Baltimore, Montreal, Rockford.

BARBER-COLMAN COMPANY
Dept. L - 1470 Rock Street, Rockford, Illinois.

Preserver of Peace...

**Wrap-around
bumper for
a continent**

NORAD



Headquarters—NORAD—Colorado Springs

Like a huge "bumper" wrapped around the North American continent and reaching down along both the Atlantic and Pacific shores, the North American Air Defense Command (NORAD) has been created for operational control of air defense units of the Army, Navy and Air Force of the U.S. and the RCAF Air Defense Command of Canada. Its field includes the vast area between the southern border of the United States and the

northernmost limits of Canada and Alaska. Under the functional control of NORAD will be BMEWS (Ballistic Missile Early Warning System) and SAGE (Semi-Automatic Ground Control Environment) for the defense of specified sectors. In addition to its responsibility as prime contractor for BMEWS, the Radio Corporation of America is working on other important electronic assignments for NORAD.



Tmk(s) ®

RADIO CORPORATION of AMERICA

DEFENSE ELECTRONIC PRODUCTS

CAMDEN, N. J.

DECEMBER 1958

847

ASI ENGINEERS & SCIENTISTS

Here is your opportunity to grow with a young, expanding subsidiary of the Ford Motor Company. Outstanding career opportunities are open in Aeronutronic's new RESEARCH CENTER, overlooking the Pacific at Newport Beach, and the facility in Glendale, California. You will have all the advantages of a stimulating mental environment, working with advanced equipment in a new facility, located where you can enjoy California living at its finest.

PhD and MS RESEARCH SPECIALISTS with 5 to 7 years' experience in heat transfer, fluid mechanics, thermodynamics, combustion and chemical kinetics, and thermoelasticity. To work on theoretical and experimental programs related to re-entry technology and advanced rocket propulsion. Specific assignments are open in re-entry body design, high temperature materials studies, boundary layer heat transfer with chemical reaction, thermal stress analysis, and high temperature thermodynamics.

PROPULSION ENGINEERS with 5 years' experience in liquid and solid rocket design and test. Familiarity with heat transfer problems in engines desirable. To work on program of wide scope in R & D of advanced concepts in rocket engine components, and for missile project work.

ADVANCED AERODYNAMIC FACILITY DESIGNER. Advanced degree desired. To supervise work in design and in instrumentation of advanced aerodynamic test facilities such as shock tubes, shock tunnels, plasma-jets, and hyper-velocity guns.

STRUCTURAL ANALYSIS SECTION SUPERVISOR with 8 to 10 years' experience, including supervision, in the missile field. Graduate degree for design and analysis required. Will be required to apply knowledge of high temperature materials and methods, thermal stress, dynamics, etc. to advanced hypersonic vehicles, re-entry bodies, and space vehicles.

FLIGHT TEST & INSTRUMENTATION ENGINEERS with 5 to 10 years' experience in laboratory and flight test instrumentation techniques. Will develop techniques utilizing advanced instrumentation associated with space vehicles.

THEORETICAL AERODYNAMICIST. Advanced degree and at least 5 years' experience in high-speed aerodynamics. Knowledge of viscous and inviscid gas flows required. To work on program leading to advanced missile configurations. Work involves analysis of the re-entry of hypersonic missiles and space craft for determining optimum configuration.

DYNAMICIST. Advanced degree, applied mathematics background, and experience in missile stability analysis desirable. Work involves re-entry dynamics of advanced vehicles and dynamic analysis of space craft.

ENGINEER or PHYSICIST. With experience in the use of scientific instruments for making physical measurement. Work related to flight test and facility instrumentation. Advanced degree desired with minimum of 3 years of related experience.

Qualified applicants are invited to send resumes and inquiries to Mr. L. R. Stapel.

AERONUTRONIC SYSTEMS, INC.

A subsidiary of Ford Motor Company
1234 Air Way, Bldg. 19, Glendale, Calif.
Chapman 5-6651

for deflections in a single degree of freedom. A generator signals any deflection from a neutral position, and a force generator is energized in a direction to reduce the deflection of the element.

Target position indicator (2,853,701). J. Freedman, R. O. Schlegelmilch and H. Sherman, Lexington, Mass., assignors to the U. S. Air Force.

Transparent screen, with translucent backing, on which recorded data are projected. Plotter's marks on the screen, together with projected recorded data, are sharper and clearer than the projected data. A rapid process camera is set to be sensitive only to the more visible plotter's marks and insensitive to the projected image.

Moving target cancellation circuit (2,853,702). M. C. Johnson and R. F. Ahrens, Eatontown, N. J., assignors to the U. S. Air Force.

Modulation of the beam of a cathode-ray tube in accordance with an alternating voltage, input and output circuits and a transformer with two primary windings coupled to a secondary winding. Voltages induced in the secondary winding by the input circuit currents cancel, and the output circuit is coupled to the secondary winding.

Video train bracketed by time-spaced control pulses (2,853,703). H. T. Hayes, Long Beach, Calif., assignor to Gilfillan Bros., Inc.

Generator for developing range marks and modulating them in accordance with voltages representing the scanning movements of a radiated antenna beam. Cursor voltages derived electronically establish a predetermined glide path course line in relation to runway course line.

Radio direction finders (2,853,704). A. J. Ortusi and A. Robert, Paris, France, assignors to Compagnie Generale de Telegraphie Sans Fil Corp.

System for determining the angular position of a first point with respect to a second point. UHF energy is emitted over a single carrier wave from one of the points. Energy is alternately concentrated at the second point. Current from the two points is measured, and the ratio between the currents establishes the distance relationship between the points.

Jet engine thrust control (2,853,851). M. E. Chandler, New Britain, Conn., assignor to Pratt & Whitney Co.

Engine mounted in movable relationship to the aircraft and moved in proportion to the reaction thrust, so the aircraft is propelled in a definite selected speed throughout the speed range of the aircraft.

Boundary layer control for aerodynamic ducts (2,853,852). A. G. Bodine Jr., Van Nuys, Calif.

Control of the aerodynamic-acoustic vibration originating in a layer of air next to the wall surface of a jet engine duct through which air travels at sonic speed. Frequencies in the region are controlled by a sound wave attenuator mounted outside the duct, a part extending through the wall and communicating with the air layer in the vibration area.

Rocket (2,853,946). A. C. Loedding, Princeton, N. J., assignor to Unexcelled Chemical Corp.

Lightweight shell with elongated propellant charges each having a polygonal cross section and operating at a pressure of 500 psi. Spaces between charges are filled with an elastic inhibitor to form a solid unit between the shell and charges.

Acceleration pressurized bipropellant liquid fuel rocket (2,850,975). W. D. Teague Jr., Alpine, N. J., assignor to Bendix Aviation Corp.

Thrust to the rocket is initiated by a booster charge using either hypergolic or nonhypergolic propellants, avoiding the need of a staging system in the injector system.

Thrust modifying device (2,847,822). G. F. Hausmann, Glastonbury, Conn., assignor to United Aircraft Corp.

Streamlined fins upstream of the nozzle of a jet powerplant, the rear portions movable for diverting the gases transversely of the duct axis.

Reversible thrust nozzle construction (2,847,823). T. L. Brewer, Ridgewood, N. J., assignor to Curtiss-Wright Corp.

Tail pipe extension for jet engines with vanes shaped to close the side walls and pivotally movable to direct the exhaust flow outward.

Wing tip jets (2,848,181). W. L. Landers, Smithburg, Md., assignor to Fairchild Engine and Airplane Co.

Pair of auxiliary jet engines mounted at the wing tips providing supplemental thrust to the airplane. Failure of one of the wing tip engines automatically cuts off the fuel supply to the engine on the opposite wing tip.

Ultrasonic apparatus for the non-destructive evaluation of structural bonds (2,851,876). J. S. Arnold, Palo Alto, Calif., assignor to the U. S. Air Force.

Ultrasonic frequency modulated cyclically over a narrow band of frequencies outside the resonant frequencies of the structure being tested.



Rocket motor with recrystallized silicon carbide throat insert (2,849,860). E. C. Lowe, Niagara Falls, Ontario, Canada, assignor to Norton Co.

Silicon carbide used for throat insert because of its high resistance to the non-oxidizing flame of a rocket motor reaction blast. The material can withstand temperatures as high as 2250 deg and is extremely erosion resistant.

Pressure vessels (2,848,133). E. M. Ramberg, Glen Head, N. Y.

Cylindrical container for fluids, constructed of a solid assembly of non-metallic fibrous strands of threads and helical wrappings. A solidified bonding material impregnates the threads, and a layer of metal foil is interposed between some of the wrappings.

Temperature responsive fuel control for gas turbine (2,848,868). R. W. Jensen, Encino, Calif., assignor to the Garrett Corp.

Needle valve for varying the flow of the fuel supply through a restricted inlet of one of two parallel flow paths, in response to temperature changes of the combustion air.

Blast release detent (2,848,925). D. W. Hood, Sherman Oaks, Calif., assignor to the U. S. Navy.

Rocket launcher casing and tube adapted to contain a rocket having tail elements and a retaining element at the rear end. Blast from an ignited rocket releases a detent from the retaining flange engaging position.



*The
Inquiring
Mind
at
Oldsmobile*

no. 6
OF A SERIES

TWO STEPS TO NEW FUEL ECONOMY

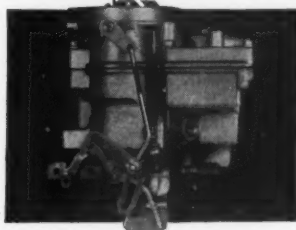
Unique Oldsmobile-developed two-stage automatic choke is a major step forward in improving automobile operating economy.

One of the important carburetor developments during the past few years was the automatic choke, a device that allows the automobile to be started in cold weather, and then keeps it running until the engine is sufficiently warmed up to sustain itself. Every automatic choke has two separate functions: 1) choking, which enriches the fuel-air mixture for starting, and 2) the idle speed control, which keeps the engine from stalling once it is started. In the past, and on all present carburetors except those used on the 1959 Oldsmobile, these two functions have operated simultaneously with the result that the engine ran on a rich mixture for the same length of time that the fast idle was "on". This resulted in excess fuel consumption.

With the introduction of the 1959 Oldsmobile, the two functions have been separated with a new and exclusive

two-stage automatic choke developed by Oldsmobile engineers. An ingenious system of over-running levers allows the choke fly to open 75% sooner than previously required. The fast idle, however, remains "on" for

the full warm-up period so the engine will not stall. This early elimination of the choking function represents a considerable fuel saving in cold weather when numerous short trips are made.



At Oldsmobile the Inquiring Mind is always at work, finding new and better ways to design, engineer and build finer automobiles for the most discriminating of buyers—the Oldsmobile owner. Discover the difference for yourself by visiting your local Oldsmobile Quality Dealer and taking a demonstration ride in a 1959 Oldsmobile.

OLDSMOBILE DIVISION, GENERAL MOTORS CORPORATION

OLDSMOBILE ➤

**Pioneer in Progressive Engineering
... Famous for Quality Manufacturing**

Book Reviews

Ali Bulent Cambel, Northwestern University, Associate Editor

Thermodynamics of One-Component Systems, by William N. Lacey and Bruce H. Sage, Academic Press, Inc., New York, 1957, xi + 376 pp. \$8.00.

Reviewed by JOHN F. LEE
North Carolina State College

The author states in the preface that this is a textbook intended to "help the student in his transit from science studies to engineering, from idealized thermodynamics to the combinations of thermodynamics with mechanics needed for dealing with everyday problems of the engineer." However, the book fails in its avowed purpose as a textbook and appears more appropriate as a review volume for an engineer or scientist who has already had a thorough and complete course in the basic thermodynamic principles and their applications. Part I of the book is devoted to a summary in rather a catalog form of the more important basic thermodynamic principles. Part II is devoted to applications in the restricted area of the traditional flow processes covered in most thermodynamics textbooks. The applications are covered in a most cursory fashion. The coverage is not only limited in scope, but is even more severely limited in depth. The basic principles of thermodynamics are stated concisely, accurately and clearly. The interpretation, the subtleties and the implications of the basic principles are left to the creative imagination or ingenuity of the reader. There is considerable merit in this approach, but one cannot avoid the feeling that the authors have previously carried it to an extreme.

One might expect that in Part II some of the deficiencies mentioned previously in presenting the thermodynamics principles in Part I might be alleviated. However, the applications covered in Part II are linked only inferentially to the principles discussed in Part I. It is difficult to see how the material presented in this book could serve as a basis for either scientific or engineering action on the part of a student or practicing engineer. Nevertheless, despite the shortcomings mentioned in this review, the volume should serve as a useful topical summary of thermodynamics for students or engineers whose interests fall within the scope of the book.

The Exploration of Space by Radio, by R. Hanbury Brown and A. C. B. Lovell, John Wiley & Sons, Inc., New York, 1958, 207 pp. \$6.50.

Reviewed by J. G. BOLTON
California Institute of Technology

This book gives an excellent account of the first twelve years work in the new science of Radio Astronomy. The authors are two men who have directed the efforts of the Jodrell Bank Experimental Station of Manchester University, which is one of the world's foremost radio observatories.

It is written chiefly from an experimentalist's point of view and can be understood by anyone who can follow articles in, say, the *Scientific American*. The book is copiously illustrated with explanatory diagrams and photographs, and only a bare minimum of mathematics is used.

The book is divided into 11 chapters. The first two contain a brief résumé of the necessary astronomical background and the factors governing the reception of extraterrestrial radio waves through the Earth's upper and lower atmosphere. The third chapter gives an account of some of the specialized antenna and receiver techniques used in radio astronomy. It is, however, principally confined to the meter wave lengths; that is the range in which the authors have been accustomed to work. It is somewhat surprising that the authors make no mention of the new high-frequency devices, such as the maser and the parametric amplifier, which promise such great increases in receiver sensitivity for the future.

There are then seven chapters on the results of various phases of radio astronomical investigation. These chapters are on galactic and extragalactic radio emissions (including the "radio stars"), the hydrogen line, the scintillation of radio stars, solar radio waves, meteors, radio and the aurora borealis, and finally radio investigations of the moon planets and the Earth satellites. The last three are concerned with radar-astronomy in which echo techniques are used, the others with reception of radio waves emitted by extraterrestrial objects. The better chapters are those on galactic and extragalactic radio emission, scintillation and meteors. These, rather logically, are the subjects with which the authors have been intimately concerned. The chapters on the 21-cm hydrogen line and the sun seem relatively brief compared with the amount of experimental work which has been done in these two fields. The chapter on the sun, for instance, contains only a brief reference to the work by Wild and his associates on the dynamic spectrum of solar disturbances. There is also no reference in the scintillation chapter to Wild's classification of scintillations using the same dynamic spectrograph.

As a matter of correction, in the chapter on the hydrogen line and that on radio stars, it is mentioned that there is a discrepancy between the distance of the Cassiopeia radio-star as determined optically and by means of the 21-cm absorption spectrum. Since the book was written, Dr. Walter Baade, of the Mount Wilson and Palomar Observatories, has made a new determination of the distance based on a longer period of observation of the expansion of the visible remnant. His recent determination of the distance is in excellent agreement with the rather easier radio measurement.

The final chapter of the book is on the giant 250-ft steerable telescope at Jodrell Bank. In collecting area, this instrument is larger by a factor of 10 than any other similar instrument in operation or under construction. Its successful completion represents a triumph in engineering skill on the part of the designer and in forethought for its originators. The reviewer can remember gazing down into the foundation pit for the central pivot at a time when most of the world's radio telescopes would have fitted into that pit. Extremely valuable work has been done by this instrument in both radar and radio tracking of the Sputniks and American Earth satellites.

The minor criticisms of this review detract only slightly from the value of this book. In general it is very well written and is sure to appeal to a widespread audience. There are few, if any, typographical errors. The upper diagram in Fig. 33 might amuse those acquainted with pen recorders. This surely is a case of over-idealization.

Jet Propulsion, by Walter J. Hesse, Pitman Publishing Corp., New York, 1958, 585 pp.

Reviewed by P. ROY CHOUDHURY
University of Southern California

Because of the increasing student interest in the field of jet propulsion, this book is welcome as an undergraduate text.

During the last academic year, this reviewer had the difficult job of selecting an undergraduate textbook for a course in Rockets and Thermal Jets, which covered, among other topics, not only the fundamentals of jet propulsion systems but also the fundamentals of gasdynamics. Because of the meager supply of books covering these subjects in one volume, the reviewer feels that the present text has made a timely arrival in its field. Besides the basic fundamentals of operation of rockets and air-breathing engines, the book covers a review of thermodynamics, compressible flow, turbomachinery, charts of standard atmospheric data, tables of compressible isentropic flow and normal shock tables.

"Jet Propulsion" is most appropriate as a text for an undergraduate course. It can be covered in two quarters of the senior year. However, the graduate students in the field would have had a major part of the material in other required courses. Nonetheless, non-mechanical or -aeronautical graduate students (e.g., civil engineering, etc.) can profitably use this as a survey course for one quarter.

In the review of the basic physical laws, the author writes the equation of motion with friction and calls it Bernoulli's equation. According to most authors, Bernoulli's equation is an integrated form of Euler's equation and does not contain

AERO-THERMODYNAMICISTS EXPLORE HIGH-SPEED RE-ENTRY

*A report to Engineers
and Scientists from
Lockheed Missile Systems —
where expanding missile
programs insure more
promising careers*

Advanced weapon system technology has brought to the forefront problem areas requiring attention to interaction between aerodynamic and thermodynamic phenomena. Typical of these is the problem of high-speed atmospheric re-entry.

Expanding research and development activities have coincided with acceleration on top priority programs like our Polaris IRBM. At the same time, positions for qualified engineers and scientists have opened up that are unequalled in responsibility or in opportunities for moving ahead.

Positions in **aero-thermodynamics** include such areas as: aerodynamic characteristics of missiles at high Mach numbers; missile and weapon system design analysis; boundary layer and heat transfer analyses in hypersonic flow fields; and calculation of transient structural and equipment temperatures resulting from aerodynamic heating and radiation.

In addition, openings exist at all levels in **Gas Dynamics, Structures, Propulsion, Test Planning and Analysis, Test Operations, Information Processing, Electronics, and Systems Integration**. For these and other positions, qualified engineers and scientists are invited to write Research and Development Staff, Dept. 2512, 962 W. El Camino Real, Sunnyvale, California.

Lockheed / **MISSILE SYSTEMS DIVISION**

SUNNYVALE, PALO ALTO, VAN NUYS, SANTA CRUZ, SANTA MARIA, CALIFORNIA
CAPE CANAVERAL, FLORIDA • ALAMOGORDO, NEW MEXICO

Maurice Tucker, Aero-Thermodynamics Department Manager, right, discusses combined aero-thermodynamic re-entry body tests being conducted in Division's new "hot-shot" wind tunnel. Others are Dr. Jerome L. Fox, Assistant Department Manager, Thermodynamics, left, and Robert L. Nelson, Assistant Department Manager, Aerodynamics.



any term due to friction. Perhaps, for the benefit of the students, it would have been better to conform to the common terminology. In another instance, in order to illustrate that in a cyclic process, energy in the form of heat can not be completely converted to continuous useful work, the author states "...heat energy is a low grade type energy..." Although this statement, in the author's mind, may describe the situation adequately, its place in a textbook of this sort is not very appropriate.

In the section on afterburners, a brief discussion of flame stabilization by different types of flameholders would not have been out of place. Lastly, in view of the ever-increasing importance of solid propellants, the chapter on rockets should definitely have included a discussion of the internal ballistics of rockets of this type.

Aircraft and Missile Propulsion, Volume I, Thermodynamics of Fluid Flow and Application to Propulsion Engines, by M. J. Zucrow, John Wiley & Sons, New York, 1958, xiv + 538 pp. \$11.50.

Reviewed by A. E. Fuchs
Northwestern University

Ten years ago, the first edition of Professor Zucrow's book "Principles of Jet Propulsion and Gas Turbines" was published. In the intervening period there has been an immense growth in the field of jet propulsion. The second edition, also, has grown and comprises three volumes, the first of which is reviewed here. Volume II deals with the cycle analysis and performance calculations of ramjets, rocket engines and the gas

turbine power plant as applied to the turboprop and turbojet. Volume III discusses the components of these engines.

In the preface the author states that the prime objective of the second edition is to furnish the student and the practicing engineer with an understanding of the fundamental principles governing the functioning and operating characteristics of the engines employed for propelling high speed aircraft and missiles. To achieve this objective, the five chapters of Volume I are devoted to a review of the fundamental principles, the general characteristics of propulsion systems, the thermodynamics of compressible fluid flow, flow through nozzles and flow through diffusers. Throughout Volume I, the author follows the policy of deriving general results and then eliminating those terms irrelevant to a specific application.

Compared to the first edition, this book has considerably more examples with detailed solutions integrated into the text. The engineer who wishes to enhance his knowledge through self study and the professor who may want to use Volume I as a classroom text will be pleased to know that there are a generous number of exercises. All the tables have been grouped in the appendix. Some of the notation has also been changed, adding to the clarity of the presentation. The extensive lists of references, for which the first edition was noted, have been brought up to date.

Since Volume I deals mainly with the fundamentals which are as valid today as they were when originally discovered by Newton, Euler, Mach, Rayleigh and others, it is not possible to evaluate how

successfully the author has "modernized" the text. It is apparent, however, that the author's viewpoint includes propulsion as applied to missiles as well as aircraft.

The value of this book arises not so much from the precision with which the fundamental facts concerning thermodynamics and fluid mechanics have been stated, but from the completeness of the material included and the variety of applications treated. This book, like the first edition, will be a useful reference for engineers working in the field, as well as a good introductory text for newcomers to jet propulsion.

Books Received

Separation and Purification of Materials, by R. Hammond, Philosophical Library, New York, 1958, 327 pp. \$10.

Dispersion of Materials, by R. Hammond, Philosophical Library, New York, 1958, 230 pp. \$10.

Impedance Matching, edited by A. Schure, J. F. Rider Publisher, Inc., New York, 1958, 128 pp. \$2.90.

Nuclear Energy, by A. Efron, J. F. Rider Publisher, Inc., New York, 1958, 72 pp. \$1.25.

Mechanics, by A. Efron, J. F. Rider Publisher, Inc., New York, 1958, 112 pp. \$1.50.

Conductance Curve Design Manual, by K. A. Pullen Jr., J. F. Rider Publisher, Inc., New York, 1958, 128 pp. \$4.25.

Physics and Mathematics in Electrical Communication, by J. O. Perrine, J. F. Rider Publisher, Inc., New York, 1958, 268 pp. \$7.50.

Technical Literature Digest

M. H. Smith, Associate Editor, and M. H. Fisher, Contributor
The James Forrestal Research Center, Princeton University

Jet and Rocket Propulsion Engines

Results of Static Test Experiment with Hot Water Rocket Model, by E. Shafer and W. Michely, *Forschungsinstitut für Physik der Strahlantriebe E. V. Mitteilungen* 11, Aug. 1957, 47 pp. (in German).

A Rocket Drive for Long Range Bombers, by Eugen Sanger and Irene Bredt, *Forschungsinstitut für Physik der Strahlantriebe E. V. Mitteilungen* 13, Oct. 1957, 266 pp. (Reprint of ZWB Untersuchungen und Mitteilungen 3538, Aug. 1944.) (In German.)

Propulsion Systems for Space Flight, by R. B. Dillaway, *Aeron. Engng. Rev.*, vol. 17, April 1958, pp. 42-49, 52.

Rocket Pumps Have Reached High Efficiency, by Kurt R. Stehling, *Aviation Age*, vol. 29, pp. 32-33, 35, 37, 41-42.

Taming the Supersonic Turbojet, by Edward A. Simonis, *Aviation Age*, vol. 29, April 1958, pp. 60-69.

EDITOR'S NOTE: Contributions from Professors E. R. G. Eckert, J. P. Hartnett, T. F. Irvine, Jr. and P. J. Schneider of the Heat Transfer Laboratory, University of Minnesota, are gratefully acknowledged.

Summary Progress Report on the Experimental Investigation of the RPI Wave Engine, by H. J. Lopez and R. E. Jensen, *Rensselaer Polytech. Inst., Dept. Aeron. Engng., Tech. Rep. AE 5801*, Feb. 1958, 23 pp.

Booster Propulsion for Space Vehicles, by R. S. Wentink, *Inst. Aeron. Sci., Preprint 828*, Jan. 1958, 29 pp. 2 figs.

An Optimum Design for a Semi Infinite Rocket Wall Containing a Circumferential Keyway, by Bernard W. Shaffer, Ira Cochran and Morton Mantus, *Inst. Aeron. Sci., Preprint 767*, Jan. 1958, 26 pp., 9 figs.

Photographic Study of Rotary Screaming and Other Oscillations in a Rocket Engine, by Theodore Male, William R. Kerslake and Adelbert O. Tischler, *NACA Res. Mem. E54A29*, May 1954, 37 pp. (Declassified from Confidential by authority of NACA Res. Abstr. 125, p. 20, 3/18/58.)

Propellant Vaporization as a Criterion for Rocket Engine Design; Relation Between Percentage of Propellant Vaporized and Engine Performance, by Marcus F. Heidmann and Richard J. Priem, *NACA TN 4219*, March 1958, 19 pp.

Application of a High-temperature Static

Strain Gage to the Measurement of Thermal Stresses in a Turbine Stator Vane, by R. H. Kemp, C. R. Morse and M. H. Hirschberg, *NACA TN 4215*, March 1958, 36 pp.

High-altitude Performance of 9.5-inch-diameter Tubular Experimental Combustor with Fuel Staging, by Wilfred E. Scull, *NACA Res. Mem. E54A06*, March 1954, 55 pp. (Declassified from Confidential by authority of NACA Res. Abstr. 125, p. 20, 3/18/58.)

Component and Over-all Performance Evaluation of an Axial-flow Turbojet Engine over a Range of Engine-inlet Reynolds Numbers, by Curtis L. Walker, S. C. Huntley and W. M. Braithwaite, *NACA Res. Mem. E52B08*, July 1952, 42 pp. (Declassified from Confidential by authority of NACA Res. Abstr. 125, p. 19, 3/18/58.)

Performance of an Impulse-type Supersonic Compressor with Stators, by John F. Klapproth, Guy N. Ullman and Edward R. Tysl, *NACA Res. Mem. E52B22*, April 1952, 22 pp. (Declassified from Confidential by authority of NACA Res. Abstr. 125, p. 19, 3/18/58.)

Design Procedure and Limited Test Results for a High Solidity, 12-inch Tran-

Two new Du Pont products to

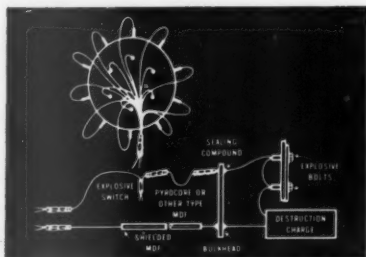
- (1) *Speed rocket-fuel ignition*
- (2) *Provide remote detonations*

When you ignite a rocket propellant . . . actuate a valve . . . release a switch . . . you often rest the success or failure of the flight on some form of detonation. Now Du Pont research brings you two new products that reduce the chances of failure almost to the vanishing point . . . and give you faster and better controlled detonation.

DU PONT "MDF" MILD DETONATING FUSE

. . . carries non-destructive detonation safely past delicate instruments to perform remote functions

"MDF" is a small diameter flexible metal tubing, available in practically any length you desire, and containing a detonating composition as its core.



USES OF "MDF" include: shearing or severing covers or diaphragms; activating various valves, releases, arming devices, etc.; simultaneously initiating multiple explosive charges.

Five strengths are available (1, 2, 5, 10 and 20 grains of PETN per foot), providing a mild explosive power sufficient to carry a detonation from one point to another, but usually not enough to ignite or initiate other explosives or to burst violently out of its tubing.

Thus "MDF" may be used to transfer a detonation through or around delicate instruments.

Strength, velocity and temperature resistance can be varied according to your needs, and other types of tubing can be provided, including plastics, wires and textiles to overcome problems of abrasion, corrosion, damaging effect and noise control.

You can plan precise detonation speeds with "MDF" because velocity for a given core loading is accurate within $\pm 1\%$.

And you can depend on each detonation coming off as planned. In recent tests, thousands and thousands of feet of "MDF" were fired, without a single failure. Approaching 200,000 feet, the tests were discontinued because they failed to produce any failures on which to base reliability figures.

Handling of "MDF" is safe and convenient compared to ordinary commercial explosives, because only small quantities of explosives are involved and even these are insensitive to ordinary shock. The tubing is quite flexible and lends itself easily to stringing, wrapping, threading.

DU PONT "PYROCORE" IGNITER

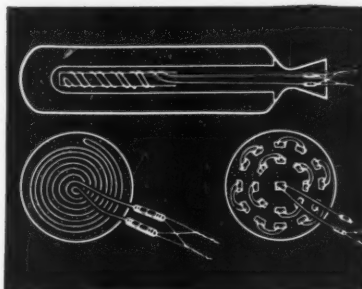
. . . provides faster, more uniform ignition of rocket propellants

"Pyrocore," too, is a flexible metal

tubing available in any length. Its core is a detonating-ignition composition.

Propellant ignition may be effected along its length at velocities ranging from 12,000 to 21,000 feet per second, depending upon the type and amount of core composition you specify.

In laboratory tests, "Pyrocore" cut ignition time 99.5% when compared with a standard primer. Total ignition of a $21\frac{1}{2}$ " length of cannon primer was achieved in less than $\frac{1}{4}$ millisecond, as against 50 milliseconds required with a squib primer.



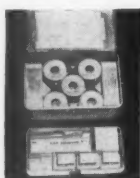
TYPICAL APPLICATIONS OF "PYROCORE" IGNITER. You can string, thread, weave it through or around the propellant.

The stringlike form of "Pyrocore" gives you new freedom in designing rocket motors. For example, you can thread "Pyrocore" through jelly roll or basket type igniter assemblies, or string it around the propellant grains. Or you can weave coils or loops of "Pyrocore" directly into the propellant grain either during or after grain formation.

Further, "Pyrocore" has very low brisance (shattering effect) and can convey a non-electric stimulus safely past expensive equipment and bulkheads.

Initiator assemblies may be located outside the propellant chamber, eliminating a major source of residue in the reaction zone. The "Pyrocore" itself leaves very little residue. The portion of "Pyrocore" not actually used for ignition may be easily insulated with any one of a variety of plastic compounds.

"Pyrocore" is a Du Pont trade mark.



Sample Kits Available • Sample kits containing either "MDF" or "Pyrocore," plus various primers and accessories, are available from Du Pont. Kit prices and technical bulletins can be obtained by writing to E. I. du Pont de Nemours & Co. (Inc.), Explosives Department, Wilmington 98, Delaware.

EXPLOSIVES DEPARTMENT



Better Things for Better Living . . . through Chemistry

sonic Impeller with Axial Discharge, by Linwood C. Wright and Karl Kovach, *NACA Res. Mem.* E53B09, April 1953, 37 pp. (Declassified from Confidential by authority of NACA Res. Abstr. 125, p. 20, 3/18/58.)

Altitude Performance Investigation of Two Flame-holder and Fuel-system Configurations in Short Afterburner, by S. C. Huntley and H. D. Wilsted, *NACA Res. Mem.* E52B25, May 1952, 41 pp. (Declassified from Confidential by authority of NACA Res. Abstr. 125, p. 19, 3/18/58.)

Altitude Starting Characteristics of an Afterburner with Autoignition and Hot-streak Ignition, by P. E. Renas, R. W. Harvey Sr. and E. T. Jansen, *NACA Res. Mem.* E53B02, April 1953, 25 pp. (Declassified from Confidential by authority of NACA Res. Abstr. 125, p. 19, 3/18/58.)

Turboprop-engine Design Considerations, I: Effect of Mode of Engine Operation on Performance of Turboprop Engine with Current Compressor Pressure Ratio, by Elmer H. Davison, *NACA Res. Mem.* E54D19, May 1955, 34 pp. (Declassified from Confidential by authority of NACA Res. Abstr. 125, p. 21, 3/18/58.)

Turboprop-engine Design Considerations, II: Design Requirements and Performance of Turboprop Engines with a Single-spool High-pressure-ratio Compressor, by Elmer H. Davison and Margaret C. Stalla, *NACA Res. Mem.* E55B18, May 1955, 32 pp. (Declassified from Confidential by authority of NACA Res. Abstr. 125, p. 22, 3/18/58.)

Correlation of Turbine-blade-element Losses Based on Wake Momentum Thickness with Diffusion Parameter for a Series of Subsonic Turbine Blades in Two-dimensional Cascade and for Four Transonic Turbine Rotors, by Robert Y. Wong and Warner L. Stewart, *NACA Res. Mem.* E55B08, April 1955, 31 pp. (Declassified from Confidential by authority of NACA Res. Abstr. 125, p. 22, 3/18/58.)

Photographic Investigation of Air-flow Patterns in Transparent One-sixth Sector of Annular Turbojet-engine Combustor with Axial-slot-type Air Admission, by Charles C. Graves and J. Dean Gernon, *NACA Res. Mem.* E54128a, Dec. 1954, 24 pp. (Declassified from Confidential by authority of NACA Res. Abstr. 125, p. 21, 3/18/58.)

Effect of Nozzle Secondary Flows on Turbine Performance as Indicated by Exit Surveys of a Rotor, by Warren J. Whitney, Howard A. Buckner Jr. and Daniel E. Monroe, *NACA Res. Mem.* E54B03, April 1954, 11 pp. (Declassified from Confidential by authority of NACA Res. Abstr. 125, p. 20, 3/18/58.)

The Transonic Flow Field of an Axial Compressor Blade Row, by James E. McCune, *Inst. Aeron. Sci., Preprint* 792, Jan. 1958, 26 pp., 6 figs.

Use of Effective Momentum Thickness in Describing Turbine Rotor-blade Losses, by Warner L. Stewart, Warren J. Whitney and James W. Miser, *NACA Res. Mem.* E56B29, May 1956, 26 pp. (Declassified from Confidential by authority of NACA Res. Abstr. 125, p. 23, 3/18/58.)

Low-velocity Turning as a Means of Minimizing Boundary-layer Accumulations Resulting from Secondary Flows within Turbine Stators, by Warner L. Stewart and Robert Y. Wong, *NACA Res. Mem.* E54B16, May 1954, 18 pp. (Declassified from Confidential by authority of NACA Res. Abstr. 125, p. 21, 3/18/58.)

Performance Characteristics of Several Short Annular Diffusers for Turbojet Engine Afterburners, by William E.

Mallett and James L. Harp Jr., *NACA Res. Mem.* E54B09, May 1954, 31 pp. (Declassified from Confidential by authority of NACA Res. Abstr. 125, p. 21, 3/18/58.)

Effect of Ambient Conditions on the Performance of a Pressure-jet Powerplant for a Helicopter, by Richard P. Krebs, *NACA Res. Mem.* E56B21, June 1956, 49 pp. (Declassified from Confidential by authority of NACA Res. Abstr. 125, p. 22, 3/18/58.)

Exploratory Investigation of a Helicopter Pressure-jet System on the Langley Helicopter Test Tower, by Robert A. Makofski and James P. Shivers, *NACA Res. Mem.* L56B17, July 1956, 38 pp. (Declassified from Confidential by authority of NACA Res. Abstr. 125, p. 26, 3/18/58.)

Ram-jets, by R. P. Probert, *J. Roy. Aeron. Soc.*, vol. 62, March 1958, pp. 151-173.

Altitude Performance Investigation of Two Single-annular Type Combustors and the Prototype J40-WE-8 Turbojet Engine Combustor with Various Combustor Inlet-air-pressure Profiles, by Adam E. Sobolewski, Robert R. Miller and John E. McAulay, *NACA Res. Mem.* E52J07, May 1953, 46 pp. (Declassified from Confidential by authority of NACA Res. Abstr. 124, p. 10, 2/10/58.)

Compressor Turbine Matching of Two-spool Turbo-props, by A. W. Morley, *Aeron. Quart.*, vol. 9, Feb. 1958, pp. 17-33.

The High-density Turbojet: The Vanguard Examined, by Roy Allen, *Aeronautics*, vol. 38, March 1958, pp. 47-51.

Propulsion, by Jerry Grey, *Aviation Age*, vol. 28, March 1958, pp. 36-43.

Acoustic, Thrust, and Drag Characteristics of Several Full-scale Noise Suppressors for Turbojet Engines, by Carl C. Ciepluch, Warren J. North, Willard D. Coles and Robert J. Antl, *NACA TN* 4261, April 1958, 48 pp.

Transonic Drag of Several Jet-noise Suppressors, by Warren J. North, *NACA TN* 4269, April 1958, 34 pp.

Discharge Coefficients for Combustor-liner Air-entry holes, II: Flush Rectangular Holes, Step Louvers, and Scoops, by Ralph T. Dittich, *NACA TN* 3924, April 1958, 56 pp.

Effect of Prior Air Force Overtemperature Operation on Life of J47 Buckets Evaluated in a Sea-level Cyclic Engine Test, by Robert A. Signorelli, James R. Johnston and Floyd B. Barrett, *NACA TN* 4263, April 1958, 41 pp.

Maximum Theoretical Tangential Velocity Component Possible from Straight-back Converging and Converging-diverging Stators at Super-critical Pressure Ratios, by Thomas P. Moffitt, *NACA TN* 4271, April 1958, 21 pp.

Equivalent Performance Parameters for Turboblenders and Compressors, by Hunt Davis, *Trans. ASME*, vol. 80, Jan. 1958, pp. 108-116.

A Method for Calculating Vibration Frequency and Stress of a Banded Group of Turbine Buckets, by M. A. Prohl, *Trans. ASME*, vol. 80, Jan. 1958, pp. 169-180.

High-frequency Vibration of Steam-turbine Buckets, by F. L. Weaver and M. A. Prohl, *Trans. ASME*, vol. 80, Jan. 1958, pp. 181-194.

F-104 Intake Ducts Save Weight and Complexity, by A. F. Watts, *Aviation Age*, vol. 29, May 1958, pp. 60-67.

Testing Paper Gas Turbines: Applying the Digital Computer to Engine Design,

by Paul T. Vickers and Charles A. Amann, *General Motors Engng. J.*, vol. 5, April-June, 1958, pp. 6-16.

Boost Systems for Helicopter Gas Turbines, by A. W. Morley, *J. Helicopter Assoc. of Gt. Brit.*, vol. 12, April 1958, pp. 66-83; Discussion, pp. 84-90.

A Combination Powerplant for High-performance Aircraft, by J. Dupin, *Interavia*, vol. 13, April 1958, pp. 349-351.

Measurement of Ignition Delay at Simulated Altitude of Hypergolic Liquid Rocket Motors, by Pierre Sarrat, *La Recherche Aeronautique*, No. 62, Jan.-Feb. 1958, pp. 15-25 (in French).

Aerodynamics of Jet Propelled Vehicles

Experimental Study of the Equivalence of Transonic Flow about Slender Conical and Elliptic Cross Section, by William A. Page, *NACA TN* 4233, April 1958, 45 pp.

A Second-order Shock-expansion Method Applicable to Bodies of Revolution Near Zero Lift, by Clarence A. Syvertson and David H. Dennis, *NACA Rep.* 1328, 1957, 20 pp. (Supersedes Res. Mem. L55G05.)

Stagnation-point Heat Transfer to Blunt Shapes in Hypersonic Flight, Including Effects of Yaw, by A. J. Eggers Jr., C. Frederick Hansen and Bernard E. Cunningham, *NACA TN* 4229, April 1958, 54 pp.

Stationary Wall Temperature of a Body under the Influence of Aerodynamic Heating Flying at Mach Numbers from 1 to 10 and up to 30 km, by H. G. L. Krause and M. E. Kubler, *Forschungsinstitut für Physik der Strahlantreibung V., Mitteilungen* 7, Oct. 1956, 138 pp. (in German).

The Structure of a Steady State One Dimensional Detonation Wave Supported by a Reversible Reaction, by B. Linder, C. F. Curtiss, and J. O. Hirschfelder, *Univ. of Wisconsin, Naval Res. Lab.*, CM-911a, Dec. 1957, 11 pp.

A Discussion of Higher-order Approximations for the Flow Field about a Slender Elliptic Cone, by Roberto Vaglio-Laurin and M. D. Van Dyke, *J. Fluid Mech.*, vol. 3, March 1958, pp. 638-644.

Hypersonic Flight and the Re-entry Problem (Twenty-first Wright Brothers Lecture), by H. Julian Allen, *J. Aeron. Sci.*, vol. 25, April 1958, pp. 217, 229, 262.

On Optimum Nose Curves for Super-aerodynamic Missiles, by H. S. Tan, *J. Aeron. Sci.*, vol. 25, April 1958, pp. 263-264.

Drag Due to Lift of a Not So Slender Configuration, by Hsien K. Cheng, *Wright Air Dev. Center, Tech. Rep.* 57-316, Part I. (ASTIA AD 118336), Sept. 1957, 38 pp.

The Supersonic Blunt Body Problem—Review and Extension, by Milton D. Van Dyke, *Inst. Aeron. Sci., Preprint* 801, Jan. 1958, 19 pp., 18 figs.

Examples of Detached Bow Shock Waves in Hypersonic Flow, by P. R. Garabedian and H. M. Lieberstein, *Inst. Aeron. Sci., Preprint* 817.

The Dynamics and Certain Aspects of Control of a Body Re-entering the Atmosphere at High Speed, by Joseph D. Welch and S. L. Shih, *Inst. Aeron. Sci., Preprint* 818, Jan. 1958, 12 pp., 12 figs.

Experimental Pressure Distribution on an Asymmetrical Nonconical Body at Mach Number 1.90, by De Marquis D. Wyatt, *NACA Res. Mem.* E9B03, Feb. 1949, 58 pp. (Declassified from Confidential by authority of NACA Res. Abstr.

SENIOR SCIENTISTS AND ENGINEERS

AVCO—PIONEER IN RE-ENTRY—IS EXPLORING

NEW APPROACHES TO SPACE AND MISSILE TECHNOLOGY

The Avco Research and Advanced Development Division is conducting an extensive program of basic and applied research in the physics, chemistry and engineering associated with space and missile technology. Supervisory and staff positions are available for creative senior physicists and engineers—both theoretical and experimental—and for electrical engineers with a strong physics background.

Unusual and challenging openings exist in the following fields:

High-intensity arcs, gaseous discharge phenomena, properties of gases at high temperatures, radiation measurements

High-temperature reflectivity and emissivity measurements

High-temperature properties of materials

Infrared

Terminal ballistics of high-velocity particles

Chemical physics, spectroscopy, surface physics, hydrodynamics, fluid dynamics, free molecule flow studies, upper atmosphere phenomena

Missile detection and discrimination, advanced missile warfare concepts

Ultra-high-speed electronic and optical instrumentation

Microwaves, telemetry systems, radar, propagation through ionized plasmas, space communication studies

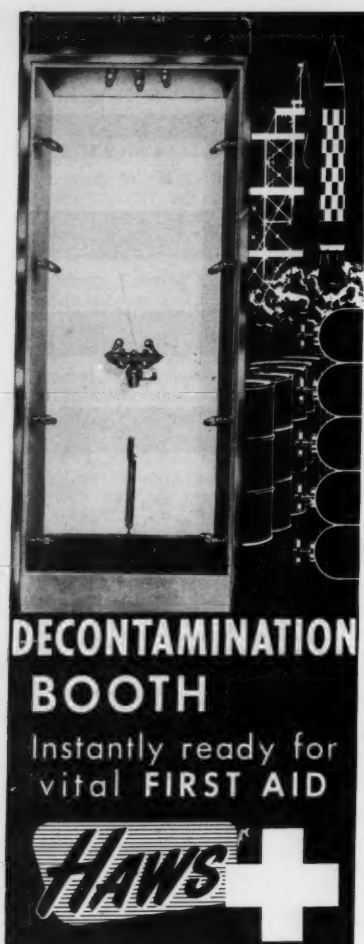
The division's new suburban location provides an unusually attractive working environment outside of metropolitan Boston. The large, fully equipped, modern laboratory is in pleasant surroundings, yet close to Boston educational institutions and cultural events. Publications and professional development are encouraged, and the division offers a liberal educational assistance program for advanced study.

AVCO

Research and Advanced Development
division

Address all inquiries to:

Dr. R. W. Johnston,
Scientific and Technical Relations,
Avco Research and Advanced Development Div.,
201 Lowell Street, Wilmington, Massachusetts



Miscues and accidental exposure to dangerous propellants and other chemicals can occur with shocking suddenness. Adequate water irrigation is an important key to minimizing such injuries and subsequent claims. HAWS Decontamination Booth is the answer... a complete safety station for immediate first aid.

HAWS MODEL 8600 DECONTAMINATION BOOTH

is made of durable, lightweight reinforced fiberglass plastic, and features Haws Eye-Face Wash Fountain, eight lateral body sprays and overhead spray unit. All are simultaneously activated by weight on the base-mounted foot treadle! Contaminated victims are instantly "covered" with water that floats away foreign matter from body and clothing.

At aeronautical and astronautical installations everywhere, HAWS Safety Facilities are important in boosting air-age safety programs. Find out what this equipment can mean to your operation. Full details sent on request, with no obligation.

HAWS DRINKING FAUCET CO.

1443 FOURTH ST. • BERKELEY 10 • CALIFORNIA

EXPORT DEPARTMENT • 19 COLUMBUS STREET
SAN FRANCISCO 11, CALIFORNIA

125, p. 18, 3/18/58.)

Effect of Mach Number on Boundary-layer Transition in the Presence of Pressure Rise and Surface Roughness on an Ogive-cylinder Body with Cold Wall Conditions, by Robert J. Carros, *NACA Res. Mem.* A56B15, April 1956, 30 pp. (Declassified from Confidential by authority of NACA Res. Abstr. 125, p. 18, 3/18/58.)

Transonic Free-flight Drag Results of Full-scale Models of 16-inch Diameter Ram-jet Engines, by Wesley E. Messing and Loren W. Acker, *NACA Res. Mem.* 52B19, April 1952, 17 pp. (Declassified from Confidential by authority of NACA Res. Abstr. 125, p. 19, 3/18/58.)

Effect of Jet-Nozzle-expansion Ratio on Drag of Parabolic Afterbodies, by Gerald W. Englert, Donald J. Vargo and Robert W. Cubbison, *NACA Res. Mem.* E54B12, April 1954, 26 pp. (Declassified from Confidential by authority of NACA Res. Abstr. 125, p. 21, 3/18/58.)

Aerodynamic Characteristics of a Cruciform-wing Missile with Canard Control Surfaces and of Some Very Small Span Wing-body Missiles at a Mach Number of 1.41, by M. Leroy Spearman and Ross B. Robinson, *NACA Res. Mem.* L54B11, April 1954, 27 pp. (Declassified from Confidential by authority of NACA Res. Abstr. 125, p. 24, 3/18/58.)

A Linear Perturbation Method for Stability and Flutter Calculations on Hypersonic Bodies, by Maurice Holt, *Inst. Aeron. Sci., Preprint* 793, Jan. 1958, 20 pp.

Similitude of Hypersonic Flows over Thin and Slender Bodies—an Extension to Real Gases, by Hsien K. Cheng, *Cornell Aeron. Lab., Inc., Rep.* AD-1052-A-6 (AFOSR-TN-58-87; *ASTIA* AD148136), Feb. 1958, 13 pp., 6 figs.

Preliminary Investigations of Spiked Bodies at Hypersonic Speeds, by S. M. Bogdonoff and I. E. Vas, *Princeton Univ. Dept. of Aeron. Engng., Rep.* 412, (Wright Air Dev. Center, TN 58-7; *ASTIA* AD 142280), March 1958, 10 pp., 16 figs.

Molecular Approach to Problems of High Altitude, High Speed Flight, by G. N. Patterson, *NATO, Advis. Group for Aeron. Res. and Dev., Rep.* 134, July 1957, 58 pp.

The Direct Measurement of Local Skin Friction on Viking No. 13 During Ascending Flight, by Felix W. Fenter and W. C. Lyons Jr., *Univ. of Texas, Defense Res. Lab., CM* 917 (DRL-414), Jan. 1958, 32 pp., 4 tabs., 16 figs.

On the Drag of a Sphere at Extremely High Speeds, by V. C. Liu, *J. Appl. Phys.*, vol. 29, Feb. 1958, pp. 194-195.

A Model of Supersonic Flow Past Blunt Axisymmetric Bodies, with Applications to Chester's Solution, by M.D. Van Dyke, *J. Fluid Mech.*, vol. 3, Feb. 1958, pp. 515-526.

An Approximate Method of Determining Axisymmetric Inviscid Supersonic Flow over a Solid Body and Its Wake, by Sin-I Cheng, *J. Aeron. Sci.*, vol. 25, March 1958, pp. 185-193.

Approximate Solution for Slightly Yawed n -Power Bodies at Hypersonic Speeds, by Robert W. Truitt, *J. Aeron. Sci.*, vol. 25, March 1958, pp. 206-207.

On Optimum Nose Shapes for Missiles in the Superaerodynamic Region, by David H. Dennis, *J. Aeron. Sci.*, vol. 25, March 1958, p. 216.

Boundary Layer Growth on a Spinning Body: Accelerated Motion, by Y. D. Wadhwa, *Phil. Mag.*, vol. 3, Feb. 1958, pp. 152-158.

On Optimum Nose Shapes for Missiles in the Superaerodynamic Region, by I. D. Chang, *J. Aeron. Sci.*, vol. 25, Jan. 1958, pp. 57-58.

On Hypersonic Blunt Body Flow with a Magnetic Field, by Nelson H. Kemp, *Avco Mfg. Corp., Avco Res. Lab., Res. Rep.* 19, Feb. 1958, 9 pp., 2 figs.

Lift and Drag on Cone Cylinders, by T. Nark, *Univ. of Calif., Inst. Engng. Res., Tech. Rep.* HE-150-154, Dec. 1957, 32 pp., 10 figs.

Pressure and Wave Drag Coefficients for Hemispheres, Hemisphere Cones, and Hemisphere Ogives, by Jerome R. Katz, *NAVORD Rep.* 5849 (NOTS 1947), March 1958, 17 pp.

Heat Transfer and Fluid Flow

Crococo's Vorticity Law in a Non-uniform Material, by C. S. Wu and W. D. Hayes, *Quart. Appl. Math.*, vol. 16, April 1958, pp. 81-82.

Temperature Dependence of Vibrational Relaxation Times in Gases, by P. G. Corran, J. D. Lambert, R. Salter and B. Warburton, *Proc. Roy. Soc., vol.* 244A, no. 1237, March 11, 1958, pp. 212-219.

The Determination of the Lorenz Number at High Temperatures, by M. R. Hopkins and R. L. Griffith, *Zeitschrift für Physik*, vol. 150, no. 3, Feb. 14, 1958, pp. 325-331 (in English).

Aerodynamic Research on Accelerating Cascade; Cascade Test of the Nozzle Blades, by Isamu Wada, *Proc., Japan, 6th Natl. Congr. Appl. Mech.*, 1956 (pub. 1957), pp. 333-336.

Design of Cascade in Compressible Fluid and Application, by Ichiro Hamamoto, *Proc., Japan, 6th Natl. Congr. Appl. Mech.*, 1956 (pub. 1957), pp. 337-340.

On the Evaporation, Ignition Lags and Combustion of Fuel Droplets, by Niichi Nishiwaki, Masaru Hirata, Sanni Hagi and Shin-ichiro Yamazaki, *Proc., Japan, 6th Natl. Congr. Appl. Mech.*, 1956 (pub. 1957), pp. 407-410.

Thermodynamics, by R. A. Budenholzer and Alfred Ritter, *Aviation Age*, vol. 28, March 1958, pp. 44-49.

Fluid Dynamics, by A. K. Oppenheim, C. L. Coldren, L. M. Grossman and C. V. Sterling, *Ind. and Engng. Chem.*, vol. 50 March 1958, Pt. 2, pp. 525-542.

Heat Transfer, by E. R. G. Eckert, J. P. Hartnett and T. F. Irvine Jr., *Ind. and Engng. Chem.*, vol. 50, March 1958, Pt. 2, pp. 543-554.

Mass Transfer, by C. R. Wilke and J. M. Prausnitz, *Ind. and Engng. Chem.*, vol. 50, March 1958, Pt. 2, pp. 555-560.

Thermodynamics, by J. M. Smith and G. M. Brown, *Ind. and Engng. Chem.*, vol. 50, March 1958, Pt. 2, pp. 561-568.

Non-linear Interactions in a Viscous Heat-conducting Compressible Gas, by Boa-Teh Chu and Leslie S. G. Kovasznay, *J. Fluid Mech.*, vol. 3, Feb. 1958, pp. 494-504.

Pyrolysis of Simple Hydrocarbons in Shock Waves, by E. F. Greene, R. L. Taylor and W. L. Patterson Jr., *J. Phys. Chem.*, vol. 62, Feb. 1958, pp. 238-243.

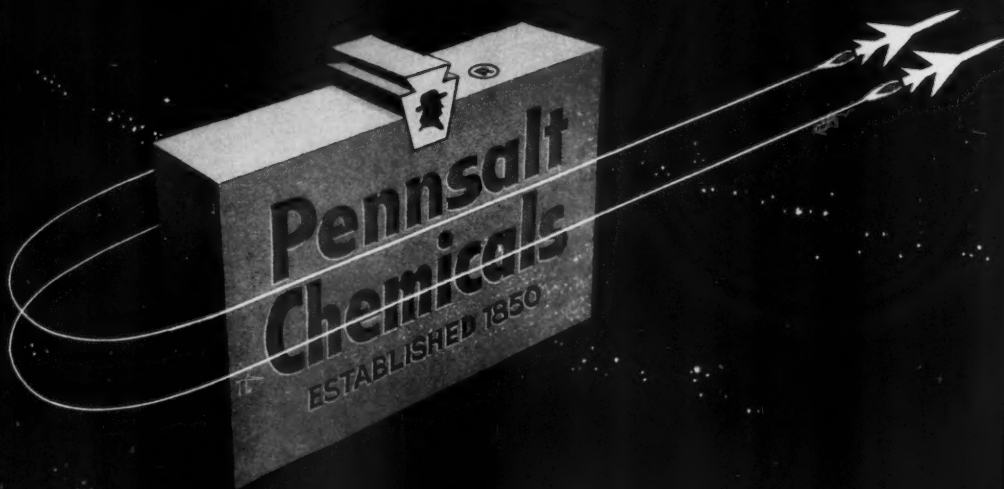
Incompressible Two-dimensional Stagnation-point Flow of an Electrically Conducting Viscous Fluid in the Presence of a Magnetic Field, by Joseph L. Neuringer and William Mclroy, *J. Aeron. Sci.*, vol. 25, March 1958, pp. 194-198.

(Continued on page 859)

JET PROPULSION

for solid propellants—

A new source of AMMONIUM PERCHLORATE



Pennsalt announces completion of its first facility at its Portland, Oregon plant for the production of AMMONIUM PERCHLORATE, a leading oxidizer used in solid propellants. Sodium chlorate, necessary for AMMONIUM PERCHLORATE manufacture, has been produced by Pennsalt at this location for over 17 years.

This is another contribution to the missile age by Pennsalt, a pioneer in the development of elemental fluorine and other high energy fluorine chemicals, and a basic producer of quality chemicals for more than one hundred years. We invite you to call or write Pennsalt of Washington Division for detailed information.

PENNSALT OF WASHINGTON DIVISION
PENNSALT CHEMICALS CORPORATION
TACOMA 1, WASHINGTON

PLANTS AND OFFICES:

Los Angeles and Menlo Park, Calif. • Philadelphia, Pa. • Portland, Ore.





There is a creative engineering assignment for you with IBM



Assignments now open include...

SYSTEMS ENGINEER to develop complex devices in fields of servo-mechanisms, radar, or computers, and integrate these elements in weapons systems. Must have 3 to 5 years' experience in such activity and two years' experience in over-all systems analysis. Assignment involves design and analysis of closed-loop systems, consisting of inertial and radar equipment, display materials, and digital or analog computers.
Qualifications: B.S. or Advanced Degree in E.E. or A.E.

INERTIAL GUIDANCE ENGINEER to assume broad project leadership in the planning and control of development projects. Must have 3 to 5 years' experience in servo-mechanisms or development of complex devices for military applications, including 2 years as technical leader of inertial guidance system development. Must have experience in astro-compass, with ability to

analyze relationship of inertial equipment with bombing and navigation computer.

Qualifications: B.S. or M.S. in E.E. or Physics.

RADAR ENGINEER to analyze ultimate limits of present techniques and develop new concepts of providing topographical sensors for advanced airborne and space systems; to design airborne radar pulse, microwave and deflection circuitry; to analyze doppler radar systems in order to determine theoretical accuracy and performance limitations.

Qualifications: B.S. or Advanced Degree in E.E. and 3 to 5 years' experience in radar system development, including display equipment and circuits, control consoles, and doppler or search radar design.

CONTROL SYSTEM ANALYST to perform physical and mathematical analyses needed to solve complex inertial control problems with real-time digi-

tal computers. Applications in area of bombing navigation systems, missile systems, special-purpose computer systems such as DDA.

Qualifications: M.S. or Ph.D. in Physics or related fields with strong math minor and up to 2 years' experience.

COMPUTER ENGINEER to undertake logical design of airborne digital computer equipment; transistorizing computer circuitry for size and weight reduction. Assignment entails: Mechanization of computer circuitry and packaging; interpreting problems for solution with the IBM 7090.
Qualifications: B.S. or Advanced Degree in Engineering or Physics and 3 to 5 years' experience in design of digital or analog computer equipment. Experience desirable in transistor technology, computer logic, programming, instrumentation, computer system evaluation, or servo-mechanism design.

Are you making full use of your creative abilities . . . do you want to undertake challenging, important career assignments . . . are you looking for career opportunities . . . then you should consider a position with IBM. In Owego, IBM's vast wealth of computer technology is applied to completely integrated B-70 bombing-navigation systems; you'll work alongside such men as Engineer David R. Baldauf, who says: "With IBM I have the opportunity to work on completely integrated B-70 bombing-radar-navigation systems. This means that my assignments have tremendous scope and versatility. For instance, I'm now evaluating several contractor proposals for a monopulse radar system, and at the same time I'm performing a study on attaching a unique radar indicator to the presently produced bombing system. I've had rapid advancement at IBM, and there are still plenty of opportunities for me to grow."

IBM is a recognized leader in the electronic systems field. Its products are used for military as well as commercial work. You will find opportunities for professional advancement at IBM, where the "small-team" approach assures quick recognition of individual merit. Company benefits set standards for industry today, and salaries are commensurate with your abilities and experience.

Ideally situated in rolling New York State countryside, Owego, in the Binghamton Triple City area, provides an excellent environment for gracious, relaxed family life. Owego's proximity to both New York City and the Finger Lakes region offers a pleasant variety of recreational opportunities.

CAREER OPPORTUNITIES IN THESE AREAS . . .

- Airborne digital & analog computers
- Ground support equipment
- Inertial guidance & missile systems
- Information & network theory
- Magnetic engineering
- Maintainability engineering
- Optics
- Radar electronics & systems
- Servo-mechanism design & analysis
- Theoretical design & analysis
- Transistor circuits

Qualifications: B.S., M.S., or Ph.D. in Electrical or Mechanical Engineering, Physics, Mathematics—and proven ability to assume a high degree of technical responsibility in your sphere of interest.

There are other openings in related fields.

FOR DETAILS, write, outlining your background and interest, to:

Mr. P. E. Strohm, Dept. 572-Z
International Business Machines Corporation
Owego, New York

IBM®

MILITARY PRODUCTS

Flows in Partly Dissociated Gases, by Hans-Joachim Metzendorf, *J. Aeron. Sci.*, vol. 25, March 1958, pp. 200-201.

Experiments on Chemical Kinetics in a Supersonic Nozzle, by Peter P. Wegener, Jack E. Marte and Carl Thiele, *J. Aeron. Sci.*, vol. 25, March 1958, p. 205.

An Energy Principle for Hydromagnetic Stability Problems, by J. B. Bernstein, E. A. Frieman, M. D. Kruskal and R. M. Kulsrud, *Proc. Roy. Soc.*, vol. 244A, Feb. 25, 1958, pp. 17-29.

Turbulent Heat Transfer through a Highly Cooled Partially Dissociated Boundary Layer, by P. H. Rose, R. F. Probst and M. C. Adams, *Avco Mfg. Corp., Avco Res. Lab., Res. Rep.* 14, Jan. 1958, 52 pp.

Tables of Radiation from High Temperature Air, by B. Kivel and K. Bailey, *Avco Mfg. Corp., Avco Res. Lab., Res. Rep.* 21, Dec. 1957, 29 pp.

Heat Transfer Economics as Related to Design of Nuclear Fuel Elements, by D. Kallman, *Chem. Engng. Progr.*, vol. 53, 1957, pp. 289-292.

A Method of Heating Matter of Low Density to Temperatures in the Range 10^6 to 10^8 K, by F. B. Knox, *Australian J. Phys.*, vol. 10, June 1957, pp. 221-225.

Prediction of Heat Transfer Burnout, by Louis Bernath, *Chem. Engng. Progr.*, vol. 53, 1957, pp. 1-6.

Pressure Drop During Forced-circulation Boiling, by Max Jakob, George Lepert and J. B. Reynolds, *Chem. Engng. Progr.*, vol. 53, 1957, pp. 29-36.

Effect of Agitation on the Critical Temperature Difference for a Boiling Liquid, by F. S. Pramuk and J. W. Westwater, *Chem. Engng. Progr.*, vol. 53, 1957, pp. 79-83.

Some Experiments Related to the Noise from Boundary Layers, by Harvey H. Hubbard, *J. Acoustical Soc. of America*, vol. 29, 1957, pp. 331-334.

Investigation of Burnout Heat Flux in Rectangular Channels at 2000 Psia, by H. S. Jacket, J. D. Roarty and J. E. Zerbe, *Westinghouse Electric Corp. Atomic Power Div. (U.S. Atomic Energy Comm.), WAPD-A1W (IM)-3*, Dec. 1955, 1 vol.

An Empirical Correlation for Velocity Distribution of Turbulent Fluid Flow, by B. F. Ruth and H. H. Lang, *J. Am. Inst. Chem. Engrs.*, vol. 3, 1957, pp. 117-120.

Determination of Burnout Limits of Polyphenyl Coolants, by K. Sato, *Aerojet-General Corp. (U.S. Atomic Energy Comm.), AGC-AE-32*, Feb. 1957, 67 pp.

Measurement of Local Heat Transfer Coefficients with Sodium-potassium Eutectic in Turbulent Flow, by K. D. Kuczen and T. R. Bump, *Nuclear Sci. and Engng.*, vol. 2, 1957, pp. 181-198.

The Heat Transfer and High-temperature Properties of Liquid Alkali Metals, by I. I. Novikov, *J. Nuclear Energy*, vol. 4, 1957, pp. 387-408.

Thermal Conductivity of Some Refractory Materials, by J. F. Clements and J. Vyse, *Trans. British Ceramics Soc.*, vol. 56, 1957, pp. 296-308.

Thermal Relaxation in Carbon Dioxide as a Function of Temperature, by F. Douglas Shields, *J. Acoustical Soc. of America*, vol. 29, 1957, pp. 450-454.

Radiative Transfer in Discontinuous Media, by R. G. Giovanelli, *Australian J. Phys.*, vol. 12, no. 2, June 1957, pp. 227-239.

Rotational Waves in Turbulent Liquid, by R. V. L. Hartley, *J. Acoustical Soc. of America*, vol. 29, 1957, pp. 195-196.

Material Transport in Turbulent Gas Streams; Radial Diffusion in Circular

Conduit, by S. Lynn, W. H. Corcoran and B. H. Sage, *J. AICHE*, vol. 3, 1957, pp. 11-15.

Velocity Distribution in Vortices, by A. Timme, *Ingenieur-Archiv*, vol. 25, no. 3, 1957, pp. 205-226 (in German).

Ground Reflection of Jet Noise, by Walton L. Howes, *NACA TN* 4260, April 1958, 56 pp.

Near Field Jet Noise, by M. O. W. Wolfe, *NATO, AGARD, Rep.* 112, April-May 1957, 41 pp.

Cloud-droplet Ingestion in Engine Inlets with Inlet Velocity Ratios of 1.0 and 0.7, by Rinaldo J. Brun, *NACA Rep.* 1317, 1957, 35 pp. (Supersedes TN 3593.)

Experiments in Liquid Atomization by Air Streams, by Henry F. Hruby, *J. Appl. Phys.*, vol. 29, March 1958, pp. 572-578.

The Prospects for Magneto-aerodynamics, by E. L. Resler Jr. and W. R. Sears, *J. Aeron. Sci.*, vol. 25, April 1958, pp. 235-245, 258.

Note on Hydrogen as a Real-gas Driver for Shock Tubes, by Paul W. Huber, *J. Aeron. Sci.*, vol. 25, April 1958, p. 269.

Hypersonic Heat Transfer to Catalytic Surfaces, by Sinclair M. Scala, *J. Aeron. Sci.*, vol. 25, April 1958, pp. 273-275.

A Note on Isentropic Compressible Flow of Air with Variable Specific Heats, by K. E. Tempelmeyer and L. Self, *J. Aeron. Sci.*, vol. 25, April 1958, pp. 278-279.

Propagation of Weak Waves in a Dissociated Gas, by F. K. Moore, *J. Aeron. Sci.*, vol. 25, April 1958, pp. 279-280.

Wall Effects in Shock Tube Flow, by Raymond J. Emrich and Donald B. Wheeler Jr., *Physics of Fluids*, vol. 1, Jan.-Feb. 1958, pp. 14-23.

Effect of Radiation on Shock Wave Behavior, by R. E. Marshak, *Physics of Fluids*, vol. 1, Jan.-Feb. 1958, pp. 24-29.

Hydromagnetic Stability of a Conducting Fluid in a Circular Magnetic Field, by Frank N. Edmonds Jr., *Physics of Fluids*, vol. 1, Jan.-Feb. 1958, pp. 30-41.

Statistical Behavior of a Reacting Mixture in Isotropic Turbulence, by Stanley Corrsin, *Physics of Fluids*, vol. 1, Jan.-Feb. 1958, pp. 42-47.

On the Diffusion of a Chemically Reactive Species in a Laminar Boundary Layer Flow, by Paul L. Chambré and Jonathan D. Young, *Physics of Fluids*, vol. 1, Jan.-Feb. 1958, pp. 48-54.

An Energy Principle for Hydromagnetic Problems, by I. B. Bernstein, E. A. Friedman, M. D. Kruskal and R. M. Kulsrud, *Roy. Soc.*, vol. 244A, Feb. 25, 1958, pp. 17-40.

Chemical Relaxation in Air, Oxygen and Nitrogen, by M. Camac, J. Camm, S. Feldman, J. Keck and C. Petty, *Inst. Aeron. Sci.*, Preprint 802, Jan. 1958, 21 pp., 15 figs.

The Interaction of a Reflected Shock Wave with the Boundary Layer in a Shock Tube, by Herman Mark, *NACA Tech. Mem.* 1418, March 1958, 128 pp.

On the Mixing Theory of Crocco and Lees and Its Application to the Interaction of Shock Wave and Laminar Boundary Layer, Part II: Results and Discussion, by Sin I. Cheng and I. D. Chang, *Princeton Univ., Dept. Aeron. Engng., Rep.* 376 (AFOSR-TN-58-3; ASTIA AD 148042), Nov. 1957, 32 pp.

Supersonic Mixing of Jets and Turbulent Boundary Layers, by Harry E. Bailey and Arnold M. Kuethe, *Wright Air Dev. Center, Tech. Rep.* 57-402 (ASTIA AD 150992), June 1957, 45 pp.

New Approach for the Calculation of Laminar and Turbulent Boundary Layers in Compressible Flow, Case of a Pressure Gradient; Peculiarities—Examples, by Alfred Walz, *France, Ministère de l'Air, Publications Scientifiques et Techniques* 336, 1957, 48 pp. (in French).

Light Diffusion through High-speed Turbulent Boundary Layers, by Howard A. Stine and Warren Winovich, *NACA Res. Mem.* A56B21, May 1956, 46 pp. (Declassified from Confidential by authority of NACA Res. Abstr. 125, p. 18, 3/18/58.)

Approximations for the Thermodynamic and Transport Properties of High-temperature Air, by C. Frederick Hansen, *NACA TN* 4150, March 1958, 67 pp.

Incompressible Two Dimensional Stagnation Point Flow of an Electrically Conducting Viscous Fluid in the Presence of a Magnetic Field, by Joseph L. Neuringer and William McIlroy, *Inst. Aeron. Sci., Preprint* 764, Jan. 1958, 19 pp., 1 tab., 4 figs.

Charts for Flow Parameters of Helium at Hypersonic Speeds; Mach Number 10 to 20, Princeton University, James Forrestal Res. Center, Gas Dynamics Lab., *Wright Air Dev. Center, TN* 57-377 (ASTIA AD 142310), Nov. 1957, 62 pp., 18 figs.

On Reducing Aerodynamic Heat Transfer Rates by Magneto-hydrodynamic Techniques, by Rudolf C. Meyer, *Inst. Aeron. Sci., Preprint* 816, Jan. 1958, 25 pp., 7 figs.

Approximate Three Dimensional Solutions for Transient Temperature in Shells of Revolution, by Maurice A. Brull and Jack R. Vinson, *Inst. Aeron. Sci., Preprint* 775, Jan. 1958, 29 pp., 3 figs.

The Hecker Method of Transient Temperature Calculation, by A. W. Trimpi, *Inst. Aeron. Sci., Preprint* 774, Jan. 1958, 24 pp.

On the Hydrodynamic Stability of Curved Laminar Compressible Flows, by M. Lessen, *Inst. Aeron. Sci., Preprint* 812, Jan. 1958, 16 pp., 5 figs.

The Shock Wave in a Nonmonatomic Fluid, by Phrixos Theodorides, *Maryland Univ., Inst. Fluid Dynam. and Appl. Math., TN* BN-123 (AFOSR-TN-58-156; ASTIA AD 152182), Feb. 1958, 20 pp.

Numerical Analysis of Inviscid Supersonic Flows, Utilizing the Stream Surface Characteristics Method, by C. Cobb, H. G. Loos and S. Manus, *Propulsion Res. Corp., Rep.* R-279 (AFOSR-TN-58-105; ASTIA AD 152014), Jan. 1958, 31 pp.

Critical Study of Certain Extensions in Rational Mechanics; Thermodynamics and Viscosity, by Henry Du Bose De Beaumont, *France, Ministère de l'Air, Publications Scientifiques et Techniques, Notes Tech.* 72, 1957, 46 pp. (in French).

Experimental Study of Turbulent Flow in a Two Dimensional Variable Diffuser, by Jean Pierre Milliat, *France, Ministère de l'Air, Publications Scientifiques et Techniques* 335, 1957, 134 pp. (in French).

A Numerical Method for Calculating the Starting and Perturbation of a Two Dimensional Jet at Low Reynolds Number, by R. B. Payne, *Gl. Brit., Aeron. Res. Council, Rep. & Mem.* 3407, (formerly ARC Tech. Rep. 18846), 1958, 50 pp.

Boundaries of Supersonic Axisymmetric Free Jets, by Eugene S. Love, Mildred J. Woodling and Louise P. Lee, *NACA Res. Mem.* L56G18, Oct. 1956, 98 pp. (Declassified from Confidential by authority of NACA Res. Abstr. 125, p. 24, 3/18/58.)

An Analogue Computer for Convective Heating Problems, by H. G. R. Robinson, *Gl. Brit., Aeron. Res. Council, Curr. Paper*

374 (formerly ARC Tech. Rep. 19098; Roy. Aircr. Estab., TN G. W. 434), 1957, 15 pp., 10 figs.

The Conservation Property of the Heat Equation on Riemannian Manifolds, by Matthew P. Gaffney, *Northwestern Univ. (AFOSR-TN-58-145; ASTIA AD 152-172)*, Feb. 1958, 12 pp.

Heat Transfer in Turbulent Pipe Flow, by Raul R. Hunziker, *J. Franklin Inst.*, vol. 265, March 1958, pp. 205-225.

On Time Smoothing, a Model for Momentum Transport, by Marshall Fixman, *J. Chem. Phys.*, vol. 28, March 1958, pp. 397-400.

Thermal Conductivities of Gases at Low Pressures, I: Monatomic Gases, Helium and Argon, by F. G. Waelbroeck and P. Zuckerbrodt, *J. Chem. Phys.*, vol. 28, March 1958, pp. 523-524.

Thermal Conductivities of Gases at Low Pressures, II: Rotational Relaxation Times in Hydrogen and Oxygen, by F. G. Waelbroeck and P. Zuckerbrodt, *J. Chem. Phys.*, vol. 28, March 1958, pp. 524-526.

Drop-size Distributions for Impinging-jet Breakup in Airstreams Simulating the Velocity Conditions in Rocket Combustors, by Robert D. Ingebo, *NACA TN* 4222, March 1958, 23 pp.

Thermodynamics of Electrically Conducting Fluids and Its Application to Magneto-Hydrodynamics, by Boia-Teh Chu, *Wright Air Dev. Center, TN* 57-350 (ASTIA AD 142039), Dec. 1957, 32 pp.

The Shock Tunnel and Its Applications to Hypersonic Flight, by A. Hertzberg, *NATO, Adv. Group for Aeron. Res. and Dev., Rep.* 144, July 1957, 32 pp.

Correlation of Turbulent Heat Transfer in a Tube for the Dissociating System $N_2O_4 \rightleftharpoons 2NO_2$, by R. S. Brokaw, *NACA Res. Mem.* E57K19a, March 1958, 17 pp.

Effect of Jet Temperature on Jet-noise Generation, by Vern G. Rollin, *NACA TN* 4217, March 1958, 13 pp.

A Theory about the Secondary Flow in Cascades, by Shintaro Otuka, *Proc., Japan, 8th Natl. Congr. Appl. Mech.*, 1956 (pub. 1957), pp. 327-332.

Combustion, Fuels and Propellants

Relation of the Turbojet and Ramjet Combustion Efficiency to Second-order Reaction Kinetics and Fundamental Flame Speed, by J. Howard Childs, Thaine W. Reynolds and Charles C. Graves, *NACA Rep.* 1334, 1957, 13 pp.

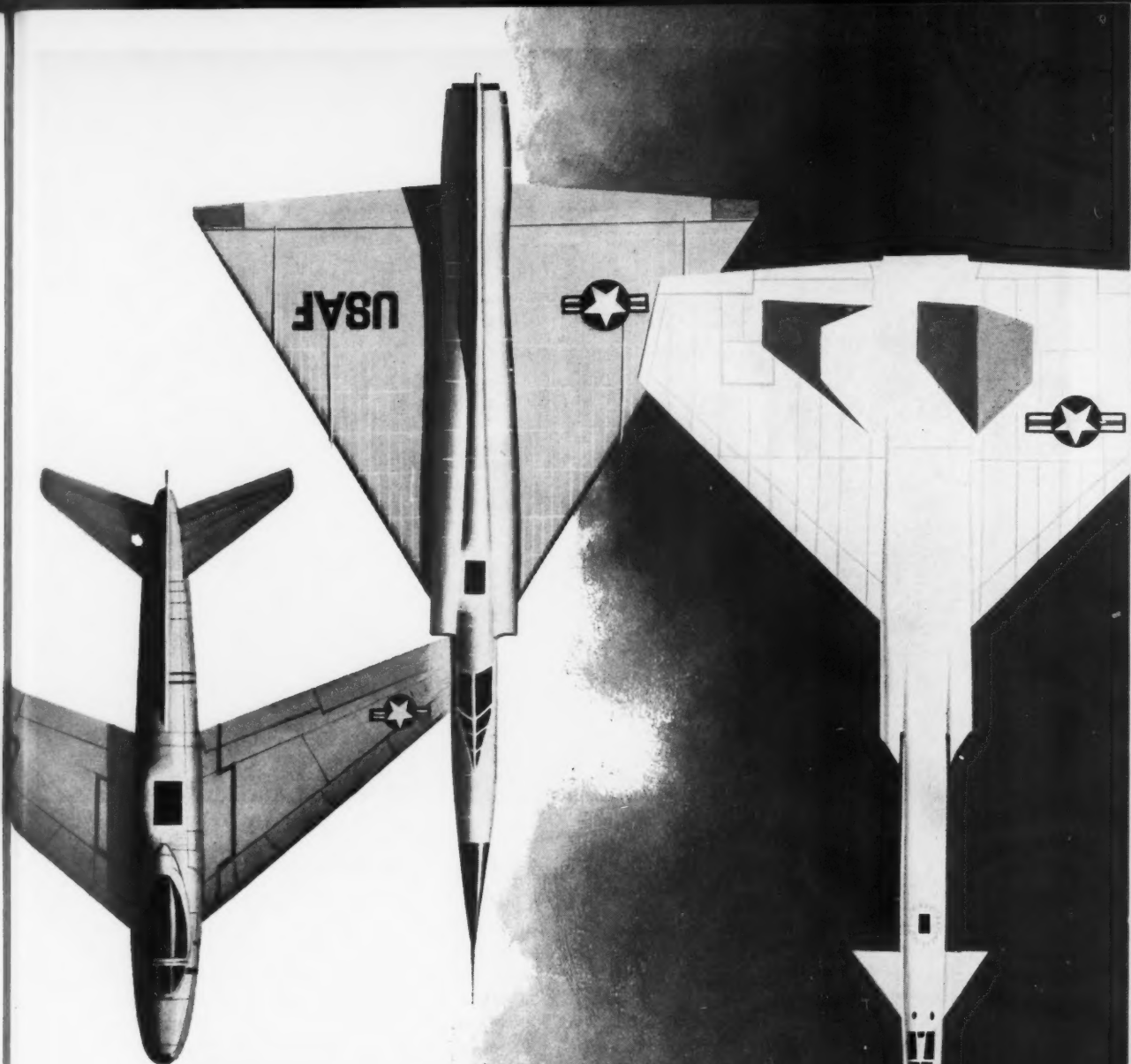
Development of an Automatic System for Measuring Time in the Determination of Burning Rates of Propellants, by H. M. Burns and W. A. Hendricks, *Hercules Powder Co., Allegany Ballistics Lab., Rep.* ABL/B-16, Jan. 1958, 28 pp.

The Equations of Motion in a Multicomponent Chemically Reacting Gas, by Sinclair M. Scala, *General Electric Co., Tech. Info. Series, Rep.* R58SD205, Dec. 1957, 38 pp.

Irreversible Stochastic Thermodynamics and the Transport Phenomena in a Reacting Plasma, by H. J. Kaeppler and G. Baumann, *Forschungsinstitut für Physik der Strahlentriebe, E. V. Mitteilungen* 8, Nov. 1956, 104 pp.

Composition and Thermodynamic Functions of the Chemically Reactive Combustion Gas: Hydrocarbon Air Mixture, by H. J. Kaeppler and G. Baumann, *Forschungsinstitut für Physik der Strahlentriebe, E. V. Mitteilungen* 10, April 1957, 221 pp. (in German).

(Continued on page 864)

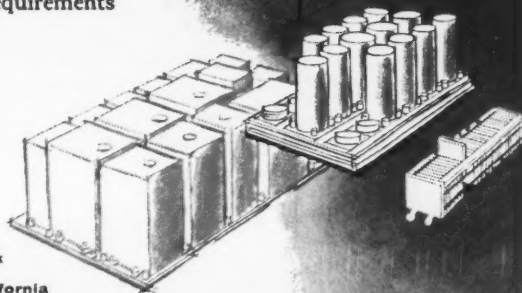


SPACE-ABILITY

Servomechanisms' proven ability to design and produce consistently smaller and more reliable Central Data Computers, has established SMI as the pace-setter in this exacting science. This experience, coupled with our major scientific advances in new materials research and deposited film circuitry techniques, will meet the requirements of even smaller and more reliable subsystems for the spacecraft of tomorrow.



SUBSYSTEMS DIVISION, Hawthorne, California
 MECHATROL DIVISION, Westbury, L.I., New York
 SPECIAL PRODUCTS DIVISION, Hawthorne, California
 RESEARCH LABORATORY, Goleta, California
 GENERAL OFFICES • 12500 Aviation Boulevard, Hawthorne, California



The products of SMI are available in Canada and throughout the world through Servomechanisms (Canada) Limited, Toronto 16, Ontario.



Photograph of the repetitive orbit of a 20 micron diameter charged aluminum particle suspended in a vacuum chamber by oscillating and static electric fields

ELECTRODYNAMIC ORBITS

By the application of properly chosen alternating and static electric fields, electrically charged particles can be maintained in dynamic equilibrium in a vacuum against interparticle and gravitational forces. This is illustrated in the above photograph of the orbit of a charged dust particle. During the time of exposure the particle traversed the closed orbit several times, yet it retraced its complicated path so accurately that its various passages can barely be distinguished.

The range of particles of different charge-to-mass ratios which can be contained in this manner is determined by the gradients of the static and alternating electric field intensities and by the frequencies of the latter. In the absence of static fields and for a given electric field strength, the minimum frequency required for stable containment of the particles is proportional to the square root of their charge-to-mass ratios. Thus, charged colloidal particles require the use of audio frequencies, atomic ions need HF frequencies, while electrons require the use of VHF and higher frequencies.

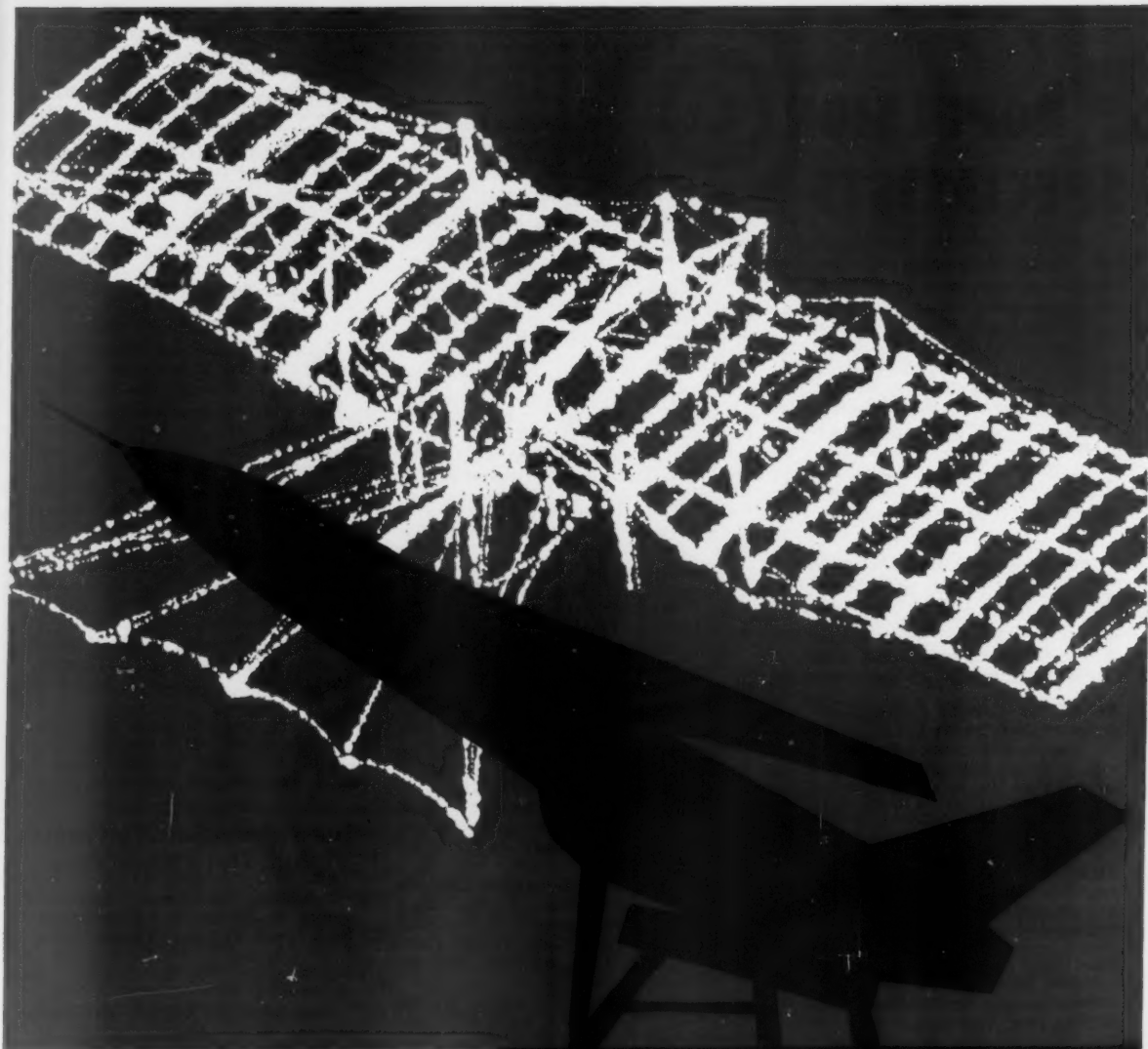
Under the confining influence of the external fields,

the particles are forced to vibrate with a lower frequency of motion which is determined by the external field intensities, space charge, and the driving frequencies. If the initial thermal energy is removed, a number of particles may be suspended in space in the form of a crystalline array which reflects the symmetry properties of the external electrodes. These "space crystals" can be repeatedly "melted" and re-formed by increasing and decreasing the effective electrical binding force. These techniques offer a new approach in the study of plasma problems and mass spectroscopy in what may be properly termed "Electrohydrodynamics."

At The Ramo-Wooldridge Corporation, work is in progress in this and other new and interesting fields. Scientists and engineers are invited to explore current openings in Electronic Reconnaissance and Countermeasures; Microwave Techniques; Infrared; Analog and Digital Computers; Air Navigation and Traffic Control; Antisubmarine Warfare; Electronic Language Translation; Radio and Wireline Communication, and Basic Electronic Research.

The Ramo-Wooldridge Corporation

LOS ANGELES 45, CALIFORNIA



REVOLUTION IN DESIGN

Grove Regulators As revolutionary in design and engineering as the technological transition from flying machine to space vehicle... Achieved a quarter of a century ago, the only regulators which could be used in the early space labs of Annapolis... still today the standard for the critical control of high pressure fluids... Now on the threshold of space, Grove is uniquely prepared—through advance research and development—to meet the challenge of even higher pressures ahead.

GROVE POWREACTOR DOME REGULATOR MODEL GH-408—50-6000 PSI INLET... 5-3000 PSI REDUCED PRESSURE

GROVE VALVE and REGULATOR COMPANY

6529 Hollis St., Oakland 8, California • 2559 W. Olympic Blvd., Los Angeles 6, California
Offices in other principal cities



PROPULSION SPECIALISTS

Bell Aircraft Corporation offers you outstanding high level positions in the Propulsion Department of its Space Flight and Missiles Division.

Experienced specialists are needed to assume the responsibility for conducting analytical and/or experimental investigations in specified fields as related to advanced propulsion technology. These challenging and unique positions offer you opportunities for technical advancement as well as professional and financial growth.

AEROTHERMODYNAMIC SPECIALIST

to work on supersonic aerodynamics, boundary layer flow, heat transfer and combustion problems. 5-7 years of experience related to supersonic inlet and exhaust nozzle design including dissociation effects required. Ph D desirable.

RAMJET SPECIALIST for preliminary design, evaluation and selection of ramjet engines and components for advanced missile programs. MS degree or equivalent plus 10 years progressive and intensive experience in all phases of ramjet engine research, design and development desired.

TURBOJET SPECIALIST to assume responsibility for preliminary design, evaluation and selection of turbojet engines and components for advanced missile programs. MS degree or equivalent plus 10 years progressive and intensive experience in all phases of turbojet engine research design and development desired.

THERMOCHEMICAL SPECIALIST to deal with transport properties of gases at high temperatures, dissociation and recombination phenomena and rates, high temperature gas and surface interaction and boundary layer flows involving sublimation or combustion. Ph D plus 5-7 years directly related experience desired.

SOLID PROPELLANT ROCKET ENGINE SPECIALIST to engage in preliminary design, evaluation and selection of solid propellant rocket engines for advanced missile programs. MS degree or equivalent plus 10 years progressive and intensive experience in solid propellants, grain configuration, combustion and hardware desired.

Salaries are commensurate with your background. Living and working conditions are excellent and employee benefits outstanding.

Write:

SUPERVISOR, ENGINEERING
EMPLOYMENT, DEPT. K-62
BELL AIRCRAFT CORPORATION
BUFFALO 5, NEW YORK

Reaction Kinetics, Thermodynamics, and Transport in the Hydrogen-bromine System; A Survey of Properties for Flame Studies, by Edwin S. Campbell and Robert M. Fristrom, *Chem. Rev.*, vol. 58, April 1958, pp. 173-234.

The Ignition of Combustible Gases by Flames, by H. G. Wolfhard and D. S. Burgess, *Combustion and Flame*, vol. 2, March 1958, pp. 3-12.

Application of Well-stirred Reactor Theory to the Prediction of Combustor Performance, by H. C. Hottel, G. C. Williams and A. H. Bonnell, *Combustion and Flame*, vol. 2, March 1958, pp. 13-34.

A Review of Some Unusual Stationary Flame Reactions, by W. G. Parker, *Combustion and Flame*, vol. 2, March 1958, pp. 69-82.

The Methyl Nitrite Decomposition Flame, by E. A. Arden and J. Powling, *Combustion and Flame*, vol. 2, March 1958, pp. 55-68.

Use of an Electro-optical Method to Determine Detonation Temperatures in High Explosive, by F. C. Gibson, M. L. Bowser, C. R. Sommers, F. H. Scott and C. M. Mason, *J. Appl. Phys.*, vol. 29, April 1958, pp. 628-632.

Measurement of Rate Constants of Fast Reactions in a Supersonic Nozzle, by Peter P. Wegener, *J. Chem. Phys.*, vol. 28, April 1958, pp. 724-725.

Heats of Combustion of Some Organic Compounds Containing Chlorine, by G. C. Sinke and D. R. Stull, *J. Phys. Chem.*, vol. 62, April 1958, pp. 397-401.

Cyanogen Derivatives as Rocket Propellants, by Eckart W. Schmidt, *Raketentechnik und Raumfahrtforschung*, vol. 2, no. 1, 1958, pp. 20-21 (in German).

Flow Visualization Techniques Applied to Combustion Problems, by E. F. Winter, *J. Roy. Aeron. Soc.*, vol. 62, April 1958, pp. 268-276.

The Point of Oxygen Attack in the Combustion of Hydrocarbons, I: The Origin of Carbon Monoxide, by C. F. Cullis, F. R. F. Hardy and D. W. Turner, *Proc. Roy. Soc.*, vol. 244A, April 22, 1958, pp. 573-580.

Reactions of Nitrogen Atoms, II: H₂, CO, NH₃, NO, and NO₂, by B. G. Kistiakowsky and G. G. Volpi, *J. Chem. Phys.*, vol. 28, April 1958, pp. 665-667.

Materials of Construction

A Vibration Manual for Engineers, by R. T. McGoldrick, 2d ed., *David Taylor Model Basin, Rep. R-189*, Dec. 1957, 27 pp.

New Graphites Beat Missile Hot Spots, by Irwin Stambler, *Aviation Age*, vol. 29, April 1958, pp. 150-154.

Thin Pressurized Shells Look Best for Space Structures, by Joseph S. Lewin, *Aviation Age*, vol. 29, April 1958, pp. 86-92.

Orbital Re-entry Will Intensify Demands on Structures, by J. S. Butz Jr., *Aviation Week*, vol. 68, April 21, 1958, pp. 50-51, 53, 55, 57, 59.

The Minimum Weight of a Structure Protected Against Short Duration Aerodynamic Heating by Means of Thermal Diffusion, by Richard A. Dobbins, *Inst. Aeron. Sci., Preprint 773*, Jan. 1958, 20 pp., 9 figs.

Ignition of Kel-F and Teflon, by Lewis Greenspan, *Rev. Sci. Instr.*, vol. 29, Feb. 1958, pp. 172-173.

Cermets as Potential Materials for High Temperature Service, by O. A. Sandven, *NATO, Adv. Group. for Aeron. Res. and*

Dev., Rep. 101, April 1957, 25 pp.

Structures and Materials, by Paul E. Sandorff, *Aviation Age*, vol. 28, March 1958, pp. 50-63.

High Temperatures Spur Use of Nickel-base Alloys, II, by T. E. Kihlgren, *Aviation Age*, vol. 28, March 1958, pp. 130-137.

1958 Missile Materials Review, by Alfred J. Zaehring and Raymond M. Nolan, *Missiles and Rockets*, vol. 3, March 1958, pp. 69-75.

Aluminum for Missiles in Production, by Don Fabun, *Missiles and Rockets*, vol. 3, March 1958, pp. 85-87.

Materials Build a New Technology, by W. C. Rous Jr., *Missiles and Rockets*, vol. 3, March 1958, pp. 91-92, 95-96, 98, 100.

Welded Stainless Steel Hollow Core, by Dr. Michael Watter, *Missiles and Rockets*, vol. 3, March 1958, pp. 104-105, 107-110.

High Temperature Brazing Looks Good for Missile Parts, by John V. Long and George D. Dremer, *Aviation Age*, vol. 29, May 1958, pp. 30-31, 33.

Lithia Agents Boost Heat Resistance of Ceramic Coatings, by Paul A. Huppert, *Aviation Age*, vol. 29, May 1958, pp. 56-58.

Ceramic Nozzles for Uncooled Rocket Motors, by W. L. Wroten, *Raketentechnik und Raumfahrtforschung*, vol. 2, no. 1, 1958, pp. 21-22 (in German).

Axial - temperature - gradient Bending Stresses in Tubes, by F. G. Hammitt, *J. Appl. Mech.*, vol. 25, no. 1, March 1958, pp. 109-114.

Thermal Stress Analysis of a Cylinder of Semi-plastic Material, by Donald Hunter and Glenn Murphy, *Ames Lab. (U.S. AEC) ISC-839*, Dec. 1956, 31 pp.

Instrumentation, Telemetering, Data Recording

Extending Transducer Transient Response by Electronic Compensation for High-Speed Physical Measurements, by F. F. Liu and T. W. Berwin, *Rev. Sci. Instrum.*, vol. 29, no. 1, Jan. 1958, pp. 14-22.

Description of a Sensitive Micromanometer, by R. Eichhorn and T. F. Irvine Jr., *Rev. Sci. Instr.*, vol. 29, no. 1, Jan. 1958, pp. 23-27.

Industry Strives for Missile Telemetry Economy, by John Kinkle, *Missiles and Rockets*, vol. 3, no. 2, Feb. 1958, pp. 87-88.

Industry's Answer to the Data-processing Challenge, by H. H. Rosen, *Missiles and Rockets*, vol. 3, no. 2, Feb. 1958, pp. 95-102.

Challenge to Industry: Spaceship Telemetry, by Henry P. Steier, *Missiles and Rockets*, vol. 3, no. 2, Feb. 1958, pp. 105-110.

Vortex Tube Performance Data Sheets, by R. Westley, *Cranfield, Coll. Aeron.*, Note 67, July 1957, 7 pp., 65 figs.

Digital Computer Calculation of Transducer Frequency Response from Its Response to a Step Function, by Ralph B. Bowersox and Joseph Carlson, *Calif. Inst. Techn., Jet Propulsion Lab., Progr. Rep. 20-331*, July 1957, 12 pp.

Information Criteria for Estimation of Telemetering Systems, by M. M. Bachmetiev and R. R. Vasiliev, *Automatika i Telemekanika*, vol. 18, no. 4, 1957, pp. 371-375 (in Russian).

Static Transfer Device of a Pulse-frequency Telemetering System, by A. M. Pshenichnikov, *Automatika i Telemekanika*, vol. 18, no. 5, 1957, pp. 444-448 (in Russian).

Kodak reports on:

why 5,000 \$5 bills were stuffed into our till... a large optical device...
the boys who do their arithmetic in advance

The stickum of last resort

For *Eastman 910 Adhesive*, of which the active ingredient is methyl-2-cyanoacrylate, we now have a slogan—"the adhesive to try if no other will do."

We are just being sensible. Its price by the ounce is \$10; special pound price, \$75. It *does* make possible some distinctly advantageous new assembly techniques in a large number of industries. So we gather from the correspondence incidental to the 5,000 orders filled during the past year. It bonds virtually everything (except silicones and polyolefins, else how could we deliver it?).

The biggest plus is the speed at which enormous bond strength is developed within minutes after application of this thin, clear liquid to one of the adherents. Within hours the tensile strength of its bond to steel is in the thousands of pounds per square inch. In the case of glass, rubber, or wood, bonds are stronger than the material itself. There is virtually no shrinkage on setting. No heating, no great squeezing, no evaporation is required. The bond, however, should not be depended on for too many weeks at temperatures above 175°F, particularly in the presence of much moisture. That's the minus.

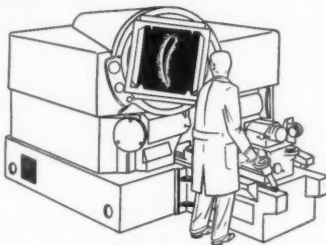
In case *Eastman 910 Adhesive* sounds more interesting now than it did when we practically swamped our boat by offering samples at \$5 an ounce, write to *Eastman Chemical Products, Inc., Department E 910A, Kingsport, Tenn.* (Subsidiary of *Eastman Kodak Company*).

For blades (also vanes and buckets)



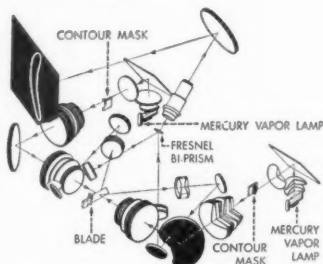
This is a blade from a jet engine. Many mathematical minds, mighty mathematical machines, and much aerodynamical experimentation have created its shape. Violation of the plan to the extent of a few thousandths of an inch in a single cross-section of a single blade sucks at efficiency like a little leech. And

there are so many blades in a single compressor or turbine that the total number of them made in the brief span of air-breathing non-reciprocating history must compare with all the wooden spokes in all the wagon wheels of all the supply trains in all armies since Alexander the Great. Tolerances on wooden spokes have always been broad.



Therefore we have been busily building this large optical device.

It works like this.



Not long before this periodical reached its subscribers, the two mercury lamps were turned on and the first cross-section of the first blade was seen thus in magnification against its tolerance envelope scribed on the screen. Inspection from now on should go rapidly and well.

The device has been named *Kodak Section-Profile Projector*, and it is enough to restore a man's faith in the future of geometrical optics. Inquiries go to *Eastman Kodak Company, Military and Special Products Sales, Rochester 4, N. Y.*

A fast film with a quiet name

Dearly as a hunting-and-fishing editor loves to describe some high Andean stream which only a major general has ever had occasion to

whip, so the photographic press dotes on miracles in making pictures with a parsimony of radiant energy that few occasions demand. We would no more discourage this than we would the game of bridge.

The fastest film that can be obtained by walking up to a film counter without previous notice and plunking down the money is labeled *Kodak Royal-X Pan Film*. It comes either as roll film or sheet film. It is grainy. The average photo-hobbyist needs it about as badly as he needs a fishing trip to the Andes, except that a roll of the 120 size lists for only 75¢.

On the other hand, take a fellow whose hobby is bridge but whose job is to record the path of a piece of metal hurtling through the twilight a thousand miles above him. Or take his classmate who needs to analyze the first microsecond of a thermonuclear explosion. These boys are not apt to mail in their negatives to us with a letter asking how come they turned out so dark. They have been in close touch with us before going out to their stations. In their behalf we have very carefully considered all the data on the *Royal-X Pan* emulsion and concluded that for the present putting it on 16mm, 35mm, or 70mm film would not be a good idea. Furthermore, the arithmetic indicates that the most sensitive regular-production films in these widths, *Kodak Tri-X Film* and *Kodak Linagraph Pan Film*, might not be quite sensitive enough.

No, this is not leading up to some new "Quadruple Grand Ducal Whoosh-X Film." In these cases of speed-above-all what we often recommend bears the quieter name, *Kodak Spectroscopic Film, Type I-D(2)*. It is one of 111 special emulsions we make for astrophysicists and the like. By some tests it is faster than *Royal-X Pan*, but we are not prepared to prove this. By advance arrangement through *Eastman Kodak Company, Special Sensitized Products Division, Rochester 4, N. Y.*, as little as 100 feet of it in 35mm perforated form can be furnished for \$10, or two 100-foot 16mm rolls for \$6.60 apiece (list).

Prices stated are subject to change without notice.

This is another advertisement where *Eastman Kodak Company* probes at random for mutual interests and occasionally a little revenue from those whose work has something to do with science

Kodak
TRADE MARK

Index of Papers Published in JET PROPULSION

A Publication of the American Rocket Society

Volume 28—January through December 1958

Issue	Pages
January	1-72
February	73-148
March	149-212
April	213-292
May	293-364
June	365-436
July	437-504
August	505-572
September	573-640
October	641-712
November	713-788
December	789-872

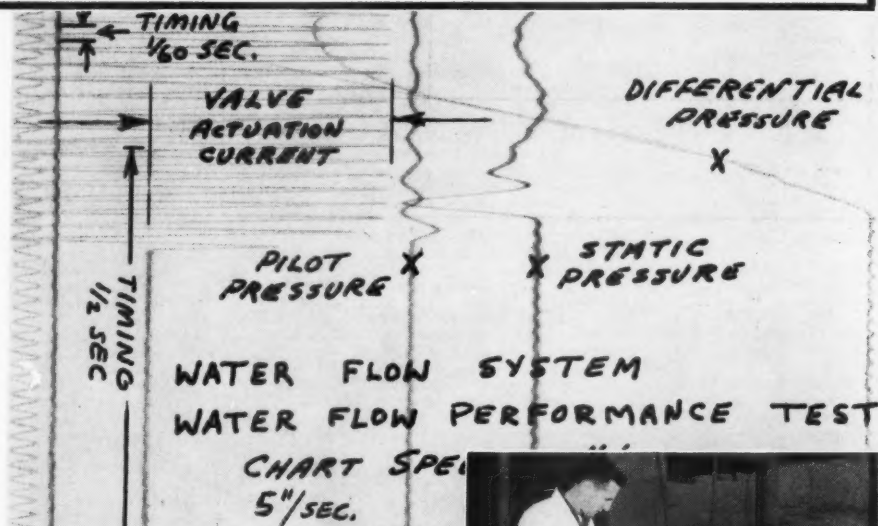
ADAMS, MAC C. and PROBSTEN, RONALD F. On the Validity of Continuum Theory for Satellite and Hypersonic Flight Problems at High Altitudes..... See also PROBSTEN, RONALD F.	86
ADLER, ALFRED A. Calculation of Re-Entry Velocity Profile	827
AGOSTON, GEORGE A., WOOD, BERNARD J. and WISE, HENRY Influence of Pressure on the Combustion of Liquid Spheres.....	181
ANDERSEN, W. H., BILLS, K. W., DEKKER, A. O., MISHUCK, E., MOE, G. and SCHULTZ, R. D. The Gasification of Solid Ammonium Nitrate	831
ARENS, M. A Comparison of Turbojets and Ram-jets for High Speed Flight..... On a Generalized Optimization Procedure for N-Staged Missiles.....	620 766
AROSTE, HENRY and RUDIN, MORTON Relaxation Lags in Gas Flow.....	690
BAJER, J. J., see SEARS, G. A.	
BAKER, ROBERT M. L., JR. Note on Interplanetary Navigation.... See also HERRICK, SAMUEL	834
BARTZ, D. R. Factors Which Influence the Suitability of Liquid Propellants as Rocket Motor Regenerative Coolants..... See also HASTRUP, R. C.	46
BAUMANN, ROBERT C. Design, Fabrication and Testing of the Vanguard Satellite.....	244
BENNETT, D. J. Escape From a Circular Orbit Using Tangential Thrust.....	167
BENTON, MILDRED Artificial Satellites—A Bibliography of Recent Literature Part I—1956..... Part II—1957-1958.....	301 399
BERGER, WILLIAM J. Celestial Iconospherics, the Ultimate Astronomy	337
BERGER, W. J. and RICUPITO, J. R. Visibility of Orbital Points.....	825
BERWIN, T. W., see LIU, F. F.	
BEUTLER, F. J. and RAUCH, L. L.	

Precision Measurement of Supersonic Rocket Sled Velocity—Part II.....	809
BILLS, K. W., see ANDERSEN, W. H.	
BLOXSOM, D. E., JR. Supersonic Aerodynamic Experiments Using Very High Temperature Air Wind Tunnels..... Use of Capacitor Discharges to Produce High Temperature, High Pressure Air	603 609
BOGDONOFF, S. M., see VAS, I. E.	
BOLLINGER, LOREN E. Evaluation of Flame Stability at High Reynolds Numbers.....	334
BOND, J. W., JR. Plasma Physics and Hypersonic Flight	228
BRAGG, S. L. and BYWORTH, S. P. Q. Combustion Chamber Pressure Loss....	829
BRAGG, S. L. and RATCIFFE, H. Characteristic Velocity as a Measure of Available Work.....	762
BREHM, R. L., see DUNLAP, R.	
BROBECK, W. M., CLEMENSEN, R. E. and VORECK, W. E. A Recording Sodium-Line Reversal Pyrometer	249
BROMBERG, R. and LIPKIS, R. P. Heat Transfer in Boundary Layers With Chemical Reactions Due to Mass Addition	668
See also COHEN, C. B.	
BRYSON, A. E., JR. and ROSS, STANLEY E. Optimum Rocket Trajectories With Aerodynamic Drag.....	465
BURGESS, D. S., see RICHMOND, J. K.	
BUSSARD, ROBERT W. Concepts for Future Nuclear Rocket Propulsion	223
BYWORTH, S. P. Q., see BRAGG, S. L.	
CAMBEL, ALI BULENT, see ZIEMER, RICHARD W.	
CHANG, CHIEH-CHIEN and HSU, CHENG-TING Solutions to Stoolman's External Diffusion Equation for Instability of a Normal Shock Inlet Diffuser.....	457
CHRIST, O. J. W. and SMALL, B. B. Direct Digital Read-Out of Missile Role From Film Records.....	406
CHU, S. T. An Iterative Method of Determining Equilibrium Compositions of Reacting Gases	252
CLEMENSEN, R. E., see BROBECK, W. M.	
COHEN, C. B., BROMBERG, R. and LIPKIS, R. P. Boundary Layers With Chemical Reactions Due to Mass Addition.....	659
COLBOURN, JOSEPH L., see ROTHBERG, SIDNEY	
COURTNEY, WELBY G. Ignition by Flow Over Hot Surfaces..	836
COX, W. T. Comment on "Stresses in Rocket Grains"	342
CROCCO, LUIGI Comments on the Zucrow-Oshorn Paper on Combustion Oscillations.....	843
CROCCO, LUIGI, GREY, JERRY and HARRJE, DAVID T. On the Importance of the Sensitive Time Lag in Longitudinal High-Frequency Rocket Combustion Instability.....	841
DAWLEY, RICHARD E., see GEDEON, GEZA S.	
DEAN, LEO E. and SHURLEY, LUCIAN A. Analysis of Regenerative Cooling in	

Rocket Thrust Chambers.....	104
DEKKER, A. O., see ANDERSEN, W. H.	
DESSLER, A. J., HANSON, W. B. HERTZBERG, M., MCKIBBIN, D. D. and WRIGLEY, R. C. A New Instrument for Measuring Atmospheric Density and Temperature at Satellite Altitudes.....	837
DIETZ, ROBERT O., JR. and HINNERS, ARTHUR H., JR. Ramjet Test Facility Planning.....	315
DOBROWOLSKI, A. Satellite Orbit Perturbations Under a Continuous Radial Thrust of Small Magnitude	687
DONALDSON, W. F., see RICHMOND, J. K.	
DUNCAN, D. B. Analysis of an Inertial Guidance System	111
DUNLAP, R., BREHM, R. L. and NICHOLLS, J. A. A Preliminary Study of the Application of Steady-State Detonative Combustion to a Reaction Engine.....	451
DUSSOURD, JULES L. and SHAPIRO, ASCHER H. A Deceleration Probe for Measuring Stagnation Pressure and Velocity of a Particle-Laden Gas Stream.....	24
ECKERT, E. R. G., SCHNEIDER, P. J., HAYDAY, A. A. and LARSON, R. M. Mass-Transfer Cooling of a Laminar Boundary Layer by Injection of a Light-Weight Foreign Gas.....	34
EVANS, MARJORIE W., GIVEN, FRANK I. and MULLER, G. M. Ignition of Electrolytic Monopropellants by Submerged Electrical Discharge..	255
FARBER, MILTON Thermodynamics of AlO_2	760
FARREL, E. C., see KLUGER, P.	
FINKELSTEIN, A. B., see YUAN, S. W.	
FRIED, BURTON D. Corrections to "Comments on the Powered Flight Trajectory of a Satellite"	342
GAMBILL, W. R. and GREENE, N. D. A Preliminary Study of Vortex-Boiling Burnout Heat Fluxes.....	192
GARWIN, RICHARD L. Solar Sailing—A Practical Method of Propulsion Within the Solar System	188
GEDEON, GEZA S. and DAWLEY, RICHARD E. The Influence of the Launching Conditions on the Orbital Characteristics	759
GERARD, GEORGE An Evaluation of Structural Sheet Materials in Missile Applications.....	511
GIEDT, W. H. and RALL, D. L. Bore-Surface Temperature Variation During Rapid Firing of a 40-mm Gun	116
GIN, W. Calculated Viscosity of a Solid Propellant Rocket Exhaust Gas Mixture....	127
GIVEN, FRANK I., see EVANS, MARJORIE W.	
GOETTELMAN, R. C. Measurement of Satellite Erosion Rates by the Backscattering of Beta-Rays	753
GOLDSMITH, M. The Optimization of Nozzle Area Ratio for Rockets Operating in a Vacuum	170

(Continued on page 868)

This is a record of a missile component



Visicorder Record—actual size

Wyle Laboratories in El Segundo, California, have used a battery of four Visicorder consoles like the one shown (right) to run a series of tests on a vital missile component. In the Wyle test project, the unique Visicorder consoles are easy to operate. Most parameters are low frequency, requiring response on the order of 5 to 60 cycles.

The two calibrator control panels in each Visicorder console accommodate 10 plug-in balance and matching units—designed to match tachometer generators, pressure transducers, thermocouples, expanded-scale voltmeters, etc., to the Heiland galvanometers.

Dick Johnson, Instrumentation Branch Head at Wyle, says, "This system, I feel, is one of the most efficient instrumentation consoles in operation. Set-up and calibration time has been reduced by the use of Visicorders by approximately 50%. This is due to the simplicity of operation and trouble-free performance. There are no inking pens to clean, high-gain amplifier maintenance, and so on, and we can also use these consoles together to form systems of more than six channels."



Tom Jackson, Wyle engineer, examines Visicorder record

The HONEYWELL VISICORDER is the first high-frequency, high-sensitivity direct recording oscillograph. In laboratories and in the field everywhere, instantly-readable Visicorder records are pointing the way to new advances in product design, rocketry, computing, control, nucleonics... in any field where high speed variables are under study.

To record high frequency variables—and monitor them as they are recorded—use the Visicorder Oscillograph. Call your nearest Minneapolis-Honeywell Industrial Sales Office for a demonstration.

Honeywell



Industrial Products Group


Reference Data: Write for Visicorder Bulletin

Minneapolis-Honeywell Regulator Co., Industrial Products Group, Heiland Division, 5200 E. Evans Ave., Denver 22, Colorado

GORDON, JOHN S. High Temperature Chemistry as Applied to Metal-Based Propellants.....	769	LOGAN, JOSEPH G., JR. Recent Advances in Determination of Radiative Properties of Gases at High Temperatures.....	795	RICHMOND, J. K., DONALDSON, W. F., BURGESS, D. S. and GRUMER, J. Evidence for the Wrinkled Continuous Laminar Wave Concept of Turbulent Burning.....	393
GOULARD, R. On Catalytic Recombination Rates in Hypersonic Stagnation Heat Transfer	737	LUDWIG, G. H., <i>see</i> VAN ALLEN, J. A.		RICHTER, HENRY L., JR., SAMPSON, WIL- LIAM F. and STEVENS, ROBERTSON Microluck: A Minimum Weight Radio Instrumentation System for a Satellite	532
GRANTON, JAMES, JR., <i>see</i> STRUBLE, RAYMOND A.		MARCIANEK, J. J. On the Free Vibration of a Variable Mass.....	198	RICUPITO, J. R., <i>see</i> BERGER, W. J.	
GREEN, LEON, JR. Some Effects of Oxidizer Concentration and Particle Size on Resonance Burn- ing of Composite Solid Propellants	159	MATSNAGA, SYOGO On Radiation From Combustion Gas... On the Thermal Resistance of the Water Droplet on the Metallic Surface.....	125 126	ROBERSON, ROBERT E. Air Density Determination by Observa- tion of a Satellite.....	330
Some Properties of a Simplified Model of Solid Propellant Burning.....	386	McALEVY, R. F., III, <i>see</i> SUMMERFIELD, MARTIN		Effect of Air Drag on Elliptic Satellite Orbits.....	90
Some Effects of Charge Configuration in Solid Propellant Combustion....	483	McILWAIN, C. E., <i>see</i> VAN ALLEN, J. A.		Optical Determination of Orientation and Position Near a Planet.....	747
GREEN, L., JR. and NACHBAR, W. A Comment on Combustion Instability in Solid Propellant Rocket Motors...	769	McKIBBIN, D. D., <i>see</i> DESSLER, A. J.		Vertical Ballistic Trajectories Over an Oblate Earth.....	333
GREENBERG, RAYMOND Techniques of Flight Simulation for Ramjet Engines.....	308	MICKELSEN, WILLIAM R. An Analysis of Fuel-Oxidant Mixing in Screaming Combustors.....	172	ROSE, PETER H., <i>see</i> PROBSTEN, RONALD F.	
GREENE, N. D., <i>see</i> GAMBELL, W. R.		MIELE, ANGELO Minimality for Arbitrarily Inclined Rocket Trajectories.....	481	ROSEN, GERALD On the Classification of the Chemistry in Combustion Experiments.....	839
GREENWOOD, S. W. Solar Sailing—Practical Problems....	765	Some Recent Advances in the Mechanics of Terrestrial Flight.....	581	ROSNER, DANIEL E. Boundary Conditions for the Flow of a Multicomponent Gas.....	555
GREY, JERRY, <i>see</i> CROCCO, LUIGI		On the Brachistochronic Thrust Program for a Rocket Powered Missile Travel- ing in an Isothermal Medium.....	675	Recent Advances in Convective Heat Transfer With Dissociation and Atom Recombination.....	445
GRIFFITH, WAYLAND C. Recent Advances in Real Gas Effects in Hypersonic Flow.....	157	MIESSE, C. C. Effect of High Altitude Conditions on Atomization Phenomena.....	335	Wall Temperature Instability for Con- vective Heating With Surface Radica- l Recombination.....	402
GRUMER, JOSEPH Flashback and Blowoff Limits of Un- piloted Turbulent Flames.....	756	MIRELS, HAROLD Flat Plate Laminar Skin Friction and Heat Transfer in the Free Molecule to Continuum Flow Regimes.....	689	ROSS, PETER A. Some Observations of Flame Stabiliza- tion in Sudden Expansions.....	123
GRUMER, J. F., <i>see</i> RICHMOND, J. K.		MISHUCK, E., <i>see</i> ANDERSEN, W. H.		ROSS, STANLEY Minimality for Problems in Vertical and Horizontal Rocket Flight.....	55
HAITE, W. F. Propellant Explosives Classification and the Effect on Field Handling of Missiles.....	489	MOE, G., <i>see</i> ANDERSEN, W. H.		ROSS, STANLEY E., <i>see</i> BRYSON, A. E., JR.	
HALL, J. GORDON and HERTZBERG, A. Recent Advances in Transient Surface Temperature Thermometry.....	719	MORRELL, GERALD An Empirical Method for Calculating Heat Transfer Rates in Resonating Gaseous Pipe Flow.....	829	ROTHBERG, SIDNEY, COLBOURN, JOSEPH L. and SALVATORE, ROBERT Toxicity and Personal Decontamination of Boron Hydride Propellant Fuels	762
HALL, H. H. and ZAMBELLI, E. D. On the Optimization of Multistage Rockets.....	463	MULLER, G. M., <i>see</i> EVANS, MARJORIE W.		RUDIN, MORTON, <i>see</i> AROESTE, HENRY	
HAMMITT, A. G., <i>see</i> VAS, I. E.		NACHBAR, W. R., <i>see</i> GREEN, L., JR.		RUSSELL, WILLIAM T. Inertial Guidance for Rocket-Propelled Missiles.....	17
HANSON, W. B., <i>see</i> DESSLER, A. J.		NEWTON, ROBERT R. Lifetimes of Artificial Satellites.... On the Optimization of Physical Propul- sion Systems.....	331 752	SABERSKY, R. H., <i>see</i> HASTRUP, R. C.	
HARRJE, DAVID T., <i>see</i> CROCCO, LUIGI		NICHOLLS, J. A., <i>see</i> DUNLAP, R.		SACKMAN, J. L. A Remark on an Iterative Method of Determining Equilibrium Composi- tions of Reacting Gases.....	765
HARTNETT, J. P., <i>see</i> TURNACLIFF, R. D.		NIELSEN, CARL L. Principles and Applications of Phase- Lock Detection in Phase-Coherent Systems.....	541	SALVATORE, ROBERT, <i>see</i> ROTHBERG, SIDNEY	
HASTRUP, R. C., SABERSKY, R. H., BARTZ D. R. and NOEL, M. B. Friction and Heat Transfer in a Rough Tube at Varying Prandtl Numbers...	259	NOEL, M. B., <i>see</i> HASTRUP, R. C.		SAMPSON, WILLIAM F., <i>see</i> RICHTER, HENRY L., JR.	
HAYDAY, A. A., <i>see</i> ECKERT, E. R. G.		OLDS, R. H. Optimum Variation of Exhaust Velocity During Burning.....	405	SCALA, SINCLAIRE M. Surface Combustion in Dissociated Air	340
HERRICK, SAMUEL and BAKER, ROBERT M. L., JR. Recent Advances in Astrodynamics...	649	ORR, ELSIE C., <i>see</i> WILLINSKI, MARTIN I.		SCHAAF, S. A., <i>see</i> TALBOT, L.	
HERTZBERG, A., <i>see</i> HALL, J. GORDON		OSBORN, J. R., <i>see</i> ZUCROW, M. J.		SCHNEIDER, P. J., <i>see</i> ECKERT, E. R. G.	
HERTZBERG, M., <i>see</i> DESSLER, A. J.		PAIEWONSKY, BERNARD H. Transfer Between Vehicles in Circular Orbits.....	121	SCHULTZ, R. D., <i>see</i> ANDERSEN, W. H.	
HIDALGO, HENRY On the Application of Van Driest's Method to a Highly Cooled Partially Dissociated Turbulent Boundary Layer.....	487	PARKS, DRUEY P., <i>see</i> WINZEN, OTTO C.		SEARS, G. A. and BAJEK, J. J. Testing Air-Breathing Supersonic Power- plants.....	303
HILDENBRAND, D. L. and REID, W. P. Burning Rate Studies. III. Correlation of Experimental Results With the Thermal Model.....	194	PERRIN, J. R., <i>see</i> SHANLEY, E. S.		SHANLEY, E. S. and PERRIN, J. R. Prediction of the Explosive Behavior of Mixtures Containing Hydrogen Peroxide.....	382
HINNERS, ARTHUR H., JR., <i>see</i> DIETZ, ROBERT O., JR.		PERSEN, LEIF N. Motion of a Satellite With Friction...	750	SHAPIRO, ASCHER H., <i>see</i> DUSSOURD, JULES L.	
Hsu, CHENG-TING, <i>see</i> CHANG, CHIEH- CHEN		PETERSON, J. B., <i>see</i> WANG, C. J.		SHURLEY, LUCIAN A., <i>see</i> DEAN, LEO E.	
HURLBUT, F. C., <i>see</i> TALBOT, L.		PRICE, E. W. Terminology in Rocket Combustion In- stability.....	197	SIBULKIN, MERWIN Estimation of Turbulent Heat Transfer at the Sonic Point of a Blunt-Nosed Body.....	548
KLUGER, P. and FARREL, E. C. Digital Computer Analysis of Transients in Liquid Rocket Engines.....	804	PRICE, E. W. and SOFFERIS, J. W. Combustion Instability in Solid Propel- lant Rocket Motors.....	190	SIMONS, DAVID G. Observations Made During Manhigh II Flight.....	521
LATTONE, E. V. and STOUT, J. E. Mach Reflections in Two-Dimensional Diffusers From Hydraulic Analogy Experiments.....	257	PROBSTEN, RONALD F., ADAMS, MAC C. and ROSE, PETER H. On Turbulent Heat Transfer Through a Highly Cooled Partially Dissociated Boundary Layer.....	56	SINGER, S. F. and WENTWORTH, R. C. A Method for Calculating Impact Points of Ballistic Rockets: Convenient Representations.....	684
LARSON, R. M., <i>see</i> ECKERT, E. R. G.		<i>See also</i> ADAMS, MAC C.		SMALL, B. B., <i>see</i> CHRIST, O. J. W.	
LAWRENCE, H. R., WANG, C. J. and REDDY, R. B. Variational Solution of Fuel Sloshing Modes.....	729	PUTNAM, ABBOTT A. On the Rational Choice of Flame- Holder Shape.....	60	SMALL, LANCE W. Possibility of Aerodynamic Descent on the Moon.....	765
LEITMANN, GEORGE A Remark on the Free Vibration of a Variable Mass.....	197	RABINOWICZ, JOSEF Measurement of Turbulent Heat Trans- fer Rates on the Aft Portion and Blunt Base of a Hemisphere Cylinder in the Shock Tube.....	615	SNYDER, WILLIAM T. Influence of Approach Boundary Layer Thickness on Premixed Propane-Air Flames Stabilized in a Sudden Ex- pansion.....	822
LIEBERMAN, P. Simulation of Free Flight Structural Characteristics by Captive Missile I. Computer Analysis.....	622	RAINS, DEAN A. Head-Flow Characteristics of Axial Flow Helical Inducers.....	557	SOFFERIS, J. W., <i>see</i> PRICE, E. W.	
LINNELL, R. D. Vertical Re-entry Into the Earth's At- mosphere for Both Light and Heavy Bodies.....	329	RALL, D. L., <i>see</i> GIEDT, W. H.		SPARROW, E. M. Combined Effects of Unsteady Flight Velocity and Surface Temperature on Heat Transfer.....	403
LIPKIS, R. P., <i>see</i> BROMBERG, R.; <i>see</i> <i>also</i> COHEN, C. B.		RAO, G. V. R. Exhaust Nozzle Contour for Optimum Thrust.....	377	SQUIRE, WILLIAM Some Comments on Generalized Trajec- tories for Free Falling Bodies of High Drag.....	838
LIPOW, M. Recent Advances in Rocket Reliability Concepts.....	373	RATCLIFFE, H., <i>see</i> BRAGG, S. L.			
LIU, F. F. and BERWIN, T. W. Recent Advances in Dynamic Pressure Measurement Techniques.....	83	RAUCH, L. L., <i>see</i> BEUTLER, F. J.			
		RAY, E. C., <i>see</i> VAN ALLEN, J. A.			
		REDDY, R. B., <i>see</i> LAWRENCE, H. R.			
		REID, W. P., <i>see</i> HILDENBRAND, D. L.			
		REISMANN, HERBERT Liquid Propellant Inertia and Damping Due to Airframe Roll.....	746		
		RESHOTKO, ELI Heat Transfer to a General Three- Dimensional Stagnation Point.....	58		

(Continued on page 870)

EXCELCO



Builders of more large, thin wall,
high strength solid propellant
rocket engine cases and nozzles
for development purposes than
any other company in America.

RV-A-10 SERGEANT
NIKE-HERCULES JUPITER JR.
JUPITER SR. POLARIS O
POLARIS A POLARIS A-1
AIR FORCE - RE-ENTRY - X-17
POLARIS - RE-ENTRY - X-36
MINUTEMAN PERSHING

AND MANY OTHER CLASSIFIED PROJECTS

A small experienced organization geared to handle
your development and prototype requirements for
static and flight tests in the shortest possible time.

Call or write

EXCELCO DEVELOPMENTS

MILL STREET • PHONE 101

SILVER CREEK, NEW YORK

CONTINENTAL Ground Support



Boosts Air Time

Continental's TC-106 turbine air compressor, developed in conjunction with the United States Air Force, is now available for commercial jet liner ground support. The unit, supplying low pressure air, is especially suited to engine starting, cabin air conditioning and actuation of electrical generating equipment for ground operations of the aircraft . . . Continental Turbo-Compressors have been in operation with the Air Force for more than four years, compiling an enviable service record for dependability and long life . . . Continental's new Snow and Ice Removal Nozzle unit, designed to be used with the TC-106 air compressor, reduces man hours and material costs for ice removal from aircraft surfaces. Warm bleed air from the compressor is converted to a high-energy air shaft which erodes through the ice, lifting it from the surface and blowing it away. The Snow and Ice Removal Nozzle is equipped with a glycol spray attachment for quick application of anti-ice protection after the surface has been cleared.



SNOW AND ICE
REMOVAL NOZZLE



CONTINENTAL AVIATION & ENGINEERING CORPORATION

12700 KERCHEVAL AVENUE, DETROIT 15, MICHIGAN

SUBSIDIARY OF CONTINENTAL MOTORS CORPORATION

STRINITZ, ROBERT	
Recent Advances in Cermets	15
STEVENS, ROBERTSON, <i>see</i> RICHTER,	
HENRY L., JR.	
STEWART, CHARLES E., <i>see</i> STRUBLE,	
RAIMOND A.	
STONE, MAX W.	
A Practical Mathematical Approach to	
Grain Design	236
STOUT, J. E., <i>see</i> LAITONE, E. V.	
STROUD, W. G.	
Meteorological Rocket Soundings in the	
Arctic	817
STRUBLE, RAIMOND A., STEWART,	
CHARLES E. and GRANTON, JAMES, JR.	
The Trajectory of a Rocket With Thrust	
Subotowicz, M.	472
The Optimization of the N-Step Rocket	
With Different Construction Param-	
eters and Propellant Specific Im-	
pulses in Each Stage	460
SUMMERFIELD, MARTIN and McALEVY,	
R. F., III	
The Shock Tube as a Tool for Solid	
Propellant Ignition Research	478
SUTTON, GEORGE W.	
The Temperature History in a Thick	
Skin Subjected to Laminar Heating	
During Entry Into the Atmosphere	
TALBOT, L., SCHAAF, S. A. and HURLBUT,	
F. C.	40
Pressure Distribution on Blunt-Nosed	
Cones in Low Density Hypersonic	
Flow	832
TEN DYKE, RICHARD P.	
Computation of Rocket Step Weights	
to Minimize Initial Gross Weight . . .	338
TURNACLIFFE, R. D. and HARTNETT,	
J. P.	
Generalized Trajectories for Free-Falling	
Bodies of High Drag	263
VAN ALLEN, J. A., LUDWIG, G. H., RAY,	
E. C. and McILWAIN, C. E.	
Observation of High Intensity Radiation	
by Satellites 1958 Alpha and Gamma	
VANDENKERCKHOVE, JEAN A.	
Comment on "A Practical Approach to	
Grain Design"	766
Erosive Burning of a Colloidal Solid	
Propellant	599
VARGO, LOUIS G.	
Criteria for Orbital Entry	54
VAS, I. E., BOGDANOFF, S. M. and HAM-	
MUTT, A. G.	
An Experimental Investigation of the	
Flow Over Simple Two-Dimensional	
and Axial Symmetric Bodies at Hy-	
personic Speeds	97
VORECK, W. E., <i>see</i> BROBECK, W. M.	
WANG, C. J. and PETERSON, J. B.	
Spreading of Supersonic Jets From	
Axially Symmetric Nozzles	321
<i>See also</i> LAWRENCE, H. R.	
WEISBORD, LEON	
A Generalized Optimization Procedure	
for N-Staged Missiles	164
WENTWORTH, R. C., <i>see</i> SINGER, S. F.	
WIEGAND, JAMES H.	
Simplified Equations for Transient	
Heat-Conduction to Insulated Metal	
Slab	456
WILDE, KENNETH A.	
Effect of Radical Recombination Ki-	
netics on Specific Impulse of High	
Temperature Systems	119
WILLINSKI, MARTIN I. and ORR, ELSIE C.	
Project Snooper, A Program for Un-	
manned Interplanetary Reconnaissance	
WINZEN, OTTO C. and PARKS, DRUEY, P.	
Operation Manhigh II	523
WISE, HENRY, <i>see</i> AGOSTON, GEORGE A.	
WOLFHARD, H. G.	
The Ignition of Combustible Mixtures	
by Hot Gases	798
WOOD, BERNARD J., <i>see</i> AGOSTON, GEORGE	
A.	
WRIGLEY, R. C., <i>see</i> DESSLER, A. J.	
YUAN, S. W. and FINKELSTEIN, A. B.	
Heat Transfer in Laminar Pipe Flow	
With Uniform Coolant Injection . . .	178
ZAMBELLI, E. D., <i>see</i> HALL, H. H.	
ZIEMER, RICHARD W. and CAMBEL, ALI	
BULENT	
Flame Stabilization in the Boundary	
Layer of Heated Flat Plates	592
ZIGRANG, D. J.	
Comments on "An Approximate Specific	
Impulse Equation for Condensable	
Mixtures"	409
ZUCROW, M. J. and OSBORN, J. R.	
An Experimental Study of High-Fre-	
quency Combustion Pressure Oscilla-	
tions	654

JET PROPULSION

5
8
7
2
0
3
0
2
3
3
3
3
9
4
7
0
4
1
3
3